



R/V Mirai Cruise Report MR02-K06 (Leg 3-4)

*January 13, 2003 – January 31, 2003 (Leg 3)
February 2, 2003 – February 14, 2003 (Leg 4)*

Primary productivity in the equatorial Pacific

Biogeochemical and optical research



Edited by
Kazuhiko Matsumoto

Japan Marine Science and Technology Center
(JAMSTEC)

Contents

1. Introduction
2. Cruise summary
 - 2.1 Ship
 - 2.2 Period
 - 2.3 Ports of call
 - 2.4 Cruise code
 - 2.5 Cruise name
 - 2.6 Chief scientist
 - 2.7 Cruise log
 - 2.7.1 Leg. 3
 - 2.7.2 Leg. 4
 - 2.8 Cruise track
3. Participants list
 - 3.1 R/V MIRAI scientist and technical staff
 - 3.2 R/V MIRAI crew member
4. General observation
 - 4.1 Meteorological measurement
 - 4.1.1 Surface meteorological observation
 - 4.1.2 Ceilometer
 - 4.2 CTD/XCTD
 - 4.2.1 CTD
 - 4.2.2 XCTD
 - 4.3 Shipboard ADCP
 - 4.4 Underway geophysics
 - 4.4.1 Sea surface gravity
 - 4.4.2 Surface three-component magnetometer
 - 4.4.3 Multi-narrow beam echo sounding system
5. Special observations
 - 5.1 Dissolved oxygen
 - 5.2 Salinity measurement
 - 5.3 Nutrients
 - 5.3.1 Nitrate, Nitrite, Silicic acid, Phosphate
 - 5.3.2 Low level Ammonia
 - 5.4 Phytoplankton pigment analysis
 - 5.4.1 Chlorophyll *a* measurements by fluorometric determination
 - 5.4.2 Size fraction of phytoplankton by fluorometric determination
 - 5.5 The measurement of marine phytoplankton pigments by HPLC
 - 5.6 Characterization of light absorption coefficients of phytoplankton
 - 5.7 Phytoplankton abundances

- 5.8 Distribution of heterotrophic microflagellates and ciliates
- 5.9 Primary productivity
- 5.10 Distribution of microplankton (>15 µm) along the Western Equatorial Pacific Ocean in winter 2003
- 5.11 Study on the biogeography of the coccolithophorid assemblage in the Western and Central Equatorial Pacific Ocean
- 5.12 Distribution of diatoms in sea-surface waters in the western and central equatorial Pacific
- 5.13 Distributions of planktic foraminifera and radiolarians in the Equatorial Pacific Ocean
- 5.14 Distribution of planktic foraminifera in the surface water in the western Pacific Ocean
- 5.15 Continuous monitoring of surface seawater
 - 5.15.1 Integrated monitoring system of surface seawater
 - 5.15.2 Nutrients monitoring in surface seawater
- 5.16 CO₂ concentration in the atmosphere and CO₂ system in the ocean
- 5.17 Greenhouse Effects Gasses at the Equatorial Area
- 5.18 Volatile organic compounds
- 5.19 Stable isotope biogeochemistry of the greenhouse and trace gases in the equatorial Pacific Ocean
- 5.20 Radionuclides in settling particles and suspended particles in the equatorial Pacific
- 5.21 Rare earth element and heavy metal distributions in seawater of the equatorial Pacific Ocean
- 5.22 Relationship between cadmium and phosphate in the equatorial Pacific
- 5.23 Sediment trap experiments in the equatorial Pacific
- 5.24 ²³⁴Th/²³⁸U and ²¹⁰Po/²¹⁰Pb Disequilibria as indicators of removal rates and particulate organic carbon fluxes in the western and central equatorial Pacific
- 5.25 Satellite observation with SeaWiFS for primary productivity research
- 5.26 Optical measurements, nitrate sensor and production
- 5.27 ARGO float deployment
- 5.28 TRITON Buoy recovery
- 5.29 Aerosol Measurement
- 5.30 Lidar observations of clouds and aerosols
- 5.31 Microwave radiometer and micro rain radar
- 5.32 Surface Atmospheric Turbulent Flux

1. Introduction

The equatorial Pacific has distinguished into distinct two regions: the western warm pool or the oligotrophic waters and the equatorial upwelling or the high nutrient low chlorophyll waters. The western warm pool, where nitrate is depleted and formed deep chlorophyll maximum in the vicinity of nitracline. The equatorial upwelling, where nutrients are sufficient and chlorophyll *a* concentrations are higher in surface water. However, the concentrations were not as high as expected from nutrients concentration. Phytoplankton species, biomass and vertical distributions are different in two regions. Primary productivity is small in the warm pool and higher in the upwelling region.

Two regions area are shifted with ENSO event, phytoplankton distribution and primary productivity are affected by seasonal and interannual fluctuations associated with ENSO event.

Japan Marine Science and Technology Center (JAMSTEC) conducted MR02-K06 leg-3 cruise along the equator between 160°E and 160°W. The western warm pool extended to the east, the sea surface temperature was higher than 28°C in all observation area, since this year corresponds to El Nino conditions.

Furthermore, we conducted MR02-K06 leg-4 cruise from Honolulu to Sekinehama to clarify the subduction process in the mid-latitude.

2. Cruise summary

2.1. Ship

R/V MIRAI

2.2. Period

Jan. 13, 2003 – Jan. 31, 2003 (Leg 3: Chuuk – Honolulu)

Feb. 1, 2003 – Feb. 14, 2003 (Leg 4: Honolulu – Sekinehama)

2.3. Ports of call

- 1) Chuuk, F.S.M
- 2) Honolulu, U.S.A
- 3) Hachinohe, Japan
- 4) Sekinehama, Japan

2.4. Cruise code

MR02-K06 (leg3 – leg4)

2.5. Cruise name

Primary productivity in the equatorial Pacific
(Biogeochemical and optical research)

2.6. Chief scientist

Kazuhiko Matsumoto
Ocean Research Department, JAMSTEC

2.7. Cruise Log

2.7.1. Leg. 3

Date	Start Time	Date	Start Time	Station	Position(start)		Events
	(U.T.C.)		(L.S.T.)		Lat.	Lon.	
		1.13	10:00				Departure from Chuuk
		1.14	7:56	Triton	04-58.00N	156-02.00E	TRITON recovery
1.15	02:31	1.15	13:31	6	00-03.03N	159-57.20E	Arrival at Stn. 6
			13:31	6	00-03.03N	159-57.20E	Sediment trap recovery
			15:13	6	00-00.12N	160-00.20E	CTD Shallow cast 3
			15:21	6	00-00.07N	160-00.24E	Sea surface sampling
			16:03	6	00-00.21S	160-00.55E	Plankton net calibration
		1.16	00:55	6	00-00.80S	159-59.80E	Plankton net
			03:58	6	00-00.14S	159-59.82E	CTD Shallow cast 1
			04:02	6	00-00.16S	159-59.82E	Sea surface sampling
			05:17	6	00-00.07N	160-00.03E	In-situ incubator deployment
			05:59	6	00-00.03N	159-59.52E	In-situ filtration
			10:53	6	00-00.18N	160-01.02E	CTD Shallow cast 2
			11:00	6	00-00.12N	160-01.05E	Sea surface sampling
			11:43	6	00-00.07N	160-01.48E	Freefall
			11:52	6	00-00.11S	160-01.41E	Freefall
			12:06	6	00-00.16S	160-01.35E	Hyperspectral Freefall
			12:16	6	00-00.10S	160-01.36E	Hyperspectral Freefall
			13:54	6	00-00.11N	160-01.07E	CTD Deep cast
			17:56	6	00-01.07N	160-09.72E	In-situ incubator recovery
1.16	07:21			X01	00-01.40N	160-10.73E	XCTD observation
	10:27			X02	00-02.00N	161-00.16E	XCTD observation
	14:12			X03	00-01.35N	162-00.03E	XCTD observation
	17:57			X04	00-00.44N	163-00.01E	XCTD observation
	21:45			X05	00-00.64N	164-00.00E	XCTD observation
	23:55	1.17	10:55	7	00-00.49N	164-31.30E	Arrival at Stn. 7
			10:55	7	00-00.49N	164-31.30E	CTD Shallow cast 4-1
			11:47	7	00-00.89N	164-31.50E	Freefall
			11:57	7	00-00.90N	164-31.72E	Freefall
			12:08	7	00-00.91N	164-31.97E	Hyperspectral Freefall
			12:19	7	00-00.90N	164-32.14E	Hyperspectral Freefall
			12:59	7	00-00.60N	164-33.02E	CTD Shallow cast 4-2
			13:02	7	00-00.65N	164-33.04E	Sea surface sampling
1.17	02:36			X06	00-00.87N	164-33.81E	XCTD observation
	04:20			X07	00-00.81N	165-00.00E	XCTD observation
	08:09			X08	00-00.50N	165-59.74E	XCTD observation
	12:00			X09	00-00.05N	167-00.03E	XCTD observation
	15:55			X10	00-00.43N	168-00.00E	XCTD observation

Date	Start Time	Date	Start Time	Station	Position(start)		Events
	(U.T.C.)		(L.S.T.)		Lat.	Lon.	
1.17	19:51			X11	00-00.03S	169-00.03E	XCTD observation
	23:53	1.18	10:53	8	00-00.11S	169-59.31E	Arrival at Stn. 8
			10:53	8	00-00-11S	169-59.31E	CTD Shallow cast 4-1
			11:42	8	00-00.28N	169-59.00E	Freefall
			11:54	8	00-00.21N	169-59.03E	Freefall
			12:06	8	00-00.14N	169-59.10E	Hyperspectral Freefall
			12:16	8	00-00.08N	169-59.09E	Hyperspectral Freefall
			12:54	8	00-00.36S	169-59.39E	CTD Shallow cast 4-2
			12:58	8	00-00.34S	169-59.35E	Sea surface sampling
1.18	02:45			8	00-00.22S	169-59.98E	ARGO float deployment
	02:36			X12	00-00.21S	169-59-35E	XCTD observation
	06:44			X13	00-03.19S	171-00.01E	XCTD observation
	10:39			X14	00-05.97S	172-00.06E	XCTD observation
	14:31			X15	00-08.93S	173-00.01E	XCTD observation
	18:27			X16	00-07.25S	174-00.02E	XCTD observation
	22:30	1.19	10:30	9	00-00.09S	174-59.65E	Arrival at Stn. 9
			10:30	9	00-00.09S	174-59.65E	CTD Shallow cast 3
			10:35	9	00-00.16S	174-59.63E	Sea surface sampling
			11:12	9	00-00.42S	174-59.76E	In-situ filtration
		1.20	00:53	9	00-00.02N	174-59.97E	Plankton net
			03:53	9	00-00.28N	175-00.31E	CTD Shallow cast 1
			03:59	9	00-00.32N	175-00.27E	Sea surface sampling
			05:11	9	00-01.19N	175-02.65E	In-situ incubator deployment
			07:32	9	00-02.42N	174-55.75E	Sediment trap recovery
			10:54	9	00-00.01S	174-59.80E	CTD Shallow cast 2
			10:57	9	00-00.02S	174-59.77E	Sea surface sampling
			11:41	9	00-00.02S	174-59.49E	Freefall
			11:53	9	00-00.30S	174-59.22E	Freefall
			12:11	9	00-00.46S	174-58.86E	Hyperspectral Freefall
			12:21	9	00-00.47S	174-58.62E	Hyperspectral Freefall
			13:56	9	00-00.16S	175-00.20E	Sea surface sampling
			13:46	9	00-00.12S	175-00.20E	CTD Deep cast
			18:09	9	00-02.64N	175-05.72E	In-situ incubator recovery
1.20	06:36			9	00-02.84N	175-06.11E	ARGO float deployment
	06:40			X17	00-02.81N	175-06.34E	XCTD observation
	10:06			X18	00-00.05S	176-00.02E	XCTD observation
	13:51			X19	00-00.06N	177-00.02E	XCTD observation
	17:38			X20	00-00.31S	178-00.00E	XCTD observation
	21:30			X21	00-00.29S	179-00.02E	XCTD observation

Date	Start Time	Date	Start Time	Station	Position(start)		Events
	(U.T.C.)		(L.S.T.)		Lat.	Lon.	
1.20	22:55	1.21(A)	10:55	10	00-00.18S	179-19.21E	Arrival at Stn. 10
			10:55	10	00-00.18S	179-19.21E	CTD Shallow cast 4-1
			11:47	10	00-00.51S	179-18.57E	Freefall
			11:59	10	00-00.42S	179-18.44E	Freefall
			12:12	10	00-00.35S	179-18.32E	Hyperspectral Freefall
			12:25	10	00-00.40S	179-18.18E	Hyperspectral Freefall
			13:00	10	00-00.44S	179-18.38E	CTD Shallow cast 4-2
			13:01	10	00-00.45S	179-18.37E	Sea surface sampling
1.21	01:52			10	00-00.97S	179-17.89E	ARGO float deployment
	01:55			X22	00-01.05S	179-18.06E	XCTD observation
	04:45			X23	00-00.98S	179-59.99E	XCTD observation
	08:50			X24	00-00.26S	179-00.02W	XCTD observation
	12:58			X25	00-00.43N	178-00.01W	XCTD observation
	17:02			X26	00-00.17N	177-00.00W	XCTD observation
	21:10			X27	00-00.05N	176-00.01W	XCTD observation
	22:53	1.21(B)	10:53	11	00-00.89N	175-37.97W	Arrival at Stn. 11
			10:53	11	00-00.89N	175-37.97W	CTD Shallow cast 4-1
			11:35	11	00-01.10N	175-38.29W	Freefall
			11:46	11	00-01.10N	175-38.21W	Freefall
			11:58	11	00-01.15N	175-38.21W	Hyperspectral Freefall
			12:09	11	00-01.18N	175-38.24W	Hyperspectral Freefall
			12:53	11	00-00.53N	175-37.42W	CTD Shallow cast 4-2
			12:59	11	00-00.56N	175-37.49W	Sea surface sampling
1.22	01:35			11	00-00.80N	175-37.82W	ARGO float deployment
	01:38			X28	00-00.79N	175-37.69W	XCTD observation
	04:18			X29	00-00.04S	175-00.01W	XCTD observation
	08:28			X30	00-00.48N	174-00.01W	XCTD observation
	12:34			X31	00-00.14S	173-00.03W	XCTD observation
	16:38			X32	00-00.53S	171-59.96W	XCTD observation
	20:43			X33	00-00.75S	171-00.01W	XCTD observation
1.23	00:52	1.22	13:52	12	00-00.71S	170-09.96W	Arrival at Stn. 12
			13:52	12	00-00.71S	170-09.96W	Sediment trap recovery
			16:30	12	00-00.00N	170-00.76W	CTD Shallow cast 3
		1.23	00:52	12	00-00.03S	170-00.19W	Plankton net
			03:53	12	00-00.17S	169-59.43W	CTD Shallow cast 1
			04:00	12			Sea surface sampling
			05:12	12	00-00.14S	169-53.27W	In-situ incubator deployment
			10:54	12	00-00.24N	169-58.86W	CTD Shallow cast 2
			11:00	12	00-00.26N	169-58.99W	Sea surface sampling

Date	Start Time	Date	Start Time	Station	Position(start)		Events
	(U.T.C.)		(L.S.T.)		Lat.	Lon.	
		1.23	11:37	12	00-00.52N	169-59.24W	Freefall
			11:47	12	00-00.59N	169-59.28W	Freefall
			11:58	12	00-00.66N	169-59.35W	Hyperspectral Freefall
			12:11	12	00-00.70N	169-59.52W	Hyperspectral Freefall
			13:09	12	00-00.30N	169-59.10W	CTD Deep cast
			18:18	12	00-02.67N	170-00.67W	In-situ incubator recovery
		1.24	06:55	12	00-00.03S	170-00.01W	In-situ filtration
1.24	23:28			12	00-00.08S	169-58.93W	ARGO float deployment
1.25	03:40			X34	00-00.30S	169-00.01W	XCTD observation
	07:59			X35	00-00.29N	168-00.01W	XCTD observation
	16:29			X36	00-00.58S	166-00.20W	XCTD observation
	20:50			X37	00-00.39S	165-00.00W	XCTD observation
	21:56	1.25	10:56	13	00-00.28S	164-47.65W	Arrival at Stn. 13
			10:56	13	00-00.28S	164-47.65W	CTD Shallow cast 4-1
			11:41	13	00-00.04S	164-48.13W	Freefall
			11:52	13	00-00.01S	164-48.23W	Freefall
			12:03	13	00-00.02S	164-48.34W	Hyperspectral Freefall
			12:12	13	00-00.00S	164-48.48W	Hyperspectral Freefall
			12:53	13	00-00.01S	164-47.80W	CTD Shallow cast 4-2
			12:57	13	00-00.01S	164-47.90W	Sea surface sampling
1.26	00:38			13	00-00.18N	164-48.32W	ARGO float deployment
	04:17			X38	00-00.05N	164-00.02W	XCTD observation
	08:44			X39	00-00.25N	163-00.02W	XCTD observation
	13:10			X40	00-00.07N	162-00.02W	XCTD observation
	17:39			X41	00-00.37N	161-00.00W	XCTD observation
	22:11	1.26	11:11	14	00-00.02N	160-01.01W	Arrival at Stn. 14
			11:11	14	00-00.02N	160-01.01W	CTD Shallow cast 3
			11:14	14	00-00.05N	160-01.13W	Sea surface sampling
			12:47	14	00-00.21S	160-00.87W	Sediment trap recovery
			15:05	14	00-00.32S	159-59.68W	CTD Deep cast
		1.27	00:54	14	00-00.11S	159-59.36W	Plankton net
			03:55	14	00-00.02S	159-58.80W	CTD Shallow cast 1
			03:57	14	00-00.02S	159-58.80W	Sea surface sampling
			05:08	14	00-00.24N	159-53.20W	In-situ incubator deployment
			05:47	14	00-00.02S	159-55.29W	In-situ filtration
			10:58	14	00-00.22N	159-56.37W	CTD Shallow cast 2
			11:03	14	00-00.23N	159-56.40W	Sea surface sampling
			11:40	14	00-00.52N	159-56.44W	Freefall
			11:50	14	00-00.58N	159-56.44W	Freefall

Date	Start Time	Date	Start Time	Station	Position(start)		Events
	(U.T.C.)		(L.S.T.)		Lat.	Lon.	
		1.27	12:01	14	00-00.64N	159-56.46W	Hyperspectral Freefall
			12:13	14	00-00.69N	159-56.59W	Hyperspectral Freefall
			17:34	14	00-04.10N	159-58.49W	In-situ incubator recovery
1.28	05:01			14	00-04.23N	159-58.36W	ARGO float deployment
	12:22				01-59.65N	159-48.52W	ARGO float deployment
1.29	07:30				06-59.37N	159-17.96W	ARGO float deployment
1.30	03:05				11-59.37N	158-46.81W	ARGO float deployment
	19:24				15-59.64N	158-24.74W	ARGO float deployment
		1.31	13:50				Arrival at Honolulu

2.7.2. Leg 4

Date	Start Time	Date	Start Time	Station	Position(start)		Events
	(U.T.C.)		(L.S.T.)		Lat.	Lon.	
		2.1	23:30				Departure from Honolulu
2.3	20:03				25-28.38N	165-59.46W	ARGO float deployment
	15:34			X01	24-45.46N	165-00.00W	XCTD observation
	20:07			X02	25-28.51N	165-59.70W	XCTD observation
2.4	08:17				26-59.80N	168-59.18W	ARGO float deployment
	20:51				28-21.73N	171-59.24W	ARGO float deployment
	00:07			X03	25-59.16N	167-00.02W	XCTD observation
	04:08			X04	26-29.50N	168-00.01W	XCTD observation
	08:22			X05	26-59.93N	168-59.46W	XCTD observation
	12:40			X06	27-29.99N	170-00.01W	XCTD observation
	17:17			X07	28-00.17N	171-08.12W	XCTD observation
	20:55			X08	28-21.86N	171-59.44W	XCTD observation
2.5	20:38				29-17.60N	175-59.14W	ARGO float deployment
	01:03			X09	28-47.85N	173-00.01W	XCTD observation
	06:30			X10	29-15.61N	174-05.36W	XCTD observation
	13:48			X11	29-14.85N	175-00.02W	XCTD observation
	20:41			X12	29-17.71N	175-59.39W	XCTD observation
2.6	07:50				30-17.89N	177-59.28W	ARGO float deployment
	20:53				32-02.48N	179-00.84E	ARGO float deployment
	02:28			X13	29-45.05N	177-00.02W	XCTD observation
	07:53			X14	30-17.98N	177-59.51W	XCTD observation
	12:33			X15	30-53.96N	179-00.01W	XCTD observation
	16:52			X16	31-29.50N	179-59.99W	XCTD observation
	20:53			X17	32-02.60N	179-00.62E	XCTD observation
2.7	07:43				32-58.79N	176-01.04E	ARGO float deployment
	22:11				32-59.03N	173-01.18E	ARGO float deployment
	00:31			X18	32-21.90N	177-59.98E	XCTD observation
	04:02			X19	32-40.83N	176-59.98E	XCTD observation
	07:45			X20	32-58.85N	176-00.88E	XCTD observation
	09:55			X21	32-59.74N	175-29.98E	XCTD observation
	12:11			X22	32-59.05N	175-00.00E	XCTD observation
	14:28			X23	32-59.33N	174-30.00E	XCTD observation
	17:03			X24	32-58.96N	173-59.98E	XCTD observation
	19:44			X25	32-58.51N	173-30.02E	XCTD observation
	22:14			X26	32-59.02N	173-00.83E	XCTD observation
2.8	13:11				32-58.78N	170-01.08E	ARGO float deployment
	00:38			X27	32-59.44N	172-29.99E	XCTD observation

Date	Start Time	Date	Start Time	Station	Position(start)		Events
	(U.T.C.)		(L.S.T.)		Lat.	Lon.	
2.8	02:53			X28	32-59.68N	172-00.00E	XCTD observation
	05:12			X29	32-59.36N	171-29.98E	XCTD observation
	07:36			X30	32-59.31N	170-59.99E	XCTD observation
	13:13			X31	32-58.76N	170-01.00E	XCTD observation
	16:01			X32	32-57.98N	169-29.99E	XCTD observation
	18:43			X33	32-57.56N	168-59.98E	XCTD observation
	21:44			X34	32-58.46N	168-30.02E	XCTD observation
2.9	06:51				33-12.78N	167-01.21E	ARGO float deployment
	16:58				33-54.35N	165-01.23E	ARGO float deployment
	00:48			X35	33-00.89N	168-00.15E	XCTD observation
	04:00			X36	33-07.22N	167-30.02E	XCTD observation
	06:53			X37	33-12.79N	167-01.04E	XCTD observation
	09:48			X38	33-23.53N	166-30.00E	XCTD observation
	12:25			X39	33-34.80N	166-00.01E	XCTD observation
	17:00			X40	33-54.40N	165-01.06E	XCTD observation
	21:02			X41	34-12.62N	164-00.00E	XCTD observation
2.10	00:48				34-30.57N	163-00.59E	ARGO float deployment
	08:19				35-05.74N	161-01.09E	ARGO float deployment
	15:04				35-40.38N	159-00.52E	ARGO float deployment
	00:49			X42	34-30.61N	163-00.49E	XCTD observation
	04:32			X43	34-49.64N	162-00.00E	XCTD observation
	08:20			X44	35-05.77N	161-00.97E	XCTD observation
	11:46			X45	35-23.57N	159-59.99E	XCTD observation
	15:13			X46	35-40.70N	158-59.03E	XCTD observation
	18:34			X47	35-58.79N	157-59.97E	XCTD observation
	21:40			X48	36-17.04N	156-58.95E	XCTD observation
2.11	10:27				37-24.45N	153-00.18E	ARGO float deployment
	00:48			X49	36-33.11N	155-59.98E	XCTD observation
	04:03			X50	36-50.97N	155-00.19E	XCTD observation
	07:17			X51	37-08.65N	153-59.99E	XCTD observation
	10:29			X52	37-24.49N	153-00.04E	XCTD observation
	13:42			X53	37-41.81N	152-00.01E	XCTD observation
		2.13	12:50				Arrival at Hachinohe
			16:00				Departure from Hachinohe
		2.14	9:00				Arrival at Sekinehama

2.8. Cruise track

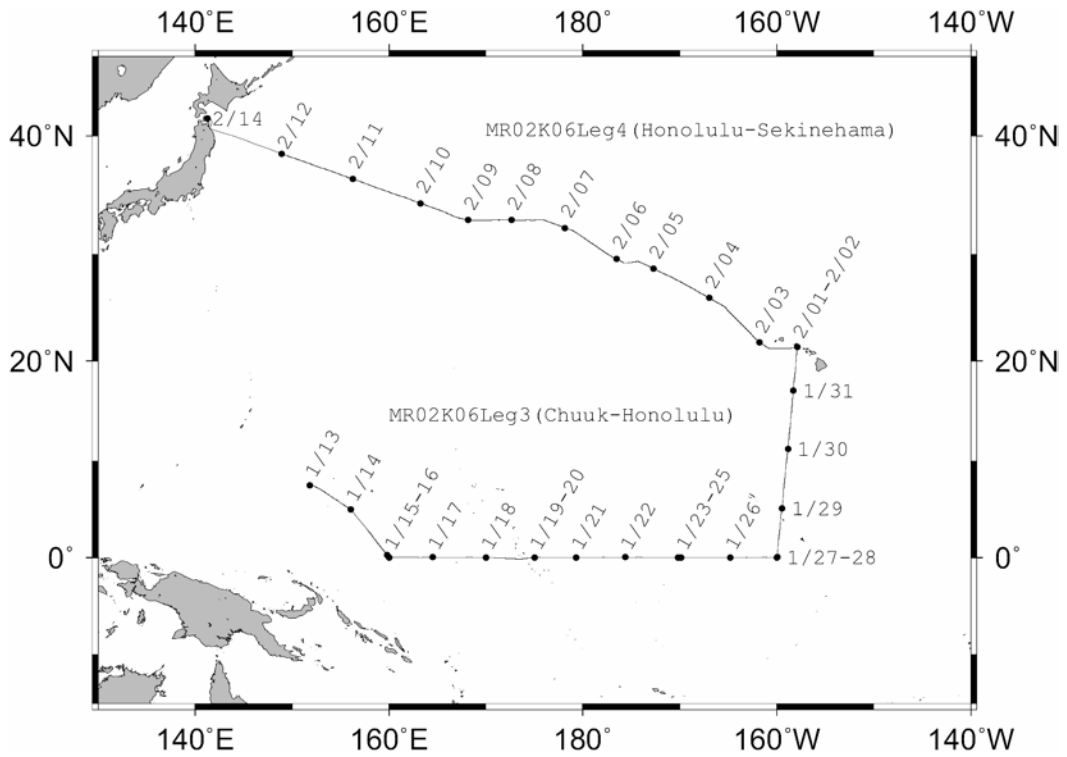


Fig.2.8-1 Cruise track

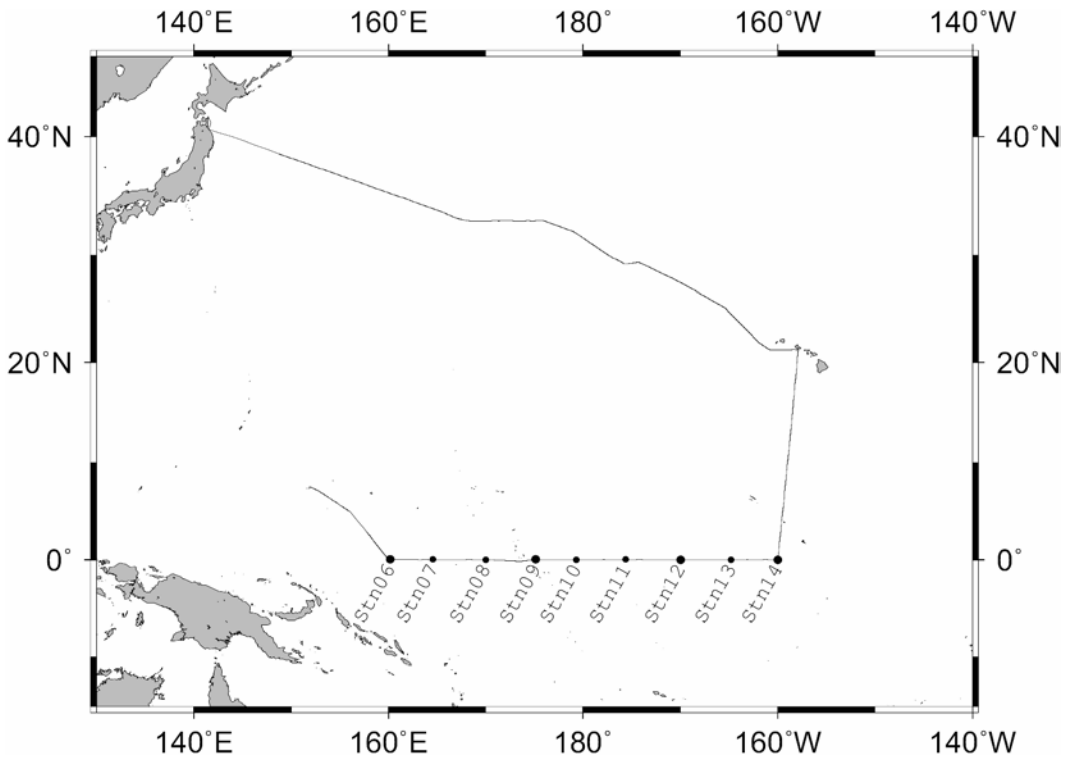


Fig.2.8-2 Observation stations

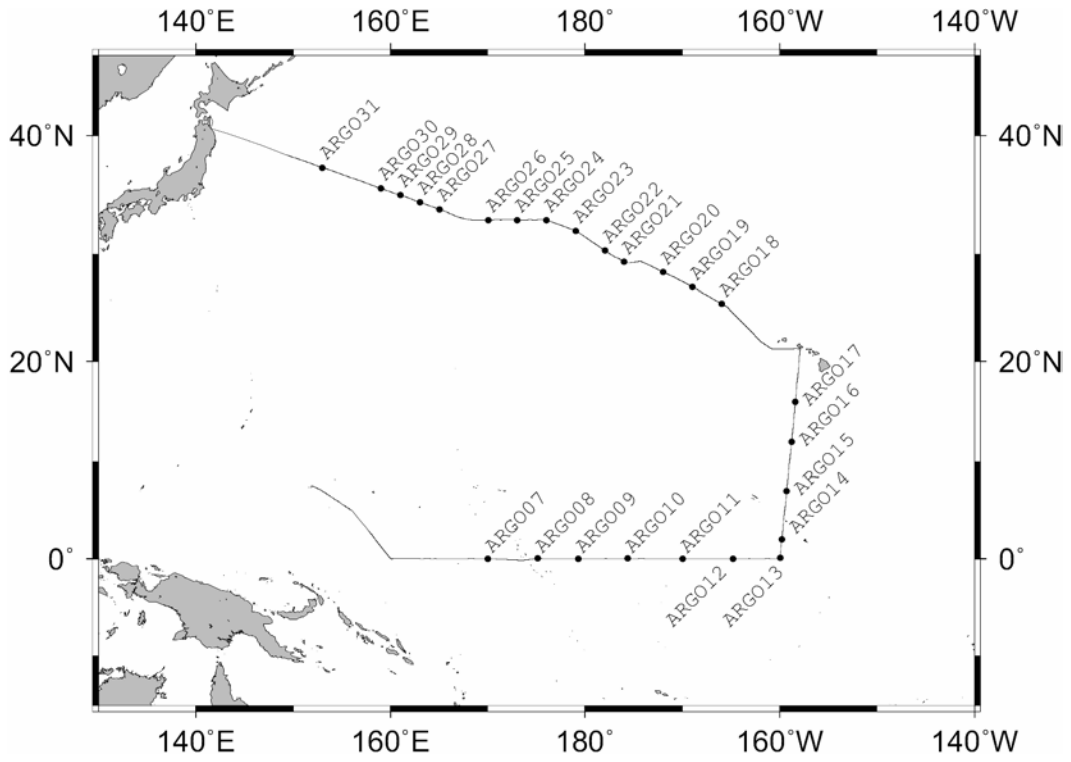


Fig.2.8-3 ARGO float deployment stations

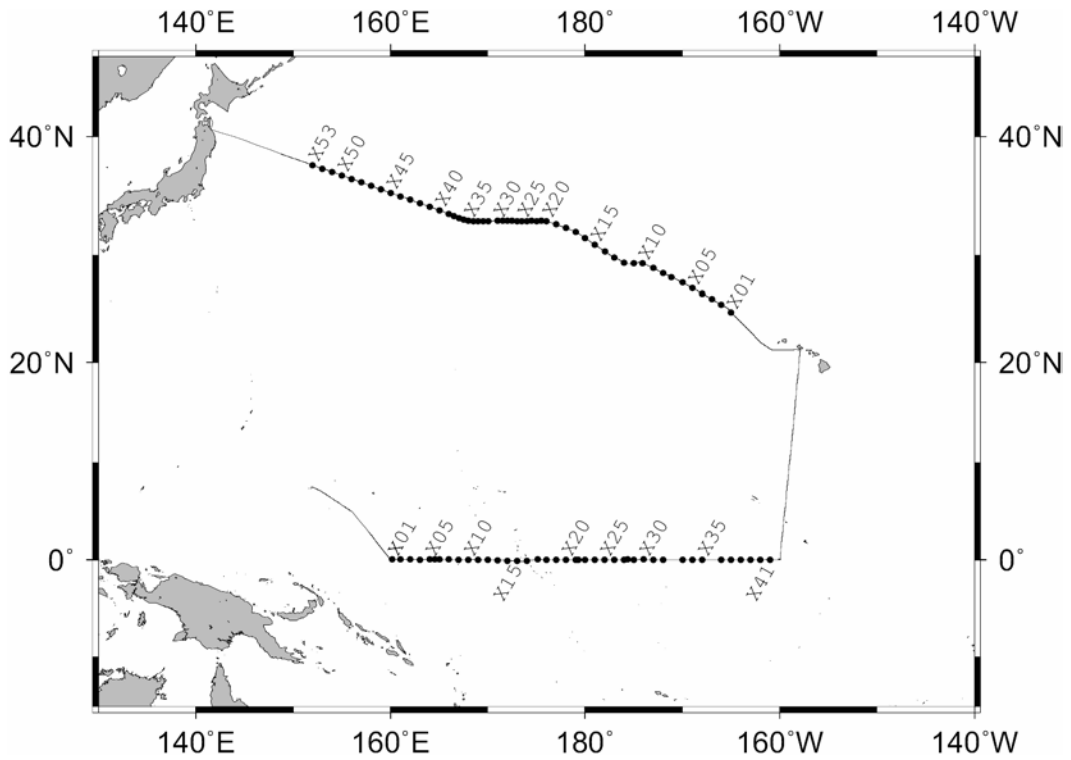


Fig.2.8-4 XCTD observation points

3. Participants list

3.1. R/V MIRAI scientists and technical staffs

	NAME	ORGANIZATION	POSITION	ADDRESS
1	Kazuhiko Matsumoto (Leg. 3 – 4)	JAMSTEC	CHIEF SCIENTIST	2-15 Natsushima-cho Yokosuka Kanagawa 237-0061 JAPAN
2	Akihiko Murata (Leg. 3)	JAMSTEC	SCIENTIST	2-15 Natsushima-cho Yokosuka Kanagawa 237-0061 JAPAN
3	Eitaro Oka (Leg. 4)	FORSGC	SCIENTIST	2-15 Natsushima-cho Yokosuka Kanagawa 237-0061 JAPAN
4	Masatoshi Yamada (Leg. 3)	NIRS	SCIENTIST	3609 Isozaki Hitachinaka Ibaraki 311-1202 JAPAN
5	Tatsuo Aono (Leg. 3)	NIRS	SCIENTIST	3609 Isozaki Hitachinaka Ibaraki 311-1202 JAPAN
6	Zhong-Liang Wang (Leg. 3)	NIRS	SCIENTIST	3609 Isozaki Hitachinaka Ibaraki 311-1202 JAPAN
7	Masao Ishii (Leg. 3)	MRI	RESEARCHER	1-1 Nagamine Tsukuba Ibaraki 305-0052 JAPAN
8	Shu Saito (Leg. 3 – 4)	MRI	RESEARCHER	1-1 Nagamine Tsukuba Ibaraki 305-0052 JAPAN
9	Kazuo Abe (Leg. 3)	SNFRI	RESEARCHER	148-446 Fukaiota Aza Ishigaki Okinawa 907-0451 JAPAN Phone +81-9808-8-2571, Fax +81-9808-8-2573
10	Akifumi Shimamoto (Leg. 3 – 4)	KANSO	TECHNICIAN	1-3-5 Azuchimachi Chuo-ku Osaka 541-0052 JAPAN
11	Shinya Endo (Leg. 3 – 4)	KANSO	TECHNICIAN	1-3-5 Azuchimachi Chuo-ku Osaka 541-0052 JAPAN
12	Shingo Maeda (Leg. 3 – 4)	NHE	TECHNICIAN	2-40-7 Higashikanagawa Kanagawa-ku Yokohama 221-0044 JAPAN Phone +81-45-453-6914, Fax +81-45-453-6919
13	Yuichi Koike (Leg. 3)	Bio-Environment Research CO. LTD	SCIENTIST	1646 Abiko Abiko Chiba 270-1166 JAPAN
14	John George MACINTYRE (Leg. 3)	Dalhousie Univ.	SCIENTIST	1355 Oxfprd St. Halifax N.S. CANADA B3H4J1
15	Michael D. MACDONALD (Leg. 3)	Dalhousie Univ	RESEARCHER	1355 Oxfprd St. Halifax N.S. CANADA B3H4J1
16	Toaea Beiateuea (Leg. 3)	Fisheries Division	FISHERIES ASSISTANT	P.O.Box 276, Bikenibeu Tarawa Republic of KIRIBATI Phone +686-28061

17	Fernando GOMEZ (Leg. 3 – 4)	Univ. of Tokyo	RESEARCHER	1-1-1 Yayoi Bunkyo-ku Tokyo 113-8657 JAPAN
18	Akira Sasaki (Leg. 3 – 4)	Tohoku Univ.	GRADUATE STUDENT	Aoba Aza Aramaki Aoba-ku Sendai Miyagi 980-8578 JAPAN
19	Kota Katsuki (Leg. 3 – 4)	Kyushu Univ.	STUDENT	6-10-1 Hakozaki Higashi-ku Fukuoka 812-8581 JAPAN
20	Daisuke Matsueda (Leg. 3 – 4)	Kyushu Univ.	STUDENT	6-10-1 Hakozaki Higashi-ku Fukuoka 812-8581 JAPAN
21	Tatsuya Shinmura (Leg. 3 – 4)	Hokkaido Univ.	GRADUATE STUDENT	Kita10 Nishi8 Sapporo Hokkaido 060-0810 JAPAN Phone +81-11-716-2111, Fax +81-746-0394
22	Yuji Fujitani (Leg. 3 – 4)	Hokkaido Univ.	GRADUATE STUDENT	Kita13 Nishi8 Kita Sapporo Hokkaido 060-8628 JAPAN Phone +81-11-716-2111, Fax +81-706-6832
23	Miyuki Ota (Leg. 3 – 4)	Tsukuba Univ.	GRADUATE STUDENT	1-1-1 Tennoudai Tsukuba Ibaraki 305-8571 JAPAN
24	Atsuhiko Tsuchiya (Leg. 3 – 4)	Univ. of Shizuoka	GRADUATE STUDENT	52-1 Yada Shizuoka Shizuoka 422-8526 JAPAN
25	Michiko Kinoshita (Leg. 3 – 4)	Univ. of Shizuoka	GRADUATE STUDENT	52-1 Yada Shizuoka Shizuoka 422-8526 JAPAN
26	Hiroaki Yamagishi (Leg. 3 – 4)	Tokyo Institute of Technology	GRADUATE STUDENT	4256 Nagatsuta Midori-ku Yokohama 226-8502 JAPAN
27	Ai Yasuda (Leg. 3 – 4)	MWJ	TECHNICIAN	2-15 Natsushima-cho Yokosuka Kanagawa 237-0061 JAPAN
28	Fujio Kobayashi (Leg. 3 – 4)	MWJ	TECHNICIAN	2-15 Natsushima-cho Yokosuka Kanagawa 237-0061 JAPAN
29	Keisuke Wataki (Leg. 3 – 4)	MWJ	TECHNICIAN	2-15 Natsushima-cho Yokosuka Kanagawa 237-0061 JAPAN
30	Yuichi Sonoyama (Leg. 3 – 4)	MWJ	TECHNICIAN	2-15 Natsushima-cho Yokosuka Kanagawa 237-0061 JAPAN
31	Asako Kubo (Leg. 3 – 4)	MWJ	TECHNICIAN	2-15 Natsushima-cho Yokosuka Kanagawa 237-0061 JAPAN
32	Tomoko Miyashita (Leg. 3 – 4)	MWJ	TECHNICIAN	2-15 Natsushima-cho Yokosuka Kanagawa 237-0061 JAPAN
33	Taeko Ohama (Leg. 3)	MWJ	TECHNICIAN	2-15 Natsushima-cho Yokosuka Kanagawa 237-0061 JAPAN
34	Kentaro Shiraishi (Leg. 3)	MWJ	TECHNICIAN	2-15 Natsushima-cho Yokosuka Kanagawa 237-0061 JAPAN
35	Naoko Takahashi (Leg. 3)	MWJ	TECHNICIAN	2-15 Natsushima-cho Yokosuka Kanagawa 237-0061 JAPAN
36	Masahiko Nishino (Leg. 3 – 4)	MWJ	TECHNICIAN	2-15 Natsushima-cho Yokosuka Kanagawa 237-0061 JAPAN

37	Osamu Kawai (Leg. 3 – 4)	MWJ	TECHNICIAN	2-15 Natsushima-cho Yokosuka Kanagawa 237-0061 JAPAN
38	Toshiko Nakashima (Leg. 3 – 4)	MWJ	TECHNICIAN	2-15 Natsushima-cho Yokosuka Kanagawa 237-0061 JAPAN
39	Noriaki Teramae (Leg. 3 – 4)	MWJ	TECHNICIAN	2-15 Natsushima-cho Yokosuka Kanagawa 237-0061 JAPAN
40	Masato Sugiyama (Leg. 3 – 4)	MWJ	TECHNICIAN	2-15 Natsushima-cho Yokosuka Kanagawa 237-0061 JAPAN
41	Yasutaka Imai (Leg. 3 – 4)	GODI	TECHNICIAN	1-13-8 Kamiookanishi Kohnan-ku Yokohama 233-0002 JAPAN
42	Norio Nagahama (Leg. 3 – 4)	GODI	TECHNICIAN	1-13-8 Kamiookanishi Kohnan-ku Yokohama 233-0002 JAPAN
43	Takeshi Kawano (not on board)	JAMSTEC	SCIENTIST	2-15 Natsushima-cho Yokosuka Kanagawa 237-0061 JAPAN
44	Kunio Yoneyama (not on board)	JAMSTEC	SCIENTIST	2-15 Natsushima-cho Yokosuka Kanagawa 237-0061 JAPAN
45	Toshiya Fujiwara (not on board)	JAMSTEC	SCIENTIST	2-15 Natsushima-cho Yokosuka Kanagawa 237-0061 JAPAN
46	Ichio Asanuma (not on board)	NASDA	SCIENTIST	Harumi Island Triton Square Office Tower X23F 1/8-10 Harumi Chuo-ku Tokyo 104-6023 JAPAN
47	Masayuki Sasaki (not on board)	NASDA	SCIENTIST	Harumi Island Triton Square Office Tower X23F 1/8-10 Harumi Chuo-ku Tokyo 104-6023 JAPAN
48	Tatsuo Endo (not on board)	Hokkaido Univ.	ASSISTANT PROFESSOR	Kita 19 Nishi 8 Sapporo Hokkaido 060-0819 JAPAN
49	Ichiro Matsui (not on board)	NIES	SCIENTIST	16-2 Onogawa Tsukuba Ibaraki 305-8506 JAPAN

JAMSTEC: Japan Marine Science and Technology Center

FORSGC: Frontier Observational Research System for Global Change

NIRS: National Institute of Radiological Sciences

MRI: Meteorological Research Institute

SNFRI: Seikai National Fisheries Research Institute

KANSO: Kansai Environmental Engineering Center CO., LTD

NHE: Nippon Hakuyo Electronics, LTD.

Fisheries Division: Ministry of Natural Resources Development Fisheries Division, Government of Kiribati

MWJ: Marine Works Japan

GODI: Global Ocean Development. Inc

NASDA: National Space Development Agency of Japan

NIES: National Institute for Environmental Studies

3.2. R/V MIRAI crew member

Takaaki Hashimoto	Master
Hiroki Maruyama	Chief Officer
Takeshi Isohi	1st Officer
Keitaro Inoue	2nd Officer
Nobuo Fukaura	3rd Officer
Akiteru Ono	Chief Engineer
Nobuya Araki	1st Engineer
Koji Masuno	2nd Engineer
Takahiro Machino	3rd Engineer
Keiichirou Shishido	C.R.Officer
Naoto Morioka	2nd.R.Officer
Kenetsu Ishikawa	Boatswain
Hisashi Naruo	Able Seaman
Kunihiko Omote	Able Seaman
Hisao Oguni	Able Seaman
Masaru Suzuki	Able Seaman
Yosuke Kuwahara	Able Seaman
Kazuyoshi Kudo	Able Seaman
Tsuyoshi Sato	Able Seaman
Tsuyoshi Monzawa	Able Seaman
Masashige Okada	Able Seaman
Shuji Komata	Able Seaman
Sadanori Honda	No.1 Oiler
Kiyoharu Emoto	Oiler
Yoshihiro Sugimoto	Oiler
Takashi Miyazaki	Oiler
Toshio Matsuo	Oiler
Daisuke Taniguchi	Oiler
Yasuaki Koga	Chief Steward
Yasutaka Kurita	Cook
Takayuki Akita	Cook
Hitoshi Ota	Cook
Tatsuya Hamabe	Cook
Wataru Sasaki	Cook

4. General observation

4.1. Meteorological measurement

4.1.1. Surface Meteorological observation

(1) Personnel

Yasutaka Imai (GODI): Operation Leader
Norio Nagahama (GODI)

(2) Objective

The surface meteorological parameters are observed as a basic dataset of the meteorology. These parameters bring us the information about temporal variation of the meteorological condition surrounding the ship.

(3) Methods

The surface meteorological parameters were observed throughout MR02-K06 cruise from the departure of Chuuk on 13 January 2003 to the arrival of Sekinehama on 14 February 2003, excluding territorial waters of the Federation States of Micronesia and the United States of America.

This cruise, we used 2 systems for the surface meteorological observation.

1. Mirai meteorological observation system
2. Shipboard Oceanographic and Atmospheric Radiation (SOAR) system

(3-1) Mirai meteorological observation system

Instruments of Mirai meteorological system are listed in Table 4.1-1 and measured parameters are listed in Table 4.1-2. Data was collected and processed by KOAC-7800 weather data processor made by Koshin Denki, Japan. The data set has 6-second averaged every 6-second record and 10-minute averaged every 10-minute record.

Table 4.1-1: Instruments and their installation locations of Mirai met system

Sensors	type	manufacturer	location (altitude from surface)
anemometer	KE-500	Koshin Denki, Japan	foremast (24m)
thermometer	FT	Koshin Denki, Japan	compass deck (21m)
	RFN1-0	Koshin Denki, Japan	4th deck (-1m, inlet -5m) SST
dewpoint meter	DW-1	Koshin Denki, Japan	compass deck (21m)
barometer	F-451	Yokogawa, Japan	weather observation room captain deck (13m)
rain gauge	50202	R. M. Young, USA	compass deck (19m)
optical rain gauge	ORG-115DR	Osi, USA	compass deck (19m)
radiometer (short wave)	MS-801	Eiko Seiki, Japan	radar mast (28m)
radiometer (long wave)	MS-202	Eiko Seiki, Japan	radar mast (28m)
wave height meter	MW-2	Tsurumi-seiki, Japan	bow (10m)

Table 4.1-2: Parameters of Mirai meteorological observation system

Parameters	Units	Remarks
1 latitude	degree	
2 longitude	degree	
3 ship's speed	knot	Mirai log, DS-30 Furuno
4 ship's heading	degree	Mirai gyro, TG-6000, Tokimec
5 relative wind speed	m/s	6 sec./10 min. averaged
6 relative wind direction	degree	6 sec./10 min. averaged
7 true wind speed	m/s	conducted by 3/4/5/6 6 sec./10 min. averaged
8 true wind direction	degree	conducted by 3/4/5/6 6 sec./10 min. averaged
9 barometric pressure	hPa	adjusted to the sea surface level 6 sec./10 min. averaged
10 air temperature (starboard side)	degC	6 sec./10 min. averaged
11 air temperature (port side)	degC	6 sec./10 min. averaged
12 dewpoint temperature (starboard side)	degC	6 sec./10 min. averaged
13 dewpoint temperature (port side)	degC	6 sec./10 min. averaged
14 relative humidity (starboard side)	%	6 sec./10 min. averaged conducted by 9/10/12
15 relative humidity (port side)	%	6 sec./10 min. averaged conducted by 9/11/13
16 sea surface temperature	degC	6 sec./10 min. averaged
17 rain rate (optical rain gauge)	mm/hr	hourly accumulation
18 rain rate (capacitive rain gauge)	mm/hr	hourly accumulation
19 down welling shortwave radiometer	W/m ²	6 sec./10 min. averaged
20 down welling infra-red radiometer	W/m ²	6 sec./10 min. averaged
21 significant wave height (fore)	m	hourly
22 significant wave period (fore)	second	hourly

(3-2) Shipboard Oceanographic and Atmospheric Radiation (SOAR) system

SOAR system, designed by BNL (Brookhaven National Laboratory, USA), is consisted of 3 parts.

1. Portable Radiation Package (PRP) designed by BNL – short and long wave down welling radiation
2. Zeno meteorological system designed by BNL – wind, Tair/RH, pressure and rainfall measurement
3. Scientific Computer System (SCS) designed by NOAA (National Oceanographic and Atmospheric Administration, USA) – centralized data acquisition and logging of all data sets

SCS recorded PRP data every 6.5 seconds, Zeno/met data every 10 seconds.

Instruments and their locations are listed in Table 4.1-3 and measured parameters are listed in Table 4.1-4.

Table 4.1-3: Instrument installation locations of SOAR system

sensors	type	manufacturer	location (altitude from the baseline)
Zeno/Met			
anemometer	05106	R. M. Young, USA	foremast (25m)
T/RH	HMP45A	Vaisala, USA	foremast (24m)
	with 43408 Gill aspirated radiation shield (R. M. Young)		
barometer	61201	R. M. Young, USA	foremast (24m)
	with 61002 Gill pressure port (R. M. Young)		
rain gauge	50202	R. M. Young, USA	foremast (24m)
optical rain gauge	ORG-815DA	Osi, USA	foremast (24m)
PRP			
radiometer (short wave)	PSP	Eppley labs, USA	foremast (25m)
radiometer (long wave)	PIR	Eppley labs, USA	foremast (25m)
fast rotating shadowband radiometer		Yankee, USA	foremast (25m)

Table 4.1-4: Parameters of SOAR system

Parameters	Units	Remarks
1 Latitude	degree	
2 Longitude	degree	
3 Sog	knot	
4 Cog	degree	
5 Relative wind speed	m/s	
6 Relative wind direction	degree	
7 Barometric pressure	hPa	
8 Air temperature	degC	
9 Relative humidity	%	
10 Rain rate (optical rain gauge)	mm/hr	
11 Precipitation (capacitive rain gauge)	mm	reset at 50mm
12 Down welling shortwave radiation	W/m2	
13 Down welling infra-red radiation	W/m2	
14 Defuse irradiation	W/m2	

(4) Preliminary results

Tair (SOAR), SST (from EPCS), RH, rainfall intensity, pressure, solar radiation (from SOAR) and Wind (converted to U, V component, from SOAR), observed during this cruise are shown in Figure 4.1-1. In the figures, 30 minutes accumulated precipitation data from SOAR capacitive rain gauge was converted to the rainfall intensity and obvious noises were eliminated but not calibrated. Other figures show the uncorrected data at every 5 minutes.

(5) Data archives

These raw data will be submitted to the Data Management Office (DMO) in JAMSTEC just after the cruise.

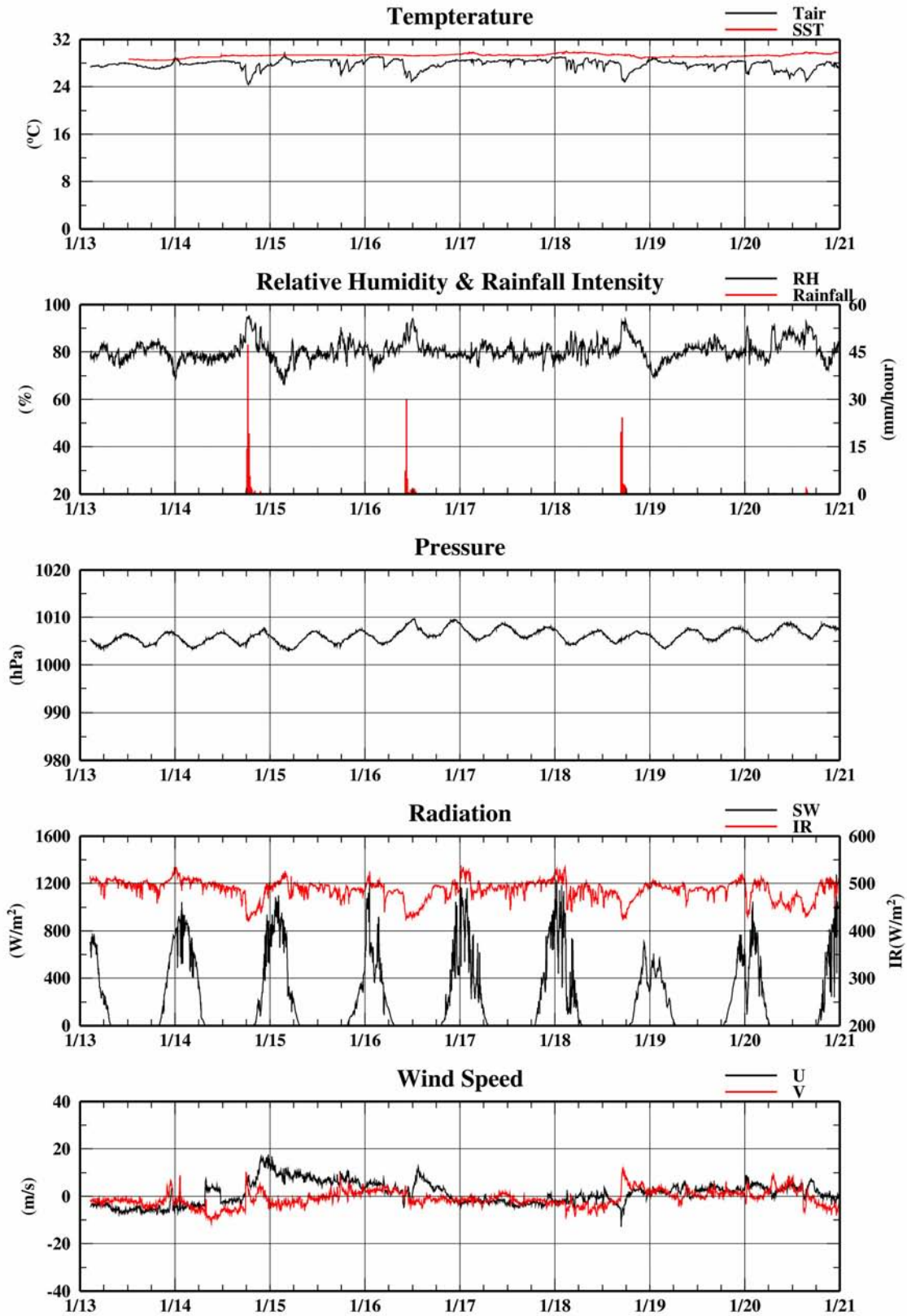


Figure 4.1-1: Time series of surface meteorological parameters during MR02K06 cruise.

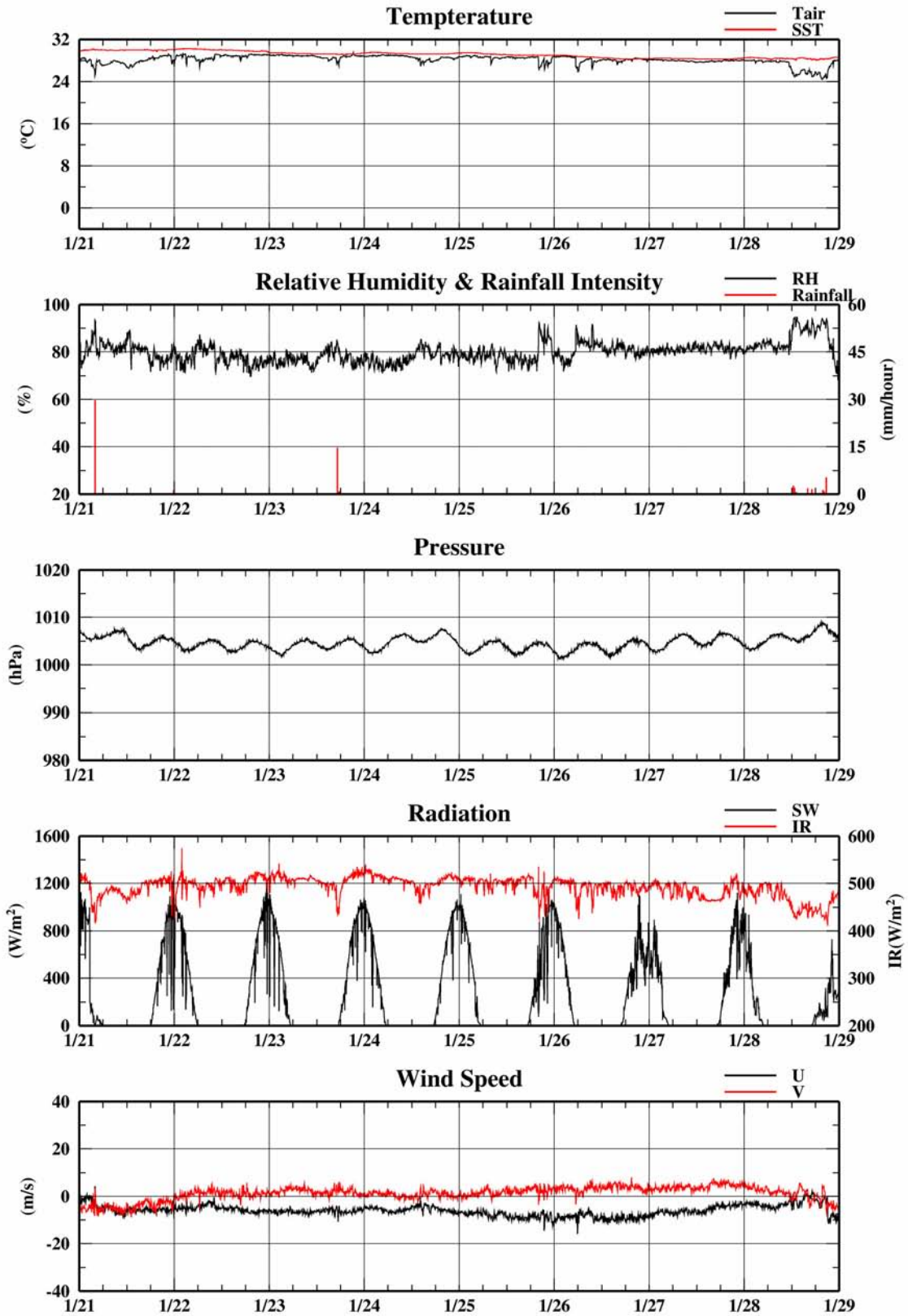


Figure 4.1-1: (continued)

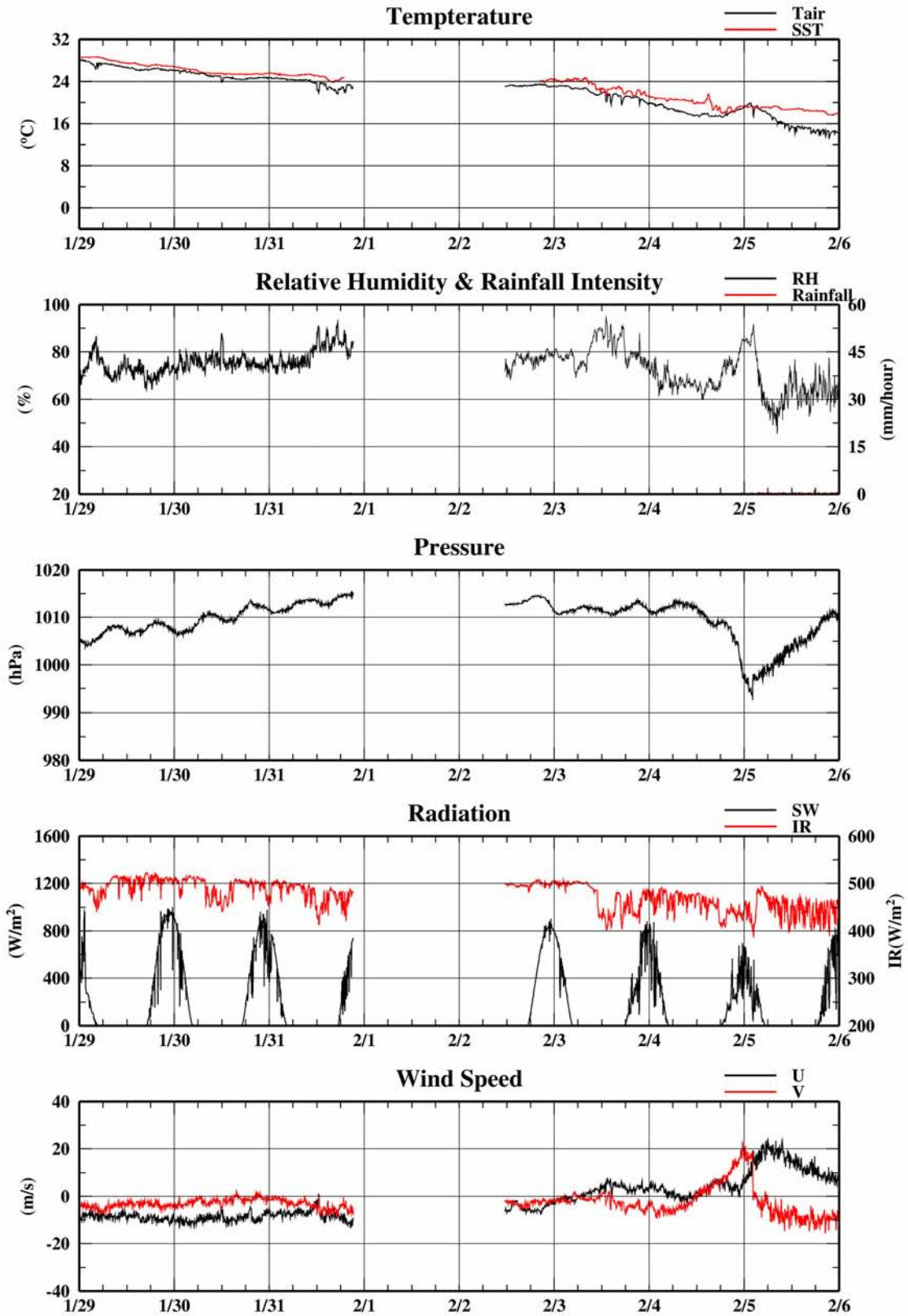


Figure 4.1-1: (continued)

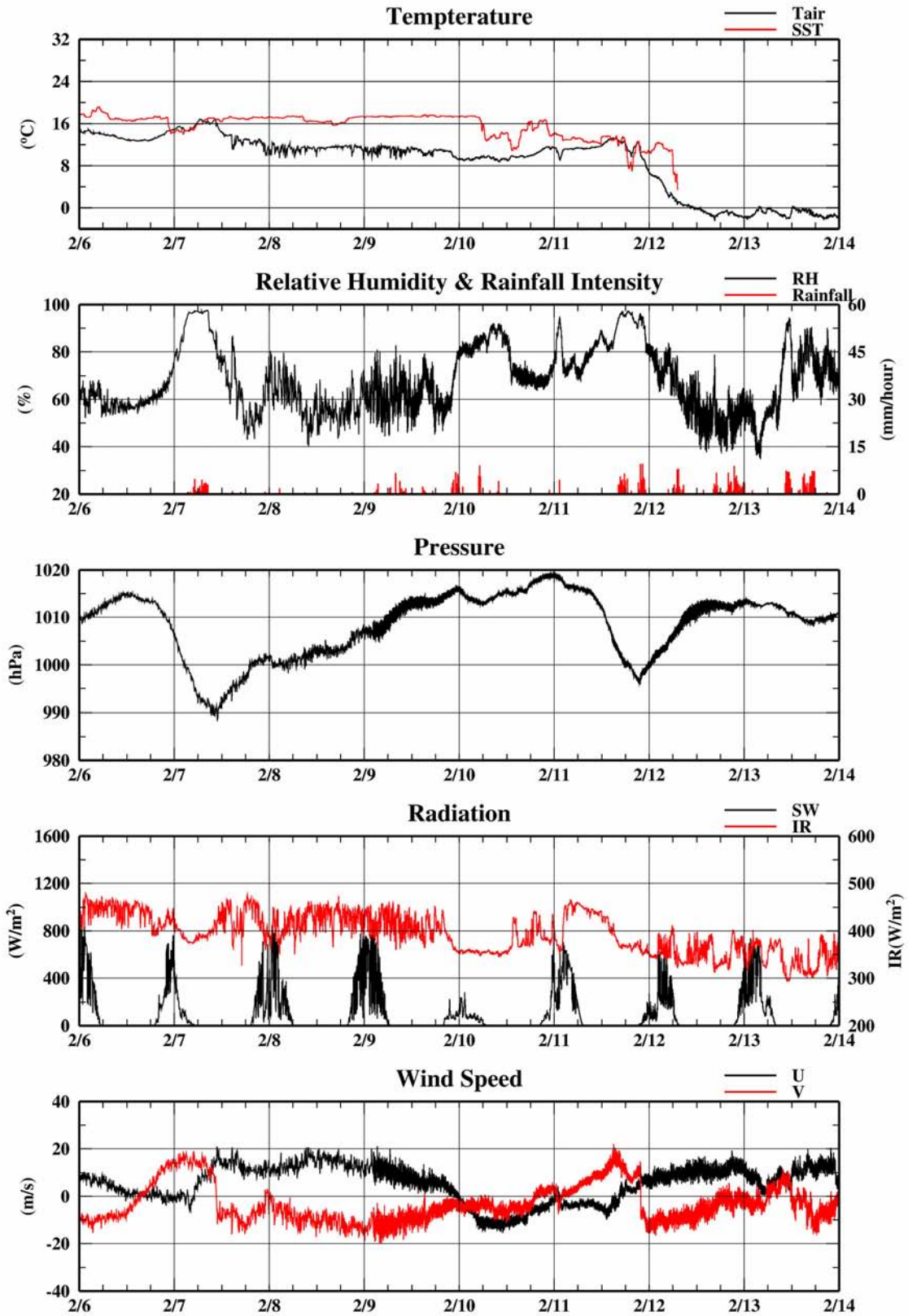


Figure 4.1-1: (continued)

4.1.2. Ceilometer

(1) Personnel

Yasutaka Imai (GODI): Operation Leader
Norio Nagahama (GODI)

(2) Objective

The information of the cloud base height and the liquid water amount around cloud base is important to understand the processes on the formation of the cloud. As one of the methods to measure them, the ceilometer observation was carried out.

(3) Methods

We measured cloud base height and backscatter profile using CT-25K (VAISALA, Finland) ceilometer throughout MR02-K06 cruise from the departure of Chuuk on 13 January 2003 to the arrival of Sekinehama on 14 February 2003, excluding territorial waters of the Federation States of Micronesia and the United States of America.

Major parameters for the measurement configuration are as follows;

Laser source:	Indium Gallium Arsenide (InGaAs) Diode
Transmitting wave length:	905 ± 5 nm at 25 deg-C
Transmitting average power:	8.9 mW
Repetition rate:	5.57kHz
Detector:	Silicon avalanche photodiode (APD)
Responsibility at 905 nm:	65 A/W
Measurement range:	0~7.5 km
Resolution:	50 ft in full range
Sampling rate:	60 sec

On the archived dataset, cloud base height and backscatter profile are recorded with the resolution of 30 m (100 ft.).

(4) Preliminary results

The first, second and third lowest cloud base height which the ceilometer detected during the stationary observation are plotted in Fig. 4.2-1. Sometimes the ceilometer records calculated vertical visibility and the height of detected highest signal instead of the cloud base heights. But they are not plotted in the figure.

(5) Data archives

Ceilometer data obtained during this cruise will be submitted to and archived by the DMO (Data Management Office) of JAMSTEC.

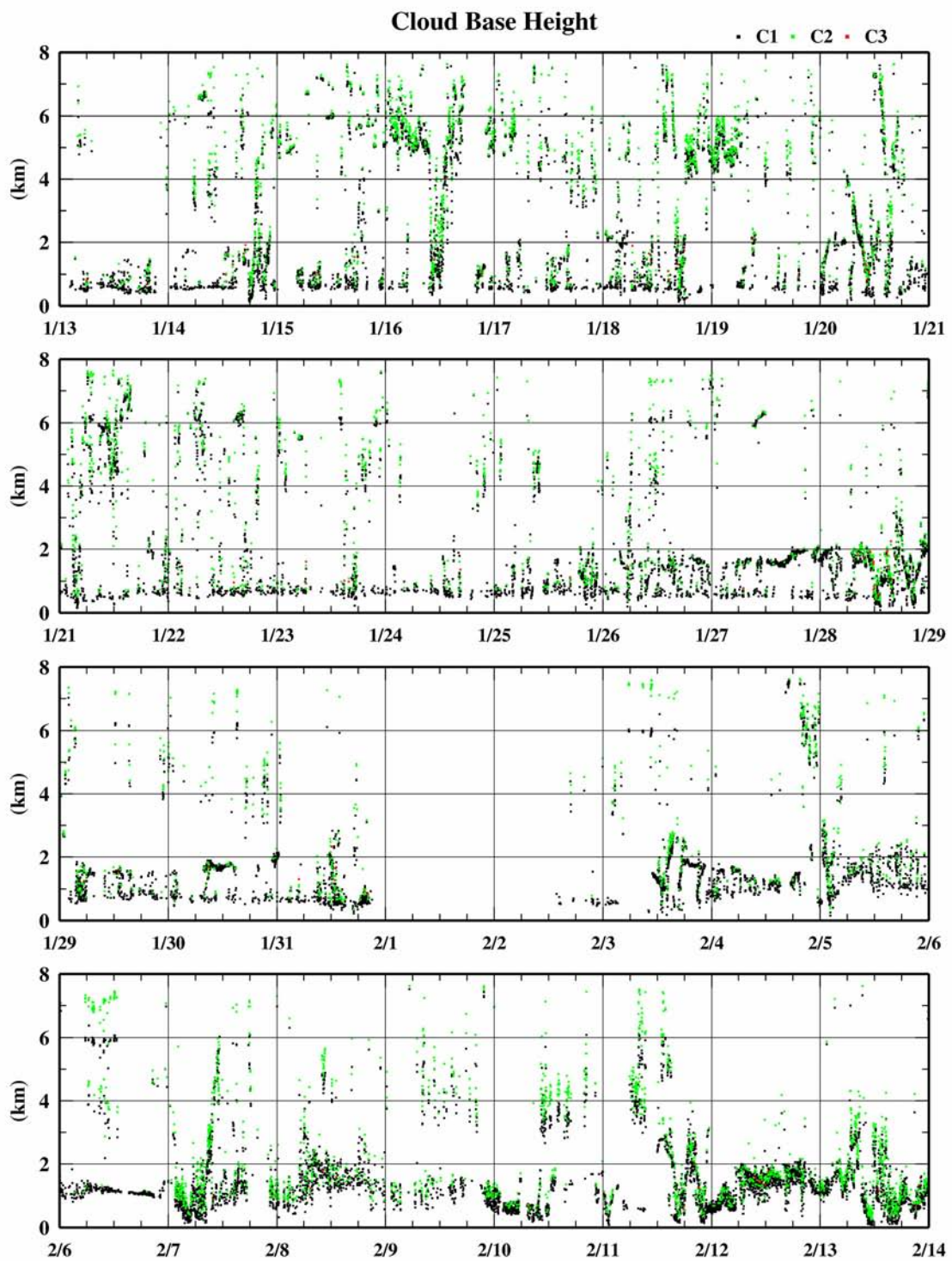


Figure 4.2-1 1st, 2nd and 3rd lowest cloud base height during MR02K06 cruise.

4.2. CTD/XCTD

4.2.1. CTD

(1) Personnel

Fujio KOBAYASHI (MWJ): Operation Leader
Naoko TAKAHASHI (MWJ)
Kentaro SHIRAISHI (MWJ)

(2) Introduction

Temperature and salinity were measured with CTD (SBE 911plus; Sea-Bird Electronics, Inc.) and the seawater samplings for chemical analysis were conducted with Carousel Water Sampler (CWS: SBE 32; Sea-Bird Electronics, Inc.). In addition, the dissolved oxygen sensor (D.O. sensor: SBE 43; Sea-Bird Electronics, Inc.), the fluorometer (Seapoint Chlorophyll Fluorometer: Seapoint Sensors, Inc.), the transmissometer (C-Star: WET Labs, Inc.), and the altimeter (PSA-900D; Datasonics, Inc.) were attached with CTD system to measure dissolved oxygen concentration, Chl-a concentration, light transmission, and altitude from sea floor.

In this Leg3, pH sensors and a nitrate sensor were attached with CTD system particularly. But we don't describe these sensors in detail, because pH sensors were logging to inside memory and a nitrate sensor was a prototype.

(3) Methods

(a) CTD/CWS systems

We used the CTD/CWS systems which has the 12 liters 36 positions CWS. The system configuration is listed in Table 1.

Conductivity, temperature, depth, dissolved oxygen concentration, Chl-a concentration, light transmission, and altitude from sea floor were measured from sea surface to 5,479db in maximum. Seawater was sampled with CTD/CWS systems at 9 stations. The 26 water-sampling casts in total were for the chemical analysis of nutrients, dissolved gas, pH, pigment, and so on.

(b) Operation

The CTD/CWS systems were operated with the crane (Dynacon, Inc.) on the starboard side. The CTD raw data were acquired on real time by using the SEASAVE-Win32 ver.5.27b provided by Sea-Bird Electronics, Inc. and stored on the hard disk of the personal computer set in the After Wheel-house. Water sampling was made during up cast by sending a fire command from the computer. The detail information such as station name, file name, date, time, location at the start/bottom/end of observation, water sampling layers, and events were recorded in CTD cast log sheets.

(c) CTD data processing

The CTD raw data were processed by the SBE DataProcessing-Win32 ver.5.27b (Sea-Bird Electronics, Inc.) on another computer. The procedure of the data processing and used utilities in the SEASOFT and the SBE DataProcessing-Win32 were as following:

DATCNV: Convert raw data (binary format) to engineering units (ASCII format). Output items are scan number, pressure, depth, temperature, conductivity, descent rate, Oxygen concentration, altitude from sea floor, Chl-a concentration, and light transmission. This utility makes a file which includes the data when the bottles were closed.

SECTION: Exclude the data in air. Write out selected rows of converted data to a new file.

ALIGNCTD: Align oxygen measurements in time relative to pressure. This ensures that calculation of dissolved oxygen concentration is made using measurements from the same parcel of water.

WILDEDIT: Mark wild points by setting their values to the bad value specified in the input file header.

CELLTM: Use a recursive filter to remove conductivity cell thermal mass effects from the measured conductivity.

FILTER: Low pass filter pressure with a time constant to increase pressure resolution for LOOPEDIT.

LOOPEDIT: Mark scans "bad" by setting the flag value associated with the scan to bad flag in input files that have pressure reversals.

BINAVG: Average data into depth bins.

DERIVE: Compute salinity, density, and potential temperature.

SPLIT: Split the data into up cast and down cast files. The filename of down cast is d*.CNV and that of up cast is u*.CNV.

ROSSUM: Write out a summary of the bottle data to a file with a .BTL extension.

(4) Preliminary results

The information for each CTD cast was summarized in the CTD Cast Table in Table 2. The profiles are also shown in Fig. 1 to 13.

(5) Management of the CTD data

A file name of each cast consists of station name, CTD system type and cast number, e.g., C06m01. After SPLIT utility was used, up/down identification was added. As a result of data processing, 9 files were made every cast, such as .BL, .CON, .DAT, .HDR, .ROS, .BTL, d*.CNV, u*.CNV, and *.CNV files.

The Raw and the processed CTD data files were copied into CD-R disk. All data are under the control of Data Management Office in JAMSTEC (DMO).

Table 1. CTD System Configuration

CTD System	Sensor	Manufacturer	Model No.	Serial No.
12 liters 36 positions	Underwater Unit (Pressure)	Sea-Bird Electronics, Inc.	SBE <i>9plus</i>	09P27443-0677 (79511)
	Deck Unit	Sea-Bird Electronics, Inc.	SBE <i>11plus</i>	11P9833-0344
	Carousel Water Sampler	Sea-Bird Electronics, Inc.	SBE 32	3227443-0391
	Temperature	Sea-Bird Electronics, Inc.	SBE 3	031525
	Conductivity	Sea-Bird Electronics, Inc.	SBE 4C	042435
	Dissolved Oxygen Sensor	Sea-Bird Electronics, Inc.	SBE 43	430069
	Fluorometer	Seapoint Sensors, Inc.	Seapoint Chlorophyll Fluorometer	2148
	Transmissometer	WET Labs, Inc.	C-Star	CST-207RD
Altimeter	Datasonics, Inc.	PSA-900D	396	

Table 2. CTD Cast Table

Station	Cast Type	File Name	Date (UTC)	Start Time (UTC)	End Time (UTC)	Latitude	Longitude	Wire Out (m)	Depth (*MNB) (m)	Max. Pressure (db)	Remarks
06	Shallow3	C06m01	2003/1/15	4:12	4:43	00-00.08N	160-00.23E	205.9	2825	202.06	
	Shallow1	C06m02	2003/1/15	16:57	17:40	00-00.16S	159-59.82E	213.8	2825	199.12	
	Shallow2	C06m03	2003/1/15	23:52	0:33	00-00.12N	160-01.05E	310.3	2832	305.65	
	Deep	C06m04	2003/1/16	2:52	5:01	00-00.11N	160-01.11E	2817.1	2833	2817.49	
07	Shallow4-1	C07m01	2003/1/16	23:53	0:42	00-00.52N	164-31.34E	312.3	4414	306.47	
	Shallow4-2	C07m02	2003/1/17	1:57	2:32	00-00.65N	164-33.04E	203.4	4413	202.94	
08	Shallow4-1	C08m01	2003/1/17	23:54	0:36	00-00.08N	169-59.29E	322.3	4444	310.97	
	Shallow4-2	C08m02	2003/1/18	1:52	2:32	00-00.35S	169-59.36E	321.5	4443	318.01	
09	Shallow3	C09m01	2003/1/18	22:24	23:04	00-00.17S	174-59.63E	201.9	4828	202.22	
	Shallow1	C09m02	2003/1/19	15:51	16:32	00-00.31N	175-00.30E	217.2	4833	205.85	
	Shallow2	C09m03	2003/1/19	22:52	23:36	00-00.02S	174-59.77E	298.7	4829	298.53	
	Deep	C09m04	2003/1/20	1:44	5:00	00-00.15S	175-00.20E	4938.6	4831	4890.30	
10	Shallow4-1	C10m01	2003/1/20	22:53	23:41	00-00.24S	179-19.18E	319.9	5401	302.65	
	Shallow4-2	C10m02	2003/1/21	0:54	1:48	00-00.47S	179-18.36E	335.1	5387	321.70	
11	Shallow4-1	C11m01	2003/1/21	22:51	23:30	00-00.90N	175-38.02W	312.2	5451	307.11	
	Shallow4-2	C11m02	2003/1/22	0:51	1:29	00-00.54N	175-37.46W	316.2	5453	306.00	
12	Shallow3	C12m01	2003/1/23	3:29	4:07	00-00.01N	170-00.78W	206.5	5539	202.42	
	Shallow1	C12m02	2003/1/23	14:52	15:29	00-00.15S	169-59.50W	218.6	5438	213.07	
	Shallow2	C12m03	2003/1/23	21:52	22:33	00-00.25N	169-58.93W	319.0	5416	317.68	
	Deep	C12m04	2003/1/24	0:06	4:13	00-00.35N	169-59.28W	5470.9	5450	5479.14	
13	Shallow4-1	C13m01	2003/1/25	21:54	22:36	00-00.28S	164-47.73W	304.1	5632	304.65	
	Shallow4-2	C13m02	2003/1/25	23:51	0:32	00-00.00S	164-47.93W	309.2	5662	306.53	
14	Shallow3	C14m01	2003/1/26	22:08	22:39	00-00.05N	160-01.12W	214.4	5174	211.49	
	Deep	C14m02	2003/1/27	2:02	5:24	00-00.26S	159-59.82W	5204.1	5160	5195.28	
	Shallow1	C14m03	2003/1/27	14:53	15:27	00-00.01S	159-58.89W	211.3	5132	208.50	
	Shallow2	C14m04	2003/1/27	21:55	22:34	00-00.23N	159-56.40W	300.6	5131	303.36	

*MNB = Multi Narrow Beam

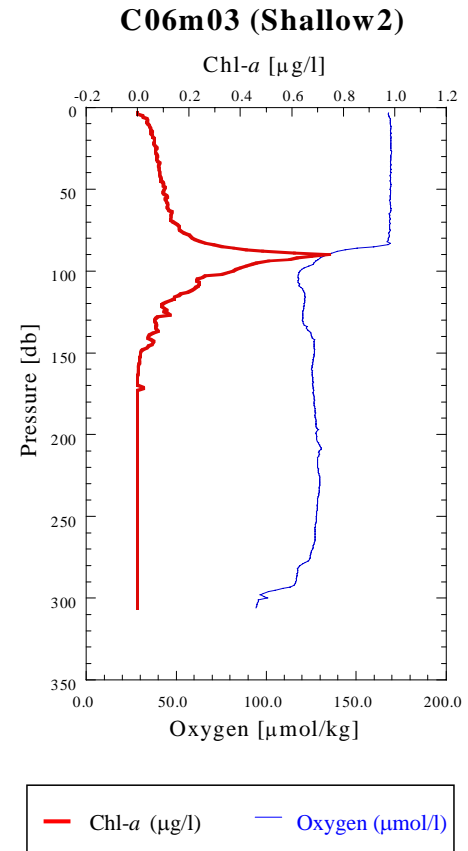
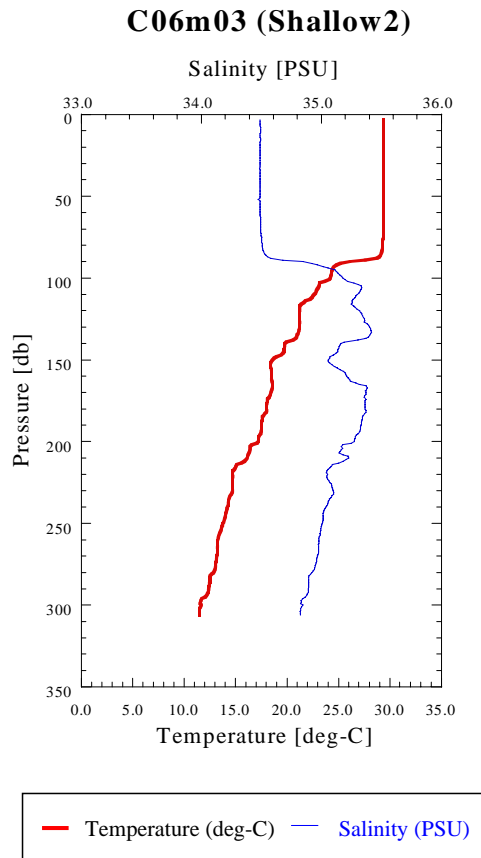


Fig. 1. CTD Profile (St.06 Shallow2)

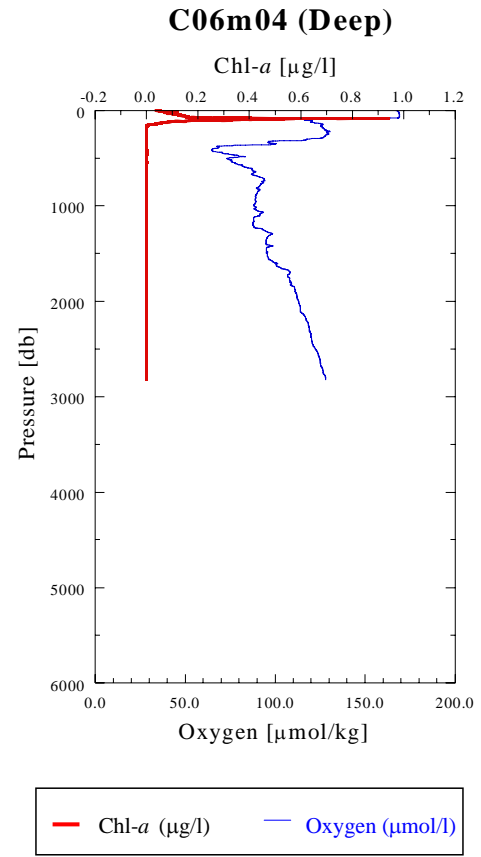
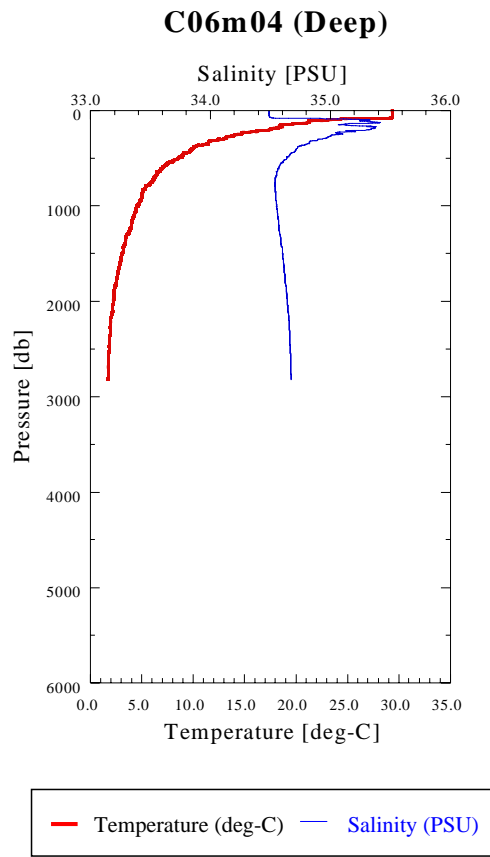


Fig. 2. CTD Profile (St.06 Deep)

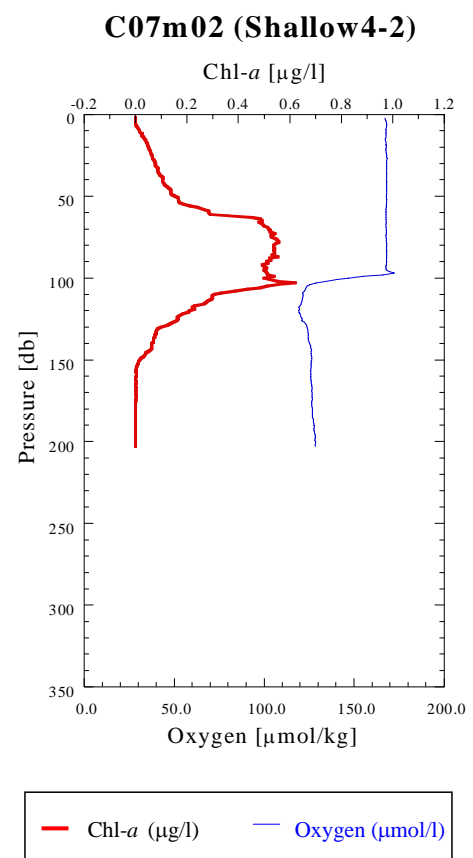
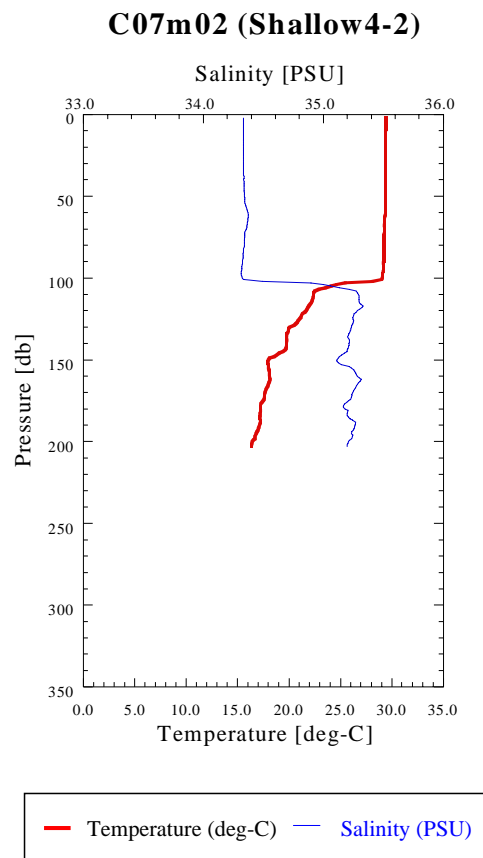


Fig. 3. CTD Profile (St.07 Shallow4-2)

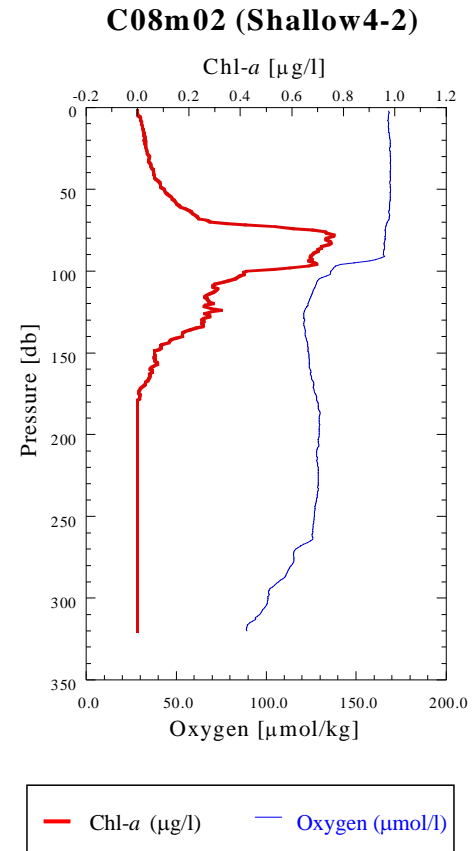
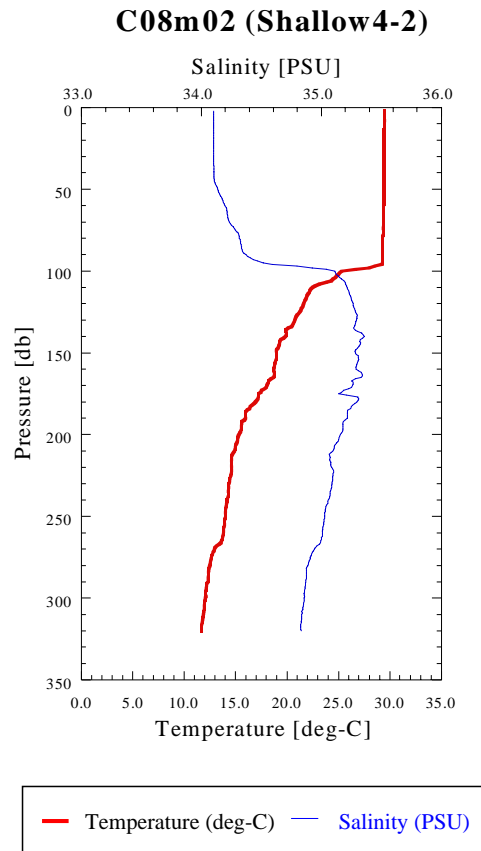


Fig. 4. CTD Profile (St.08 Shallow4-2)

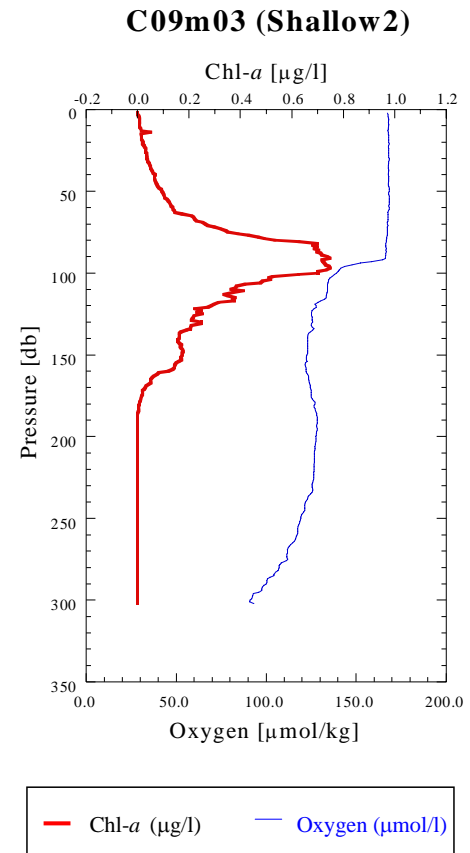
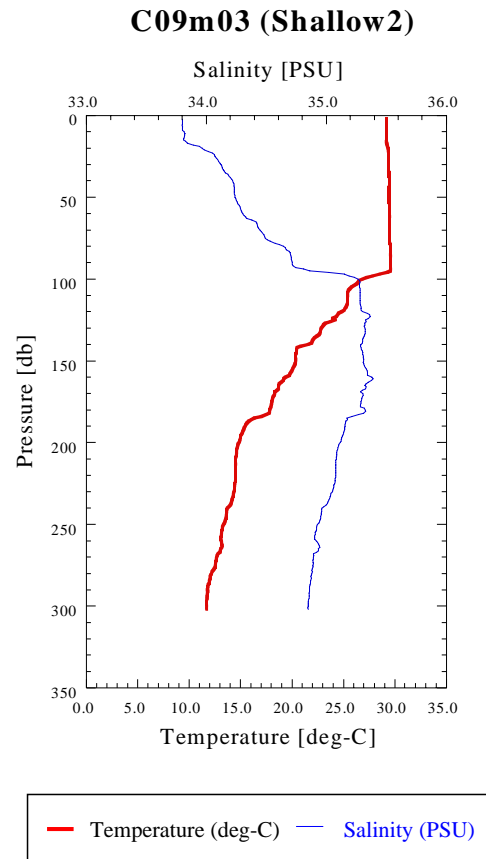


Fig. 5. CTD Profile (St.09 Shallow2)

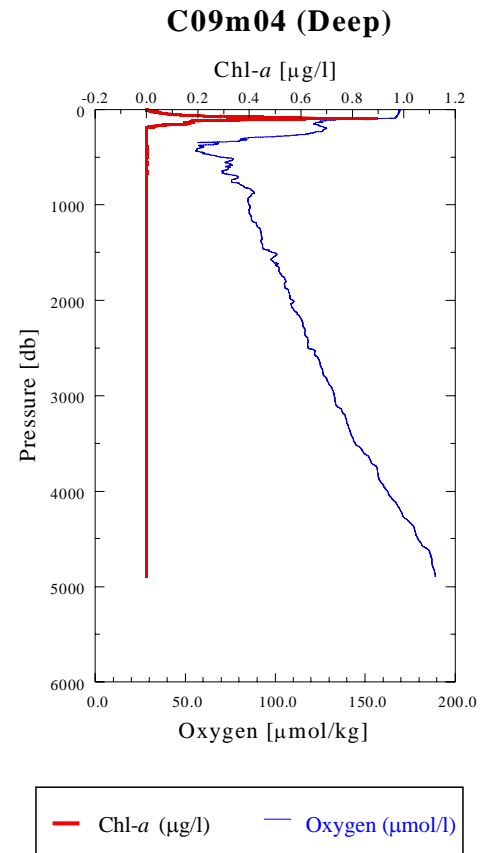
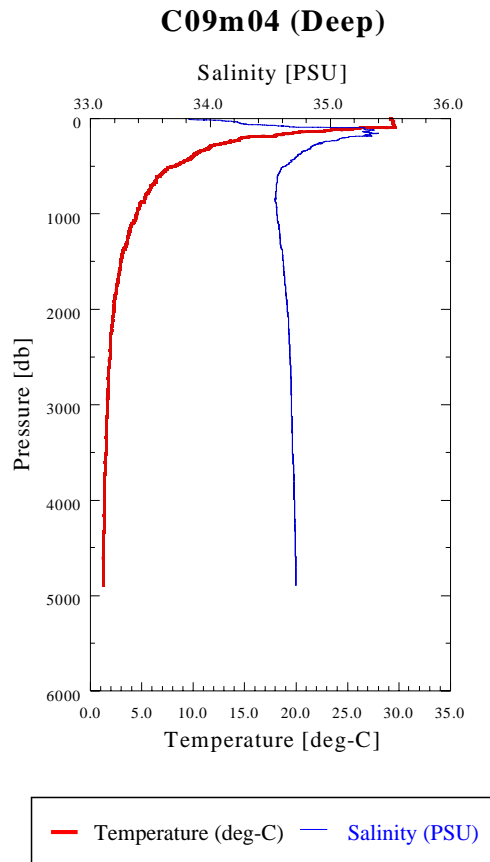


Fig. 6. CTD Profile (St.09 Deep)

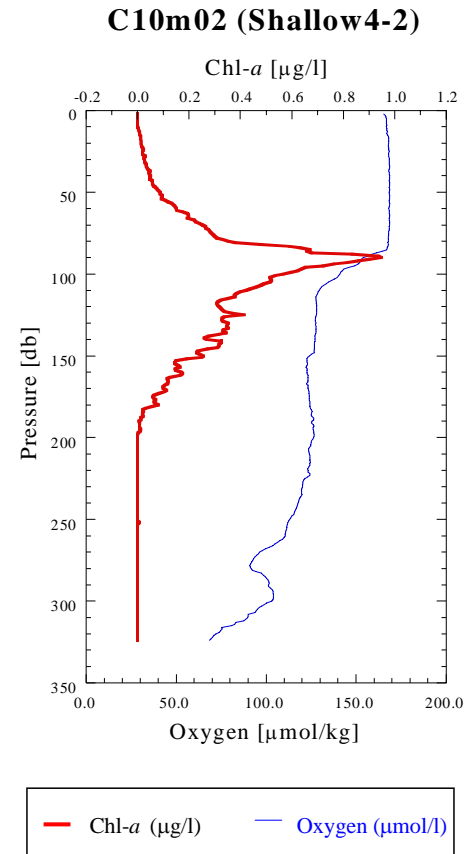
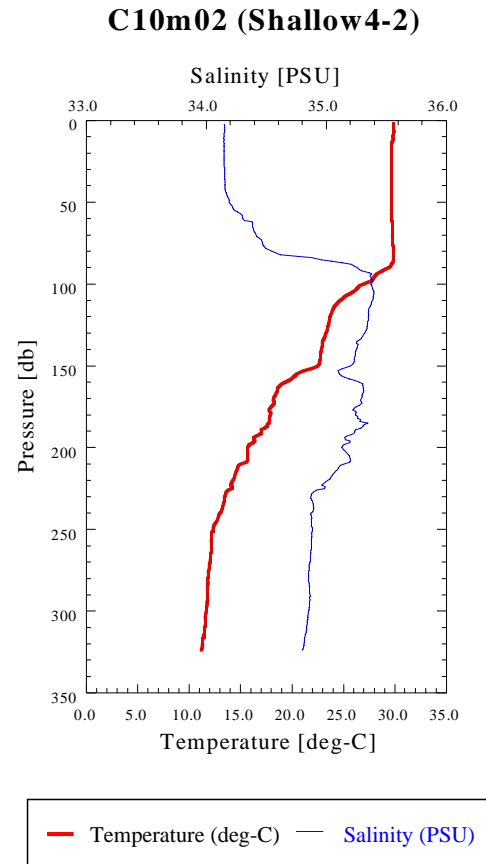


Fig. 7. CTD Profile (St.10 Shallow4-2)

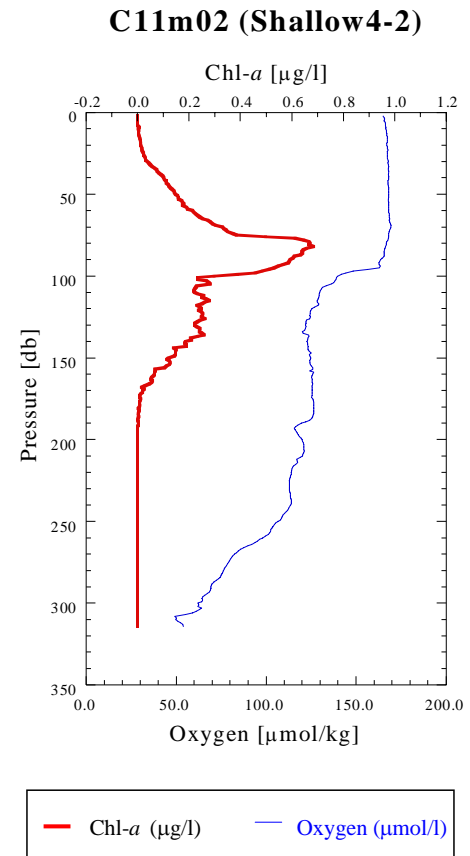
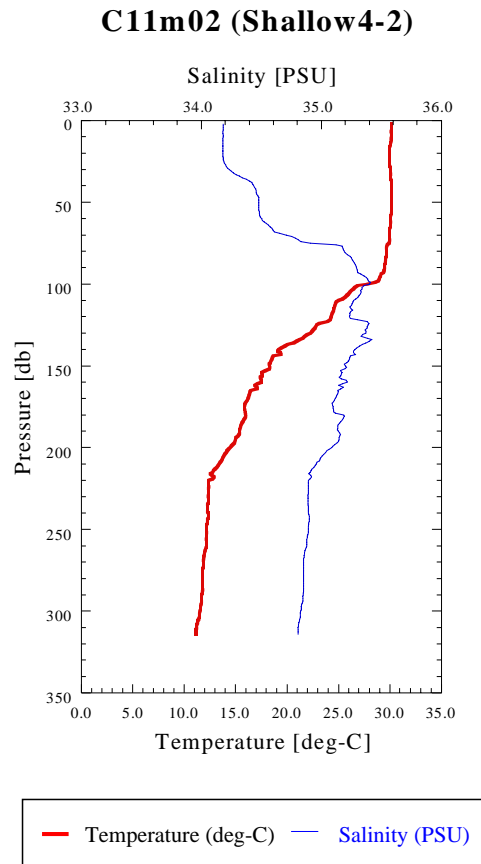


Fig. 8. CTD Profile (St.11 Shallow4-2)

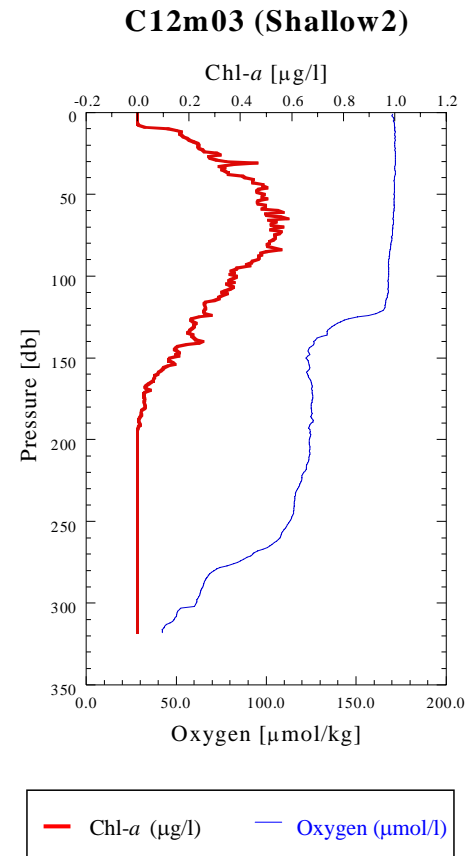
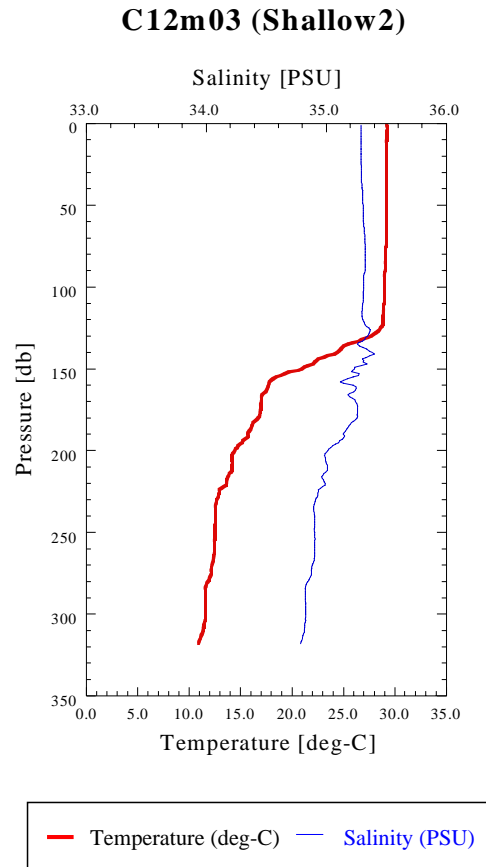


Fig. 9. CTD Profile (St.12 Shallow2)

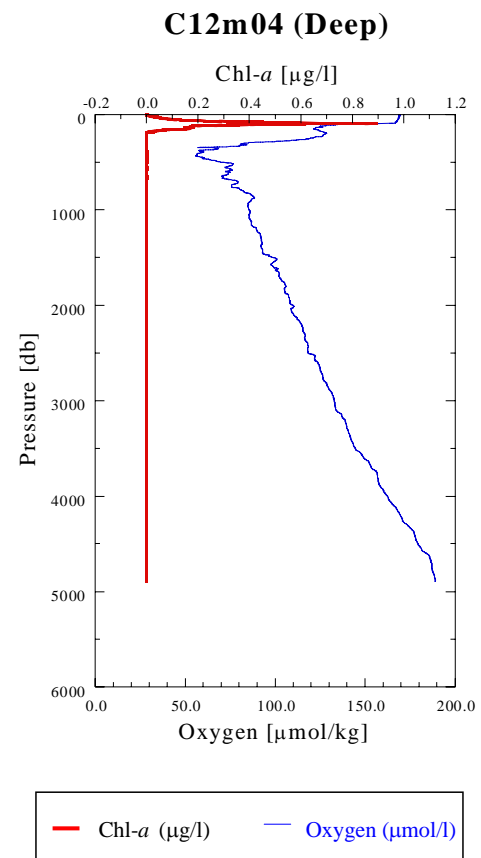
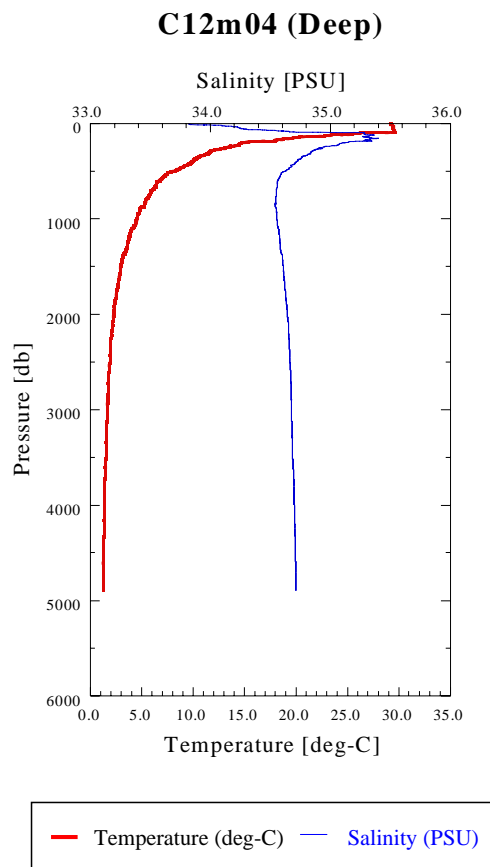
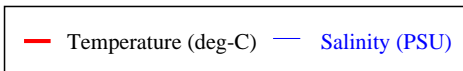
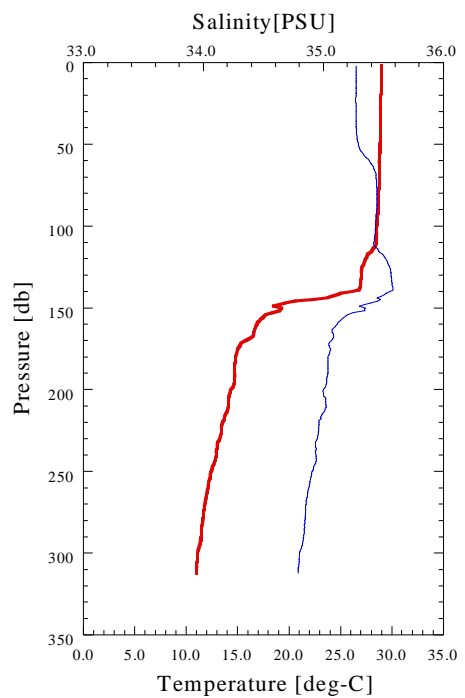


Fig. 10. CTD Profile (St.12 Deep)

C13m02 (Shallow4-2)



C13m02 (Shallow4-2)

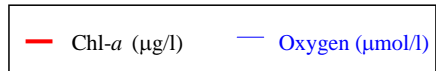
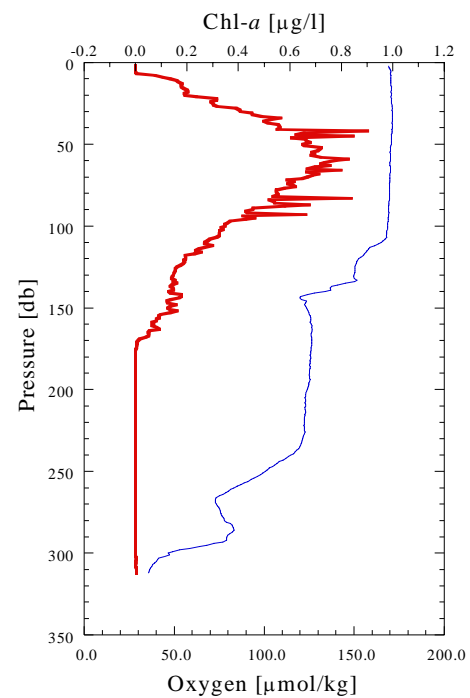


Fig. 11. CTD Profile (St.13 Shallow4-2)

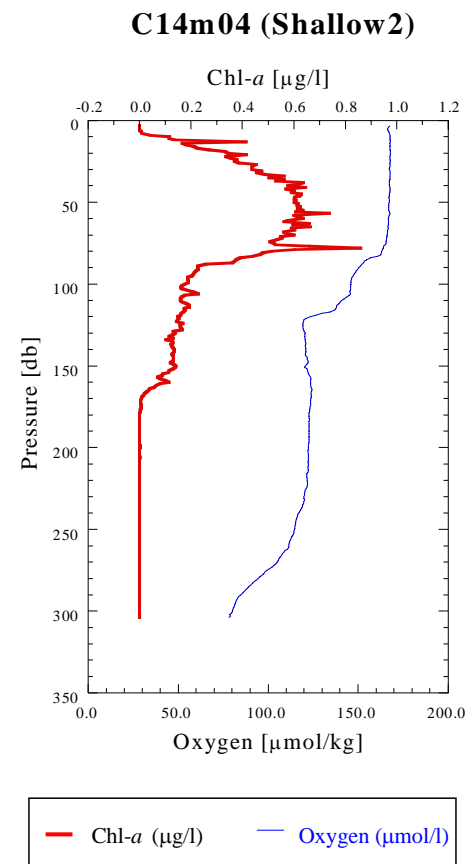
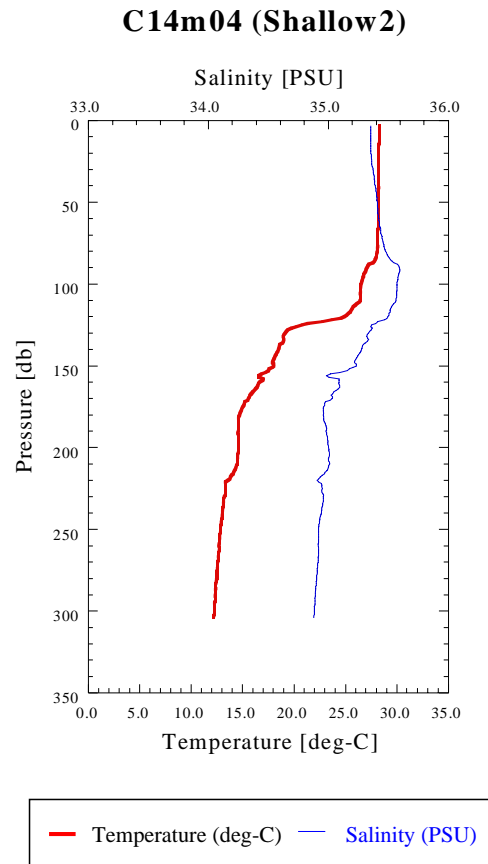


Fig. 12. CTD Profile (St.14 Shallow2)

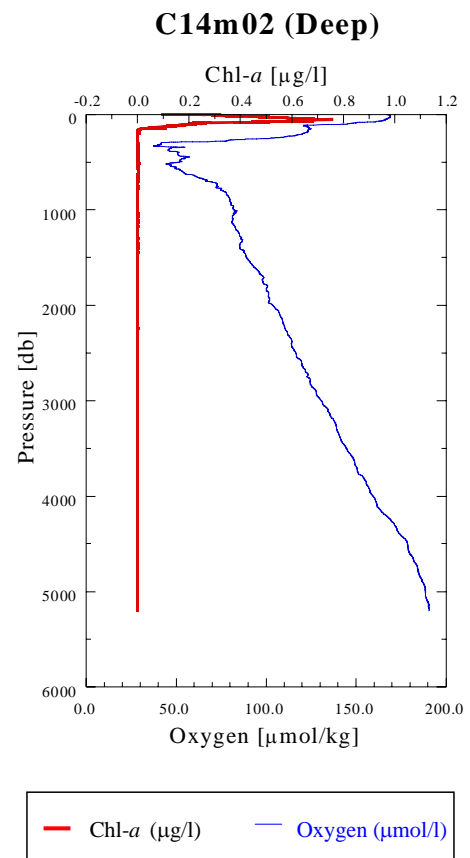
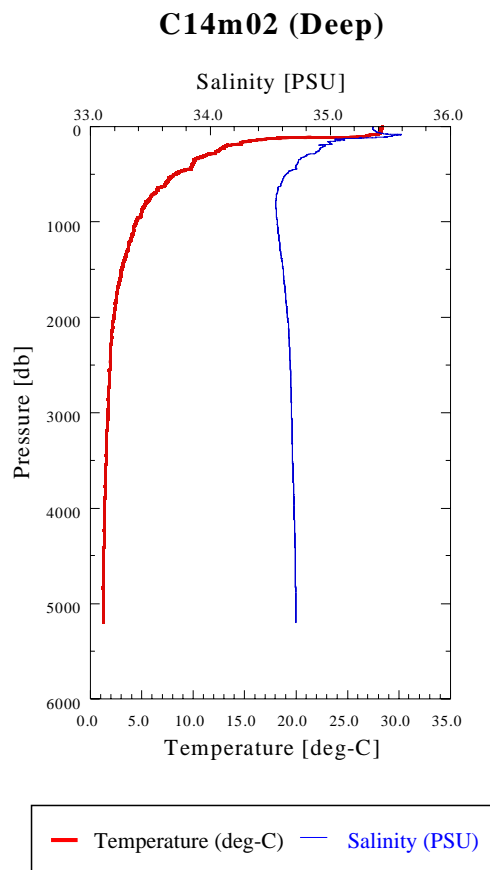


Fig. 13. CTD Profile (St.14 Deep)

4.2.2. XCTD

(1) Personnel

Kazuhiko Matsumoto (JAMSTEC) Principal investigator

Eitarou Oka (FORSGC)

Yasutaka Imai (GODI)

Norio Nagahama (GODI)

(2) Objectives

Investigation of oceanic structure.

(3) Parameters

According to manufacture's information, the range and accuracy of parameters measured by the XCTD are as follows;

Parameter	Range	Accuracy
Conductivity	0-60mS	+/-0.03mS/cm
Temperature	-2 – 35degC	+/-0.02degC
Depth	0 – 1000m	

(4) Method

We observed the vertical profiles of sea water temperature and salinity measured by the XCTD-1 manufactured by Tsurumi-Seiki Co. The signal was converted by MK-100, Tsurumi-Seiki C. and was recorded by WinXCTD software (Ver.1.06) made by Tsurumi-Seiki Co.. We dropped 94 probes (41 for Leg3 and 53 for Leg4) by using automatic launcher. Observation stations are presented in table 1.

(5) Preliminary results

Vertical profile of temperature and salinity is presented in Fig.4.2.2-1, Fig.4.2.2-2.

(6) Data archives

Magnetic force data obtained during this cruise will be submitted to the JAMSTEC DMO (Data Management Office), and archived.

Table 4.2.2-1 XCTD observations (MR02K06 Leg3)

Station	Date	Time	Lat.	Lon.	SST	SSS	MD	WD	Probe S/N
X01	2003/01/16	07:21	00-01.40N	160-10.73E	29.37	34.467	1035	2788	02090716
X02	2003/01/16	10:27	00-02.00N	161-00.16E	29.32	34.390	1034	3365	02090719
X03	2003/01/16	14:12	00-01.35N	162-00.03E	29.28	34.387	1033	4176	02090720
X04	2003/01/16	17:57	00-00.44N	163-00.01E	29.29	34.329	1035	4452	02090723
X05	2003/01/16	21:45	00-00.64N	164-00.00E	29.42	34.422	1034	4463	02090722
X06	2003/01/17	02:36	00-00.87N	164-33.81E	29.77	34.340	1034	4417	02100900
X07	2003/01/17	04:20	00-00.81N	165-00.00E	29.56	34.304	1035	4381	02100901
X08	2003/01/17	08:09	00-00.50N	165-59.74E	29.32	34.282	1035	4376	02100903
X09	2003/01/17	12:00	00-00.05N	167-00.03E	29.37	34.142	1034	4368	02100904
X10	2003/01/17	15:55	00-00.43N	168-00.00E	29.29	34.092	1035	4252	02100902
X11	2003/01/17	19:51	00-00.03S	169-00.03E	29.34	34.048	1035	4382	02100905
X12	2003/01/18	02:36	00-00.21S	169-59.35E	29.83	34.099	1035	4442	02100906
X13	2003/01/18	06:44	00-03.19S	171-00.01E	29.79	34.105	1035	4650	02100910
X14	2003/01/18	10:39	00-05.97S	172-00.06E	29.65	34.124	1033	4651	02100907
X15	2003/01/18	14:31	00-08.93S	173-00.01E	29.47	33.944	1034	4507	02100909
X16	2003/01/18	18:27	00-07.25S	174-00.02E	29.41	34.075	1035	4792	02100911
X17	2003/01/20	06:40	00-02.81N	175-06.34E	29.29	33.835	1035	4869	02090873
X18	2003/01/20	10:06	00-00.05S	176-00.02E	29.36	33.794	1034	5055	02100912
X19	2003/01/20	13:51	00-00.06N	177-00.02E	29.57	34.001	1034	5373	02090871
X20	2003/01/20	17:38	00-00.31S	178-00.00E	29.77	34.174	1033	5421	02090872
X21	2003/01/20	21:30	00-00.29S	179-00.02E	29.55	33.947	1033	5411	02090874
X22	2003/01/21	01:55	00-01.05S	179-18.06E	29.99	34.148	1035	5405	02090877
X23	2003/01/21	04:45	00-00.98S	179-59.99E	30.02	34.137	1033	5274	02090875
X24	2003/01/21	08:50	00-00.26S	179-00.02W	29.94	34.054	1034	5421	02090880
X25	2003/01/21	12:58	00-00.43N	178-00.01W	30.00	34.102	1034	4817	02100882
X26	2003/01/21	17:02	00-00.17N	177-00.00W	30.05	34.101	1036	5367	02090879
X27	2003/01/21	21:10	00-00.05N	176-00.01W	29.84	34.183	1035	5567	02100883
X28	2003/01/22	01:38	00-00.79N	175-37.69W	30.20	34.183	1035	5448	02090878
X29	2003/01/22	04:18	00-00.04S	175-00.01W	30.20	34.196	1034	5412	02100881
X30	2003/01/22	08:28	00-00.48N	174-00.01W	30.09	34.433	1036	5389	02100886
X31	2003/01/22	12:34	00-00.14S	173-00.03W	30.00	34.768	1034	5508	02100885
X32	2003/01/22	16:38	00-00.53S	171-59.96W	29.85	34.917	1034	5705	02100894
X33	2003/01/22	20:43	00-00.75S	171-00.01W	29.67	35.173	1034	5668	02100897
X34	2003/01/25	03:40	00-00.30S	169-00.01W	29.41	35.365	1034	5582	02100889
X35	2003/01/25	07:59	00-00.29N	168-00.01W	29.15	35.315	1034	5281	02100888

X36	2003/01/25	16:29	00-00.58S	166-00.20W	28.96	35.322	1035	5296	02100892
X37	2003/01/25	20:50	00-00.39S	165-00.00W	28.97	35.253	1034	5793	02100890
X38	2003/01/26	04:17	00-00.05N	164-00.02W	28.84	35.339	1032	4795	02100895
X39	2003/01/26	08:44	00-00.25N	163-00.02W	28.64	35.377	1035	5193	02100898
X40	2003/01/26	13:10	00-00.07N	162-00.02W	28.46	35.407	1034	5085	02100896
X41	2003/01/26	17:39	00-00.37N	161-00.00W	28.27	35.387	1035	5048	02100899

SST: Sea surface temperature [deg-C] measured by Continuous Sea Surface Monitoring System

SSS: Sea surface salinity [PSU] measured by Continuous Sea Surface Monitoring System

MD: Maximum measured depth [m]

WD: Water Depth [m]

Table 4.2.2-2 XCTD observations (MR02K06 Leg4)

Station	Date	Time	Lat.	Lon.	SST	SSS	MD	WD	Probe S/N
X01	2003/02/03	15:34	24-45.46N	165-00.00W	22.65	35.428	1033	5020	01116888
X02	2003/02/03	20:07	25-28.51N	165-59.70W	21.25	35.362	1034	4893	01116891
X03	2003/02/04	00:07	25-59.16N	167-00.02W	21.07	35.346	1033	4868	01116890
X04	2003/02/04	04:08	26-29.50N	168-00.01W	20.62	35.322	1035	4556	01116893
X05	2003/02/04	08:22	26-59.93N	168-59.46W	20.49	35.315	1036	4451	02069291
X06	2003/02/04	12:40	27-29.99N	170-00.01W	19.87	35.234	1035	4559	02069292
X07	2003/02/04	17:17	28-00.17N	171-08.12W	18.52	35.004	1033	2605	01116889
X08	2003/02/04	20:55	28-21.86N	171-59.44W	18.34	35.049	1033	5013	01116892
X09	2003/02/05	01:03	28-47.85N	173-00.01W	19.15	35.187	936	5174	02069299
X10	2003/02/05	06:30	29-15.61N	174-05.36W	18.88	35.147	738	2240	02069293
X11	2003/02/05	13:48	29-14.85N	175-00.02W	18.85	35.119	1034	5359	02069294
X12	2003/02/05	20:41	29-17.71N	175-59.39W	18.06	34.948	1035	5270	02069298
X13	2003/02/06	02:28	29-45.05N	177-00.02W	17.19	34.773	1034	5373	02069303
X14	2003/02/06	07:53	30-17.98N	177-59.51W	16.84	34.725	1035	5510	02069302
X15	2003/02/06	12:33	30-53.96N	179-00.01W	16.62	34.703	1035	5170	02069297
X16	2003/02/06	16:52	31-29.50N	179-59.99W	16.90	34.739	1035	2860	02069295
X17	2003/02/06	20:53	32-02.60N	179-00.62E	16.92	34.711	1034	5190	02069300
X18	2003/02/07	00:31	32-21.90N	177-59.98E	14.70	34.559	1035	5272	02070084
X19	2003/02/07	04:02	32-40.83N	176-59.98E	15.26	34.574	1034	5421	02070089
X20	2003/02/07	07:45	32-58.85N	176-00.88E	16.77	34.681	1033	4144	02070085
X21	2003/02/07	09:55	32-59.74N	175-29.98E	17.04	34.697	818	5135	02070088
X22	2003/02/07	12:11	32-59.05N	175-00.00E	16.58	34.625	890	4452	02070077
X23	2003/02/07	14:28	32-59.33N	174-30.00E	17.19	34.715	898	5063	02070082
X24	2003/02/07	17:03	32-58.96N	173-59.98E	16.98	34.682	931	5187	02070081
X25	2003/02/07	19:44	32-58.51N	173-30.02E	17.17	34.702	1020	5012	02070080
X26	2003/02/07	22:14	32-59.02N	173-00.83E	17.24	34.719	1035	5220	02070083
X27	2003/02/08	00:38	32-59.44N	172-29.99E	17.23	34.705	918	4498	02059271
X28	2003/02/08	02:53	32-59.68N	172-00.00E	17.11	34.709	826	4382	02059266
X29	2003/02/08	05:12	32-59.36N	171-29.98E	17.34	34.730	902	4965	02070087
X30	2003/02/08	07:36	32-59.31N	170-59.99E	17.25	34.739	856	5715	02059274
X31	2003/02/08	13:13	32-58.76N	170-01.00E	16.31	34.587	997	5753	02059270
X32	2003/02/08	16:01	32-57.98N	169-29.99E	15.72	34.648	875	5736	02070078
X33	2003/02/08	18:43	32-57.56N	168-59.98E	16.25	34.679	816	5771	02059276
X34	2003/02/08	21:44	32-58.46N	168-30.02E	17.25	34.751	847	5841	02059273
X35	2003/02/09	00:48	33-00.89N	168-00.15E	17.35	34.755	798	--	02069281

X36	2003/02/09	04:00	33-07.22N	167-30.02E	17.35	34.752	865	5946	02059277
X37	2003/02/09	06:53	33-12.79N	167-01.04E	17.28	34.747	1032	5967	02059279
X38	2003/02/09	09:48	33-23.53N	166-30.00E	17.39	34.753	956	5849	02059280
X39	2003/02/09	12:25	33-34.80N	166-00.01E	17.43	34.756	1016	6082	02069284
X40	2003/02/09	17:00	33-54.40N	165-01.06E	17.58	34.760	1034	6139	02069283
X41	2003/02/09	21:02	34-12.62N	164-00.00E	17.38	34.754	1034	6121	02059278
X42	2003/02/10	00:49	34-30.61N	163-00.49E	17.30	34.756	1035	5899	02059296
X43	2003/02/10	04:32	34-49.64N	162-00.00E	17.20	34.768	1035	5010	02059272
X44	2003/02/10	08:20	35-05.77N	161-00.97E	13.56	34.521	1035	4013	02069288
X45	2003/02/10	11:46	35-23.57N	159-59.99E	14.23	34.574	1035	4470	02059275
X46	2003/02/10	15:13	35-40.70N	158-59.03E	13.10	34.451	1035	4214	02069290
X47	2003/02/10	18:34	35-58.79N	157-59.97E	14.67	34.631	1034	3478	02069289
X48	2003/02/10	21:40	36-17.04N	156-58.95E	16.74	34.761	1032	5174	02069287
X49	2003/02/11	00:48	36-33.11N	155-59.98E	13.98	34.495	1034	5665	02069282
X50	2003/02/11	04:03	36-50.97N	155-00.19E	12.98	34.425	1035	5788	02059265
X51	2003/02/11	07:17	37-08.65N	153-59.99E	12.84	34.448	1035	5729	02069286
X52	2003/02/11	10:29	37-24.49N	153-00.04E	12.56	34.442	1035	5857	02059263
X53	2003/02/11	13:42	37-41.81N	152-00.01E	13.63	34.531	1035	5867	02059264

SST: Sea surface temperature [deg-C] measured by Continuous Sea Surface Monitoring System

SSS: Sea surface salinity [PSU] measured by Continuous Sea Surface Monitoring System

MD: Maximum measured depth [m]

WD: Water Depth [m]

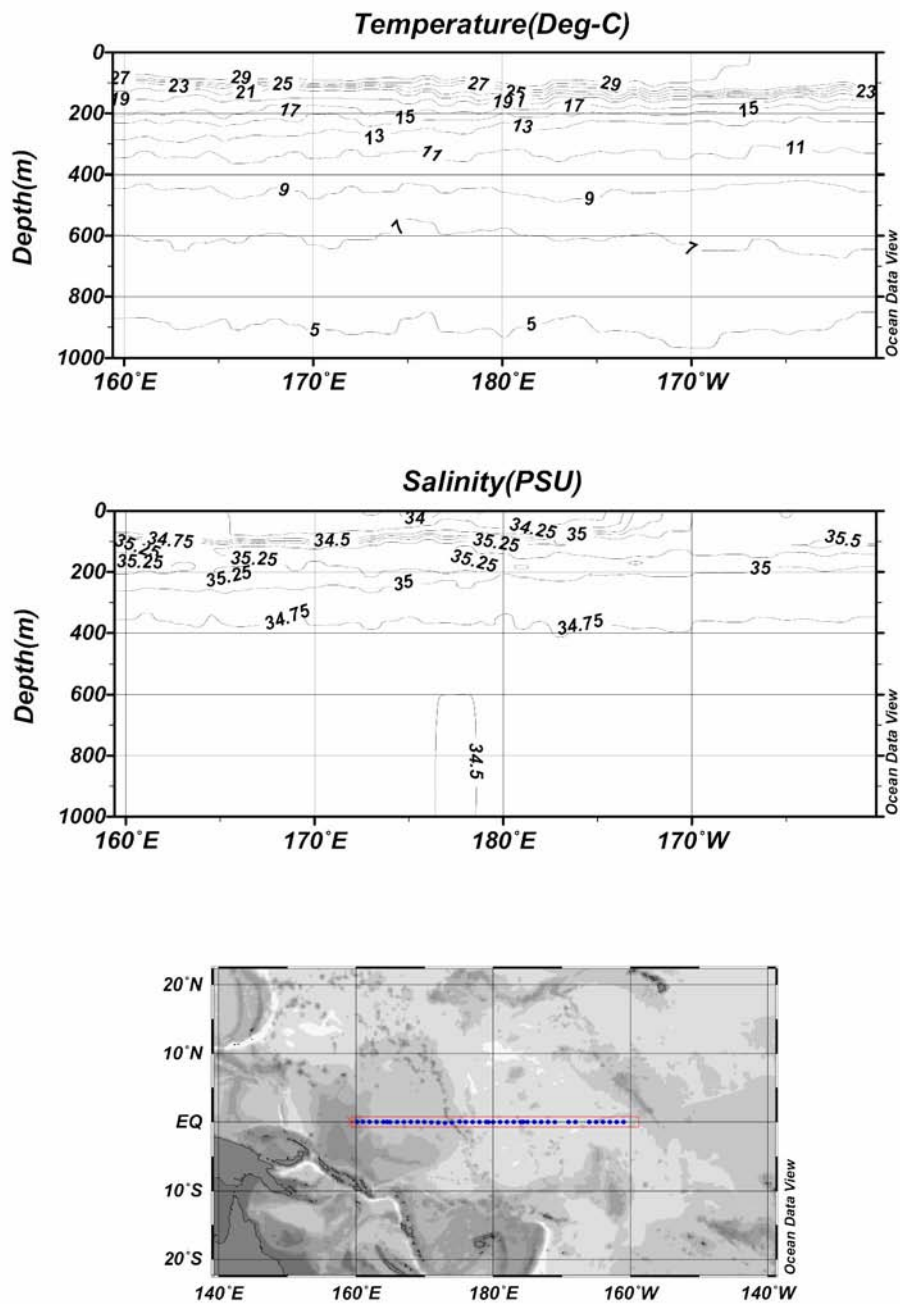


Fig.4.2.2-1 Vertical profile of temperature and salinity (MR02K06 Leg3)

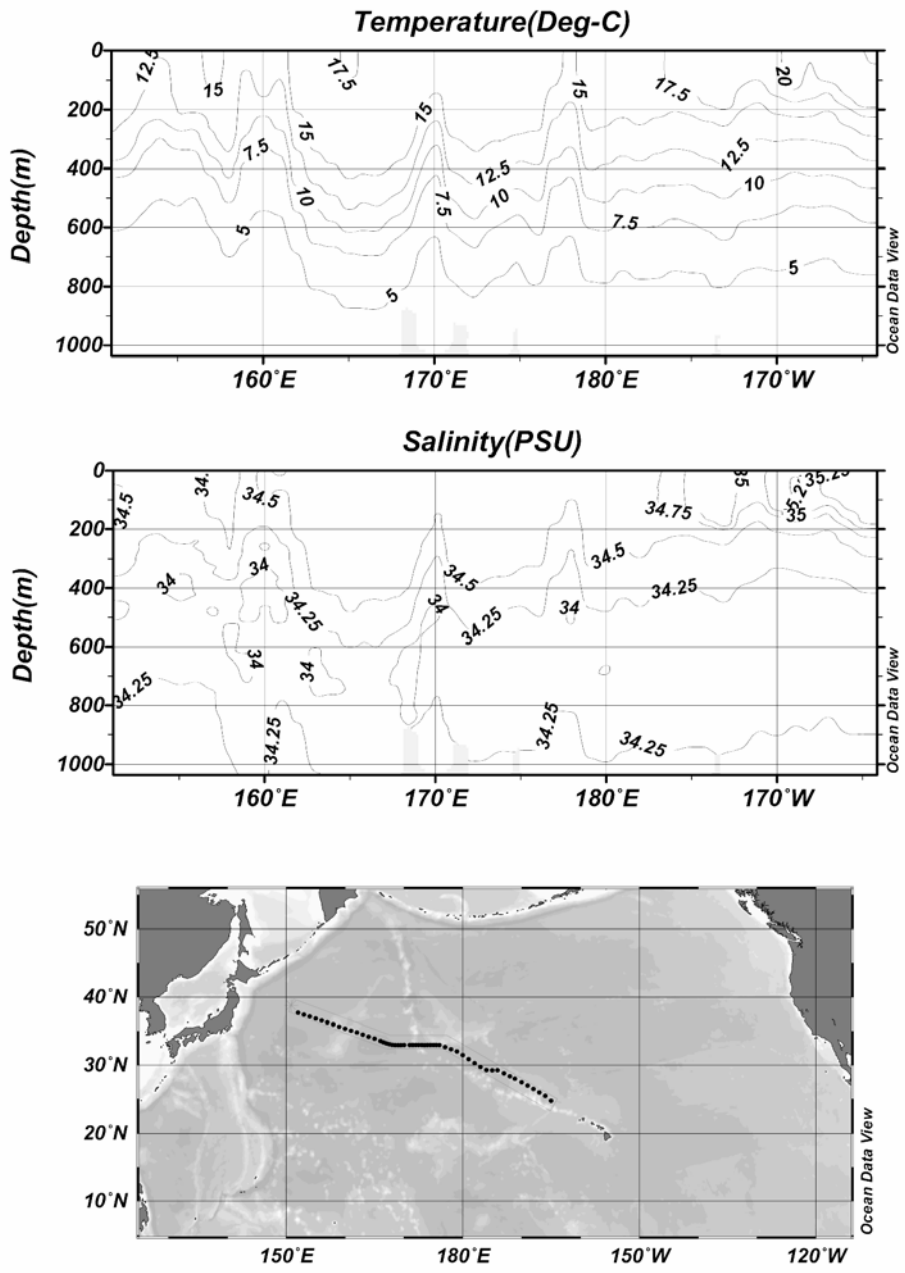


Fig.4.2.2-2 Vertical profile of temperature and salinity (MR02K06 Leg4)

4.3. Shipboard ADCP

(1) Personnel

Kazuhiko Matsumoto (JAMSTEC)

Yasutaka Imai (GODI)

Norio Nagahama (GODI)

(2) Parameters

Current velocity of each depth cell [mm/s]

(3) Methods

Upper ocean current measurements were made throughout MR02-K06 Leg3 and 4 cruise (Departure from Chuuk on 13 January 2003 to the arrival at Sekinehama on 14 February) except for the territorial waters of the Federation States of Micronesia and the United States of America, using the hull-mounted Acoustic Doppler Current Profiler (ADCP) system that is permanently installed on the R/V Mirai. The system consists of following components;

- 1) a 75 kHz Broadband (coded-pulse) profiler with 4-beam Doppler sonar operating at 75 KHz (RD Instruments, USA), mounted with beams pointing 30 degrees from the vertical and 45 degrees azimuth from the keel;
- 2) the Ship's main gyro compass (Tokimec, Japan), continuously providing ship's heading measurements to the ADCP;
- 3) a GPS navigation receiver (Leica MX9400) providing position fixes;
- 4) an IBM-compatible personal computer running data acquisition software (VmDas version 1.3 ; RD Instruments, USA). The clock of the logging PC are adjusted to GPS time every 5 minutes.

The ADCP was configured for 16-m pulse length, 16-m processing bin, and a 8-m blanking interval. The sound speed is calculated from temperature (thermistor near the transducer faces), salinity (constant value; 35.0 psu) and depth (6.5 m; transducer depth) by equation in Medwin (1975). The transducer depth was 6.5 m; 40 velocity measurements were made at 16-m intervals starting 31m below the surface. Each 1 ping was recorded as raw ensemble data. Also, 60 seconds and 300 seconds average data were recorded as short-term average (STA) and long-term average (LTA) data.

(4) Preliminary result

Horizontal Velocity along the Equator is presented in Fig.4.3-1. Vertical distribution of the current magnitude along the equator is presented in Fig.4.3-1

(5) Data archive

These data obtained in this cruise will be submitted to the JAMSTEC DMD (Data Management

Division), and will be opened to the public via “R/V Mirai Data Web Page” in JAMSTEC home page.

(6) Remarks

We did not sample the data within territorial water of the federation states of Micronesia (2003/01/13 00:00 --- 2003/01/13 02:30) and the United States of America (2003/01/31 21:16---2003/02/02 11:30).

VM-ADCP Configuration

Bottom-Track Commands

BP=000 ----- Pings per Ensemble

Environmental Sensor Commands

EA=+00000 ----- Heading Alignment (1/100 deg)

EB=+00000 ----- Heading Bias (1/100 deg)

ED=00065 ----- Transducer Depth (0 – 65535 dm)

EF=+0001 ----- Pitch/Roll Divisor/Multiplier (pos/neg) [1/99 - 99]

EH=00000 ----- Heading (1/100 deg)

ES=35 ----- Salinity (0-40 pp thousand)

EX=00000 ----- Coord Transform (Xform: Type; Tilts; 3Bm; Map)

EZ=1020001 ----- Sensor Source (C;D;H;P;R;S;T)

Timing Command

TE=00:00:02.00 ----- Time per Ensemble (hrs:min:sec.sec/100)

TP=00:02.00 ----- Time per Ping (min:sec.sec/100)

Water-Track Commands

WA=255 ----- False Target Threshold (Max) (0-255 counts)

WB=1 ----- Mode 1 Bandwidth Control (0=Wid, 1=Med, 2=Nar)

WC=064 ----- Low Correlation Threshold (0-255)

WD= 111 111 111 ----- Data Out (V;C;A PG;St;Vsum Vsum^2;#G;P0)

WE=5000 ----- Error Velocity Threshold (0-5000 mm/s)

WF=0800 ----- Blank After Transmit (cm)

WG=001 ----- Percent Good Minimum (0-100%)

WI=0 ----- Clip Data Past Bottom (0=OFF, 1=ON)

WJ=1 ----- Rcvr Gain Select (0=Low, 1=High)

WM=1 ----- Profiling Mode (1-8)

WN=040 ----- Number of depth cells (1-128)

WP=00001 ----- Pings per Ensemble (0-16384)

WQ=0 ----- Sample Ambient Sound (0=OFF, 1=ON)

WS=1600 ----- Depth Cell Size (cm)

WT=0000 ----- Transmit Length (cm) [0=Bin Length]

WV=999 ----- Mode 1 Ambiguity Velocity (cm/s radial)

WW=004 ----- Mode 1 Pings before Mode 4 Re-acquire

MR02K06Leg3

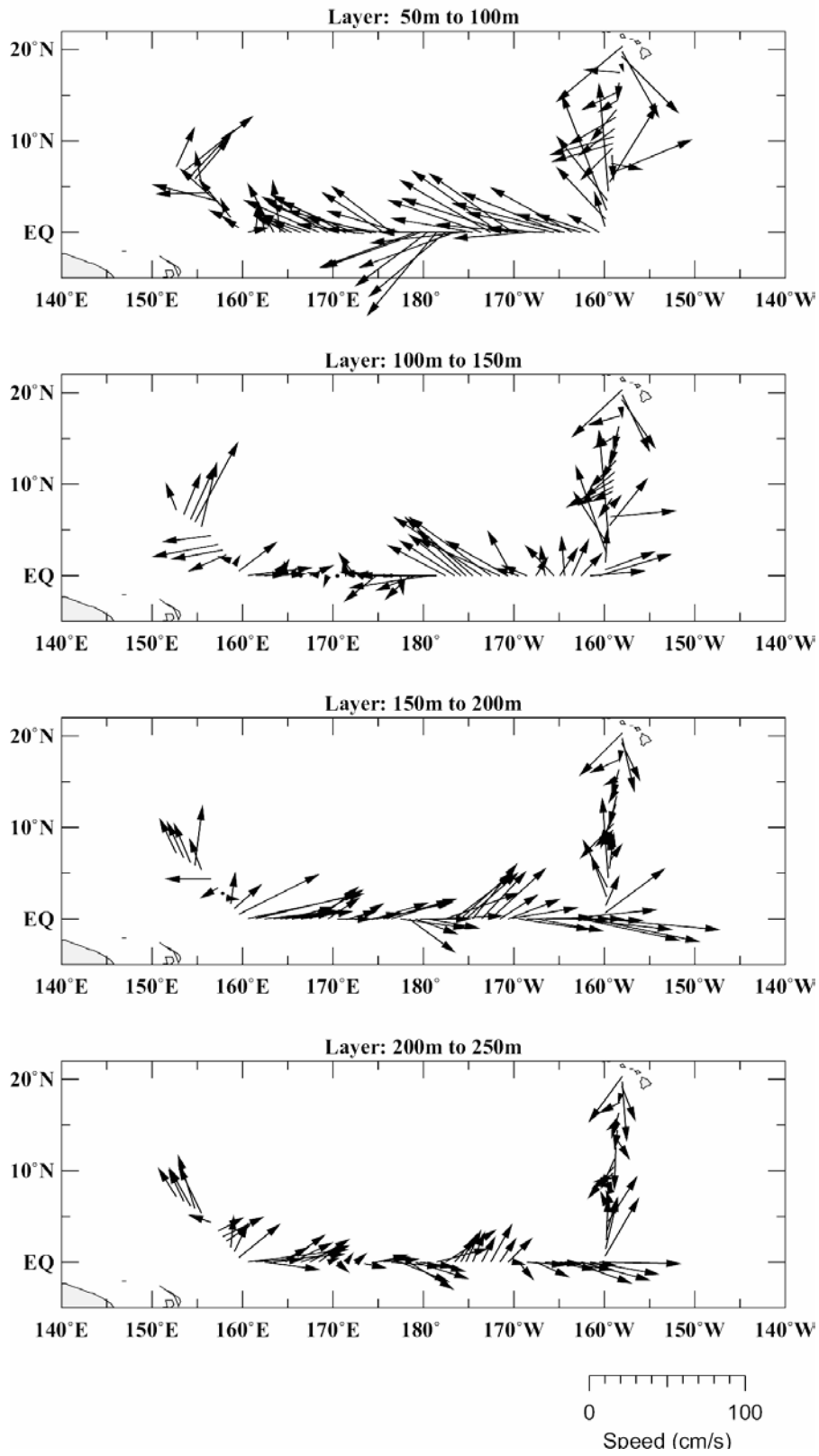


Fig 4.3-1 Horizontal Velocity along Track

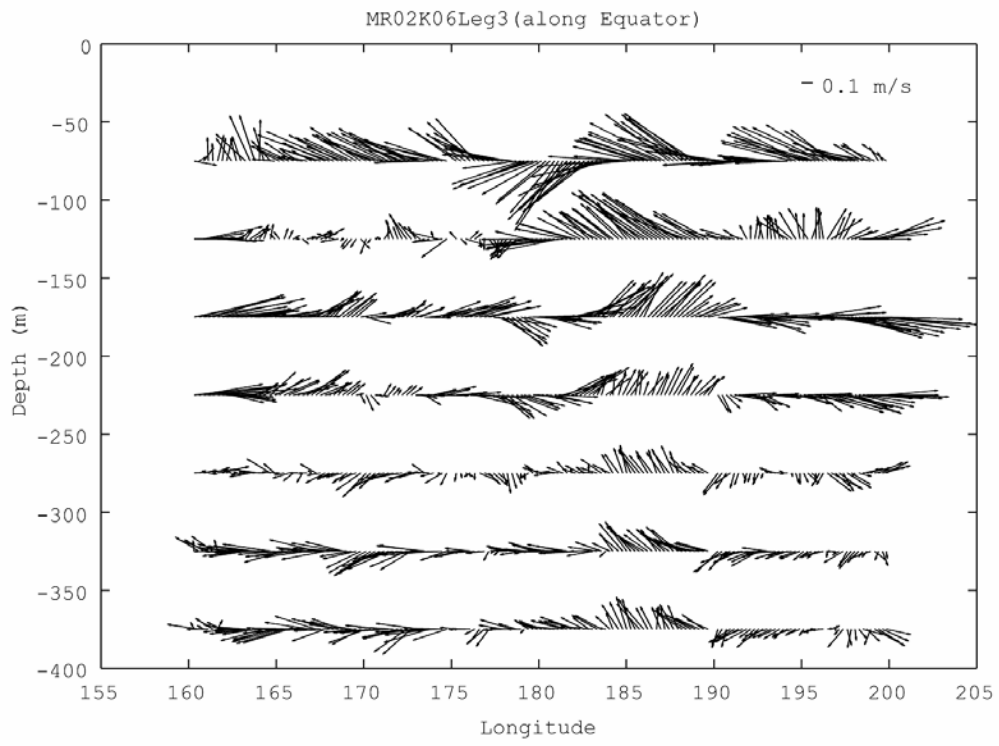


Fig 4.3-2 Vertical distribution of the current magnitude and direction (Upward: North)

4.4. Underway Geophysics

4.4.1. Sea Surface Gravity

(1) Personnel

Toshiya Fujiwara (JAMSTEC) Principal investigator (not on board)

Yasutaka Imai (GODI)

Norio Nagahama (GODI)

(2) Objectives

The difference of local gravity is an important parameter in geophysics. We measured relative gravity at the sea surface during MR02-K06 cruise (13/January/2003---14 /February/2003, Chuuk---Honolulu --- Sekinehama)

(3) Parameters

Gravity [mgal]

(4) Methods

We have measured relative gravity using LaCoste-Romberg onboard gravity meter S-116 during MR02-K06 (13/January/2003---14/February/2003, Chuuk---Honolulu---Sekinehama). To convert relative gravity to absolute one at the sensor, we measured gravity at Sekinehama gravity reference point using portable gravity meter (Scintrex gravity meter CG-3M). Information of crust and upper-mantle structures is derived from measured gravity.

(5) Results

Absolute gravity (Table 4.4.1-1).

Table 4.4.1-1

No	Date	UTC	Port	Absolute Gravity (mGal)	Sea Level (cm)	Draft (cm)	Gravity at sensor (mGal)	L&R (mGal)	Remarks
1	2003/Feb/01	17:25	Honolulu	998927.8	159	590	998928.32	112221	
2	2003/Feb/14	04:30	Sekine						

- Gravity at sensor = Absolute gravity + sea level*0.3086/100 + (Draft— 530)/100*0.0431
- L&R: LaCoste - Romberg onboard gravity meter S-116

(6) Data archives

Gravity data obtained during this cruise will be submitted to the JAMSTEC DMO (Data Management Office), and archived there.

(7) Remarks

We did not sample the data within territorial water of the federation states of Micronesia (2003/01/13 00:00---2003/01/13 02:30) and the United States of America (2003/01/31 21:16---2003/02/02 11:30).

4.4.2. Surface three-component magnetometer

(1) Personnel

Toshiya Fujiwara (JAMSTEC) Principal investigator (not on board)

Yasutaka Imai (GODI)

Norio Nagahama (GODI)

(2) Objectives

Measurements of magnetic force that is induced by magnetized body beneath the sub-bottom and the earth dipole on the sea, is required for reorganization of the geophysical crust structure. We measured a geomagnetic field at the sea surface using a three-component magnetometer, two horizontal and one vertical component.

(3) Parameters

Three-component magnetic force [nT]

Ship's attitude [1/100deg]

(4) Method

A three-component fluxgate magnetometer is set on the top of foremast. Sampling is controlled by the 1pps (pulse per second) standard clock of GPS signal. Every one-second data is composed of navigation information, 8Hz three component of magnetic forces and vertical reference unit (VRU) data.

(5) Preliminary results

The magnetic force is continuously measured during MR02-K06 cruise (13/January/2003 --- 14/February/2003, Chuuk --- Honolulu --- Sekinehama).

(6) Data archives

Magnetic force data obtained during this cruise will be submitted to the JAMSTEC DMO (Data Management Office), and archived there.

(7) Remarks

We did not sample the data within territorial water of the federation states of Micronesia (2003/01/13 00:00---2003/01/13 02:30) and the United States of America (2003/01/31 21:16---2003/02/02 11:30).

4.4.3. Multi-narrow beam echo sounding system

(1) Personnel

Toshiya Fujiwara (JAMSTEC) Principal investigator (not on board)

Yasutaka Imai (GODI)

Norio Nagahama (GODI)

(2) Objectives

To obtain the bathymetry for buoy deployment, geophysical investigation and water sampling.

(3) Methods

A multi-narrow beam echo sounding system “SeaBeam 2100” on R/V Mirai was used for bathymetry mapping during the MR02-K06 cruise (13/January/2003---14/February/2003, Chuuk---Honolulu---Sekinehama).

(4) Data archives

Bathymetry data obtained during this cruise will be submitted to the JAMSTEC DMO (Data Management Office), and archived there.

(5) Remarks

We did not sample the data within territorial water of the federation states of Micronesia (2003/01/13 00:00---2003/01/13 02:30) and the United States of America (2003/01/31 21:16---2003/02/02 11:30).

5. Special observation

5.1. Dissolved Oxygen

(1) Personal

Tomoko MIYASHITA (Marine Works Japan Ltd.)

(2) Introduction

Precise determination of Dissolved Oxygen using the Winkler titration with potentiometric detection.

(3) Methods

(a) Instruments and Apparatus

Glass bottle:

Glass bottle for D.O. measurements consist of the ordinary BOD flask (ca.100ml) and glass stopper with long nipple, modified from the nipple presented in Green and Carritt (1966).

Dispenser:

Eppendorf Comforpette 4800/1000 1 (dispensed for the 1 ml of H₂SO₄ and standard KIO₃ solution)

OPTIFIX/1ml (dispensed for the picking reagents)

Kyoto Electronics manufacturing co.,LTD Auto Piston Burette APB-510 / 20ml of titration vessel (dispensed for the standard KIO₃ solution)

Titration: Metrohm Model 716 DMS Titrino / 10 ml of titration vessel (resolution of titration is 0.001 ml)

Metrohm Pt Electrode / 6.9904.030

Software: Data acquisition and endpoint evaluation / Metrohm, Tinet2.4

(b) Methods

Sampling and analytical methods were based on to the WHP Operations and Methods (Culberson, 1991, Dickson, 1994)

(b-1) Sampling

Sea water samples for dissolved oxygen measurement were collected from 12 liter Niskin bottles to calibrated dry glass bottles. During each sampling, 3 bottle volumes of seawater sample were overflowed to minimize contamination with atmospheric oxygen and the seawater temperature at the time of collection was measured for correction of the samples volume. After the sampling, MnCl₂(aq.) 1ml and NaOH / NaI (aq.) 1ml were added into the glass bottle, and then shook the bottle well. After the precipitation has settled, we shook the bottle vigorously to disperse the precipitate.

(b-2) Dissolved Oxygen analysis

The samples were analyzed by 1 sets of Metrohm titrator with 10 ml piston burette and Pt electrode. Titration values was determined by the potentiometric methods, and the endpoint for titration was evaluated by the software of Metrohm, Titrino Workcell. From the titration values, we calculated concentration of dissolved oxygen by WHP Operations and Methods (Culberson, 1991, Dickson, 1994).

(4) Preliminary Result

The vertical profiles of Dissolved Oxygen were shown in Figs5.1-1~3.

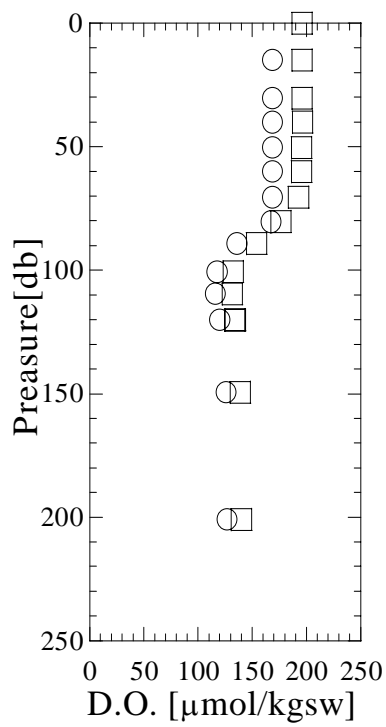
(5) References

Culberson, C.H.(1991) Dissolved Oxygen, in WHP Operations and Methods, Woods Hole.,pp1-15

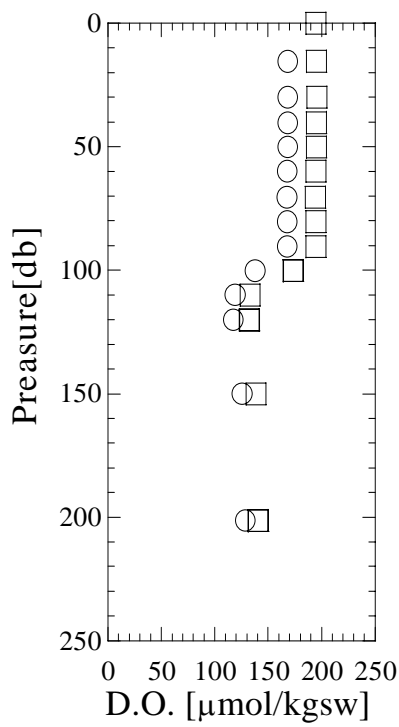
Culberson, C.H., G.Knapp, R.T.Williams and F.Zemlyak (1991) A comparison of methods for the determination of dissolved oxygen in seawater. (WHPO 91-2)

Dickson, A.G (1994) Determination of dissolved oxygen in sea water by Winkler titration, in WHP Operations and Methods, Woods Hole.,pp1-14

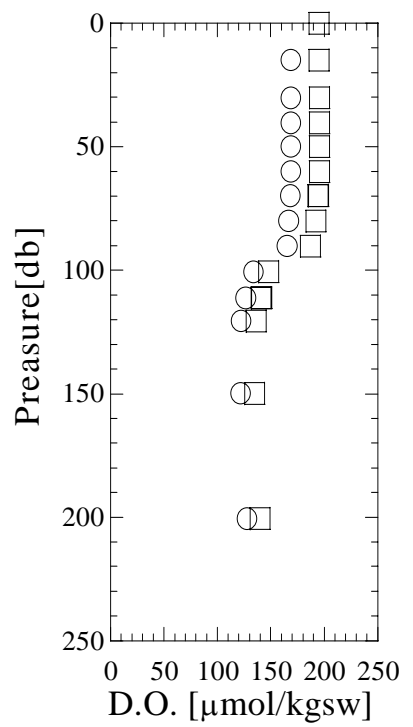
Murray, N.,J.P.Riley and T.R.S. Wilson (1968) The solubility of oxygen in Winkler reagents used for the determination of dissolved oxygen, Deep-Sea Res.,15,237-238.



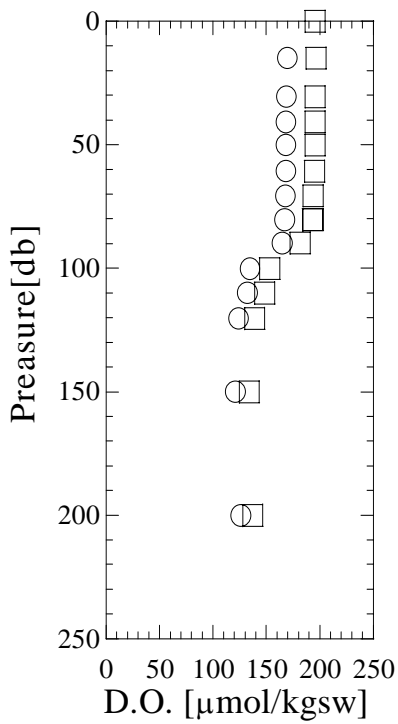
St.6 Shallow2



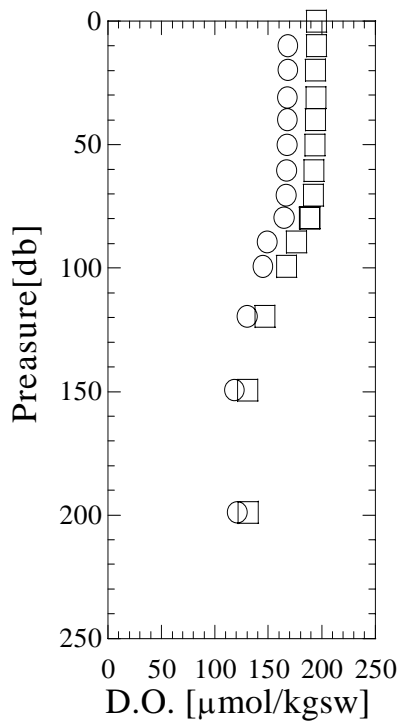
St.7 Shallow4-2



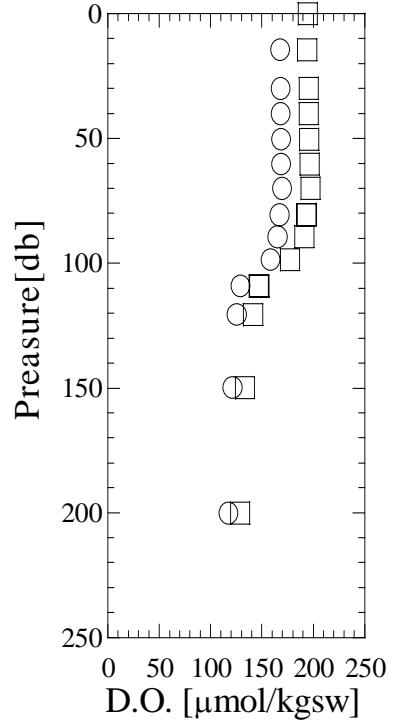
St.8 Shallow4-2



St.9 Shallow2



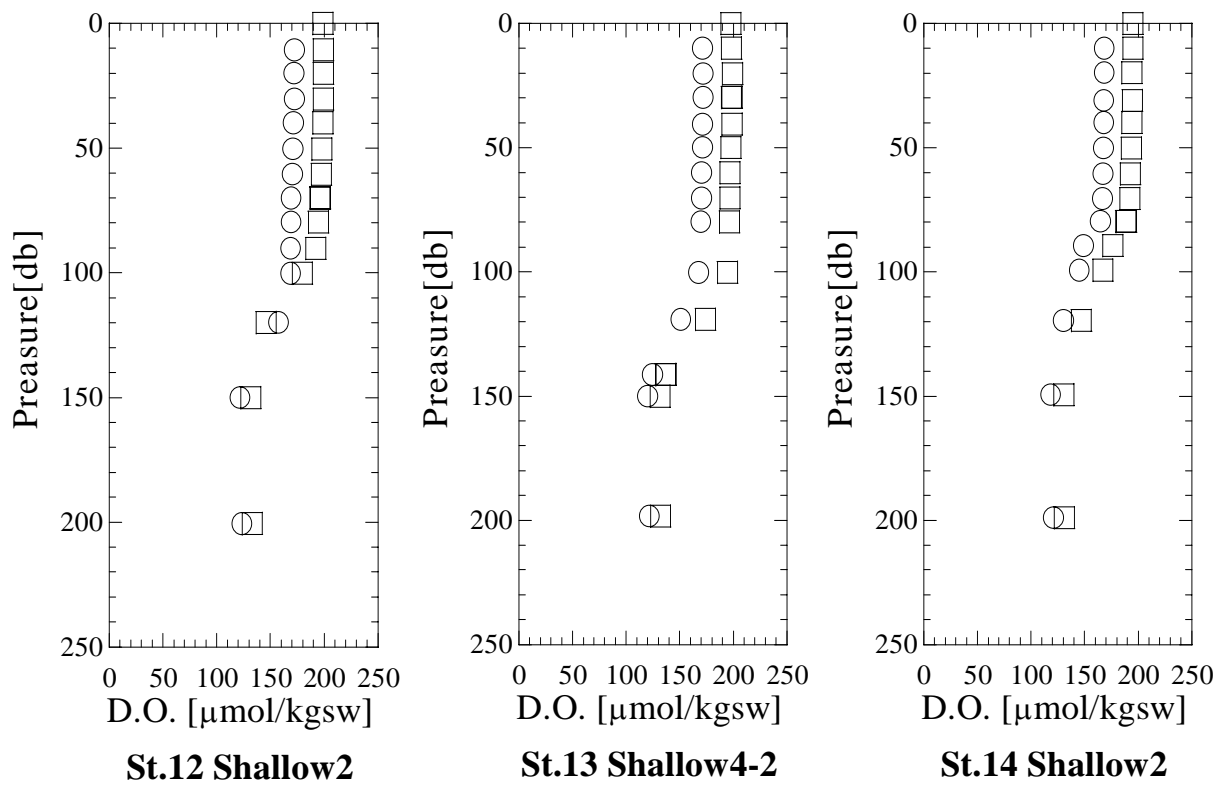
St.14 Shallow2



St.11 Shallow4-2

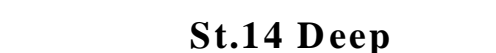
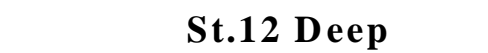
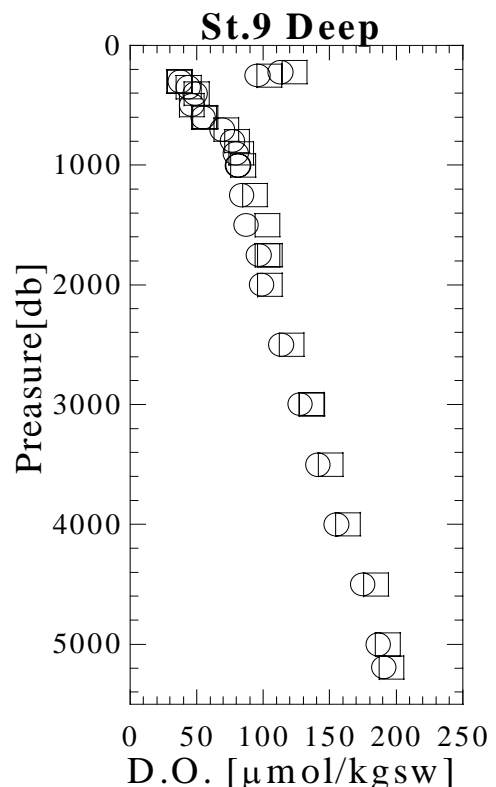
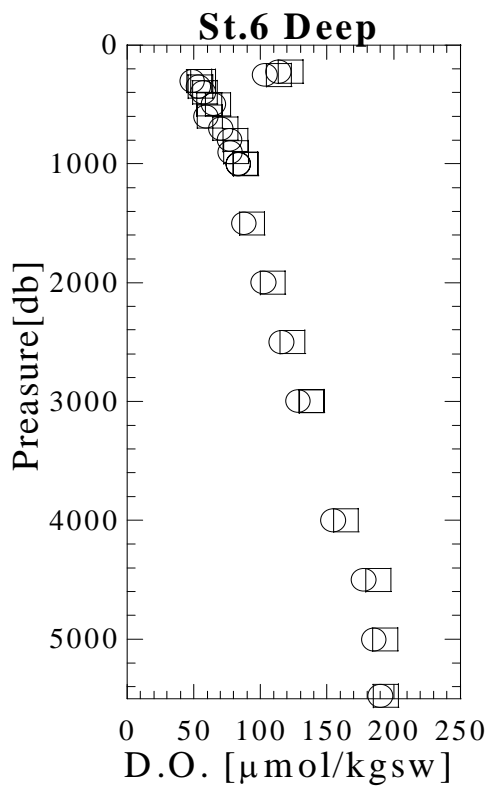
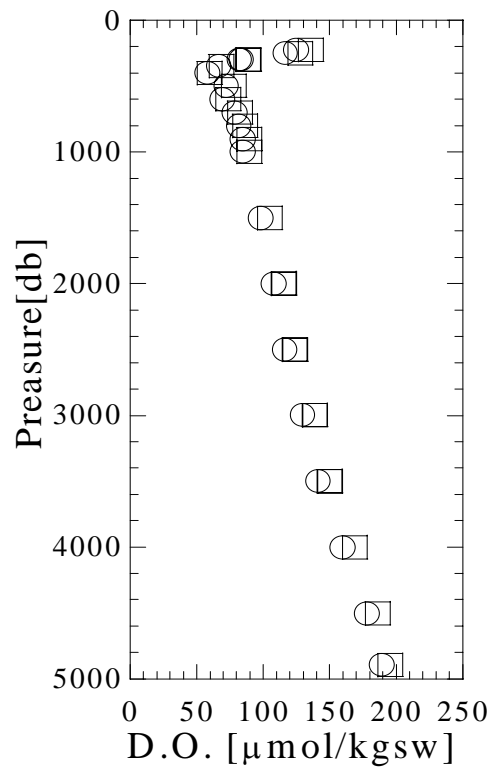
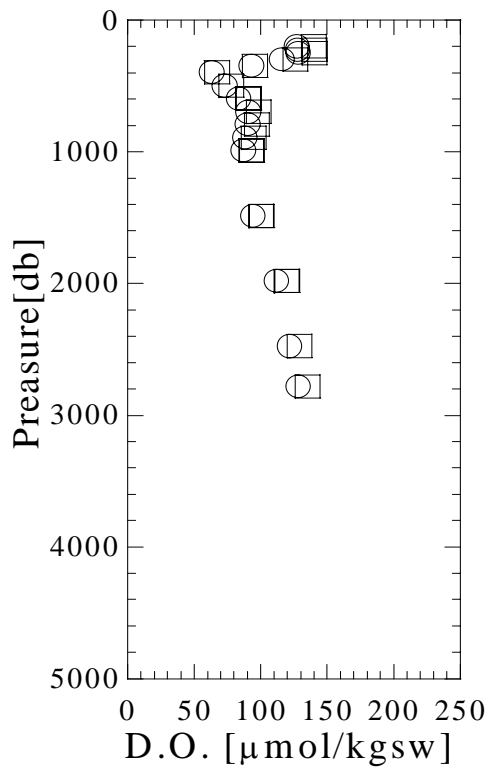
□ ; D.O.($\mu\text{mol}/\text{kg} \cdot \text{sw}$)
 ○ ; D.O.[sensor] ($\mu\text{mol}/\text{kg} \cdot \text{sw}$)

Fig.5.1-1 Vertical profiles at each stations.



□ ; D.O.(μmol/kg · sw)
 ○ ; D.O.[sensor] (μmol/kg · sw)

Fig.5.1-2 Vertical profiles at each stations.



□ ; D.O.($\mu\text{mol/kg} \cdot \text{sw}$)
 ○ ; D.O.[sensor] ($\mu\text{mol/kg} \cdot \text{sw}$)

Fig.5.1-3 Vertical profiles at each stations.

5.2. Salinity measurement

(1) Personnel

Naoko Takahashi (MWJ): operation reader

Masayuki Fujisaki (MWJ)

Fujio Kobayashi (MWJ)

(2) Objective

Calibration of salinity measured by CTD

(3) Measured Parameter

Sample water salinity

(4) Instrument and Method

The salinity analysis was carried out on R/V MIRAI during the cruise of MR02-K06 Leg3 and Leg4 by the Guildline salinometer model 8400B "AUTOSAL" (S/N 62827) modified with addition of an Ocean Scientific International peristaltic-type intake pump.

The AUTOSAL was operated in the air-conditioned "AUTOSAL Room" and its bath temperature was held at 24 degrees C. An ambient temperature varied from approximately 21 to 26 degrees C.

Standardization

AUTOSAL was standardized with the use of IAPSO Standard Seawater (Batch P141, conductivity ratio; 0.99993, salinity; 34.997) before a series of measurement.

The measurement of standard seawater was carried out every approximately 20 samples, and the drift check of AUTOSAL was performed. Total 32 ampoules of standard seawater were measured for the monitoring, that standard deviation was 0.00003.

We also used sub-standard seawater that was deep-sea water filtered by Millipore filter (pore size of 0.45 μ m) and stored in a 20 liter container made from polyethylene. It was measured every 10 samples in order to check the drift of the AUTOSAL.

Method

Seawater samples were collected from 12 liter NiskinX bottles (Non-coating for Teflon) with silicone O-rings. The salinity sample bottle was the 250 ml brown glass bottle with screw cap and was used to collect the sample water. Each bottle was rinsed three times with the sample water, and was filled with it to the shoulder of the bottle. Its cap was also thoroughly rinsed. The bottle was stored more than 24 hours in AUTOSAL Room before the salinity measurement.

A double conductivity ratio was defined as median of 31 times reading of AUTOSAL. Data collection started in 5 seconds and it took about 10 seconds to collect 31 times reading by a personal computer.

When repetition measurement was carried out a maximum of 5 times and the same value

came out, we made the measured value of a sample the determination salinity. Or, when the following value came out in ± 0.00001 , it made the mean value the determination value.

Table 1: Kind and number of samples

Kind of samples	Number of samples
Samples for CTD	221
Samples for EPCS (Leg3)	15
Samples for experiment	30
Reference Material for Nutrients	4
Samples for EPCS (Leg4)	10
Total	280

(5) Result

The preliminary results are shown in Table 2.

The average of difference between CTD data and measurement data was 0.0041 and the standard deviation (SD) was 0.0325.

The average of difference between CTD data and measurement data extracted each for deeper than 2,000db was -0.0051 and the standard deviation was 0.0011.

Table 2: Result of measurement for CTD samples

ALL (221 samples)	
AVERAGE	0.0041
SD (ABS)	0.0325
> 2,000db (32 samples)	
AVERAGE	-0.0051
SD (ABS)	0.0011

Replicate was measured to in order to check correlation of CTD profile data and the sampled seawater, the average and standard deviation of a difference between CTD data and AUTOSAL data. The replicate results are shown in Table 3.

Table 3: Result of replicate measurement for CTD samples

Replicate	11 Pairs
AVERAGE	0.00041
SD (ABS)	0.00092

(6) Data archive

The data of measured samples and worksheets of calculation for salinity were stored on CD-R disk. The data of samples will be submitted to JAMSTEC Data Management Office (DMO).

5.3. Nutrients

5.3.1. Nitrate, Nitrite, Silicic acid, Phosphate

(1) Personnel

Asako Kubo (MWJ)

(2) Objectives

Phytoplankton require nutrient elements for growth, chiefly nitrogen, phosphorus, and silicon. The data of nutrients in seawater is important for investigation of phytoplankton productivity.

(3) Measured parameters

- Nitrate
- Nitrite
- Silicic acid
- Phosphate

(4) Methods

Seawater samples were transferred into 10 ml PMMA bottles. Sample bottles were rinsed three times before filling. The samples were analyzed as soon as possible. Nutrients were measured by a TRAACS 800 continuous flow analytical system (BRAN+LUEBBE). The following analytical methods were used.

Nitrate: Nitrate in the seawater was reduced to nitrite by reduction tube (Cd-Cu tube), and the nitrite reduced was determined by the nitrite method as shown below. The flow cell was a 3 cm length type.

Nitrite: Nitrite was determined by diazotizing with sulfanilamide by coupling with N-1-naphthyl-ethylenediamine (NED) to form a colored azo compound, and by being measured the absorbance of 550 nm using a 5 cm length flow cell in the system.

Silicic acid: Silicic acid was determined by complexing with molybdate, by reducing with ascorbic acid to form a colored complex, and by being measured the absorbance of 630 nm using a 3 cm length flow cell in the system.

Phosphate: Phosphate was determined by complexing with molybdate, by reducing with ascorbic acid to form a colored complex, and by being measured the absorbance of 880 nm using a 5 cm length flow cell in the system.

(5) Results

Precision of the analysis

Coefficient of variation (CV) of nitrate, nitrite, silicic acid, and phosphate analysis at each station were less than 0.27% (50 μM), 0.59% (1.2 μM), 0.23% (170 μM) and 0.34% (3.1 μM), respectively.

(6) Data Archive

These data are stored Ocean Research Department in JAMSTEC.

5.3.2. Low level Ammonia

(1) Personal

Shinya ENDO* and Kazuhiko MATSUMOTO**

*Kansai environmental engineering center co ltd. (KANSO)

**Japan marine science and technology center. (JAMSTEC)

(2) Abstract

Knowing of ammonia's role in the marine environment with respect to a biological activity, eutrophication and continental input assessment are wide interest.

However, accurate determination of ammonia in seawater seems to be difficult.

A direct automated method for routine determination of nutrients in seawater has been developed using segmented flow analysis.

The method based on the reaction of ammonia with sodium salicylate and hypochlorite, is sensitivity and highly reproducible method.

Until now, ammonia reacts in moderately alkaline solution with hypochlorite to monochloramine, which in the presence of phenol, catalytic amounts of nitroprusside ions excess hypochlorite gives indophenol blue.

However, IPB (indophenol blue) techniques are unsuitable for most unpolluted and open seawater where NH_3 occurs lower concentration levels.

In the present cruise, we carried on new method that caused by Teflon membrane filter (PTFE) remove interference substances (e.g. magnesium) from seawater samples.

This method is application from Ion chromatography.

In ion chromatography cation exchange columns strong acidic eluents (e.g. HCl) are used to resolved ammonium and detected conductimetrically.

(3) Instruments and methods

Sample seawater was mixed with an alkaline solution containing citrate as masking agent, ammonia as gas state was formed from sample. The ammonia(gas) was absorbed in sulfuric acid solution by passing a porous teflon membrane (pore-size $0.5 \mu\text{m}$) at the dialyzer attached to analytical system. The ammonia absorbed in acidic solution was determined by coupling with salicylate and hypochlorite to form a colored compound and by being measured the absorbance of 660 nm using 5 cm length flow cell in the system.

In the system, ammonia in sample was done to react with the reagent after separating from magnesium coexisted in sample. Thus we named this method "a gas diffusion method (GDM)".

(3)-1. Regents

1. 50%-Triton X100 solution.

Dissolved 50ml of Triton X100 (aq) in ethanol, and dilute to 0.1 liter.

Store in a well-stopped polyethylene bottle.

2. Sodium salicylate solution.

Dissolved 40g of sodium salicylate, 20g of sodium hydroxide, 20g of boric acid and 4g of tri-sodium citrate dihydrate in Milli-Q water, and dilute to 0.2 liter.

Store in a well-stopped polyethylene bottle.

3. Tri-sodium citrate solution.

Dissolved 50g of tri-sodium citrate dihydrate, 0.2g of sodium hydroxide in Milli-Q water, and dilute to 0.5 liter. And add 5ml of 50%-Triton X100 solution.

Store in a well-stopped polyethylene bottle.

4. Tri-sodium citrate / NaOH solution.

Dissolved 5g of sodium hydroxide, 15g of tri-sodium citrate dihydrate and 7.5g of boric acid in Milli-Q water, and dilute 0.2 liter.

5. Nitroprusside reagent stock solution.

Dissolved 1.5g of disodium nitroprusside dihydrate, 0.1ml of hydrochloric acid in Milli-Q water, and dilute 0.1 liter.

Store in a well-stopped polyethylene bottle.

6. Sodium dichloroisocyanurate solution(SDI).

Dissolved 0.70g of sodium dichloroisocyanurate in Milli-Q water, and dilute 0.1 liter.

Store in a well-stopped polyethylene bottle.

7. Nitroprusside / H₂SO₄ solution.

Dissolved 5ml of the Nitroprusside reagent stock solution and 0.75ml of Sulfuric acid in Milli-Q water, and dilute to 0.5 liter. And add 5ml of 50%-Triton X100 solution.

Store in a well-stopped polyethylene bottle.

(3)-2. Samplings

Samples were drawn into acrylic 10ml spitz tubes from Niskin bottles mouth and bucket by directly. These were rinsed three times before filling. These samples were analyzed as soon as possible. These tubes were used at analysis too.

Before this cruise, all the acrylic spitz tubes had been washed with a detergent solution (Contaminon L solution, Wako Pure Chem. Indus, Ltd.), had been rinsed by fresh water, had been rinsed by deionized water. And so, these were dried on oven at 60 degree C at 1 hour. These were capped, and had kept in some packing vinyl bags.

As analyzing by the TRAACS 800, acrylic 10ml spitz tubes were used.

(3)-3. Gas diffusion block

All measurement was performed on a TRAACS 800 with axe module and pump-4, equipped with spectrum detector.

Axe module has consists a pair of mirror image blocks into which a shallow rectangular cross-section channel or track was cut. The two blocks 'sandwiched' the gas diffusion membrane and were secured with stainless steels screws or bolts, which were reproducibly and uniformly,

tightened using a calibrated torque-limiting screwdriver.

PTFE (Teflon) was used as the gas-permeable membrane. (W.Gibb et.al 1995)

Supplied in sheet form, these materials were cut whilst sandwiched between sheets of paper.

(3)-4. Principle

Sample is pumped and treated to $\text{pH} > 12$ by addition of alkali (NaOH). Under such conditions NH_4 cations are efficiently deprotonated ($>98\%$) to their volatile gaseous forms. (Fig 1.), which may then undergo transemembrane diffusion and accumulate in a recirculating acidic 'trapping solution' (nitroprusside solution). This flow injection step promotes continuous and selective gas diffusion of NH_3 from seawater and is, by virtue of its containment, relatively free from atmospheric contamination.

React on this solution sodium salicylate and hypochlorite gave blue colors, which determine at 50mm cell with wavelength 660nm.

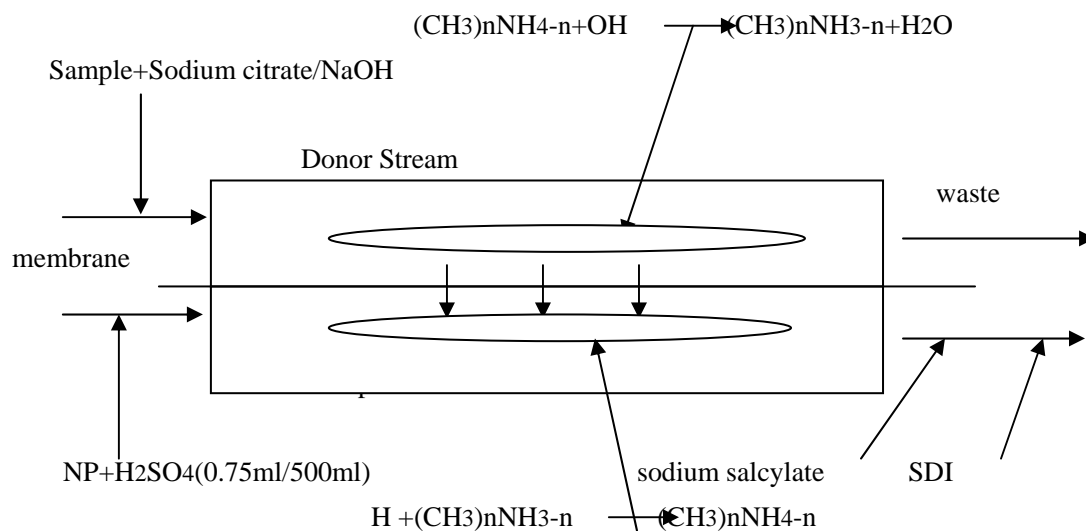


Fig 1. Schematic diagram of the speciation and diffusion of NH_3 across the PTFE.

(3)-5. Environment

The equipment of No.2 chemistry / Biology Laboratory was used.

Set up the easily ventilation system around a sampler. It is being made at aluminum frame and vinyl sheets, and an air-cleaning unit was establishment. It was possible to reduce the contamination of the ammonia from the human body.

(4) Calibration of volumetric utensil

The calibration of all volumetric flasks and micropipettes used for the cruise had been checked

before this cruise.

(5) Nutrient standards

Ammonia primary standard (stock solution) was prepared from ammonium sulfate ((NH₄)₂SO₄), that dried on oven at 110 degree C at 3 hours and cooled over silica gel in desiccater before weighting. Concentration of ammonia in the stock solution was 4,000 μ mole/l for ammonium. These working standards were named N-6, 5,4,3,2,1 and 0 (N-6=0.8, N-5=0.64, N-4=0.4, N-3=0.16, N-2=0.08, N-1=0.032 and N-0=fresh Milli-Q water).

(6) Precision check on each analysis

On each analysis, precision check was done with the working standard N-6. The results of the repeat analysis are summarized in the percent of the concentration level in 0.5 – 1.5%(CV%). (Table 1.)

(7) Preliminary results

Vertical profiles of ammonia each casts are shown in Figure 2.

Table 1-1. The results of repeat analysis for checking the precision each station.

Accuracy (NH ₄ -N)			単位: μ mol/l
Date	St. No.	Cast	STD:N-6
01/16/2003	Station.6	Shallow 1	0.80
			0.79
			0.79
			0.79
			0.80
		average	0.79
		S.D.	0.00
		C.V.(%)	0.48
		adjust-conc.	0.798
accuracy(%)	-0.46		
01/16/2003	Station.6	Shallow 2	0.81
			0.78
			0.79
			0.79
			0.80
		average	0.80
		S.D.	0.01
		C.V.(%)	1.18
		adjust-conc.	0.799
accuracy(%)	-0.39		
01/17/2003	Station.7	Shallow 4-2	0.79
			0.79
			0.80
			0.78
			0.78
		average	0.79
		S.D.	0.01
		C.V.(%)	0.70
		adjust-conc.	0.798
accuracy(%)	-0.99		
01/18/2003	Station.8	Shallow 4-2	0.79
			0.80
			0.81
			0.80
			0.80
		average	0.80
		S.D.	0.01
		C.V.(%)	0.95
		adjust-conc.	0.800
accuracy(%)	-0.01		
01/20/2003	Station.9	Shallow 1	0.82
			0.81
			0.79
			0.80
			0.80
		average	0.81
		S.D.	0.01
		C.V.(%)	1.22
		adjust-conc.	0.798
accuracy(%)	0.97		

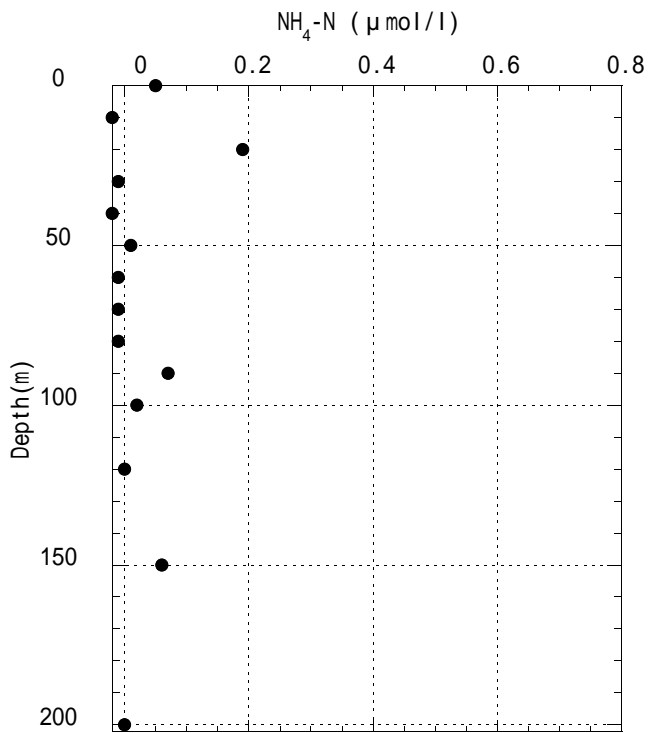
Table 1-2. The results of repeat analysis for checking the precision each station.

Accuracy (NH ₄ -N)			単位: μ mol/l	
Date	St. No.	Cast	STD:N-6	
01/20/2003	Station.9	Shallow 2	0.79	
			0.78	
			0.80	
			0.79	
			average	0.79
			S.D.	0.01
			C.V.(%)	1.18
			adjust-conc. accuracy(%)	0.799 -0.87
01/21/2003	Station.10	Shallow 4-2	0.80	
			0.80	
			0.80	
			0.79	
			0.81	
			average	0.80
			S.D.	0.01
			C.V.(%) adjust-conc. accuracy(%)	0.90 0.799 0.36
01/21/2003	Station.11	Shallow 4-2	0.79	
			0.79	
			0.81	
			0.81	
			0.81	
			average	0.80
			S.D.	0.01
			C.V.(%) adjust-conc. accuracy(%)	1.43 0.798 0.64
01/23/2003	Station.12	Shallow 1	0.81	
			0.80	
			0.81	
			0.81	
			average	0.81
			S.D.	0.01
			C.V.(%) adjust-conc. accuracy(%)	0.72 0.798 1.17
			01/23/2003	Station.12
0.79				
0.80				
0.80				
0.80				
average	0.79			
S.D.	0.01			
C.V.(%) adjust-conc. accuracy(%)	0.67 0.797 -0.62			

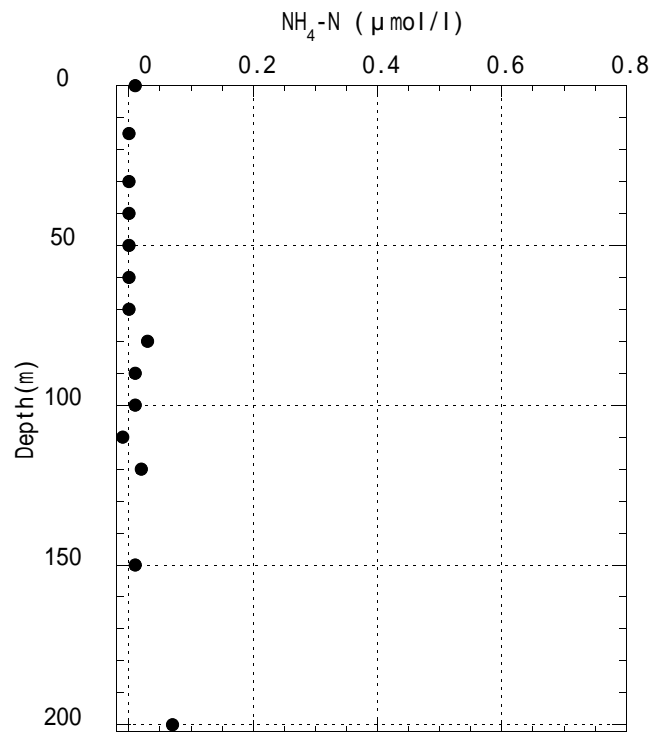
Table 1-3. The results of repeat analysis for checking the precision each station.

Accuracy (NH ₄ -N)			単位: μ mol/l
Date	St. No.	Cast	STD:N-6
01/25/2003	Station.13	Shallow 4-2	0.80
			0.80
			0.81
			0.80
			0.81
		average	0.80
		S.D.	0.01
		C.V.(%)	0.75
adjust-conc.	0.798		
accuracy(%)	0.73		
01/26/2003	Station.14	Deep	0.80
			0.81
			0.81
			0.81
			0.80
		average	0.81
		S.D.	0.01
		C.V.(%)	0.66
adjust-conc.	0.799		
accuracy(%)	0.84		
01/27/2003	Station.14	Shallow 1	0.81
			0.81
			0.79
			0.81
			0.81
		average	0.81
		S.D.	0.01
		C.V.(%)	1.17
adjust-conc.	0.799		
accuracy(%)	0.94		
01/27/2003	Station.14	Shallow 2	0.80
			0.79
			0.78
			0.79
			0.78
		average	0.79
		S.D.	0.01
		C.V.(%)	0.81
adjust-conc.	0.799		
accuracy(%)	-1.03		

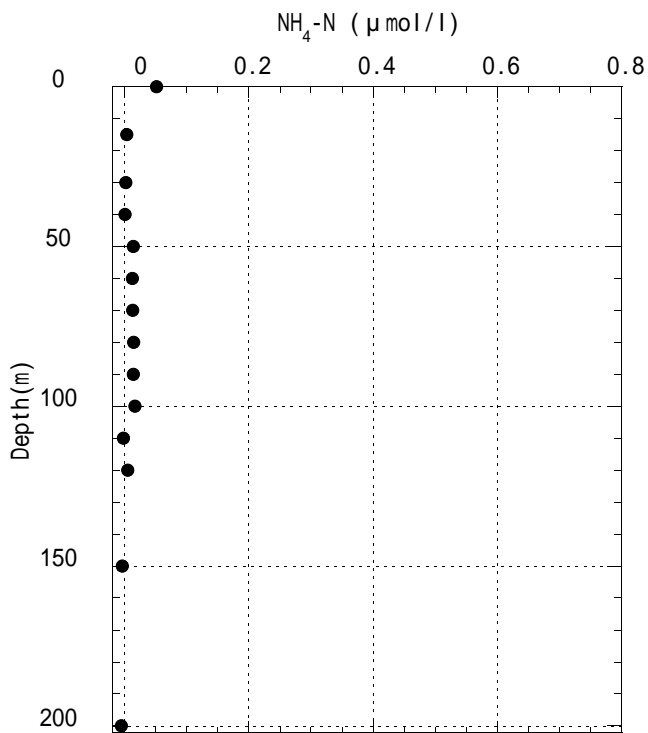
St.6 Shallow Cast 1



St.6 Shallow Cast 2



St.7 Shallow Cast 4-2



St.8 Shallow Cast 4-2

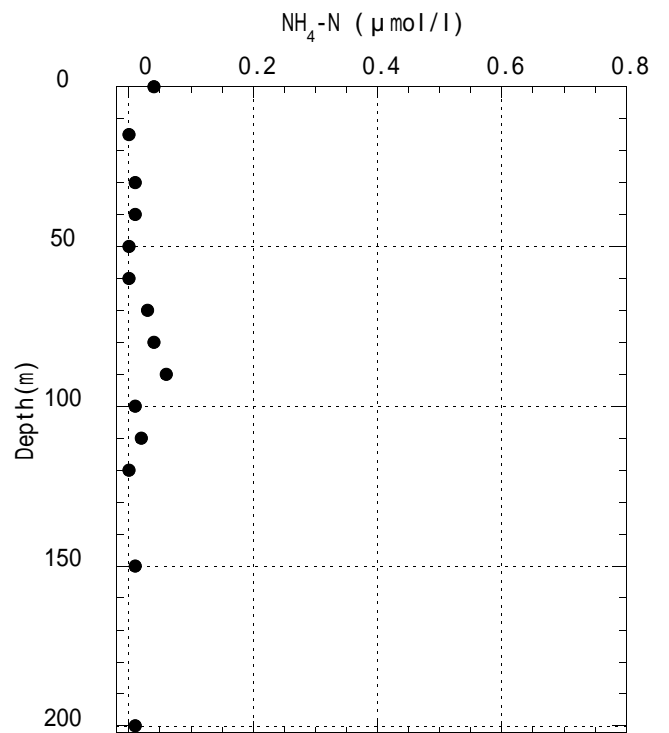
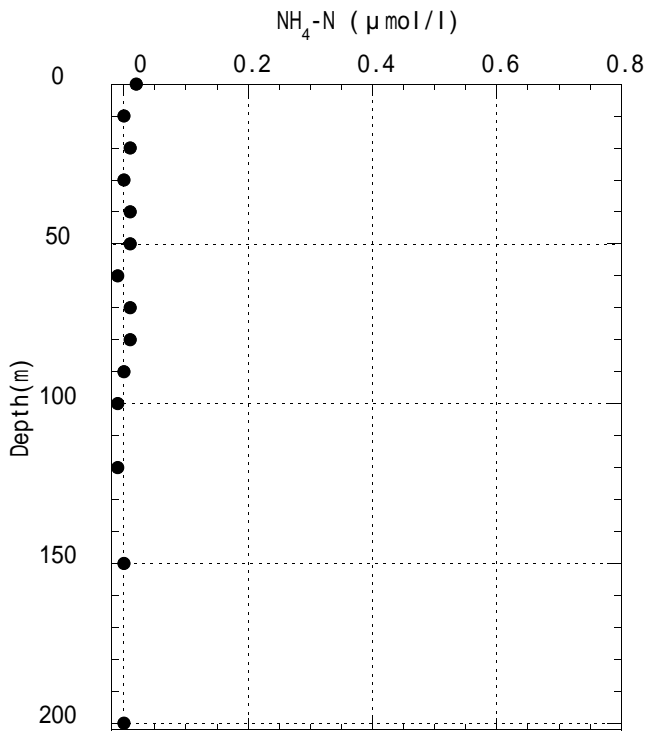
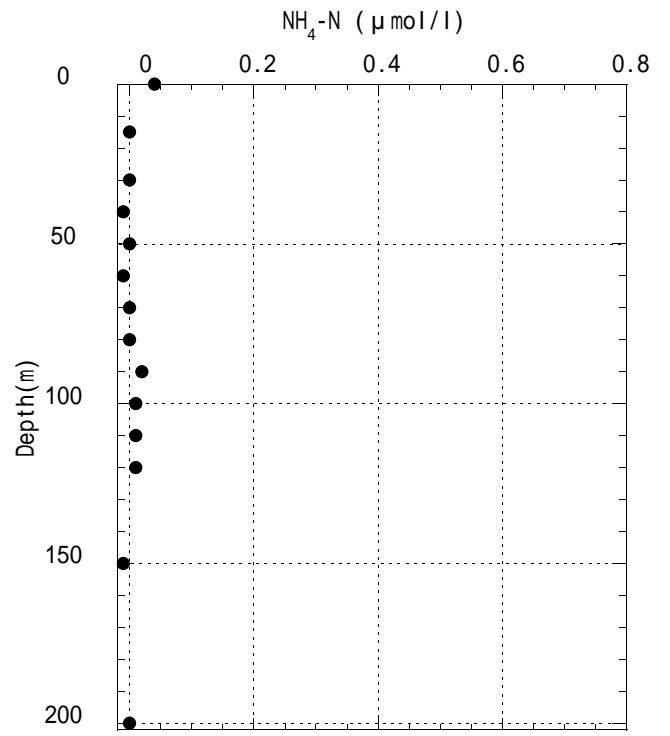


Fig2-1. Vertical profiles of Ammonia in MR02-K06 cruise.

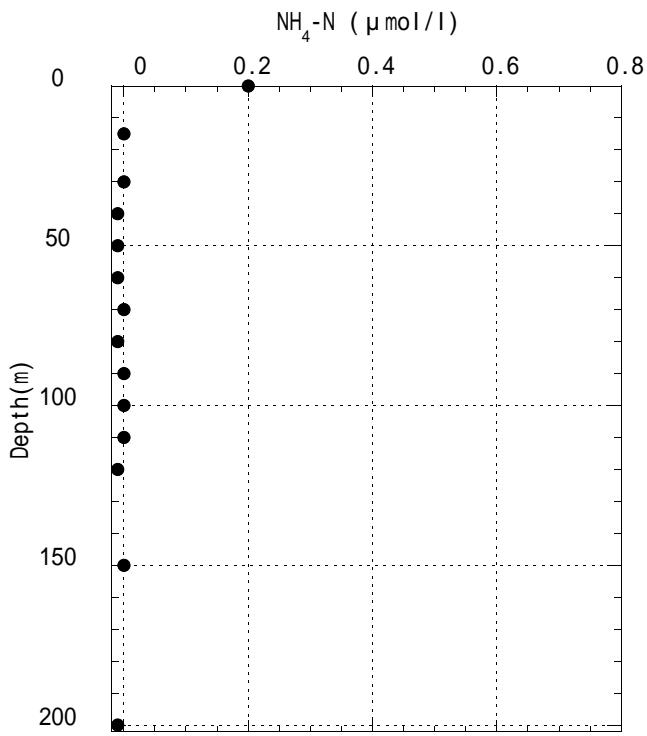
St.9 Shallow Cast 1



St.9 Shallow Cast 2



St.10 Shallow Cast 4-2



St.11 Shallow Cast 4-2

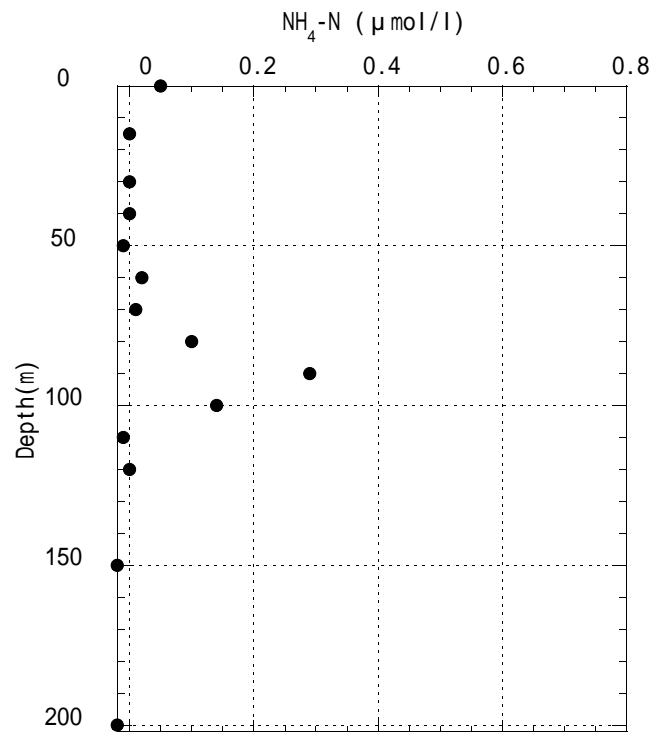
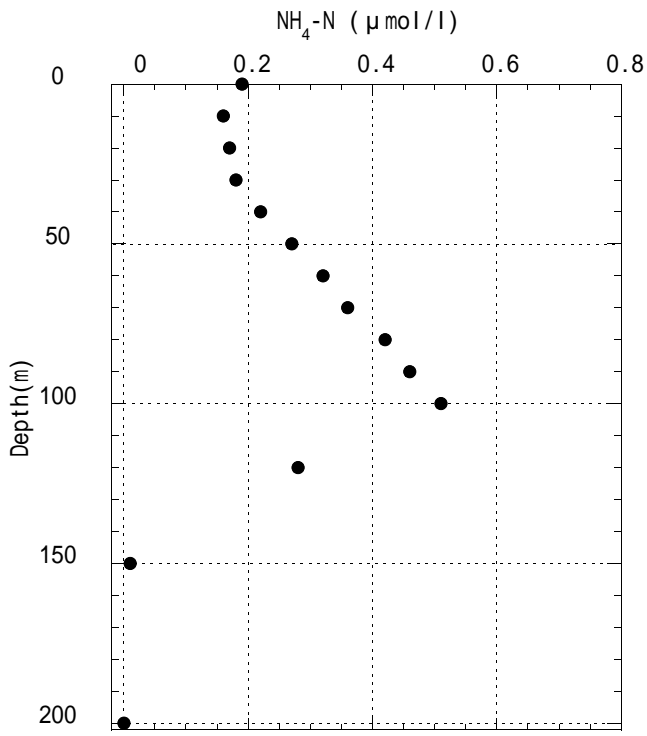
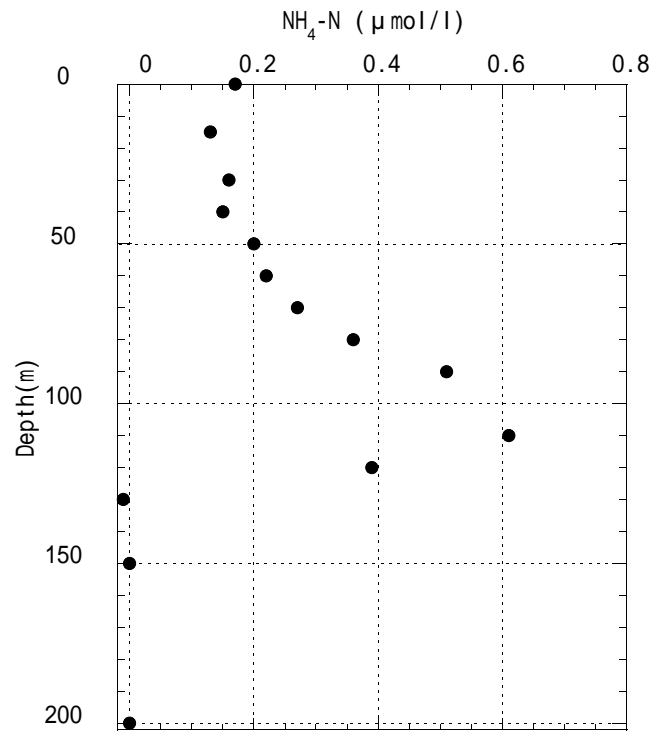


Fig2-2. Vertical profiles of Ammonia in MR02-K06 cruise.

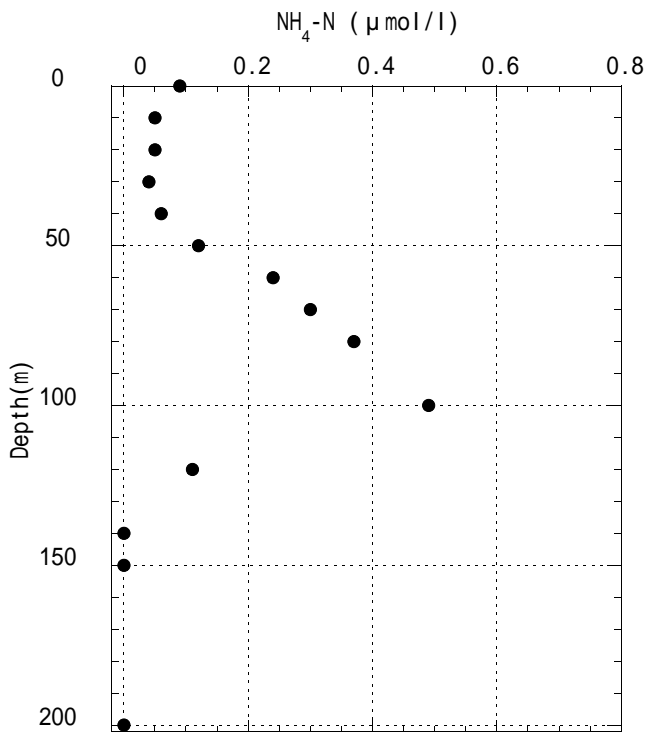
St.12 Shallow Cast 1



St.12 Shallow Cast 2



St.13 Shallow Cast 4-2



St.14 Deep Cast

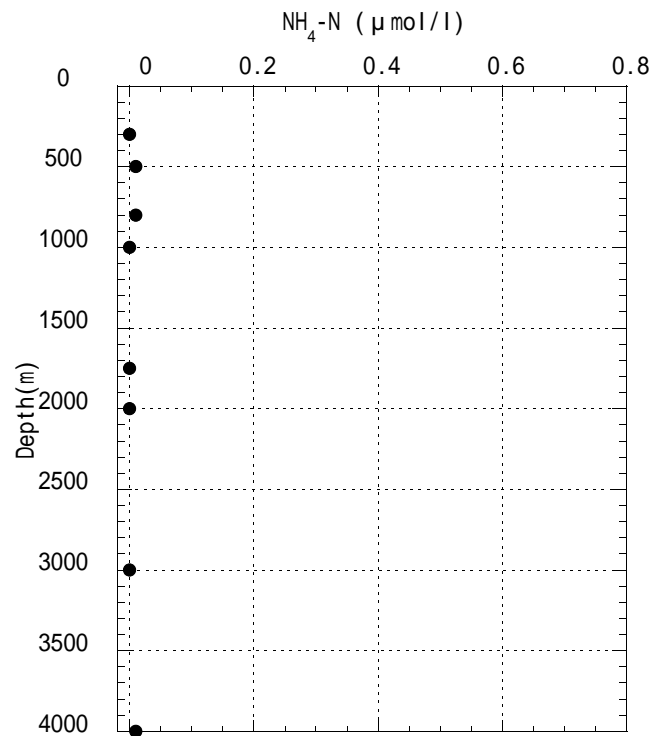
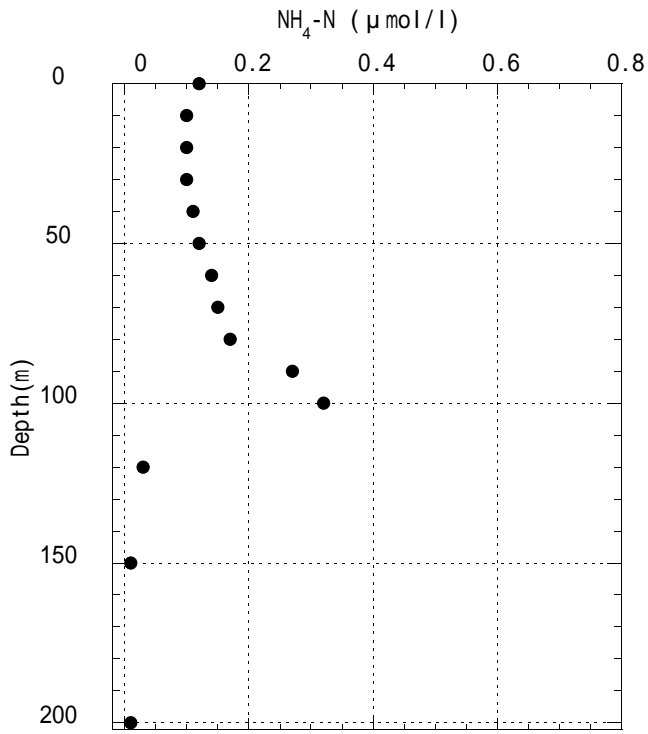


Fig2-3. Vertical profiles of Ammonia in MR02-K06 cruise.

St.14 Shallow Cast 1



St.14 Shallow Cast 2

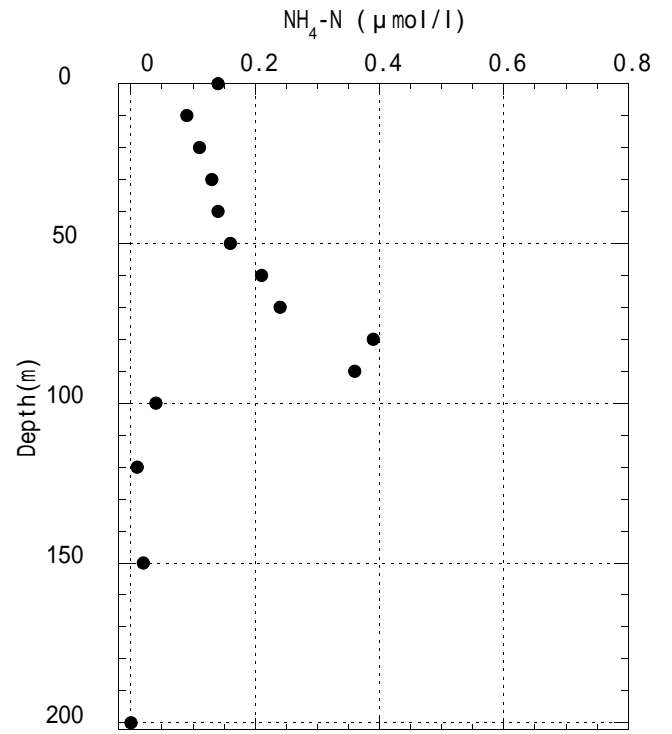


Fig2-4. Vertical profiles of Ammonia in MR02-K06 cruise.

5.4. Phytoplankton pigment analysis

5.4.1. Chlorophyll *a* measurements by fluorometric determination

(1) Personnel

Kazuhiko Matsumoto (JAMSTEC) Principal Investigator (Leg.3)

Keisuke Wataki (Marine Works Japan Ltd.)

Yuichi Sonoyama (Marine Works Japan Ltd.)

Masahiko Nishino (Marine Works Japan Ltd.)

Masato Sugiyama (Marine Works Japan Ltd.)

(2) Objective

The purpose of this study is to estimate the distributions of chlorophyll-*a* in the equatorial Pacific Ocean by fluorometric analysis. Chlorophyll-*a* measurements are carried out with two different type fluorometers (broadband filter type and narrowband filter type). Broadband filter type fluorometer is used in common, but it is recognized the errors related to the acidification technique when chlorophyll-*b* is present. The new non-acidification method was developed by Welschmeyer (1994) with narrowband filter type fluorometer to eliminate the effect of acidification error. Narrowband filter type fluorometer is the same equipment as broadband filter type fluorometer, just changed excitation-emission filters and lamp. A new non-acidification method is not need to consider the acidification error, but the new method yields some overestimate of the true chlorophyll-*a* concentration, especially when chlorophyll-*b* is present.

(3) Materials and Methods

Seawater samples were collected at 9 sampling sites between longitude 160E and 160W in the equatorial Pacific Ocean. The samples were collected 0.5 liter at 14 depths from surface to 200m with Niskin bottles, except for the surface water, which was taken by the bucket. The samples were gently filtrated by low vaccum pressure (<15cmHg) through Nuclepore filters (pore size: 0.4 μ m; diameter: 47mm) in the dark room. Phytoplankton pigments were immediately extracted in 7ml of N,N-dimethylformamide after filtration and then, the samples were stored in the freezer (-20 $^{\circ}$ C) until the analysis of fluorometric determination. The measurements were performed at room temperature after the samples were taken out of the freezer. Traditional acidification and Welschmeyer non-acidification methods were examined for the determinations of chlorophyll-*a* with Turner design model 10-AU-005 fluorometer.

Analytical conditions of two methods are indicated in Table 1, and the distributions of chlorophyll-*a* concentrations between longitude 160E and 160W with Welschmeyer method were showed in Figure 1.

Table 1 Analytical conditions of traditional acidification and Welschmeyer non-acidification methods for chlorophyll-*a* with Turner fluorometer.

	Traditional method	Welschmeyer method
Excitation filter /nm	5-60 (340-500nm)	436nm
Emission filter /nm	2-64 (>665nm)	680nm
Optical kit	10-037R	10-040R
Lamp	Daylight White F4R5D	Blue F4T5, B2/BP (F4T4, 5B2 equiv.)
Acidification	Yes (1M HCL, 1min.)	No

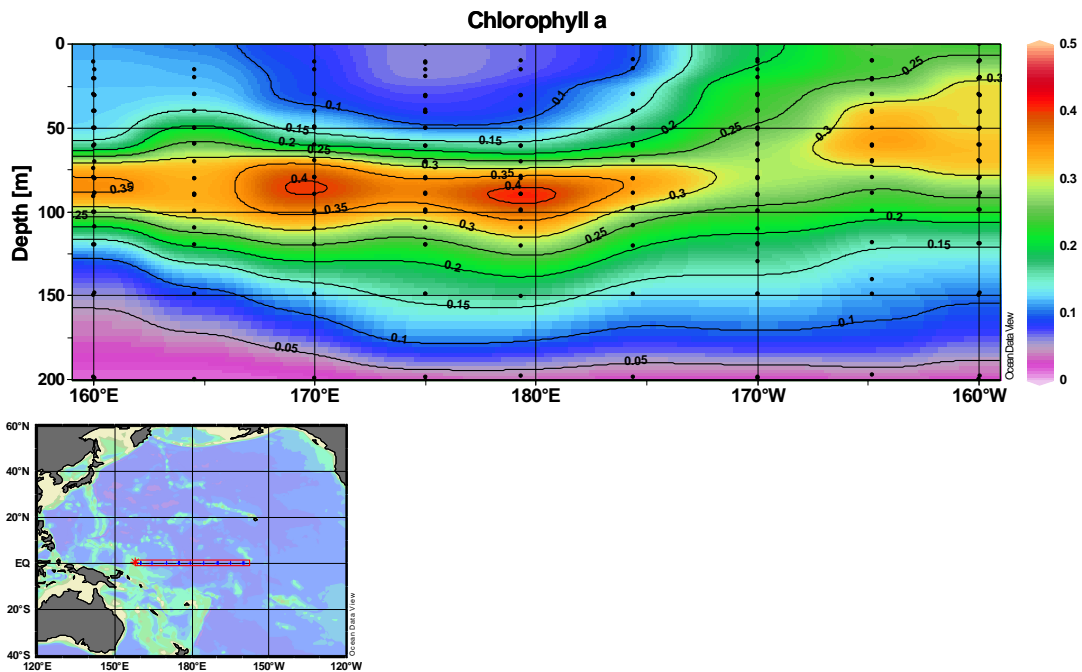


Figure 1 Distributions of chlorophyll-*a* concentrations ($\mu\text{g/L}$) between longitude 160E and 160W in the equatorial Pacific Ocean with Welschmeyer method.

5.4.2. Size fraction of phytoplankton by fluorometric determination

(1) Personnel

Kazuhiko Matsumoto (JAMSTEC) Principal Investigator (Leg.3)

Yuichi Sonoyama (Marine Works Japan Ltd.)

Osamu Kawai (Marine Works Japan Ltd.)

Noriaki Teramae (Marine Works Japan Ltd.)

(2) Objective

Phytoplankton are existed various species and size in the ocean. Phytoplankton species are roughly characterized by the cell size. The purpose of this study is to investigate the vertical distribution of phytoplankton by the size fractionation procedure in the equatorial Pacific Ocean.

(3) Materials and Methods

Seawater samples were collected at 9 sampling sites between longitude 160E and 160W in the equatorial Pacific Ocean. The samples were collected 1 liter at 14 depths from surface to 200m with Niskin bottles, except for the surface water, which was taken by the bucket. The samples were gently vacuum-filtrated (<15cmHg) through the 47mm-diameter 10.0µm mesh filter and Nuclepore filters (pore size of 2.0µm, 1.0µm and 0.4µm) after sampling. Phytoplankton pigments on the filters were immediately extracted in 7ml of N,N-dimethylformamide after filtration. Then, the extracted samples were stored in the freezer (-20 °C) for more than 24 hours before analysis. Chlorophyll-*a* was measured by the fluorometric non-acidification method using the spectrofluorophotometer (SHIMADZU RF-5300PC). Then, we attempted to measure the chlorophyll-*b* by the fluorometric determination.

Analytical conditions of chlorophyll-*a* and chlorophyll-*b* are indicated in Table 1, and the results of size fraction of chlorophyll-*a* were showed in Figure 1.

Table 1 Analytical conditions of chlorophyll-*a* and chlorophyll-*b* with SHIMADZU RF-5300PC.

	Chlorophyll- <i>a</i>	Chlorophyll- <i>b</i>
Excitation wavelength	433nm	461nm
Slit width	3.0nm	3.0nm
Emission wavelength	668nm	652nm
Slit width	5.0nm	5.0nm

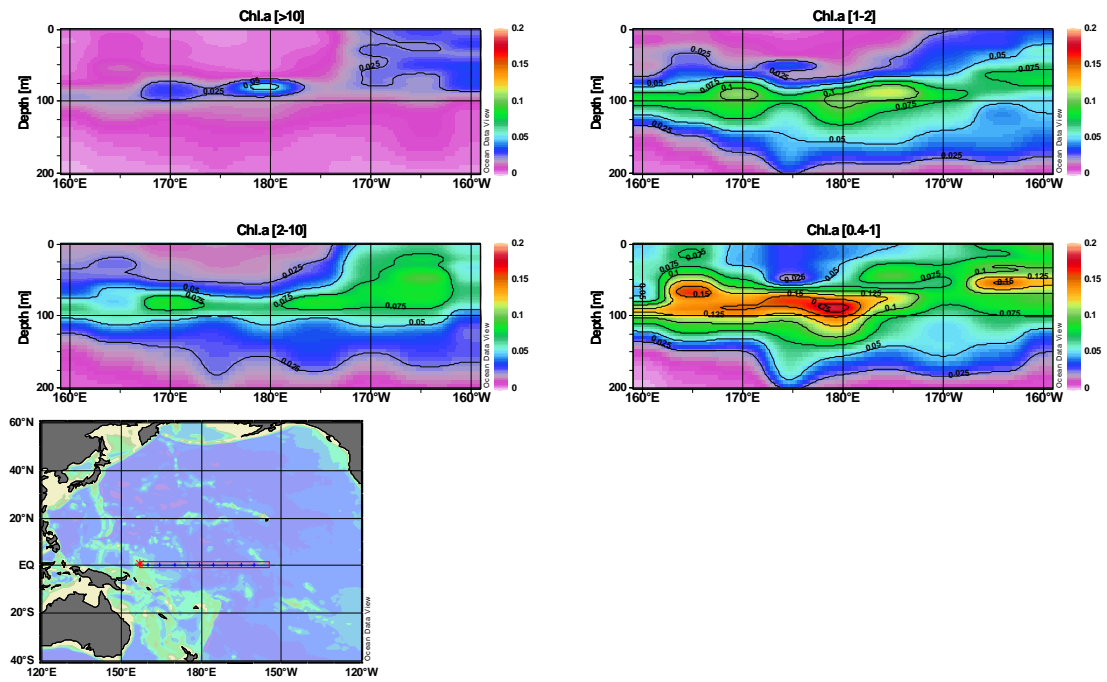


Figure 1 Size fraction of chlorophyll-*a* concentrations ($\mu\text{g/L}$) between longitude 160E and 160W in the equatorial Pacific Ocean.

5.5. The measurement of marine phytoplankton pigments by HPLC.

Keisuke WATAKI (Marine Works Japan Ltd.)

Masato SUGIYAMA (Marine Works Japan Ltd.)

Kazuhiko MATSUMOTO (JAMSTEC)

Objectives

High performance liquid chromatography (HPLC) analysis has been shown to be a conclusive method for separating and quantifying pigments in natural seawater. In this cruise, the marine phytoplankton pigments were analyzed, in order to compare the marine phytoplankton community structure.

Materials and Method

Seawater samples were filtered through a 47 mm diameter Whatman GF/F filters (nominal size 0.7 μm). Sample filters were frozen by liquid nitrogen. It was the remaining seawater in filters to remove by vacuum dry in freezer. Samples were extracted with N,N-dimethylformamid over 24 hours in freezer (-20 deg C). Extracts were then filtered through 25 mm diameter polypropylene syringe filters (0.2 μm pore size) to remove cell and filter debris. They are measured by the two way of HPLC method. As a role of ion-pair reagent, ultra pure water. It was, Canthaxanthin, as the internal standard was added to all samples, it was quickly to inject. It is showed as the following solvents and column system, which is modified the method of Zapata et al (2000).

Solvent A	methanol : acetonitrile : 0.25M pyridine solution = 50 : 25 : 25
Solvent B	acetonitrile : acetone = 80:20
Column	C-8 (Pro C8; YMC,Inc.) 4.6 x 150 mm I.D.

HPLC system is consisted as follows.

Detector	Waters 996 Photodiode Array
Pump	Waters 616
Auto Sampler	Waters 717plus
Column temperature	25degC

The HPLC system is calibrated with the following commercially pigment standards.

Chlorophyll a,b,c ₂ ,c ₃	Diadinoxanthin	Lutein	Fucoxanthin	Alpha-carotene	
Beta-carotene	Neoxanthin	Peridinin	Prasinoxanthin	Alloxanthin	Violaxanthin
19'hexanoyloxyfucoxanthin	19'butanoyloxyfucoxanthin	Canthaxanthin	Zeaxanthin		
Diatoxanthin	Divinyl-chlorophyll-a	Chlorophyllide-a	Lycopene	Crocoxanthin	
Pheophytin-a,b	Antheraxanthin	Canthaxanthin			

(Chlorophyll-a,b and Pheophytin a,b are made by Sigma Chem.Co.. Others are made by VKI.)

Concentrations of pigment standards are determined using a spectrophotometer. Chlorophyll-a and Chlorophyll-b are quantitatively evaluated by drawing the calibration curve using the amount of the standards and their respective chromatogram peak areas. Other pigments are quantitatively evaluated using the formula of JGOFS Protocols (1994). Chlorophyll-a and Chlorophyll-b, Divinyl-chlorophyll-a peak areas are measured by Photodiode Array Detector at each blue maximum wavelength. Others are measured at 440nm.

5.6. Characterization of light absorption coefficients of phytoplankton

(1) Personnel

Kazuhiko Matsumoto (JAMSTEC) Principal Investigator (Leg.3)

Yuichi Sonoyama (Marine Works Japan Ltd.)

(2) Objective

The spectral characteristics of phytoplankton absorption coefficients ($a_{ph}^*(\lambda)$) are essential parameters for bio-optical models to predict the carbon fixation rates, the heating rate of the upper ocean and the light propagation within the ocean and ocean color. The purpose of this study is to characterize the spectral absorption of phytoplankton in the equatorial Pacific ocean.

(3) Materials and Methods

Seawater samples were collected 3 liters at 14 depths from surface to 200m. Seawater samples were gently filtrated through 25 mm Whatman GF/F filters under low vacuum pressure (<15cmHg). Sample filters were stored in the deep freezer (-80°C) before the absorption measurements. Optical densities of the particulates retained on the filter ($OD_f(\lambda)$) were measured using the quantitative filter technique (QFT) based on the glass fiber filter technique, and Shimadzu MPS-2400 multi-purpose spectrophotometer, equipped with an end-on photomultiplier, was used. To determine the optical density of unpigmented detrital particles, the pigments of filters were extracted by methanol for 1 hour and washed by distilled water. Then, hot water (80°C) was added for 30 minutes to eliminate phycobiliprotein that is the water-soluble pigment and washed by filtrated seawater. The measurements $OD_f(\lambda)$ were converted to the equivalent optical densities of suspension ($OD_s(\lambda)$) using the formula to correct the path length amplification effect. In this study, we applied the correlation formula of Allali *et al.*(1997).

$$OD_s(\lambda) = 0.264 OD_f(\lambda) + 0.322 OD_f(\lambda)^2$$

The absorption coefficient of particles ($a_p(\lambda)$, (m^{-1})) and decolorized particulate matters ($a_d(\lambda)$, (m^{-1})) are computed from the corrected optical densities $OD_s(\lambda)$, according to

$$a_{p/d}(\lambda) = 2.3 \times OD_{sp/sd}(\lambda) / L; (L = V / S)$$

Where, S is the clearance area of the filter (m^2) and V is the volume of seawater sample (m^3). The subtraction of a_d from a_p shows the spectral absorption coefficient of the living phytoplankton ($a_{ph}(\lambda)$).

$$a_{ph}(\lambda) = a_p(\lambda) - a_d(\lambda)$$

Finally, the absorption coefficients of living phytoplankton ($a_{ph}(\lambda)$) were converted into chl-*a* specific absorption coefficients ($a_{ph}^*(\lambda)$) by normalizing to the sum of chlorophyll *a* and dibinyl chlorophyll *a* concentrations.

5.7. Phytoplankton abundances

(1) Personnel

Kazuhiko Matsumoto (JAMSTEC)

(2) Objectives

The main objective of our study is to clarify the relations with distribution, abundance and primary productivity of phytoplankton in the equatorial Pacific. The equatorial Pacific was distinguished spatially with hydrological condition to two major regions, where are the regions of the warm pool and the upwelling. Primary productivity is greatly different in each region, in addition, phytoplankton dominant species and the abundances are also different in each region. Primary productivity is cell-specific, phytoplankton abundance and distribution of each cell is very useful and important information to clarify the mechanism of primary productivity. We measured phytoplankton abundances with two kinds of methods: microscopy for large size phytoplankton and flowcytometry for picophytoplankton.

(3) Materials and Methods

1) Microscopy

Water samples were placed in 5000 ml plastic bottle and fixed with neutral buffered formalin solution (3% final concentration). The measurements will be scheduled at Marine biological research institute of Japan co.,ltd.

2) Flowcytometry

2)-1 Equipment

The flowcytometry system used in this research was BRYTE HS system Bio-Rad Laboratories Inc. System specification were follows:

Light source: 75W Xenon arc lamp

Excitation wavelength: 350-650 nm

Detector: high-performance PMT

Analyzed volume: 75 μ l

Flow rate: 10 μ l min⁻¹

Sheath fluid: Milli-Q water

Filter block: B2 as excitation filter block, OR1 as fluorescence separator block

B2 and OR1 have ability as follows:

B2:	Excitation filter	390-490 nm
	Beam-splitter	510 nm
	Emission filter	515-720 nm
OR1:	Emission filter 1	565-605 nm
	Beam-splitter	600 nm
	Emission filter 2	>615 nm

2)-2 Sampling

Water samples were immediately filtered with 10 μm filter which mounted with filter holder, and placed in 50 ml poly-carbonate bottle.

2)-3 Measurements

Before 30 min of measurement, the power of flowcytometer was turned on (for warm up). Internal standard beads were added before measurement. Water sample (75 μl) was run on the flowcytometer. After the measurement, the sample was fixed with glutaraldehyde (1% final concentration) for 10 min, then measured again. The analysis will be scheduled at JAMSTEC, Yokosuka.

5.8. Distribution of heterotrophic microflagellates and ciliates

(1) Personnel

Kazuhiko MATSUMOTO (JAMSTEC)

(2) Objectives

Autotrophic picoplankton (0.2-2.0 μ m) and nanoplankton (2.0-20 μ m) are major contributors to phytoplankton biomass and primary production in the equatorial Pacific. Heterotrophic microflagellates and ciliates play important role in the microbial food web as grazer of picoplankton and nanoplankton. The purpose of this study is to estimate the abundance of heterotrophic microflagellates and ciliates as grazer of phytoplankton by using fluorescence microscopy.

(3) Materials and Methods

Seawater samples were collected at twelve sampling sites between longitude 160E and 160W in the equatorial Pacific. The samples were collected at 13 depths from the depth of surface to 200m. Seawater samples were immediately treated with the final concentration of 1 % glutaraldehyde and were kept at room temperature (1 hour). Glutaraldehyde treated seawater samples were filtered through a 1 μ m pore size Nuclepore filter, pre-stained by irgalan black, at the low vacuum of < 15 cmHg. Seawater samples were double-stained with DAPI (4'-6-diamidino-2-phenylindole dihydrochloride) for the staining of DNA, and proflavine (3-6-diamidino-acridine hemisulfate) for the staining of flagella. The working solution of DAPI (10 μ g/ml) and proflavine (0.033 %) were pre-filtrated through 0.22 μ m pore size of non-pyrogenic Durapore membrane filter (Millipore, Millex-GX). At the fluorescence microscopy, heterotrophic plankton are distinguished with autotrophic plankton, because cells of autotrophic plankton are seen as orange and /or red by the autofluorescence of pigments.

The staining method was as follows;

When the seawater remained approximately 10 ml in the funnel on the filtration procedure, seawater samples were stained with the working solution of DAPI (1 ml). After 5 minutes, those were stained with the working solution of proflavine (0.4 ml) for 5 minutes. Then, seawater samples were filtered. Sample filters were put on a slide-glass with one drop of immersion oil, and covered with micro cover glass, which were stored in the deep freezer (-85 °C) until the observation.

Analysis will be scheduled at the laboratory (Marine Biological Research Institute of Japan Co., LTD., Shinagawa, Tokyo) as the selected 85 samples.

5.9. Primary productivity

Ai YASUDA 1), Taeko OHAMA 1), Toshiko Nakasima 1)

1) Marine Works Japan LTD

Objectives

The objective of this study is to know the mechanism of primary production at the open sea on the equator.

(1) In-situ Incubation

Bottles for incubation and filters

Bottles for incubation are ca. 1 liter Nalgen polycarbonate bottles with screw caps. Grass fiber filters (Wattman GF/F 25mm) pre-combusted under 450 degree C of temperature for at least 6 hours, were used for a filtration.

Incubation

In-situ incubation for 12 hours were executed at station before incubated St. 6,9,12 and 14. We took two transparent bottles samples from 13 layers took from 150m depth (every 10m from surface to 100m, 120m and 150m depth and moored these samples at each depth for 12 hours, after mooring all samples incubated in bath on deck 12 hours). All the samples were spiked with 0.2 mmoles/mL of $\text{NaH}^{13}\text{CO}_3$ solution just before mooring. Samples were filtered immediately after the incubation and the filters were kept frozen till analyze of this cruise. After that, filters were dried on the oven of 45 degree C.

Measurement

During the cruise, all samples will be made to measure by a mass spectrometer ANCA-SL system at MIRAI and JAMSTEC.

(2) Simulated in-situ incubation

Bottles for incubation and filters

Bottles for incubation are ca. 1 liter Nalgen polycarbonate bottles with screw caps. Grass fiber filters (Wattman GF/F 25mm) pre-combusted with temperature of 450 degree C for at least 6 hours, were used for a filtration.

Simulated in-situ incubation

We took four samples from the surface and one predefined depth by a bucket and Niskin bottles at St. 7,8,10,11 and 13. The depth corresponded to nominal specific optical. All samples were spiked with 0.2 mmoles/mL of $\text{NaH}^{13}\text{CO}_3$ solution. After spike, bottles were placed into incubators by neutral density filters corresponding to nominal light levels at the depth at which samples were taken. Samples were incubated in a bath on the deck for 24 hours.

Samples were filtered through the 47mm-diameter 10.0 μ m mesh filter and Nuclepore filters (pore size of 3.0 μ m and 1.0 μ m) , all samples were filtered through Grass fiber filters (Wattman GF/F 25mm) immediately after the incubation. Phytoplankton pigments on the filters were immediately extracted in 7ml of N,N-dimethyl formamide after filtration and GF/F filters were kept to freeze till analyse of this cruise. After that, filters were dried on the oven of 45 degree C.

Measurement

During the cruise, all samples will be made to measure by a mass spectrometer ANCA-SL system at MIRAI and JAMSTEC.

5.10. Distribution of microplankton (>15 µm) along the Western Equatorial Pacific Ocean in winter 2003

Fernando GOMEZ and Ken FURUYA

Department of Aquatic Biosciences, Graduate School of Agriculture and Life Sciences,
The University of Tokyo, 1-1-1 Yayoi, Bunkyo, Tokyo 113-8657, Japan.

Objectives

Two sampling strategies were applied during the cruise MR02-K066 in order to achieve the next objectives:

From non-concentrated seawater samples collected at discrete depths along the western Equatorial Pacific Ocean, the composition and abundance of microplankton (>15 µm) will be analysed. This includes the characterization of the assemblages (vertical and latitudinal distribution), mainly diatoms, dinoflagellates and tintinnids at species level and other groups as naked ciliates at supra-generic levels. The comparison with physical-chemical variables will determinate the ecological characteristic of the species. Also from the comparison with previous studies in the area, the consequences of phenomenon as El Niño/La Niña events in the structure of the microplankton communities will be evaluated.

Seawater samples for epifluorescence analysis were collected from the surface waters from all the stations in the Equatorial Pacific and also periodically (each 8 hours) during the transit to Japan. The objective is focused on the analysis of the association phytoplankton-symbiotic cyanobacteria in the surface waters. Determination of the taxa that potentially present symbiotic nitrogen fixers as well the abundance of symbionts per cell and the relationship to the environmental factors at a large-scale. The incidence of nitrogen fixation by symbiotic cyanobacteria in the NW Pacific Ocean will be indirectly estimated. Additionally from all these samples cannot be excluded that description of new taxa or new information about the distribution of rare or insufficiently known species.

Material and methods

- 1) Along the western Equatorial Pacific Ocean, 500 ml non-concentrated sea-samples were collected from discrete depths (12-13) from the surface to 200 m depth. Samples were fixed with Lugol's acid and keep in dark and cold conditions until further analysis at the laboratory.

- 2) At each station visited in the western Equatorial Pacific and further each 8 hours along the transect Equator-Hawaii-Japan, concentrated sea water samples were collected from the surface (5 m depth):
 - a) 5 l of seawater were filtered through a 10 μm pore size Nylon mesh to a final volume of 500 ml and preserved according to the previous protocol.
 - b) 5 l of seawater were also filtered through a 10 μm pore size Nylon mesh to a final volume of 10 ml, preserved with diluted glutaldehyde and kept at $-80\text{ }^{\circ}\text{C}$.

At the laboratory, Lugol-preserved seawater samples (both concentrated and non concentrated) will be settled and analysed following the Utermöhl technique by using an inverted microscope. Concentrated samples kept at a very low temperature will be analysed with an epifluorescence microscope.

5.11. Study on the biogeography of the coccolithophorid assemblage in the Western and Central Equatorial Pacific Ocean

Yuichiro TANAKA*¹, Miyuki Ota*² and Tatuya Sinmura*³

*¹: National Institute of Advanced Industrial Science and Technology.

AIST Tsukuba Central 7, 1-1-1 Higashi, Tsukuba, Ibaraki, Japan

*²: Graduate School of Science, Tsukuba University,

*³: Graduate School of Science, Hokkaido University

Introduction

Coccolithophorids are one of the important primary producers in the tropical warm ocean. Due to the production of extra cellular calcium carbonate scales (coccoliths), coccolithophorids contribute to the export flux of calcium carbonate from the sea surface to the sea floor. The standing crop and the floral composition of coccolithophorids are controlled by the topography and surface water circulation. Surface currents of the Equatorial Pacific Ocean is characterized by the westward North and South Equatorial Currents and the eastward Equatorial Counter Current. Strength of the westward transportation and the oceanographic setting are controlled by Asian Monsoon and El Nino and the Southern Oscillations (ENSO). In the Normal and La Nina phases of ENSO, stratified Western Pacific Warm Pool (WPWP) develop in the Western Equatorial Pacific due to the strong westward transportation of surface warm waters by the North and South Equatorial Currents. In the Eastern Equatorial Pacific, deep water upwells to replace the lost surface water. Therefore, strength of stratification is different between the Eastern and Western Equatorial Pacific Ocean. In the El Nino phase of ENSO, westward surface transportations is weakened, and the warm surface waters that piled up in the western Pacific during the Normal and La Nina phase flow back to the east. As a result, Central and Eastern Equatorial Pacific get stratified as well as Western Equatorial Pacific. Coccolithophorids in the Equatorial Pacific Ocean has been studied by several researchers, however, effect of environmental changes caused by ENSO on the coccolithophorid flora has not been revealed, yet. In this study, we will try to clarify the environmental control on the primary production and floral composition of coccolithophorid assemblage.

Materials and Method

For the study of the standing crop and floral composition of the coccolithophorid assemblage, surface water samples were taken during the cruises from Chuk to the site 14 and from Honolulu to Japan by using a water pump. Subsurface water samples were collected in the 9 stations by using Niskin bottles (Table 1). Immediately after sampling, 8 liter of water samples were filtered onto Millipore filter with a pore size of 0.45 μm . Filters were then air-dried by the automatic desiccator. In the laboratory, the absolute abundance and floral composition of coccolithophorid assemblage will be studied under a cross-polarized light microscope and SEM, respectively.

Table 1-a Location of samples and sampling data on the surface waters

Sample no.	Date	Time(LST)	Time(UTC)	Latitude	Longitude1	水温(RMT)	水温(SBE)	塩分(SAL)	Water(l)
1	14 Jan. 2003	8:08	22:08	04-57,681N	156-04,172E	28,469		34,411	8
2	14 Jan. 2003	18:00	8:00	03-33,029N	157-10,617E	29,185		34,541	8
3	15 Jan. 2003	7:56	20:56	00-51,401N	159-18,615E	29,264	29,311	34,480	8
4	15 Jan. 2003	18:00	7:00	00-01,127S	160-02,431E	29,345	29,397	34,451	8
5	16 Jan. 2003	18:15	7:15	00-01383N	160-10,194E	29,378	29,436	34,469	8
6	17 Jan. 2003	8:15	21:15	00-00,854N	163-51,391E	29,400	29,450	34,435	8
7	17 Jan. 2003	18:00	7:00	00-00,427S	165-70,990E	29,402	29,455	34,265	8
8	18 Jan. 2003	8:00	21:00	00-00,190N	169-16,876E	29,318	29,361	33,960	8
9	18 Jan. 2003	18:13	7:13	00-03,533S	171-06,547E	29,797	29,850	33,966	8
10	19 Jan. 2003	7:54	19:54	00-04,895S	174-21,450E	29,294	29,354	33,997	8
11	19 Jan. 2003	18:00	6:00	00-00,095S	174-59,820E	29,225	29,316	33,797	8
12	20 Jan. 2003	18:00	6:00	00-02,462N	175-05,473E	29,337	29,389	33,853	8
13	21 Jan. 2003(A)	8:00	20:00	00-00,457S	178-36,591E	29,497	29,543	33,954	8
14	21 Jan. 2003(A)	18:00	6:00	00-01,315S	179-42,114W	30,005	30,038	34,093	8
15	21 Jan. 2003(B)	8:00	20:00	00-00,248S	176-16,843W	29,980	30,020	34,122	8
16	21 Jan. 2003(B)	18:00	6:00	00-00,332N	174-36,031W	30,136	30,183	34,292	8
17	22 Jan. 2003	8:00	19:00	00-00,744S	171-25,707W	29,785	29,837	35,028	8
18	22 Jan. 2003	18:00	5:00	00-00,563N	170-02,785W	29,375	29,423	35,321	8
19	23 Jan. 2003	18:20	5:20	00-02,703N	170-00,633W	29,440	29,495	35,296	8
20	24 Jan. 2003	8:09	19:09	00-00,075S	169-59,661W	29,193	29,244	35,310	8
21	24 Jan. 2003	18:00	5:00	00-00,158S	168-42,216W	29,338	29,389	35,329	8
22	25 Jan. 2003	8:00	19:00	00-00,646S	165-25,917W	28,990	29,036	35,234	8
23	25 Jan. 2003	18:00	5:00	00-00,180N	163-51,498W	28,790	28,843	35,333	8
24	26 Jan. 2003	8:00	19:00	00-00,060N	160-42,785W	28,269	28,319	35,379	8
25	26 Jan. 2003	18:01	5:01	00-00,892N	159-59,727W	28,366	28,424	35,356	8
26	27 Jan. 2003	18:00	5:00	00-04,218N	159-58,358W	28,374	28,435	35,356	8
27	28 Jan. 2003	8:00	18:00	03-30,348N	159-39,778W	28,148	28,192	34,706	8
28	28 Jan. 2003	18:00	4:00	06-07,319N	159-21,996W	28,662	28,707	34,671	8
29	29 Jan. 2003	8:00	18:00	09-37,782N	159-02,320W	27,015	27,057	34,024	8
30	29 Jan. 2003	18:01	4:01	12-12,268N	158-45,556W	26,268	26,336	34,237	8
31	30 Jan. 2003	8:00	18:00	15-49,298N	158-24,709W	25,304	25,396	34,961	8
32	30 Jan. 2003	18:00	4:00	17-48,851N	158-14,488W	25,184	25,251	34,505	8
33	31 Jan. 2003	8:01	18:01	20-20,848N	157-59,870W	24,435	24,497	35,229	8
34	2 Feb. 2003	18:01	4:01	22-32,671N	162-37,869W	24,282	24,377	35,341	8
35	3 Feb. 2003	8:00	19:00	25-20,776N	165-44,485W	22,153	22,231	35,409	8
36	3 Feb. 2003	18:00	5:00	26-35,948N	168-12,295W	20,612	20,656	35,302	8
37	4 Feb. 2003	8:00	20:00	28-16,760N	171-48,505W	19,071	19,157	35,198	8
38	4 Feb. 2003	18:00	6:00	29-13,680N	174-01,006W	19,092	19,185	35,195	8
39	5 Feb. 2003	8:00	20:00	29-14,691N	175-53,827W	18,348	18,494	35,029	8
40	5 Feb. 2003	18:00	6:00	30-05,924N	177-38,871W	18,177	18,300	34,929	8
41	7 Feb. 2003	8:00	20:00	31-55,652N	179-13,814E	17,244	17,357	34,770	8
42	7 Feb. 2003	18:42	6:42	32-54,017N	176-16,449E	16,011	16,119	34,636	8
43	8 Feb. 2003	8:03	21:03	32-58,866N	173-14,386E	17,169	17,276	34,706	8
44	8 Feb. 2003	18:01	7:01	32-59,316N	171-07,231E	17,320	17,425	34,734	8
45	9 Feb. 2003	8:00	21:00	32-57,842N	168-36,879E	17,137	17,245	34,749	8
46	9 Feb. 2003	18:00	7:00	33-12,984N	167-00,140E	17,314	17,406	34,749	8
47	10 Feb. 2003	8:03	22:03	34-17,568N	163-44,014E	17,358	17,488	34,758	8
48	10 Feb. 2003	18:00	8:00	35-04,413N	161-05,560E	13,461	13,573	34,504	8
49	11 Feb. 2003	8:00	22:00	36-18,957N	150-53,600E	16,528	16,728	34,764	8
50	11 Feb. 2003	18:00	8:00	37-12,198N	153-47,102E	12,699	12,835	34,428	8
51	12 Feb. 2003	8:00	23:00	38-29,057N	149-10,706E	10,590	10,775	34,249	8
52	12 Feb. 2003	17:30	8:30	39-14,805N	146-25,654E	2,503	2,609	33,183	8

5.12. Distribution of diatoms in sea-surface waters in the western and central equatorial Pacific

Kota Katsuki and Daisuke Matsueda (Kyushu Univ.)

Objectives

Diatoms, which constitute one of the major primary producer groups, can be used as indicators of environmental parameters such as temperature, salinity and nutrient concentrations of the sea-surface waters. The study on the diatom assemblage distribution will enhance our basic understanding of other research such as on marine sediment and sinking particle fluxes. These researches will provide us with appreciation for past and present marine environment. The propose of this study is to characterize the relationship between diatom distribution and marine environmental conditions.

Methods

The samples were obtained from sea surface waters (5 m depth) in the western and central equatorial Pacific using a shipboard pump. They were collected at about 3 hours after sunrise every morning and at about 3 hours after sunset every evening during 8 January - 11 February 2003. Two to three liters of the samples were filtered through Gelman R membrane filter of 47 mm diameter with nominal pore size of 0.45 μ m. The filtered samples were desalted with distilled water and dried for one day. After MR02-K06 Cruise is completed, the filtered samples will be permanently mounted on microslides with Canada Balsam and will be examined in the shore laboratory at Kyushu University for further analysis.

5.13. Distribution of planktic foraminifera in the surface water in western the Pacific Ocean.

Akira Sasaki (Tohoku University)

Objective:

The purposes of this study are (1) to reveal the distribution pattern of planktic foraminifera in the surface water in the Pacific Ocean, and (2) to investigate the intensity of upwelling or downwelling in the western Pacific Ocean by measuring the difference of oxygen isotope values of foraminiferal tests.

Methods:

Plankton samples were collected from the 14th of January to the 12th of February 2003, during the R. V. MIRAI cruise MR02-K06. A continuous set of samples was obtained with an on-board surface water pump. Seawater samples (1-3 m³) were filtered through a 75 μ m mesh screen in the morning and/or evening. Planktonic organisms collected on the mesh were then preserved in approximately 50 % Ethanol.

The planktic foraminiferal specimens will be identified, and the oxygen isotope of the tests will be measured in the laboratory.

5.14. Distributions of planktic foraminifera and radiolarians in the Equatorial Pacific Ocean.

Akira Sasaki (Tohoku University), Kota Katsuki, Daisuke Matsueda (Kyushu University)

Objective:

Plankton samples were collected by a plankton net at the site of St.6, St.9, St.12 and St.14 in the Equatorial Pacific. The purpose of this study is to clarify vertical and horizontal distribution patterns, depth habitats and standing stocks of planktic foraminifera and radiolarians in the Equatorial Pacific Ocean.

Methods:

Samples were obtained by a closing type plankton net, 0.75 m in diameter, 3.5 m in length and 63 μ m in mesh size. This net can be closed by sending a messenger at a decided depth while the net was towing upward. Depth intervals of samplings were 0-20 m, 20-40 m, 40-80 m, 80-120 m, 120-160 m, 160-200 m, 200-500 m and 500-1,000 m.

Samples were preserved in seawater filtered through a screen with an opening of 63 μ m with 4 % formalin solution buffered to pH 7.6 by sodium tetraborate. And a protoplasm of plankton was dyed by Rose Bengal in order to examine which plankton was living or dead.

Samples had been kept at 4-5 °C.

Specimens of planktic foraminifera and radiolaria will be identified and counted in the laboratory.

5.15. Continuous monitoring of surface seawater

5.15.1. Integrated monitoring system of surface seawater

(1) Name & Affiliation

Tomoko MIYASHITA (Marine Works Japan LTD.)

(2) Objective

In order to measure salinity, temperature, dissolved oxygen, and fluorescence of near-sea surface water.

(3) Methods

EPCS (Nippon Kaiyo co.,Ltd.) has five kind of sensors and fluorescence photometer and can automatically measure salinity, temperature, dissolved oxygen, fluorescence and particle size of plankton in near-sea surface water continuously on real time every 1-minute. This system is located in the “*sea surface monitoring laboratory*” on R/V *Mirai*. This system is connected to shipboard LAN-system. Measured data is stored in a hard disk of PC machine every 1-minute together with time and position of ship, and displayed in the data management PC machine.

Near-surface water was continuously pumped up to the laboratory and flowed into the *EPCS* through a vinyl-chloride pipe. The flow rate for the system is controlled by several valves and was 12L/min except with fluorometer (about 0.3L/min). The flow rate is measured with two flow meters and each values were checked everyday.

Specification of the each sensor in this system of listed below.

a) Temperature and Salinity sensor

SEACAT THERMOSALINOGRAPH

Model: SBE-21, SEA-BIRD ELECTRONICS, INC.

Serial number: 2126391-3126

Measurement range: Temperature -5 to +35°C, Salinity 0 to 6.5 S m-1

Accuracy: Temperature 0.01 °C 6month-1, Salinity 0.001 S m-1 month-1

Resolution: Temperatures 0.001°C, Salinity 0.0001 S m-1

b) Bottom of ship thermometer

Model: SBE 3S, SEA-BIRD ELECTRONICS, INC.

Serial number: 032607

Measurement range: -5 to +35°C

Resolution: ±0.001°C

Stability: 0.002 °C year-1

c) Dissolved oxygen sensor

Model: 2127A, Oubisufair Laboratories Japan INC.

Serial number: 44733

Measurement range: 0 to 14 ppm
Accuracy: $\pm 1\%$ at 5 °C of correction range
Stability: 1% month-1

d) Fluorometer

Model: 10-AU-005, TURNER DESIGNS
Serial number: 5562 FRXX
Detection limit: 5 ppt or less for chlorophyll a
Stability: 0.5% month-1 of full scale

e) Particle Size sensor

Model: P-05, Nippon Kaiyo LTD.
Serial number: P5024
Measurement range: 0.02681 mmt to 6.666 mm
Accuracy: $\pm 10\%$ of range
Reproducibility: $\pm 5\%$
Stability: 5% week-1

f) Flow meter

Model: EMARG2W, Aichi Watch Electronics LTD.
Serial number: 8672
Measurement range: 0 to 30 l min-1
Accuracy: $\pm 1\%$
Stability: $\pm 1\%$ day-1

The monitoring Periods (UTC) during this cruise are listed below.

Leg.3 13-Jan.-'03 10:57 to 31-Jan.-'03 18:41

Leg.4 02-Feb.-'03 20:56 to 12-Feb.'03 08:35

(4) Preliminary Result

The profiles of temporal variation of the salinity were shown in Fig.5.15.1-1 and -2.

The profiles of temporal variation of the temperature were shown in Fig.5.15.1-3 and -4.

The profiles of temporal variation of the fluorescence were shown in Fig.5.15.1-5 and -6.

The profiles of temporal variation of the D.O. were shown in Fig.5.15.1-7 and -8.

The profiles of comparison of salinity [sensor] and salinity analysis result were shown in Fig.5.15.1-9.

The profiles of comparison of D.O.[sensor] and D.O. analysis result were shown in Fig.5.15.1-10.

(5) Date archive

The data were stored on a magnetic optical disk, which will be kept in Ocean Research Department, JAMSTEC.

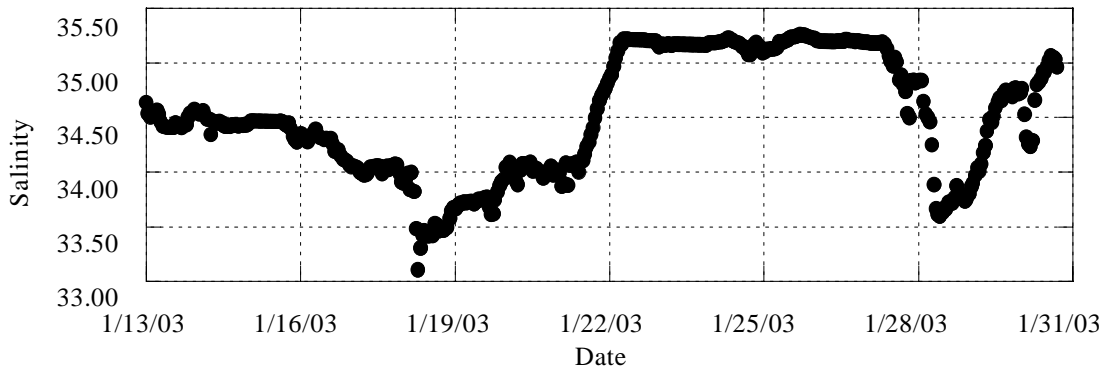


Fig.5.15.1-1:Temporal variation of the Salinity.(Leg.3)

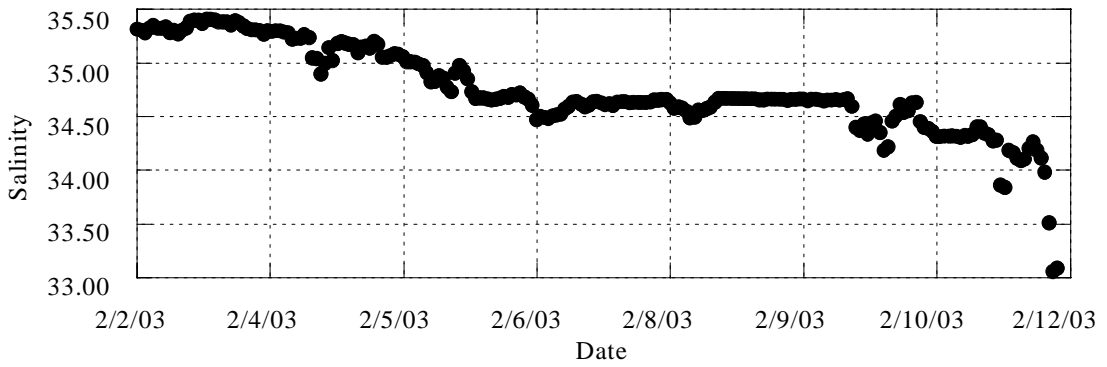


Fig.5.15.1-2:Temporal variation of the Salinity.(Leg.4)

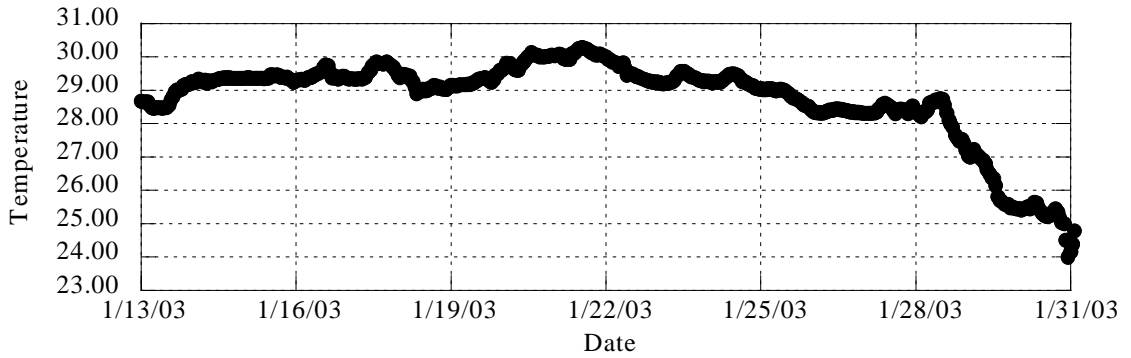


Fig.5.15.1-3:Temporal variation of the Temperature.(Leg.3)

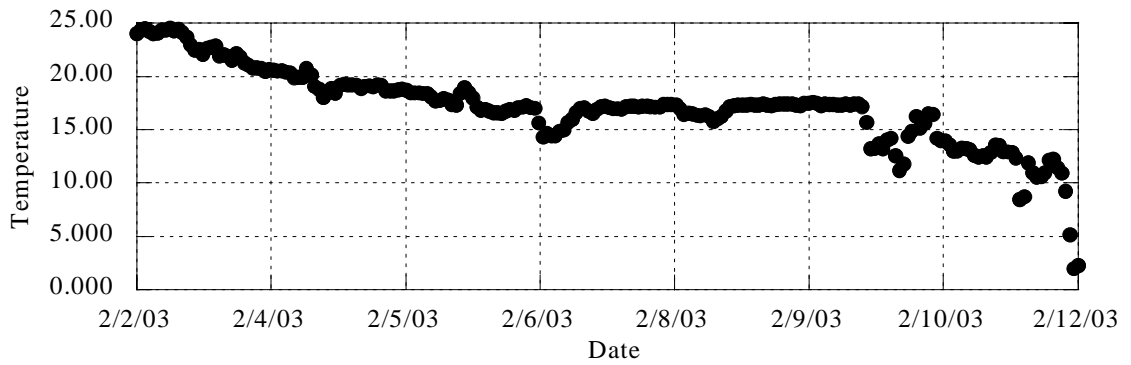


Fig.5.15.1-4:Temporal variation of the Temperature.(Leg.4)

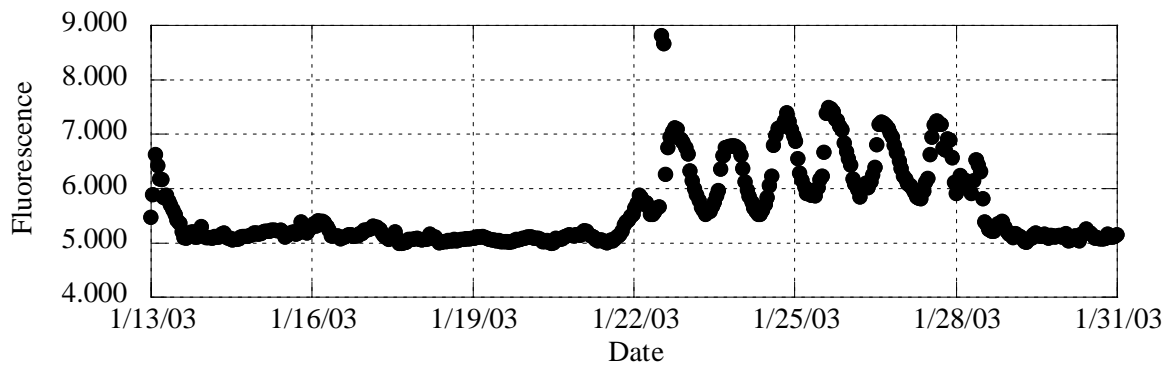


Fig.5.15.1-5:Temporal variation of the Fluorescence.(Leg.3)

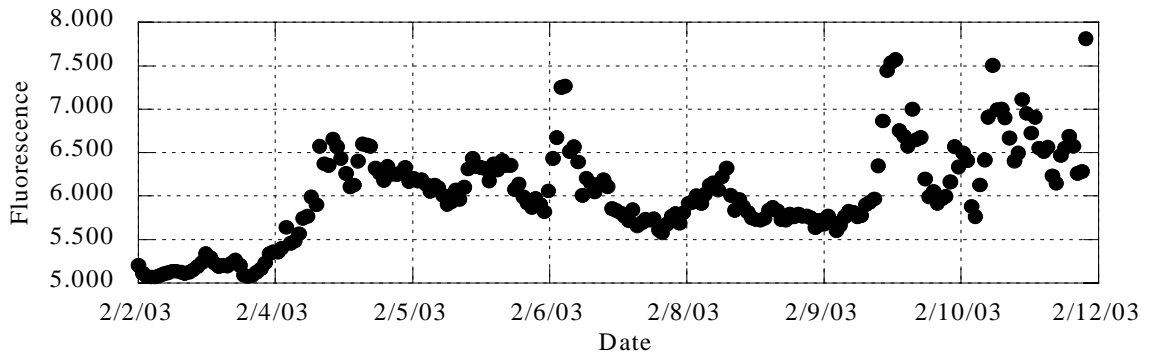


Fig.5.15.1-6:Temporal variation of the Fluorescence.(Leg.4)

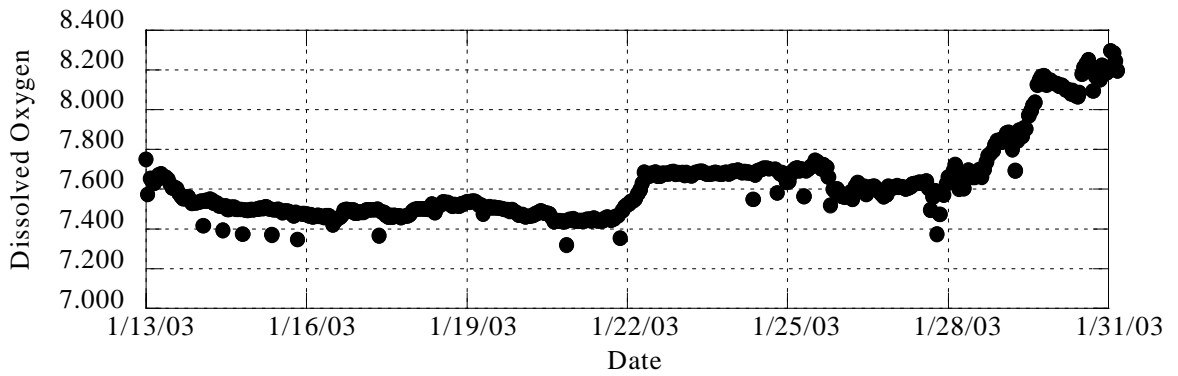


Fig.5.15.1-7:Temporal variation of the Dissolved Oxygen.(Leg.3)

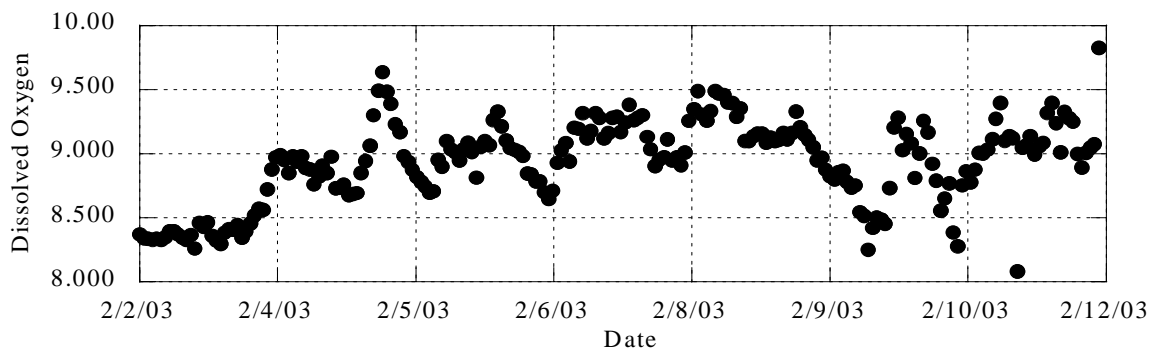


Fig.5.15.1-8:Temporal variation of the Dissolved Oxygen.(Leg.4)

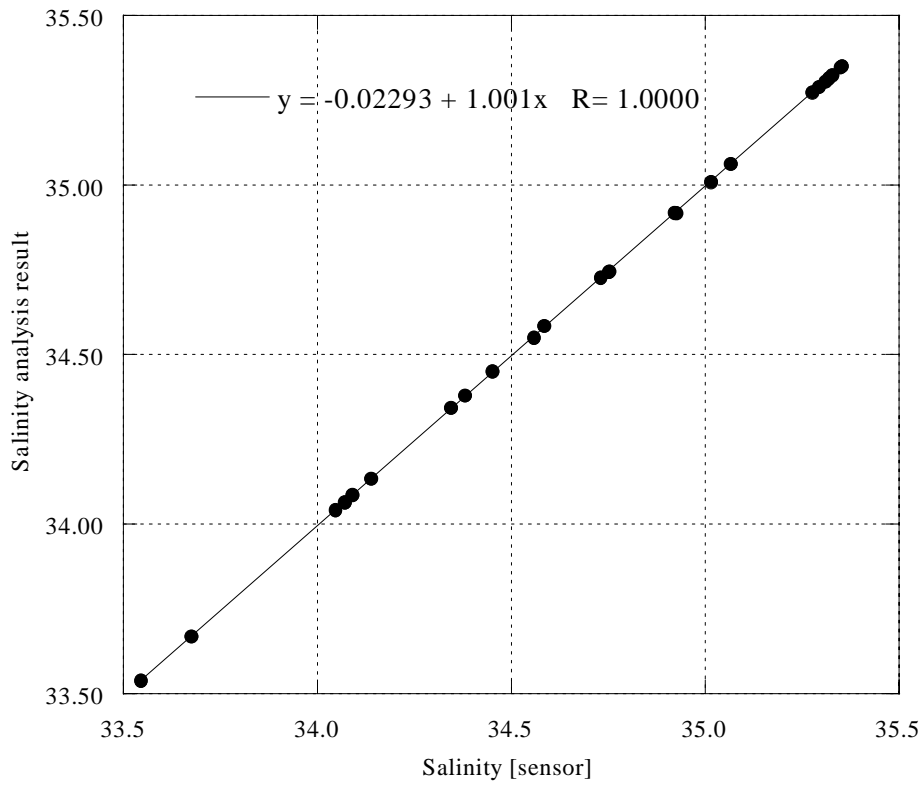


Fig.5.15.1-9:The profiles of comparison of salinity [sensor] and salinity analysis result

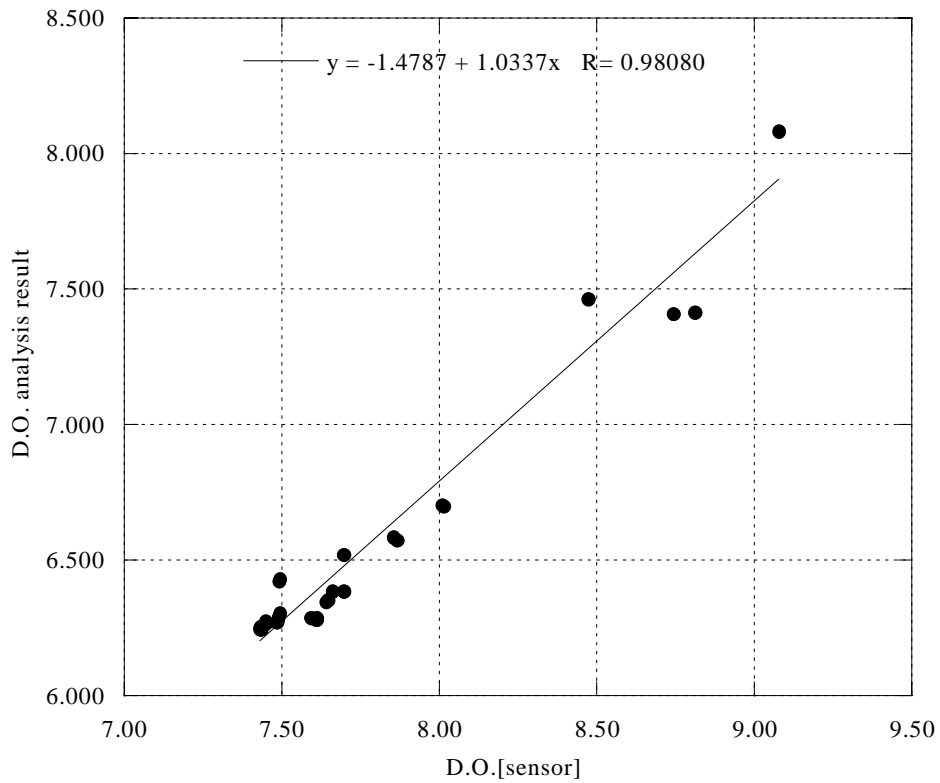


Fig.5.15.1-10:The profiles of comparison of D.O.[sensor] and D.O. analysis result

5.15.2. Nutrients monitoring in surface seawater

(1) Personnel

Asako Kubo (MWJ)

(2) Objective

We revealed the distribution of nutrients in surface seawater that is important to investigate primary production.

(3) Measured parameters

- Nitrate
- Nitrite
- Silicic acid
- Phosphate

(4) Methods

The nutrients monitoring system was performed on BRAN+LUEBBE continuous monitoring system Model TRAACS 800 (4 channels). It was located at the surface seawater laboratory for monitoring in R/V Mirai. The seawater of 4.5 m depth under sea surface was continuously pumped up to the laboratory inner R/V Mirai. The seawater was poured in 5 L of polyethylene beaker through a faucet of the laboratory. The seawater was introduced direct to monitoring system with narrow tube continuously. The methods are as follows.

Nitrate: Nitrate in the seawater was reduced to nitrite by reduction tube (Cd-Cu tube) and the nitrite reduced was determined by the nitrite method described to next, but the flow cell used in nitrate analysis was 3 cm length type. Nitrite initially present in the seawater was corrected after measuring.

Nitrite: Nitrite was determined by diazotizing with sulfanilamide by coupling with N-1-naphthyl-ethylendiamine (NED) to form a colored azo compound, and by being measured the absorbance of 550 nm using 3 cm length flow cell in the system.

Phosphate: Phosphate was determined by complexing with molybdate, by reducing with ascorbic acid to form a colored complex, and by being measured the absorbance of 800 nm using 5 cm length flow cell in the system.

Silicate: Silicate was determined by complexing with molybdate, by reducing with ascorbic acid to form a colored complex, and by being measured the absorbance of 800 nm using 3 cm length flow cell in the system.

(5) Preliminary results

The nutrients monitoring was operated during the period of Chuuk to Hachinohe. Monitoring data was obtained every 1 minute.

Monitoring period (UTC) during this cruise is listed below.

(I) 2003/1/14 (05:09) – 2003/1/17 (13:48)

(II) 2003/1/17 (14:39) – 2003/1/20 (22:47)

(III) 2003/1/21 (06:09) – 2003/1/22 (19:48)

(IV) 2003/1/23 (18:08) – 2003/1/31 (18:42)

(V) 2003/2/3 (00:02) – 2003/2/11 (01:21)

(VI) 2003/2/11 (05:43) – 2003/2/12 (08:57)

Except for the above period was not measured due to malfunction, adjustment and changing reagent.

(6) Data archive

These data are stored JAMSTEC Data Management Office.

5.16. CO₂ concentration in the atmosphere and CO₂ system in the ocean

(1) Personnel

Masao Ishii (Meteorological Research Institute)

Shu Saito (Meteorological Research Institute)

Hisayuki Yoshikawa Inoue (Hokkaido University)

(2) Objective

The equatorial Pacific is categorized into three domains: (a) the warm (~29.5°C) and saline (~34.5) region with moderate CO₂ outflux that appears in the west in the period of ENSO warm phases (El Niño); (2) the warmest (>30°C) and less saline (~34.0) region with small air-sea CO₂ flux that appears usually in the west but even in the central to eastern region in the warm phases; (3) the colder (20~28°C) and the most saline (>35.0) region with the significant CO₂ outflux that appears usually in the central to eastern region but even in the west in the cold phases (La Niña). Variability in the distribution of these domains associated with the ENSO significantly alters the CO₂ flux between the atmosphere and the ocean in the equatorial Pacific, and is considered to affect the global atmospheric CO₂ concentration. The colder domain in the equatorial Pacific is also the region of the significant biological productivity. Consequently, the equatorial Pacific is the important region for the transport of carbon between the atmosphere and the ocean as well as between the upper and deeper layers of the ocean that is subjected to drastic change with the climate.

In this cruise, we made observations that are related to the distributions of CO₂ and carbon flux in the atmosphere and in the ocean. The objectives are:

- To estimate the inter-annual variability of the air-sea CO₂ flux associated with the change in the ENSO phases.
- To detect the long-term change in the partial pressure of CO₂ in surface seawater ($p\text{CO}_{2\text{sw}}$) due to the anthropogenic CO₂ accumulation and the climate change.
- To document the CO₂ system in precise in the upper layer of the ocean and its variability associated with the change in the ENSO phases.
- To provide the precise data of CO₂ system in the deeper layers.
- To evaluate the importance of the physical and chemical factors including temperature, salinity, normalized total inorganic carbon (TCO₂), normalized total alkalinity in controlling the variability of $p\text{CO}_{2\text{sw}}$.
- To determine the role of biological activity in controlling the CO₂ system and $p\text{CO}_{2\text{sw}}$.
- To understand the budget of CO₂, including air-sea CO₂ flux, vertical and horizontal transport, and biological consumption, in the upper layer of the ocean.

(3) Parameters analyzed on board

- (a) CO₂ concentration ($x\text{CO}_2$) in marine boundary air and in the air equilibrated with surface seawater.

- (b) Total inorganic carbon (TCO₂) in surface seawater and in the water columns at hydrographic stations.
- (c) Index of the hydrogen ion concentration (pH in total hydrogen ion scale) in surface seawater and in the water columns at hydrographic stations.

(4) Methods

- (a) CO₂ concentration in marine boundary air and in the air equilibrated with surface seawater:

We made underway measurements of the CO₂ concentration (mole fraction of CO₂ in air; x_{CO_2}) in marine boundary air and in an air equilibrated with a great excess of surface seawater using the automated air-sea CO₂ analyzer (Nippon ANS Co.)(Inoue, 1999) equipped with a non-dispersive infrared (NDIR) gas analyzer BINOS 4. The measurements were made continuously in a 1.5-hour cycle, which include calibration by four standard gases (299.40, 349.11, 399.02, 449.11 ppm in air, Nippon Sanso Co., Ltd.) followed by replicate analyses of the seawater-equilibrated air, replicate analyses of the marine boundary air, and again replicate analyses of the seawater-equilibrated air.

Marine boundary air was taken continuously from the foremast (*ca.*10 m above sea level). Seawater was taken continuously from the bottom of ship located *ca.*5 m below sea level and introduced into the MRI-shower-type equilibrator where it was equilibrated with an aliquot of air in a closed circuit. Concentration of CO₂ will be reported on the MRI87 scale that can be comparable with the WMO X85 mole fraction scale. Corrections for the temperature-rise within the inner piping from the seawater intake to the equilibrator, the drift of NDIR outputs, and the drift of CO₂ concentration in standard gases, if any, are also to be made. Partial pressure of CO₂ (p_{CO_2}) will be calculated from x_{CO_2} by taking the water vapor pressure and the atmospheric pressure into account.

- (b) Total inorganic carbon (TCO₂)

We made underway measurement of TCO₂ in surface seawater and TCO₂ in the water columns at each hydrographic station using two sets of the automated TCO₂ analyzer (Nippon ANS Co., Ltd.) equipped with carbon coulometer 5012 (UIC Co., Ltd.) (Ishii et al., 1998). For the continual underway measurements, seawater was taken continuously from the bottom of the ship and a portion of the seawater (~22 cm³) was introduced into the water-jacketed pipette of the analyzer twice every 1.5 hours for analysis. At all hydrographic stations (stn.6-14, shallow casts 2, shallow casts 4-2, and deep casts), we took discrete samples for TCO₂ and pH in seawater from Niskin bottles on carousel sampler and from surface seawater taken by a bucket. These samples were stored in 250 cm³ borosilicate glass bottles with ground -glass stopcock lubricated with Apiezon-L grease after poisoning with 0.2 cm³ of saturated HgCl₂ solution.

For quality assurance, we also analyzed TCO₂ in the Certified Reference Material (batch #58) provided by Dr. A. Dickson in Scripps Institution of Oceanography and in the reference seawater prepared in MRI (batch "U"). The analysis of the reference seawater was made at least once during the each run of the coulometric cathode- and anode-solution. Data of TCO₂ is to be

finalized after the variability in the calibration factor, if any, are corrected for and data of salinity are finalized. These data will be reported in the unit of $\mu\text{mol kg}^{-1}$.

(c) pH

We made underway measurement of pH (in total hydrogen ion scale) in surface seawater and pH in the water columns at each hydrographic station by spectrophotometric method (Clayton and Byrne, 1993) using the automated pH analyzer (Nippon ANS Co., Ltd.) equipped with spectrophotometer Cary 50 (Varian Australia Pty Ltd.). Seawater samples were prepared by the same method described in the section (b). For continual underway measurements, surface seawater was measured twice every 1.5 hour. When we measure pH in bottle samples during steaming, we inserted once or twice underway measurements between 6 bottle sample measurements.

A portion of seawater ($\sim 13 \text{ cm}^3$) was introduced into sample loop that includes the water-jacketed optical cell (light path length 8 cm). Sample temperature was regulated to $25.00 \pm 0.05^\circ\text{C}$ by circulating water from thermostat through the water jacket. A portion of pH indicator dye solution (0.051 cm^3 of 1.6 mmol/kg m-cresol purple solution) was introduced into another loop. Sample and dye was mixed together by circulation in the combined loop. Absorbances at wavelengths 730, 578, 488 and 434 nm were measured before and after mixing.

pH perturbations induced by addition of dye and saturated HgCl_2 solution are to be corrected by empirical method. Indicator dye was injected twice and the difference in pH between second and first dye addition were subtracted from the pH value of first addition assuming that the difference would be identical with that of first and zero dye addition. The pH perturbation induced by addition of saturated HgCl_2 is to be corrected by similar way.

For quality assurance, we also analyzed pH in the reference seawater prepared in MRI (batch "V"). pH in the Certified Reference Material (CRM) provided by Dr. A. Dickson is potentially certified because the TCO_2 and total alkalinity has been certified. We analyzed pH in the CRM batch #58. The data will be compared with the one that is calculated with the input of TCO_2 and total alkalinity that were certified for the CRM.

(5) Results

Preliminary results of the longitudinal distributions of $x\text{CO}_2$, TCO_2 , temperature and salinity in surface water along the equator are shown in Fig.1. In this single cruise, three domains of the equatorial Pacific have been observed.

Preliminary result of the longitudinal distribution of pH in surface seawater along the equator is shown in Fig. 2. pH values changed from 8.059 to 8.147 depending on the change in water masses described above.

(6) Samples taken for the analyses on land

(a) Seawater for the analysis of $^{13}\text{C}/^{12}\text{C}$ carbon isotopic ratio in total inorganic carbon.

Samples were collected from shallow-casts at all hydrographic stations (stn.6-14, shallow

cast 2 and shallow cast 4-2). These discrete samples were taken and stored in the same method as those for TCO₂ and pH analyses.

(b) Seawater for the analysis of dissolved organic matters.

Samples were taken from shallow-casts at all hydrographic stations (stn.6-14, shallow cast 2 and shallow cast 4-2). They were collected into 100 cm³ glass test tubes (Iwaki) with Teflon-liner screw cap that have been precombusted at 450°C for 1 hour. Samples were also collected into 250 cm³ Teflon-coated polypropylene bottles (Nalgene) or 250 cm³ polypropylene bottles that have been thoroughly dried after rinsing with 1N HCl and MilliQ-purified. These samples have been stored in a refrigerator at -20°C.

(7) Data Archive

The original data will be archived at Geochemical Research Department, Meteorological Research Institute. Data will be also submitted to Data Management Office of JAMSTEC within 3 years.

References

- Clayton, T. D. and Byrne, R. H. (1993) Spectrophotometric seawater pH measurements: total hydrogen ion concentration scale calibration of m-cresol purple and at-sea results. *Deep-Sea Research I*, **40**, 2115-2129.
- Inoue, H. Y. (1999) CO₂ exchange between the atmosphere and the ocean: carbon cycle studies of the Meteorological Research Institute since 1968. In: *Dynamics and characterization of marine organic matter*, N. Handa, E. Tanoue and T. Hama, editors, Terra Scientific Publishing, Tokyo, Kluwer Academic Publishers, Dordrecht, pp. 509-531.
- Ishii, M., Inoue, H. Y., Matsueda, H., Tanoue, E. (1998) Close coupling between seasonal biological production and dynamics of dissolved inorganic carbon in the Indian Ocean sector and the western Pacific Ocean sector of the Antarctic Ocean. *Deep-Sea Research I*, **45**, 1187-1290.

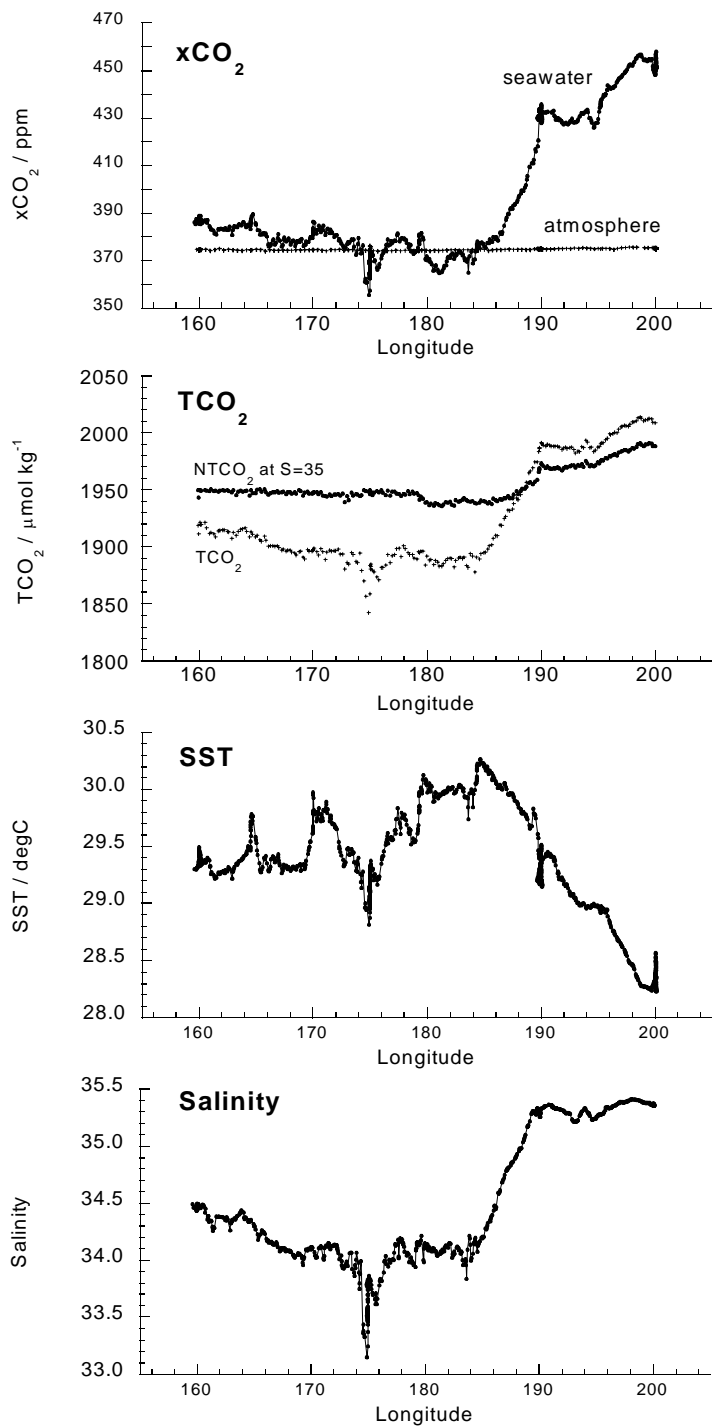


Fig. 1. Longitudinal distributions of $x\text{CO}_2$ in the atmosphere and in surface seawater, TCO_2 and TCO_2 normalized at $S=35$, temperature, and salinity along the equator.



Fig. 2. Longitudinal distribution of pH in surface seawater along the equator.

5.17. Greenhouse Effects Gasses at the Equatorial Area

(1) Personal

Yuichi KOIKE (Central Research Institute of Electric Power Industry)
(Bio-environment Research Co., Ltd.)

(2) Objectives

In the view of the problem of the global warming, it is important to know the concentration level of greenhouse effect gases in the ocean and the penetration rate of these gases through air-sea surface interface. My purpose of this cruise is to collect the data of carbonate (total carbon dioxide, alkalinity and pH), nitrogen oxide (N₂O) and sulfur hexafluoride (SF₆) at the equatorial area. I will make clear the penetration and processes of anthropogenic carbon dioxide in this area using the SF₆ data as a tracer.

(3) Parameters

Oceanic parameters for vertical profile: pH, alkalinity, total carbon dioxide (TCO₂), nitrogen oxide (N₂O) and sulfur hexafluoride (SF₆)

(4) Methods

4.1. pH

Seawater samples were collected in 100mL polyethylene bottles with inner caps from Niskin Sampler. The sample bottles were capped after an overflow of about 100mL seawater. All samples were stored at room temperature after sampling and analyzed within a few hours. Samples were transferred into a closed and jacketed glass measurement cell with a volume of ~30mL. The cell temperature was maintained at a constant temperature of 20°C±0.1°C. The electric potential and temperature of the sample were measured for 15 minutes with an Ag/AgCl combined electrode (Radiometer Analytical A/S, GK2401C) and a temperature sensor (Radiometer Analytical A/S, T901) connected to a high precision pH meter (Radiometer Analytical A/S, model PHM93). Tris and 2-Aminopyridine buffers were employed to calibrate pH electrode. Calibrations were made at the beginning and the end of set of measurement for every station.

4.2. Total Alkalinity (At)

Total Alkalinity samples were collected in 250mL polyethylene bottles with inner caps from Niskin sampler and capped after sampling and analyzed within a few hours. Samples were transferred into a glass titration cell using a 50mL transfer pipette and titrated at 20°C±0.1°C with 0.1M HCl containing 0.6M NaCl within 10 minutes. The electric potential and temperature of the sample were followed with an Ag/AgCl combined electrode (Radiometer Analytical A/S, GK2401C) and a temperature sensor (Radiometer Analytical A/S, T901) connected to the TitrLab system (Radiometer Analytical A/S). The titration was controlled automatically and the titration curve was analyzed with the inflection point titration method by the system. The precision of the

method was determined to be $\pm 0.61 \mu\text{mol/l}$ ($n=8$) from replicate analysis of the Certified Reference Solutions (CRMs (batch 42) supplied by Dr. Andrew Dickson of Scripps Institution of Oceanography (SIO)). Standardization of the titrant (0.1M HCl) was accomplished with Na_2CO_3 (99.99% pure; Asahi Grass) standards.

4.3. Total dissolved inorganic carbon (TCO₂)

The TCO₂ concentration in sea water samples was determined by using the coulometric titration system (UIC Inc., Carbon Coulometer model 5011). Samples for TCO₂ analysis were drawn from the Niskin sampler into 125mL glass vial bottles after an overflow of about 100mL of the seawater. The samples were immediately poisoned with 50 μl of 50% saturated HgCl_2 in order to restrict biological alteration prior to sealing the bottles. All samples were stored at room temperature after sampling. The analysis of TCO₂ will be carried out on land laboratory.

Seawater was introduced manually into the thermostated ($20^\circ\text{C} \pm 0.1^\circ\text{C}$) measuring pipette with a volume of $\sim 30\text{mL}$ by a pressurized headspace CO_2 -free air that had been passed through the KOH scrubber. The measured volume was then transferred to the extraction vessel. The seawater sample in the extraction vessel was acidified with 1.5mL of 3.8% phosphoric acid and the CO_2 was extracted from the sample for 5 minutes by bubbling with the CO_2 -free air. After passing through the Ag_2SO_4 scrubber, polywool and $\text{Mg}(\text{ClO}_4)_2$ scrubber to remove sea salts and water vapor, the evolved CO_2 gas was continuously induced to the coulometric titration cell by the stream of the CO_2 -free air. All reagents were renewed every day. The TCO₂ concentration in seawater was calculated using a calibration curve constructed by measuring six different concentrations (0, 500, 1000, 1500, 2000 and 2500 μML) of dissolved Na_2CO_3 (99.99% pure; Asahi Grass) used as a standard solutions. The precision of the TCO₂ measurement was tested by analyzing CRMs (batch 42) at the beginning of the measurement of samples every day. Our measurement yielded a mean value of $2030.90 \pm 0.97 \mu\text{mol/kg}$ ($n=6$), which compared with $2030.66 \pm 0.60 \mu\text{mol/kg}$ ($n=11$) certified by SIO. We also prepared and analyzed sub-standards that were bottled into 125mL glass vial bottles from a 20L bottle of filtered and poisoned offshore surface water in order to check the condition of the system and the stability of measurements every day. The resulting standard deviation from replicate analysis of 8 sub-standards was $\pm 1.00 \mu\text{mol/l}$.

4.4. Nitrogen Oxide (N₂O)

Samples for N₂O analysis were drawn from the Niskin sampler into 125mL glass vial bottles after an overflow of about 100mL of the seawater. The samples were immediately poisoned with 50 μl of 50% saturated HgCl_2 in order to restrict biological alteration prior to sealing the bottles. All samples were stored in a refrigerator before measurement. The concentration of N₂O in seawater was determined using the Shimadzu GC14A gas chromatograph (carrier gas; pure N_2 gas 40-50mL/min., column: Molecular Sieve 5A 60/80 2m x 3 ϕ) with ^{63}Ni electron capture detector. A purge-and-trap method was employed to concentrate N₂O from seawater. The analysis of N₂O will be carried out on land laboratory.

§Purge-and-trap method

Seawater was introduced into a measuring pipette with a volume of 100mL by a pressurized headspace pure N₂ gas (99.9998%). The measured volume was then transferred to the extraction vessel and N₂O was extracted from the sample for 10 minutes by bubbling with the pure N₂ gas (flow rate: 100mL/min.). After passing through the calcium chloride scrubber to remove water vapor, the evolved N₂O gas was continuously included to the a molecular sieve 13X column (60-80 μm, 0.5m) column and trapped onto the cooled (-80°C) column. After bubbling for 10 minutes, the column was heated at 80°C to desorbs the N₂O by the stream of the carrier gas (pure N₂) and the desorbed N₂O was introduced to the gas chromatograph.

§Headspace method

About 15mL of headspace gas (N₂) was introduced into a glass vial bottle by removing seawater with syringe. Subsequently, the bottle was stood in thermo stated water bath (40°C±0.5°C) for 2hours in order to make an equilibration between gas phase and liquid phase. The N₂O was taken from the headspace gas tight syringe and injected to the gas chromatograph.

4.5. Sulfur hexafluoride (SF₆)

A duplicate sample for SF₆ analysis was drawn from the Niskin sampler into 500mL SCOTT DURAN glass bottle after an overflow of about 250mL of the seawater. The bottle was sealed tightly and stored in a refrigerator before measurement. The analysis of SF₆ will be carried out on land laboratory. SF₆ in seawater was concentrated by using a purge-and-trap method and determined by the HP 5890 gas chromatograph (column: HP Molecular Sieve 5A (80-100μm) 30m x 0.53mm) with non-radioactive electron capture detector (VICI, Pulsed discharge Detector (ECD mode)). Seawater was introduced into a measuring pipette with a volume of 480mL by a pressurized headspace SF₆-free N₂ gas. The measured volume was then transferred to the extraction vessel and SF₆ was extracted from the sample for 30 minutes by bubbling with the SF₆-free N₂ gas (flow rate: 220mL/min.). After passing through the calcium chloride scrubber to remove water vapor, the evolved SF₆ gas was continuously induced to the Porapak Q (80-100μm) column and trapped onto the cooled (-80°C) column. After bubbling for 30 minutes, the column was heated 80°C to desorbs the SF₆ by the stream of the carrier gas (He + 1%H) and the desorbed SF₆ was introduced to the gas chromatograph.

4.6. Deep-Sea pH sensor

High accuracy deep-sea pH sensor (RITE-CRIEPI pH sensor) is composed from pH sensor prove, pH data logger, endurance pressure case, under water cable and battery. The system's size is 200mm in height and 85mm in diameter. The pH sensor prove is made from an ISFET (Ion Sensitive Field Effect Transistor) pH electrode and a Cl-ISE (Chloride Ion Sensitive Electrode). The ph data logger is data control base. It can accumulate on memory pH data converted from

electrical signal to pH count by pH sensor prove with temperature and time data. Endurance pressure case is made from Aluminum.

The pH electrode used by ISFET is a semiconductor made of p-type silicone coated with SiO₂ and Si₃N₄. Through this isolated coats, gate voltage V_g is impressed against reference electrode of Cl-ISE. Carrier density in the channel of semiconductor layer changes corresponds to change of V_g. As impressed source-drain voltage V_d higher carrier density causes higher current. Then, in proportion to H⁺ ion activity of the solution, interface voltage caused to determine the current between source and drain. pH sensors attached the frame of the CTD carousel sampler and measured pH value every 10 seconds during operation. Tris and 2-Aminopyridine buffers were employed to calibrate pH prove. Calibrations were made at the beginning and the end of the measurement for every station.

(5) Preliminary result

Vertical profiles of Alkalinity and pH at St.6, 9, 12 and 14 are illustrated in Figure 5.17-1 ~8. The concentrations of Alkalinity and ph at all stations are shown in Table 5.17-1 ~5.

(6) Data archive

All data will be archived at CRIEPI, RITE and Bio-environment Research Co. Ltd after checking of data quality and submitted to the DMO at JAMSTEC within 3 years.

Table 5.17-1 The concentrations of Alkalinity and ph at ST6

ST6	Depth(m)	At(uM/l)	pH
0	0	2.3388	8.1233
1	15	2.3944	8.1363
2	30	2.3734	7.9205
3	40	2.3777	8.1432
4	50	2.3821	8.1273
5	60	2.3684	8.1402
6	70	2.3452	8.1353
7	80	2.3419	8.1323
8	90	2.3350	8.0773
9	100	2.3255	7.9974
10	110	2.3367	7.9504
11	120	2.3167	7.9215
12	150	2.3872	7.8835
13	200	2.3318	7.8555
3	250	2.3824	7.7830
5	300	2.3849	7.7273
7	350	2.3708	7.5503
8	400	2.3739	7.5503
9	450	2.3800	7.5493
10	500	2.3848	7.5304
12	600	2.3965	7.5235
14	800	2.4026	7.5145
16	1000	2.4278	7.5145
18	1250	2.4433	7.5265
19	1500	2.4701	7.5344
20	1750	2.4714	7.5553
21	2000	2.4850	7.5493
22	2500	2.5056	7.5682
24	2800	2.4785	7.5722

Fig.5.17-1 ST6 Alkalinity

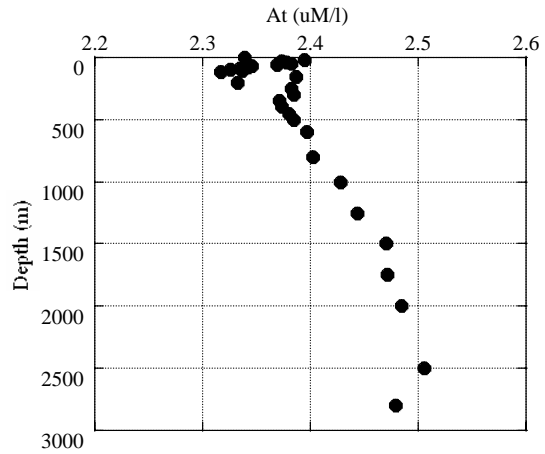


Fig.5.17-2 ST6 pH

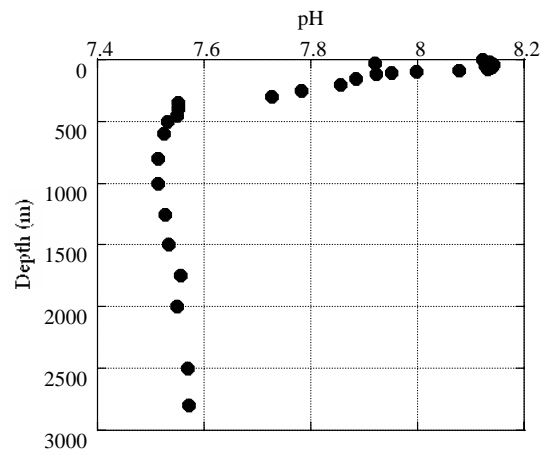


Table 5.17-2 The concentrations of Alkalinity and pH at ST9

ST9	Depth(m)	At(uM/l)	pH
0	0	2.2505	8.1434
1	15	2.2578	8.1544
2	30	2.2620	8.1484
3	40	2.2819	8.1404
4	50	2.2961	8.1494
5	60	2.2960	8.1534
6	70	2.3065	8.1484
7	80	2.3267	8.1374
8	90	2.3450	8.0953
9	100	2.3615	8.0021
10	110	2.3667	7.9781
11	120	2.3692	7.9530
12	150	2.3737	7.8919
13	200	2.3622	7.7977
1	225	2.3551	7.8107
2	250	2.3513	7.7636
3	300	2.3450	7.6524
5	350	2.3450	7.5903
6	400	2.3418	7.5372
7	500	2.3421	7.5432
9	600	2.3511	7.4921
10	700	2.3583	7.5071
11	800	2.3736	7.5201
12	900	2.3742	7.5181
13	1000	2.3859	7.5301
15	1250	2.4014	7.5281
16	1500	2.4110	7.5432
18	1750	2.4295	7.5432
19	2000	2.4333	7.5572
21	2500	2.4559	7.5702
22	3000	2.4498	7.5923
24	3500	2.4431	7.6103
25	4000	2.4342	7.6303
26	4500	2.4298	7.6103
27	4900	2.3987	7.6454

Fig.5.17-3 ST9 Alkalinity

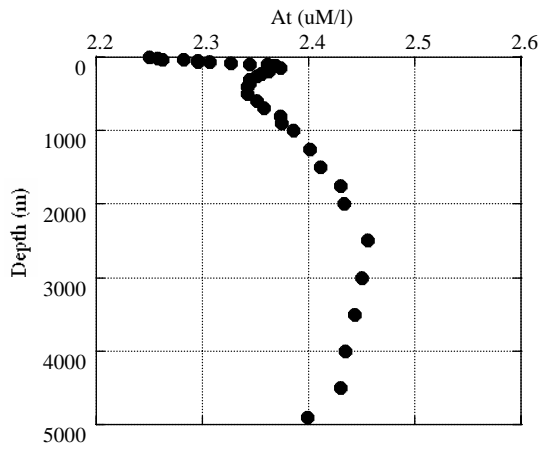


Fig.5.17-4 ST9 pH

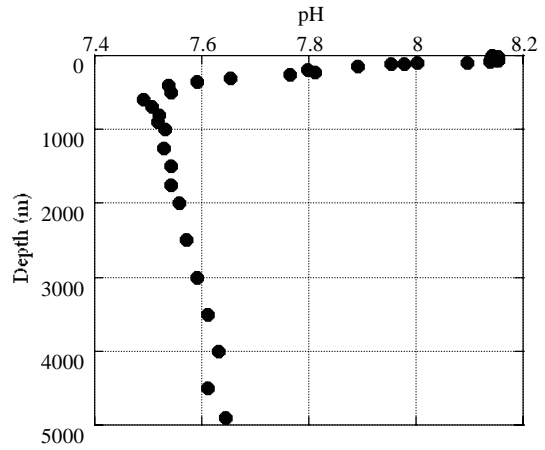


Table 5.17-3 The concentrations of Alkalinity and ph at ST12

ST12	Depth(m)	At(uM/l)	pH
0	0	2.3634	8.0893
1	15	2.3566	8.0953
2	30	2.3659	8.1488
3	40	2.3652	8.0982
4	50	2.3666	8.0873
5	60	2.3681	8.0923
6	70	2.3640	8.0943
7	80	2.3555	8.1298
8	90	2.3597	8.0843
9	100	2.3669	8.1308
10	110	2.3657	8.0476
11	120	2.3561	7.9502
12	150	2.3527	7.8637
13	200	2.3390	7.7644
1	225	2.3459	7.7236
2	250	2.3451	7.7057
3	300	2.3532	7.5676
5	350	2.3587	7.5458
6	400	2.3511	7.5398
7	500	2.3551	7.5199
9	600	2.3650	7.4861
10	700	2.3633	7.4871
11	800	2.3803	7.4951
12	900	2.3808	7.4951
13	1000	2.3927	7.5060
15	1250	2.4025	7.5508
16	1500	2.4166	7.5090
17	1750	2.4316	7.5299
18	2000	2.4337	7.5338
20	2500	2.4520	7.5547
21	3000	2.4587	7.5726
24	4000	2.4574	7.5875
25	4500	2.4216	7.6243
26	5000	2.4093	7.6263
27	5480	2.4120	7.6123

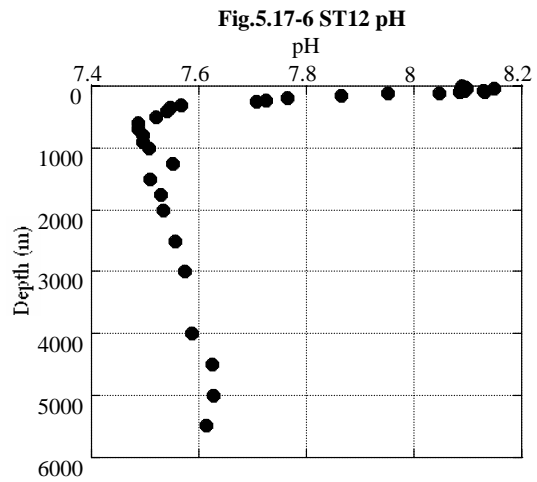
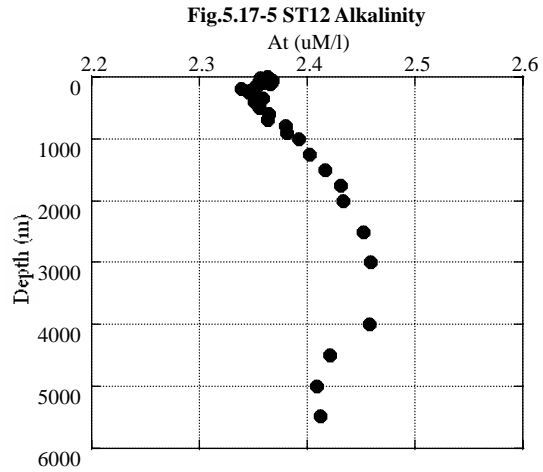


Table 5.17-4 The concentrations of Alkalinity and ph at ST14

ST14	Depth(m)	At(uM/l)	pH
0	0	2.3636	8.0893
1	15	2.3659	8.0953
2	30	2.3652	8.1488
3	40	2.3635	8.0982
4	50	2.3716	8.0873
5	60	2.3661	8.0923
6	70	2.3716	8.0943
7	80	2.3690	8.1298
8	90	2.3681	8.0843
9	100	2.3760	8.1308
10	110	2.3771	8.0476
11	120	2.3704	7.9502
12	150	2.3526	7.8637
13	200	2.3511	7.7644
1	225	2.3465	7.7393
2	250	2.3440	7.6925
3	300	2.3406	7.5225
5	350	2.3434	7.5135
6	400	2.3458	7.5195
7	500	2.3550	7.4638
9	600	2.3546	7.4737
10	700	2.3638	7.4857
11	800	2.3779	7.4946
12	900	2.3811	7.4926
13	1000	2.3913	7.4986
15	1250	2.4025	7.5445
16	1500	2.4119	7.4966
17	1750	2.4301	7.5105
18	2000	2.4645	7.5314
20	2500	2.4543	7.5593
21	3000	2.4527	7.5732
23	3500	2.4501	7.5911
24	4000	2.4395	7.6110
25	4500	2.4223	7.6209
26	5000	2.4128	7.6259
27	5200	2.4119	7.6309

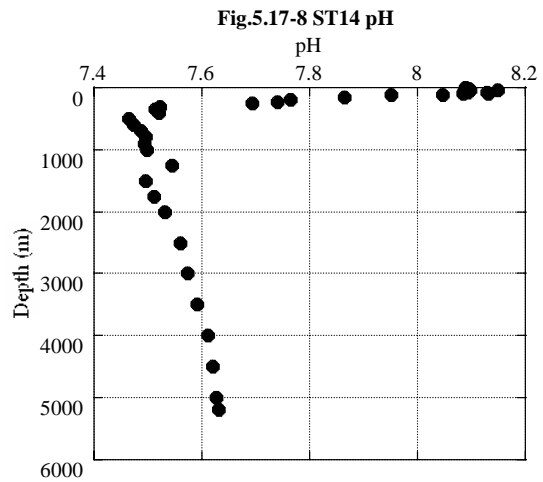
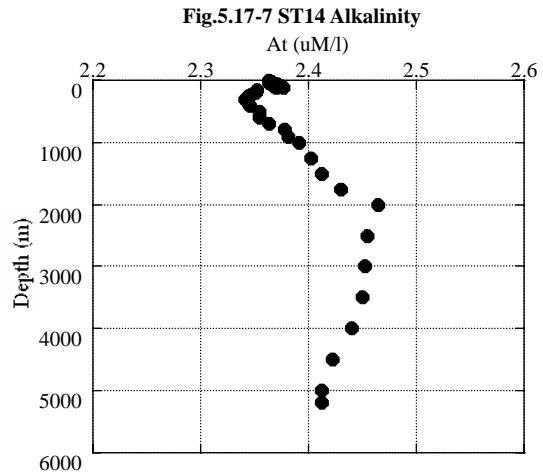


Table 5.17-5 The concentrations of Alkalinity and pH at ST7, ST8, ST10, ST11 and ST13

ST7	Depth(m)	At(uM/l)	pH
0	0	2.2898	8.1283
1	15	2.2876	8.1393
2	30	2.2872	8.1363
3	40	2.2970	8.1363
4	50	2.2954	8.1383
5	60	2.2996	8.1343
6	70	2.3008	8.1293
7	80	2.2928	8.1313
8	90	2.2846	8.1313
9	100	2.3217	8.0603
10	110	2.3583	7.9192
11	120	2.3549	7.9082
12	150	2.3475	7.8662
13	200	2.3490	7.8392

ST8	Depth(m)	At(uM/l)	pH
0	0	2.2825	8.1483
1	15	2.2792	8.1493
2	30	2.2763	8.1493
3	40	2.2792	8.1473
4	50	2.2771	8.1473
5	60	2.2829	8.1453
6	70	2.2908	8.1393
7	80	2.2977	8.1303
8	90	2.3020	8.1193
9	100	2.3616	8.1183
10	110	2.3652	7.9412
11	120	2.3658	7.9232
12	150	2.3652	7.8802
13	200	2.3608	7.8142

ST10	Depth(m)	At(uM/l)	pH
0	0	2.2771	8.1564
1	15	2.2998	8.1625
2	30	2.2704	8.1625
4	50	2.2754	8.1625
6	70	2.2964	8.1554
9	100	2.3680	8.0342
12	150	2.3453	7.9049
13	200	2.3581	7.8348

ST11	Depth(m)	At(uM/l)	pH
0	0	2.2755	8.1795
1	15	2.2691	8.1855
2	30	2.2754	8.1835
4	50	2.2998	8.1765
6	70	2.3275	8.1494
9	100	2.3643	8.1023
12	150	2.3577	7.8869
13	200	2.3514	7.7987

ST13	Depth(m)	At(uM/l)	pH
0	0	2.3637	8.0555
1	10	2.3583	8.0684
2	20	2.3565	8.0575
5	50	2.3655	8.0674
9	100	2.3646	8.0724

5.18. Volatile organic compounds

Atsuhiko Tsuchiya

Michiko Kinoshita

Shinya Hashimoto

Laboratory of Ecological Chemistry

Graduate School of Nutritional and Environmental Sciences

University of Shizuoka

Volatile organic compounds (VOCs) produced in the marine environment are thought to play a key role in atmospheric reactions, particularly those involved in the global radiation budget and the destruction of tropospheric and stratospheric ozone. Volatile organic compounds, including halogens and halocarbons that are produced by marine algae and phytoplankton, may cause ozone depletion in the troposphere and stratosphere. The assessment of numerous naturally produced VOCs in the atmosphere and in seawater is considered to be important for the estimation of the seawater/atmosphere exchange of these gases in the ocean.

The sampling was carried out during January 15-27, 2003. The sampling sites were 9 stations between 160° E and 160° W. Air samples were collected in canister at each station. Water samples were collected from 17 depths at station 6,9,12,14 and 25 depth at station 7,8,10,11,13 with a CTD-rosette sampler fitted with 24 Niskin sample bottles of 20 L volume (General Oceanics). The water sample was collected in 40 ml brown colored glass bottle (I-CHEM Certified 200, Nalge Company) for the measurement of halocarbons. After overflow of more than 100 ml of water, 0.1 ml of HgCl₂ was added to inhibit microbial activity, and the sample bottle was immediately sealed with a two layer septa (silicone/PTFE) with care to exclude air bubbles, and stored in the box (in the dark) and kept at 5 °C in refrigerator. Samples containing air bubbles were discarded. The final concentration of HgCl₂ in sample bottles was about 180 mg/l. Analysis of VOCs will be done through selected ion monitoring using purge and trap-GC-MS in the lab. 20L of water samples were also collected and after N or P was added, the samples were incubated at 25°C. The concentration of halocarbons are measured after 7 days incubation. Distribution of halocarbon concentrations of the equatorial zone in the Pacific Ocean will be examined to evaluate this oceanic area as a natural halocarbon source.

5.19. Stable isotope biogeochemistry of the greenhouse and trace gases in the equatorial Pacific Ocean

Tokyo Institute of Technology

Hiroaki Yamagishi, Keita Yamada, Hideki Nara, Sakae Toyoda, Naohiro Yoshida, and Shuichi Watanabe (JAMSTEC)

(i) Nitrous oxide

(i) -a. Objectives

Nitrous oxide (N₂O) is known as an important greenhouse gas, and involved in stratospheric ozone depletion. The concentration of nitrous oxide in the atmosphere is gradually increasing. Ocean is one of the main sources of nitrous oxide, and especially equatorial region is one of the three highly productive regions.

In natural environment, nitrous oxide is produced by nitrification and denitrification. However, dominant elementary reactions in the production processes have not been clearly understood. Therefore, the controlling factors and production mechanisms of nitrous oxide in the oceans should be revealed to forecast the response of its emission to the future climate change.

Objectives of this research are to estimate emission flux and to reveal production mechanisms of nitrous oxide in the equatorial Pacific Ocean. Our goals of this research are to combine N₂O cycle with marine ecological process in the surface layer and to parameterize them in the production-consumption model of nitrous oxide.

Analysis of isotope compositions gives information on production and decomposition processes and enables quantitative analysis. Therefore, we will analyze distributions of concentration and isotopomer compositions of nitrous oxide (Ratios of ¹⁵N¹⁴N¹⁶O, ¹⁴N¹⁵N¹⁶O, and ¹⁴N¹⁴N¹⁸O to ¹⁴N¹⁴N¹⁶O, individually). And furthermore, we ran incubation experiments and will estimate the production rate of nitrous oxide from each mechanism and the rates of nitrification and denitrification processes.

(i) -b. Sampling and experiments

Seawater was collected from station 6, 7, 9, 10, 12, and 14 for isotope analyses of nitrous oxide. Duplicate 250ml samples were collected at 13 depths between 0 and 200m deep with shallow cast (Cast 2 at Station 6, 9, 12, and 14; Cast 4-2 at Station 8 and 10). At station 6, 9, 12, and 14, duplicate 125ml of water samples were collected at 14 or 15 depths between 200 and 5000m deep with deep cast.

After seawater was overflowed, 0.5 or 1 ml of saturated HgCl₂ solution was added to the 125ml or 250ml serum vials (Maruemu Corp., Osaka, Japan), respectively as a preservative. The vials were sealed with a gray butyl rubber stopper and then crimped with aluminum cap. Samples of 200m deep were stored at 5°C in refrigerator and the rest of the samples were stored at room temperature (about 25 °C). Isotopomer compositions will be measured by purge and trap

continuous flow GC/IRMS system (HP 6890 and Finnigan MAT 252) in the laboratory at Tokyo Institute of Technology (TITech; Tokyo, Japan).

Distribution of isotopomer compositions of nitrous oxide will be analyzed in the equatorial Pacific Ocean, and then flux and production mechanisms of nitrous oxide will be discussed.

Incubation experiments were carried out at 1 or 2 depths near thermocline at station 6, 9, 12, and 14. We have received technical support from M. B. Westley (Univ. of Hawaii) on conducting this incubation experiments. Water samples for incubation experiment were collected into 250 or 650ml serum vials (250ml: Kimble Glass Inc. ,New Jersey, USA, 650ml: Maruemu Corp., Osaka, Japan) and the vials were sealed with a Viton or butyl rubber stopper, respectively, and then clipped with aluminum cap.

Incubation samples were stored in shade at the same temperature as that of collecting depth. Most of the incubation experiments started within 24 hours after collection. After the ¹⁵N labeled solution was injected into the bottle with micro-syringe, incubation was started immediately. Incubation time was about 48 hours and temperature was controlled to be kept at the same temperature as that of collecting site under dark condition. Saturated HgCl₂ solution was added to samples to analyze isotope compositions of nitrous oxide and 20% HCl solution was added to the samples to analyze isotope compositions of nitrate. Incubation time is different among each bottles but precise incubation time was recorded. Samples were stored at room temperature (about 25 °C).

Isotope compositions of nitrous oxide will be measured by purge and trap continuous flow GC/IRMS system in the laboratory of TITech. To analyze isotope compositions of nitrate, nitrate will be converted to ammonium. Nitrogen isotope compositions of collected ammonium will be analyzed by continuous flow EA/IRMS system in the laboratory of TITech. Production rate of nitrous oxide from each process and rate of nitrification and denitrification will be estimated by these incubation experiments.

Air samples were collected at each station (6, 7, 8, 9, 10, 11, 12, 13, and 14) to analyze isotope compositions of nitrous oxide and methane in the atmosphere. Air samples were compressed in 1L glass bottles by a diaphragm pump.

(ii) Methane

(ii) -a. Objectives

Supersaturation of methane in surface ocean water is a ubiquitous feature. The source of the excess methane in the open ocean, however, is not well understood. Stable isotope ratio of methane provides information on sources and sinks. The purpose of this study is to infer the source of excess methane in the equatorial Pacific Ocean by combining the isotope signatures of dissolved methane with biological information such as vertical distribution of chlorophyll-a and assemblage of plankton and flux of sinking particles.

The inference of the source of excess methane improves our insight into the methane cycle in the upper ocean water and furthermore the role of the open ocean as the atmospheric methane source and sink.

(ii) -b. Sampling and experiments

Seawater was collected from station 6, 7, 9, 10, 12, and 14 for carbon and hydrogen isotopic analyses of methane. 125ml and 650ml of seawater samples were collected from 13 depths between 0 and 200m from shallow cast (Cast 2 at Station 6, 9, 12, and 14; Cast4-2 at Station 8 and 10). 125ml of samples were collected for carbon isotope analysis and 650ml of samples were collected for hydrogen isotope analysis. After seawater was overflowed, 0.5 or 3.3 ml of saturated HgCl₂ solution was added to the 125ml or 650ml serum vials (Maruemu Corp., Osaka, Japan), respectively, as a preservative. The vials were sealed with a gray butyl rubber stopper and then crimped with aluminum cap. Samples of 200m deep were stored at 5°C in refrigerator and the rest of them were stored at room temperature (about 25 °C).

Carbon and hydrogen isotope compositions will be measured by purge and trap continuous flow GC/IRMS system in the laboratory of TITech. Carbon and hydrogen isotope compositions of the atmosphere will be analyzed by the same samples with nitrous oxide.

(iii) Methyl chloride and non-methane hydrocarbons

(iii) -a. Objectives

Methyl chloride is the most abundant halocarbon in the atmosphere, has received much attention as a natural source of chlorine atoms in the stratosphere. Recently, new sources of methyl chloride are identified one after another, although its global budget is not in balance. It is expected that this finding open up possibilities for improving our understanding of the global budget, however, there is a possibility that other new unidentified sources exist. To answer to such a question, the detailed information are necessary.

Isotopic analysis has been successfully used to improve our understanding on global budget and sink processes of CO₂, CH₄, N₂O and other trace gases in the atmosphere because isotopic analysis gives us new qualitative and quantitative information while concentration analysis gives us conventional quantitative information only. Therefore, it can be expected that isotopic analysis is useful to study atmospheric methyl chloride involving examination of an unidentified source and reaction. Estimation of its global budget by isotopic analysis needs its isotopic signature on each source and sink, however, very few observations of the isotopic composition are available. The objectives in this research is to determine $\delta^{13}\text{C}$ and $\delta^{37}\text{Cl}$ value of methyl chloride from open ocean which is one of it's major sources. Particularly, $\delta^{37}\text{Cl}$ measurement of atmospheric methyl chloride is the first measurement in the world. As it can be considered that chlorine in the methyl chloride molecule may have different control factor from carbon in the methyl chloride molecule, it can be expected that new findings on methyl chloride study such as production mechanisms in the open ocean will be available.

(iii) -b. Sampling and experiments

Air samples were collected using evacuated 6L fused-silica lined canisters (Silico-can, Resteck) at each station (6, 7, 8, 9, 10, 11, 12, 13, and 14). And seawater was also collected from station 8, 9, 10, 11, 12, 13, and 14 for isotope analyses of methyl chloride. Duplicate 650ml of seawater

samples were collected at 0m deep by bucket. At station 13, duplicate 650ml of seawater samples were collected from 8 depths from shallow cast (Cast 4-2).

After seawater was overflowed, 3.3 ml of saturated HgCl₂ solution was added to the 650ml serum vials as a preservative. The vials were sealed with a gray butyl rubber stopper and then crimped with aluminum cap. Samples were wrapped with aluminum foil to block light to prevent photochemical reaction. Samples of 200m deep were stored at 5°C in refrigerator and the rest of them were stored at room temperature (about 25 °C).

Carbon and Chlorine isotope ratio will be analyzed using by pre-concentration/ gas chromatography/ isotope ratio-monitoring mass spectrometry system (HP 6890 and Finnigan MAT 252) for air sample, and by purge and trap continuous flow GC/IRMS system (the same device above) after being transported to the TITech laboratory.

(iv) Nitrate

(iv) -a. Objectives

Nitrate plays a key role in primary production. Nitrate is supplied mainly from the lower subsurface layer to the surface layer. Upwelling promotes distribution of nitrate to the surface and then increases primary productivity. In the equatorial Pacific Ocean, the equatorial upwelling becomes gradually stronger in the eastern part than in the western part. Analysis of nitrogen isotopes of nitrate will be useful to reveal nitrate cycle and nitrogen cycle in marine ecological systems. In this research we will try to make marine ecological model using nitrogen isotopes and to combine nitrous oxide production with ecological nitrogen cycle in the oceans. This trial will result in more precise estimation of the flux of nitrous oxide emission from the oceans and give insight for controlling factors of N₂O emission.

(iv) -b. Sampling and experiments

Seawater was collected from station 6, 9, 12, and 14 for isotope analyses of nitrate. One-liter samples were collected at 13 depths between 0 and 200m with shallow cast (Cast 2; 11:00 LST). 500ml of seawater samples were collected from 10 depths from 200 to 3000m with deep cast. After seawater was collected, 2.5 or 5 ml of 20% HCl solution was added to the 500ml or 1L plastic bottles, respectively as a preservative. The bottles were sealed with screw cap and shaken well. Samples were stored at 5°C in refrigerator in the research vessel and stored at room temperature (about 25 °C) in the laboratory.

To measure nitrogen isotope compositions of nitrate, nitrate will be converted to ammonium. Nitrogen isotope compositions of collected ammonium will be analyzed by continuous flow EA/IRMS system in the laboratory of Titech.

T. Nakatsuka^{*1}, C. Yoshikawa^{*1}, K. Koba^{*2}, and Y. Yamanaka^{*1} (*1: Hokkaido Univ., *2: Kyoto Univ.) have provided technical advice for measurement of this nitrogen isotope analysis of nitrate and model construction.

5.20. Radionuclides in settling particles and suspended particles in the equatorial Pacific

Masatoshi Yamada, Tatsuo Aono and Zhong-Liang Wang

Nakaminato Laboratory for Marine Radioecology,
National Institute of Radiological Sciences
3609 Isozaki, Hitachinaka, Ibaraki 311-1202, Japan

Introduction

The Natural radionuclides ^{230}Th ($T_{1/2}=7.52 \times 10^4$ yr), ^{231}Pa ($T_{1/2}=3.28 \times 10^4$ yr), and ^{210}Pb ($T_{1/2}=22.3$ yr) can be classified into nuclides which associate with particles and are removed from seawater by scavenging or biological processes. These nuclides provide useful chronometers to determine the important rates of material transport processes in the marine environment. It is well known that ^{234}U and ^{235}U are dissolved uniformly in seawater. The production rate of ^{230}Th and ^{231}Pa in the seawater is fixed because the radioactive decay of ^{234}U and ^{235}U is the significant source. Yang et al. (1986) have reported that a fractionation between ^{230}Th and ^{231}Pa took place in the ocean. A significant fraction of ^{231}Pa relative to ^{230}Th may be transported laterally from the open ocean to the ocean margins. ^{210}Pb is transported to oceanic areas of high productivity and particle flux and scavenging by particles is a major mechanism of ^{210}Pb removal from seawater. The main purpose of this investigation is to determine the concentrations of ^{230}Th , ^{231}Pa , and ^{210}Pb in settling particles and suspended particles and to discuss the scavenging process by measuring the behavior of ^{230}Th , ^{231}Pa , and ^{210}Pb in the western and central equatorial Pacific.

Materials and Methods

Settling particle samples were collected at Stns.6, 9, 12 and 14 by using time-series sediment traps. Sampling information has been described in detail elsewhere in this cruise report (Shimamoto and Tanaka). Settling particle samples will be analyzed for their radioactivities on land laboratory after radiochemical separations. Four long-term moorings of time-series sediment traps were deployed at Stns. 3, 6, 9, and 14 in the western equatorial Pacific during the MR00-K08 cruise.

Suspended particle samples were collected at four stations in the western and central equatorial Pacific during the MR02-K06 cruise by using *in situ* particle samplers of CHALLENGER OCEANIC SYSTEMS & SERVICES. *In situ* particle sampler is designed to filter over one cubic meter of water in a few hours at midwater depths in the open ocean. The aim is to provide sufficient quantities of particulate material for the subsequent analysis of

radiochemical moieties. The basic unit consists of a 293 mm diameter polypropylene filter housing, a centrifugal pump mounted on the end cap of a pressure tube containing a motor and an alkaline battery pack (32 V). A magnetically switched preprogram able electronic timer controls the sampling and the volume sampled is monitored by a mechanical displacement flow meter. Delay to start of pumping can be from 0 to 999.9 hours and duration of sampling up to 9.9 hours, both in 6-minute steps. The volume sampled depends on the concentration of the suspended particulate matter and the duration of pumping. The units are built for a safe working depth of 5500 m. *In situ* particle samplers were deployed by wire from the piston corer winch of R/V *Mirai*. Samples will be analyzed for their radioactivities on land laboratory after radiochemical separations.

5.21. Rare earth element and heavy metal distributions in seawater of the equatorial Pacific Ocean

Zhong-Liang Wang, Masatoshi Yamada and Tatsuo Aono

Nakaminato Laboratory for Marine Radioecology,
National Institute of Radiological Sciences
Isozaki 3609, Hitachinaka, Ibaraki 311-1202, Japan

Trace elements, including rare earth elements (REEs) and heavy metals, are useful tracers in studying fundamental processes in the ocean, especially the small but systematic changes in chemical properties of REEs allow them to be used for unique tracers.

For example, except for Ce, all dissolved REEs show 'nutrient-like' gradual increase with depth across the vertical profiles for different oceanic basins, although there are small but systematic differences across the series. The vertical profile of Ce is unique among the REEs because of particle scavenging due to oxidation/reduction reactions. Generalized features common to all seawaters, shale-normalized dissolved REE patterns are a progressive heavier REE enrichment relative to the lighter ones and a pronounced depression at Ce. These features can be best understood by the conceptual model for interactions between REEs in solution and particles and subsequent removal of particulate matter by settling.

Up to now, a significant amount of data on the distribution of REEs and heavy metals have accumulated from various oceanic regions, for example Southern Ocean, North Atlantic, and North Pacific. However, there is no data of REEs and only little data of heavy metals in the equatorial Pacific Ocean

The main purpose of this research is the collection of seawater sample from the equatorial Pacific Ocean, for the determination of rare earth elements and heavy metals. Fifty seawater samples were got at four stations, station 6, 9, 12, and 14. At each station, water samples were collected along the profile from surface to deep. Sampling was made by using 5L nitric acid-cleaned polyethylene bucket firstly, and then transported rapidly to the clean room. The samples used for the determination of the dissolved REEs and heavy metals were filtered through 0.22 μ m Millipore filter membrane immediately and stored in 1L or 0.5L high-density polyethylene bottles separately. At last, all of water samples were put into the low temperature room.

5.22. Relationship between cadmium and phosphate in the equatorial Pacific

Kazuo Abe

Ishigaki Tropical Station, Seikai National Fisheries Research Institute

148-446 Fukai-Ota, Ishigaki 907-0451, Japan

TEL:0980-88-2571; FAX:0980-88-2573

Objective

The distribution of cadmium (Cd) in the ocean is strongly correlated with the behavior of phosphate (PO_4), indicating that the distribution of Cd in seawater is regulated by the marine biogeochemical processes such as uptake by phytoplankton in surface water, consequential decomposition of the organic matter, and remineralization in deep layer. Generally, the plot of dissolved Cd against PO_4 shows a good linearity and the slope varies from basin to basin. These variations in the Cd- PO_4 plots in the world oceans are considered to be influenced by multiple factors, namely biogeochemical cycle, biomass composition, preformed concentrations, atmospheric deposition, benthic input, and hydrographical conditions. The main purpose of the study in this cruise is to examine the relationship between Cd and PO_4 in the surface layer of the equatorial Pacific Ocean.

Sampling and methods

Water samples were vertically collected at 9 stations (Sts. 6-14) using rosette-mounted Niskin bottles. The water samples for dissolved Cd were transferred to acid-cleaned polyethylene bottles and Cd in samples filtered through $0.4 \mu\text{m}$ Nuclepore filter was concentrated by the APDC co-precipitation method (Boyle and Edmond, 1977) in a clean room. The determination of Cd will be carried out by flameless-Atomic Absorption Spectrophotometer.

5.23. Sediment trap experiments in the equatorial Pacific

1. Participants

Akifumi Shimamoto*¹ and Yuichiro Tanaka*²

*¹: Kansai Environmental Engineering Center Co. LTD.

Azuchimachi 1-3-5, Chuo-ku, Osaka 541-0052, Japan

*²: National Institute of Advanced Industrial Science and Technology.

AIST Tsukuba Central 7, 1-1-1 Higashi, Tsukuba, Ibaraki, Japan

2. Objective

We are planning next items about how to use collected settling particles.

A) Total mass flux and main component

To analyze total mass flux and main component (Opal, Carbonate, Organic carbon, Organic nitrogen).

B) Carbonate flux by calcareous nannoplankton.

To analyze seasonal varieties of the coccolith species, and annual and vertical changes of the coccolith flux.

C) Planktonic foraminifera flux.

To analyze planktonic foraminifera flux, and the dissolution process of settling foraminiferal shell in the water column.

D) Flux of silicoplankton (1. Diatom, 2. Radiolaria, 3. Silicofragellate, 4. Silicodinofragellate)

To estimate vertical flux of the carbon and silica based on that analyzing each species flux of the time-series settling particles.

E) Radio-nuclide (U-238, Th-230, Pa-231, Pu-239+240, Pb-210, Po-210, etc.)

To consider that settling particle flux, and horizontal and vertical transport process.

3. Recovery

We've recovered four sediment trap mooring arrays. All of them were deployed in January 2002 (MR02-K01). It seemed that most of sediment traps carried out completely.

However at Stn.14 in the shallow layer, the sediment trap was overrun for 3 terms. It's not clear what is this error caused by at present. We have to bring back to the laboratory, and to check this instrument in detail.

We named sampling bottles as follows.

[Example] “C00M06S01”

C = Mission Name (Carbon Mapping)

02 = deployed year

M = Cruise Name (MIRAI)

06 = Station Number

S = Sampling Layer (Shallow "S" or Deep "D")

01 = Collecting Number

The working record on deck is followed as next table (Table-1).

The event schedule of collected samples is followed as next table (Table-2).

There were some large organisms (Swimmer) in sediment traps set in the shallower layer (Table-3).

Table-1 Recovered mooring array data

Station number	6	9	12	14
Time lag	JST + 2hr	JST + 3hr	JST – 20hr	JST – 20hr
Released time (LST) and point	2002/1/15 13:02 00-03.12N 159-57.43E 2,809m	2002/1/20 7:00 00-02.20N 174-54.99E 4,818m	2002/1/22 13:13 00-00.74S 170-10.16W 5,638m	2002/1/26 11:55 00-00.10N 160-01.18W 5,193m
Recovery start time	13:38	7:51	13:58	13:05
Recovery end time	14:45	9:40	15:46	14:58
Collecting layer (*1)	960m 2,320m	1,100m 3,300m	950m 3,100m	1,120m 3,360m
Total depth	2,808m	4,820m	5,625m	5,130m
Event start time (JST)	2002/2/1 1:00	2002/2/1 1:00	2002/2/1 1:00	2002/1/25 1:00
Event stop time (JST)	2003/1/15 1:00	2003/1/16 1:00	2003/1/21 1:00	2003/1/24 1:00
Interval	c.a. 15days (see next time table)			
Preservative	Seawater and formalin neutralized with sodium tetraborate			

*1: the mean depth during sampling period calculated by the data of built-in depth sensors.

Table-2 Sampling schedule (JST)

EVENT #	Station#06	Station#09	Station#12	Station#14
1	2002.2.1.1:00	2002.2.1.1:00	2002.2.1.1:00	2002.1.25.1:00
2	2002.2.16.1:00	2002.2.16.1:00	2002.2.16.1:00	2002.2.1.1:00
3	2002.3.1.1:00	2002.3.1.1:00	2002.3.1.1:00	2002.2.16.1:00
4	2002.3.16.1:00	2002.3.16.1:00	2002.3.16.1:00	2002.3.1.1:00
5	2002.4.1.1:00	2002.4.1.1:00	2002.4.1.1:00	2002.3.16.1:00
6	2002.4.16.1:00	2002.4.16.1:00	2002.4.16.1:00	2002.4.1.1:00
7	2002.5.1.1:00	2002.5.1.1:00	2002.5.1.1:00	2002.4.16.1:00
8	2002.5.16.1:00	2002.5.16.1:00	2002.5.16.1:00	2002.5.1.1:00
9	2002.6.1.1:00	2002.6.1.1:00	2002.6.1.1:00	2002.5.16.1:00
10	2002.6.16.1:00	2002.6.16.1:00	2002.6.16.1:00	2002.6.1.1:00
11	2002.7.1.1:00	2002.7.1.1:00	2002.7.1.1:00	2002.6.16.1:00
12	2002.7.16.1:00	2002.7.16.1:00	2002.7.16.1:00	2002.7.1.1:00
13	2002.8.1.1:00	2002.8.1.1:00	2002.8.1.1:00	2002.7.16.1:00

Table-2 Sampling schedule (JST) (Continued)

EVENT #	Station#06	Station#09	Station#12	Station#14
14	2002.8.16.1:00	2002.8.16.1:00	2002.8.16.1:00	2002.8.1.1:00
15	2002.9.1.1:00	2002.9.1.1:00	2002.9.1.1:00	2002.8.16.1:00
16	2002.9.16.1:00	2002.9.16.1:00	2002.9.16.1:00	2002.9.1.1:00
17	2002.10.1.1:00	2002.10.1.1:00	2002.10.1.1:00	2002.9.16.1:00
18	2002.10.16.1:00	2002.10.16.1:00	2002.10.16.1:00	2002.10.1.1:00
19	2002.11.1.1:00	2002.11.1.1:00	2002.11.1.1:00	2002.10.16.1:00
20	2002.11.16.1:00	2002.11.16.1:00	2002.11.16.1:00	2002.11.1.1:00
21	2002.12.1.1:00	2002.12.1.1:00	2002.12.1.1:00	2002.11.16.1:00
22	2002.12.16.1:00	2002.12.16.1:00	2002.12.16.1:00	2002.12.1.1:00
23	2003.11.1:00	2003.1.1.1:00	2003.1.1.1:00	2002.12.16.1:00
24	2003.1.15.1:00	2003.1.16.1:00	2003.1.16.1:00	2003.1.1.1:00
25	-	-	2003.1.21.1:00	2003.1.16.1:00
26	-	-	-	2003.1.24.1:00
Bottle Name	C02M06Sxx C02M06Dxx	C02M09Sxx C02M09Dxx	C02M12Sxx C02M12Dxx	C02M14Sxx C02M14Dxx

Table-3 Sample within Swimmer

Sample number	Swimmer
C02M09S06	Fish
C02M12S10	Shrimp
C02M12S20	Shrimp
C02M14S15	Fish
C02M14S17	Fish
C02M14S19	Fish
C02M14S24	Fish

5.24. $^{234}\text{Th}/^{238}\text{U}$ and $^{210}\text{Po}/^{210}\text{Pb}$ Disequilibria as indicators of removal rates and particulate organic carbon fluxes in the western and central equatorial Pacific

Tatsuo Aono, Masatoshi Yamada and Zhong-Liang Wang

Nakaminato Laboratory for Marine Radioecology

National Institute of Radiological Sciences

3609 Isozaki, Hitachinaka, Ibaraki 311-1202, JAPAN

These nuclides, thorium-234($t_{1/2} = 24.1$ day), lead-210($t_{1/2} = 22.3$ yr) and polonium-210($t_{1/2} = 138$ days) in seawater, are especially useful for studies on material transport scavenging processes within relatively short times and on the mechanism of material transport from the surface ocean, because they are highly reactive to particulate matter and its rapid removal from the water column. The aim of this study is to investigate the removal rates of these radionuclides from the water column in the equatorial Pacific through understanding of the distributions of radionuclides in seawater and particle matter. And, the goal of this study is to clarify the material transport and the implications for POC export in the equatorial Pacific.

The study of the disequilibria of lead-210 and polonium-210 in seawater can be used to observe relatively short term oceanic particle flux processes. The seawater samples were collected at Stns. 6, 9, 12 and 14 with the CTD/RMS. The collected samples will be analyzed for activities of ^{210}Po and ^{210}Pb by an alpha spectrometry in the laboratory.

Thorium-234 produced by decay of uranium-238 in seawater, has been used to studies on removal rates and transport processes of marine particles. The seawater samples were collected at Stns. 6, 9, 12 and 14 using the CTD/RMS. The collected samples have been analyzed for ^{234}Th activity at sea and for POC in the laboratory.

The settling particles were collected using a combined drifting trap. The trap array was deployed at the depth of 210 m at Stns. 6, 9, 12 and 14. Upon recovery of the sediment traps, the sample bottles were stored under refrigeration. The collected samples have been analyzed for radioactivity of ^{234}Th and POC in the laboratory.

5.25. Satellite observation with SeaWiFS for primary productivity research

Ichio Asanuma¹, Shingo Maeda²

1: Earth Observation Research Center/NASDA

2: Nippon Hakuyo Electronics Co.

i) Objectives

It is our objectives to collect data of chlorophyll-a distribution in a high spatial resolution mode from the Sea Wide Field of View Sensor (SeaWiFS) on the OrbView-2 satellite and sea surface temperature distribution in a high spatial resolution mode from the Advanced Very High Resolution Radiometer (AVHRR) on the NOAA series satellite. We will build a time and depth resolved primary productivity model from these high resolution data.

ii) Methods

The High Resolution Picture Transmission (HRPT) receiving station on the R/V Mirai was operated to capture the HRPT signal from the OrbView-2 satellite and the NOAA satellites automatically. The HRPT signal from the OrbView-2 was decrypted following to the reception on the receiving system by a decryption key, which is assigned by the Goddard Space Flight Center (GSFC) of NASA for this research. The level-1A data were generated on the R/V. The HRPT signal from the NOAA was captured and processed by the TeraScan receiving system and its software.

The higher product, chlorophyll-a distribution, will be generated at the laboratory using the SeaWiFS Data Analysis System (SEADAS) with the algorithms dedicated for the SeaWiFS. The MSL12 in the SeaDAS is the basic function to generate a chlorophyll-a distribution as a level-2 data.

The Multi-Channels Sea Surface Temperature (MCSST) is generated and mapped by the TeraScan software.

The chlorophyll-a and sea surface temperature distribution data will be applied for the time and depth resolved primary productivity model.

iii) Data

SeaWiFS data covers a period from January 13, 2003 to February 13, 2003.

MCSST data covers a period from January 13, 2003 to February 12, 2003.

iv) Schedule

- a. Level-1A reconstruction: by the end of February, 2003
- b. Level-1A transfer to GSFC/NASA: by the middle of March 2003 (Duty of the receiving station)
- c. Level-2 production: by the end of March, 2003

- d. Level-3 mapped data production: by the end of March, 2003.
- e. Primary productivity trial: by the end of April, 2003.

v) Data availability

A distribution activity of SeaWiFS data is regulated by the agreement between the NASA and JAMSTEC in 1993.

MCSST data by the AVHRR is available from the JAMSTEC.

vi) Data list:

Following data list indicates the file name of level-1a data with the rule of notation;

Syyyyjjjhhmmss.L0_HMIR.L1A_HMIR.hdf.gz, where yyyy is a year, jjj is a Julian day of the year, hhhmmss is a hour, minute and second when data started.

SeaWiFS level-1a:

S2003013015801.L0_HMIR.L1A_HMIR.hdf.gz
S2003014010221.L0_HMIR.L1A_HMIR.hdf.gz
S2003014024032.L0_HMIR.L1A_HMIR.hdf.gz
S2003015014313.L0_HMIR.L1A_HMIR.hdf.gz
S2003016004704.L0_HMIR.L1A_HMIR.hdf.gz
S2003016022531.L0_HMIR.L1A_HMIR.hdf.gz
S2003017012659.L0_HMIR.L1A_HMIR.hdf.gz
S2003018003004.L0_HMIR.L1A_HMIR.hdf.gz
S2003018021159.L0_HMIR.L1A_HMIR.hdf.gz
S2003019011116.L0_HMIR.L1A_HMIR.hdf.gz
S2003020001355.L0_HMIR.L1A_HMIR.hdf.gz
S2003020231854.L0_HMIR.L1A_HMIR.hdf.gz
S2003021005454.L0_HMIR.L1A_HMIR.hdf.gz
S2003021235715.L0_HMIR.L1A_HMIR.hdf.gz
S2003022230058.L0_HMIR.L1A_HMIR.hdf.gz
S2003023234105.L0_HMIR.L1A_HMIR.hdf.gz
S2003024224421.L0_HMIR.L1A_HMIR.hdf.gz
S2003025002224.L0_HMIR.L1A_HMIR.hdf.gz
S2003025232411.L0_HMIR.L1A_HMIR.hdf.gz
S2003026222734.L0_HMIR.L1A_HMIR.hdf.gz
S2003027000806.L0_HMIR.L1A_HMIR.hdf.gz
S2003027230739.L0_HMIR.L1A_HMIR.hdf.gz
S2003028235037.L0_HMIR.L1A_HMIR.hdf.gz
S2003029224946.L0_HMIR.L1A_HMIR.hdf.gz
S2003030232938.L0_HMIR.L1A_HMIR.hdf.gz
S2003031223039.L0_HMIR.L1A_HMIR.hdf.gz

S2003032231000.L0_HMIR.L1A_HMIR.hdf.gz
S2003033221344.L0_HMIR.L1A_HMIR.hdf.gz
S2003033235146.L0_HMIR.L1A_HMIR.hdf.gz
S2003034225350.L0_HMIR.L1A_HMIR.hdf.gz
S2003035220034.L0_HMIR.L1A_HMIR.hdf.gz
S2003035233343.L0_HMIR.L1A_HMIR.hdf.gz
S2003036223841.L0_HMIR.L1A_HMIR.hdf.gz
S2003037231813.L0_HMIR.L1A_HMIR.hdf.gz
S2003038005443.L0_HMIR.L1A_HMIR.hdf.gz
S2003038235825.L0_HMIR.L1A_HMIR.hdf.gz
S2003040003856.L0_HMIR.L1A_HMIR.hdf.gz
S2003040234435.L0_HMIR.L1A_HMIR.hdf.gz
S2003041011840.L0_HMIR.L1A_HMIR.hdf.gz
S2003042002559.L0_HMIR.L1A_HMIR.hdf.gz
S2003043010449.L0_HMIR.L1A_HMIR.hdf.gz
S2003044014413.L0_HMIR.L1A_HMIR.hdf.gz
S2003044032031.L0_HMIR.L1A_HMIR.hdf.gz

Following data list indicates the file name of sunraster data with the rule of notation;
yyjjj.win, where yy is a year, jjj is a Julian day of the year.
yywmmdd.win, where yy is a year, mm is a month, dd is a day.

MCSST

03013.win, 03014.win, 03015.win, 03016.win, 03017.win, 03018.win,
03019.win, 03020.win, 03021.win, 03022.win, 03023.win, 03024.win,
03025.win, 03026.win, 03027.win, 03028.win, 03029.win, 03030.win,
03031.win, 03032.win, 03033.win, 03034.win, 03035.win, 03036.win,
03037.win, 03038.win, 03039.win, 03040.win, 03041.win, 03042.win,
03043.win

03w0113.win, 03w0120.win, 03w0127.win, 03w0203.win

5.26. Optical measurements, nitrate sensor and production

**MR02K06
Cruise Data Report
Equatorial Pacific
R/V Mirai**

January 13 – January 31, 2003

Prepared for: Kazuhiko Matsumoto
Chief Scientist, JAMSTEC

Prepared by: Oceanography Department
Dalhousie University
1355 Oxford Street,
Halifax, Nova Scotia, Canada
B3H 4J1
Tel: (902)494-3513

1. SCOPE	5.26-4
2. REFERENCED DOCUMENTS	5.26-4
3. BACKGROUND AND RATIONALE	5.26-4
4. PARTICIPANTS	5.26-4
5. MISSION SUMMARY	5.26-5
5.1 DEPLOYMENT COORDINATES	5.26-5
6. DESCRIPTION OF INSTRUMENTS DEPLOYED AND DATA COLLECTED...	5.26-7
6.1 SPMR/SMSR	5.26-7
6.2 HYPERSPECTRAL PROFILER	5.26-10
6.3 ISUS NITRATE SENSOR	5.26-14
6.4 METSAS	5.26-17
6.5 MICROTOPS II SUNPHOTOMETER	5.26-19
6.6 TOTAL AND NEW PRODUCTION	5.26-20
6.6.1 Methodology for measurements	5.26-20
6.6.2 Sampling.....	5.26-21
6.6.3 Data Processing	5.26-21
6.7 CHARACTERIZATION.....	5.26-22
6.8 CALIBRATION	5.26-24
6.9 OVERVIEW OF DATA TYPES.....	5.26-26
6.9.1 Reflectances and Profiles.....	5.26-26
6.9.2 Chlorophyll-a	5.26-27
6.10 QUALITY ASSURANCE	5.26-27
7. DATA REDUCTION/ANALYSIS	5.26-28
7.1 LEVEL 1 TO LEVEL 2 CONVERSION.....	5.26-28
7.2 LEVEL 2 TO LEVEL 3 CONVERSION.....	5.26-29
7.3 LEVEL 3 TO LEVEL 4 CONVERSION.....	5.26-30
7.4 PROCESSING CONFIGURATIONS	5.26-30
7.4.1 SPMR / SMSR.....	5.26-30
7.4.2 HyperPro	5.26-31
8. DATA SUBMISSION	5.26-31
9. SAMPLE PLOTS	5.26-32

Table 1. List of Symbols and Abbreviations

Symbol	Description	Units
$E(\lambda)$	Instrument measured irradiance	$\mu\text{W cm}^{-2} \text{ nm}^{-1}$
$E_d(\lambda)$	Downwelling spectral irradiance below the sea-surface	$\mu\text{W cm}^{-2} \text{ nm}^{-1}$
$E_s(\lambda)$	Downwelling spectral irradiance just above the sea-surface	$\mu\text{W cm}^{-2} \text{ nm}^{-1}$
$E_{\text{lamp}}(\lambda)$	Spectral irradiance of standard lamp at a specified distance	$\mu\text{W cm}^{-2} \text{ nm}^{-1}$
$F1(\lambda)$	Reduction in Field of View due to differences in refractive index	dimensionless
$F2(\lambda)$	Immersion reflectance changes at window - water interface	dimensionless
$\text{Imm}(\lambda)$	Total spectral immersion effects	dimensionless
$L(\lambda)$	Instrument measured radiance	$\mu\text{W cm}^{-2} \text{ nm}^{-1} \text{ sr}^{-1}$
$L_u(\lambda)$	Upwelling spectral radiance below the sea-surface	$\mu\text{W cm}^{-2} \text{ nm}^{-1} \text{ sr}^{-1}$
$L_w(\lambda)$	Upwelling spectral radiance just above the sea-surface	$\mu\text{W cm}^{-2} \text{ nm}^{-1} \text{ sr}^{-1}$
$L_T(\lambda)$	Target Radiance	$\mu\text{W cm}^{-2} \text{ nm}^{-1} \text{ sr}^{-1}$
$\eta_g(\lambda)$	Relative spectral index of refraction of optical window	dimensionless
$\eta_w(\lambda)$	Relative spectral index of refraction of water	dimensionless
NASA	National Aeronautics and Space Administration (U.S. Space Agency)	
NIST	National Institute of Standards and Technology (U.S. Standards agency)	
ONR	Office of Naval Research	
$\rho(\lambda)$	Spectral reflectance of standard target	dimensionless
R_{rs}	Remote Sensing Reflectance	sr^{-1}

1. Scope

This document summarizes scientific investigations carried out by JAMSTEC and Dalhousie University onboard the R/V Mirai in the equatorial Pacific between Jan. 13 and Jan. 31, 2003. It represents work supported by JAMSTEC, Dalhousie University, and the Office of Naval Research, HyCODE project.

2. Referenced Documents

RD 1 Mueller, J.L., and R.W. Austin, 1995: Ocean Optics Protocols for SeaWiFS Validation, Revision 1. NASA Tech. Memo. 104566, Vol. 25, S.B. Hooker, E.R. Firestone, and J.G. Acker, Eds., NASA Goddard Space Flight Center, Greenbelt, Maryland, 67 pp.

RD 2 JAMSTEC, 2002: MR02-K01 Cruise Report

3. Background and Rationale

Satellite observations of the multi-spectral reflectance of the ocean's surface, as exemplified by the Coastal Zone Color Scanner (CZCS), the Ocean Color and Temperature Sensor (OCTS) and the Sea-Viewing, Wide Field of View Sensor (SeaWiFS), have transformed perceptions of optical variability in the sea.

The objectives of Dalhousie University during this cruise were several and included:

- i. Evaluate the net vertical transport of energy associated with penetrating irradiance, for comparison with the net surface heat flux along an equatorial transect.
- ii. Carry out a collaborative effort with JAMSTEC in the development and validation of bio-optical algorithms for use with the currently operating SeaWiFS satellite.
- iii. To investigate the uptake rates of labeled ^{15}N -nitrate and labeled inorganic ^{13}C -carbon in simulated *in-situ* incubations to determine rates of new and total primary production along equatorial transect 160E to 160W.

4. Participants

Kazuhiko Matsumoto / Chief Scientist, JAMSTEC

Geoff MacIntyre M.Sc. / Research Associate, Dalhousie University

Michael MacDonald / Research Associate, Dalhousie University

Fujio Kobayashi / Technician, Marine Works Japan Ltd.

Ai Yasuda / Technician, Marine Works Japan Ltd.

5. Mission Summary

Reflectance data were collected on a series of deployments from the R/V Mirai. The Mirai departed Chuuk Island on January 13, 2003 for a transect along the equator from 160E to 160W, and arrived in Hawaii on January 31, 2003. A large number of optical, biological, physical and chemical measurements were taken, including profiler and reference optical data.

5.1 Deployment Coordinates

The locations and dates of each station are summarized below.

Table 2. Summary of station locations and dates

Location	Local Date	Position
Chuuk	Jan 13, 2003	5.00°N 156.00°E
Stn06	Jan 16, 2003	0.00°N 160.00°E
Stn07	Jan 17, 2003	0.00°N 163.97°E
Stn08	Jan 18, 2003	0.00°N 168.99°E
Stn09	Jan 20, 2003	0.00°N 175.00°E
Stn10	Jan 21a, 2003	0.00°N 180.00°W
Stn11	Jan 21b, 2003	0.00°N 175.00°W
Stn12	Jan 23, 2003	0.00°N 170.00°W
Stn13	Jan 25, 2003	0.00°N 166.07°W
Stn14	Jan 27, 2003	0.00°N 160.00°W
Hawaii	Jan 31, 2003	21.5°N 158.00°W

Table 3. Inventory of casts¹ – Locations and times

Station ID	Cast	Date [UTC]	JD [UTC]	Start Time [UTC]	Local Time	LAT Deg	LONG Deg	Cast name
SPMR06	A	16-Jan	16	00:45	11:45	0.0N	160.0E	MR02K06SPMRStn06A
SPMR06	B	16-Jan	16	00:52	11:52	0.0N	160.0E	MR02K06SPMRStn06B
NPR06	A	16-Jan	16	01:06	12:06	0.0N	160.0E	MR02K06NPRStn06A
SPMR07	A	17-Jan	17	00:50	11:50	0.0N	164.2E	MR02K06SPMRStn07A
SPMR07	B	17-Jan	17	00:57	11:57	0.0N	164.2E	MR02K06SPMRStn07B
NPR07	B	17-Jan	17	01:19	12:19	0.0N	164.2E	MR02K06NPRStn07B
SPMR08	A	18-Jan	18	00:46	11:46	0.0N	170.0E	MR02K06SPMRStn08A
SPMR08	B	18-Jan	18	00:54	11:54	0.0N	170.0E	MR02K06SPMRStn08B
NPR08	A	18-Jan	18	01:06	12:06	0.0N	170.0E	MR02K06NPRStn08A
NPR08	B	18-Jan	18	01:15	12:15	0.0N	170.0E	MR02K06NPRStn08B
SPMR09	A	19-Jan	19	23:44	11:44	0.0N	175.0E	MR02K06SPMRStn09A
SPMR09	B	19-Jan	19	23:52	11:52	0.0N	175.0E	MR02K06SPMRStn09B
NPR09	A	20-Jan	20	00:11	12:11	0.0N	175.0E	MR02K06NPRStn09A
NPR09	B	20-Jan	20	00:19	12:19	0.0N	175.0E	MR02K06NPRStn09B
SPMR10	A	20-Jan	20	23:51	11:51	0.0N	179.3E	MR02K06SPMRStn10A
SPMR10	B	20-Jan	20	23:59	11:59	0.0N	179.3E	MR02K06SPMRStn10B
NPR10	B	21-Jan	21	00:24	12:24	0.0N	179.3E	MR02K06NPRStn10B
SPMR11	A	21-Jan	21	23:39	11:39	0.0N	175.6W	MR02K06SPMRStn11A
SPMR11	B	21-Jan	21	23:46	11:46	0.0N	175.6W	MR02K06SPMRStn11B
NPR11	A	21-Jan	21	23:59	11:59	0.0N	175.6W	MR02K06NPRStn11A
NPR11	B	22-Jan	22	00:09	12:09	0.0N	175.6W	MR02K06NPRStn11B
SPMR12	A	23-Jan	23	22:40	11:40	0.0N	170.0W	MR02K06SPMRStn12A
SPMR12	B	23-Jan	23	22:47	11:47	0.0N	170.0W	MR02K06SPMRStn12B
NPR12	A	23-Jan	23	23:00	12:00	0.0N	170.0W	MR02K06NPRStn12A
NPR12	B	23-Jan	23	23:10	12:10	0.0N	170.0W	MR02K06NPRStn12B
SPMR13	A	25-Jan	25	22:44	11:44	0.0N	164.8W	MR02K06SPMRStn13A
SPMR13	B	25-Jan	25	22:51	11:51	0.0N	164.8W	MR02K06SPMRStn13B
NPR13	A	25-Jan	25	23:03	12:03	0.0N	164.8W	MR02K06NPRStn13A
NPR13	B	25-Jan	25	23:12	12:12	0.0N	164.8W	MR02K06NPRStn13B
SPMR14	A	27-Jan	27	22:43	11:43	0.0N	160.0W	MR02K06SPMRStn14A
SPMR14	B	27-Jan	27	22:50	11:50	0.0N	160.0W	MR02K06SPMRStn14B
NPR14	A	27-Jan	27	23:02	12:02	0.0N	160.0W	MR02K06NPRStn14A
NPR14	B	27-Jan	27	23:13	12:13	0.0N	160.0W	MR02K06NPRStn14B

¹ "NPR" Station ID's indicate HyperPro casts, while "SPMR" ID's refer to SPMR/SMSR casts

Table 4. Inventory of casts – Environmental conditions and processing notes

Station ID	Cast	Air temp (°C)	cloud cover	cloud Type	Sea cond. [m]	swell [m]	depth [m]	Dark correction	Cast and Processing comments
SPMR06	A	28.3	5/10ths	high cumulus	small caps	1	205	calibrated	high haze, fairly uniform sky
SPMR06	B	28.3	5/10ths	high cumulus	small caps	1	210	calibrated	high haze, fairly uniform sky
NPR06	A	28.3	5/10ths	high cumulus	small caps	1	20	shutter	many errors during cast
SPMR07	A	28.7	9/10ths	overcast	small caps	0.5-1	205	calibrated	
SPMR07	B	28.7	9/10ths	overcast	small caps	0.5-1	210	calibrated	
NPR07	B	28.7	9/10ths	overcast	small caps	0.5-1	75	shutter	seems to be working
SPMR08	A	29.3	9/10ths	high cumulus	no caps	<0.5	208	calibrated	
SPMR08	B	29.3	9/10ths	high cumulus	no caps	<0.5	208	calibrated	
NPR08	A	29.3	9/10ths	high cumulus	no caps	<0.5	75	shutter	some erratic errors still occurring
NPR08	B	29.3	9/10ths	high cumulus	no caps	<0.5	75	shutter	some erratic errors still occurring
SPMR09	A	26.7	10/10ths	overcast	no caps	<0.5	202	calibrated	
SPMR09	B	26.7	10/10ths	overcast	no caps	<0.5	203	calibrated	
NPR09	A	26.7	10/10ths	overcast	no caps	<0.5	65	shutter	using Satview2.2a, fewer errors
NPR09	B	26.7	10/10ths	overcast	no caps	<0.5	71	shutter	using Satview2.2a, fewer errors
SPMR10	A	27.8	2/10ths	clear	no caps	<1	225	calibrated	clear skies for entire cast
SPMR10	B	27.8	2/10ths	clear	no caps	<1	210	calibrated	clear skies for entire cast
NPR10	B	27.8	2/10ths	clear	no caps	<1	100	shutter	using JAMSTEC laptop WIN98; no errors
SPMR11	A	27.6	6/10ths	high cumulus	no caps	<1	208	calibrated	clear, then cloud at 100m
SPMR11	B	27.6	6/10ths	high cumulus	no caps	<1	215	calibrated	heavy clouds for entire cast
NPR11	A	27.6	7/10ths	dark clouds	no caps	<1	98	shutter	overcast, nonuniform cloud
NPR11	B	27.6	7/10ths	dark clouds	no caps	<1	100	shutter	mix of cloud and sun
SPMR12	A	30.3	2/10ths	clear	small caps	1	206	calibrated	clear skies for entire cast
SPMR12	B	30.3	2/10ths	clear	small caps	1	208	calibrated	clear skies for entire cast
NPR12	A	30.3	2/10ths	clear	small caps	1	131	shutter	clear skies for entire cast
NPR12	B	30.3	2/10ths	clear	small caps	1	109	shutter	clear skies for entire cast
SPMR13	A	28.2	5/10ths	overcast	whitecaps	1.5-2	204	calibrated	overcast but bright
SPMR13	B	28.2	5/10ths	overcast	whitecaps	1.5-2	203	calibrated	clear skies for entire cast
NPR13	A	28.2	2/10ths	clear	whitecaps	1.5-2	90	shutter	clear skies for entire cast
NPR13	B	28.2	2/10ths	clear	whitecaps	1.5-2	75	shutter	scattered clouds
SPMR14	A	28.2	8/10ths	overcast	no caps	1	212	calibrated	overcast for entire cast
SPMR14	B	28.2	8/10ths	overcast	no caps	1	212	calibrated	overcast for entire cast
NPR14	A	28.2	8/10ths	overcast	no caps	1	101	shutter	overcast for entire cast
NPR14	B	28.2	8/10ths	overcast	no caps	1	73	shutter	overcast for entire cast

6. Description of Instruments Deployed and Data Collected

6.1 SPMR/SMSR

The first instrument system deployed was the SeaWiFS Profiling Multichannel Radiometer (SPMR) and SeaWiFS Multichannel Surface Reference (SMSR). The SPMR is deployed in a freefall mode through the water column while measuring the following physical and optical parameters.

The profiler carries a 13-channel irradiance sensor (Ed) and a 13-channel radiance sensor (Lu), as well as instrument tilt, fluorometry, conductivity and an external temperature probe. The SMSR or reference sensor has a 13-channel irradiance sensor (Es), tilt meter and an internal

temperature sensor. This instrument suite is used for the derivation of the penetration of visible and ultra-violet light in the ocean, and for the determination of the vertical distribution of apparent optical properties for comparison with in-situ pigment measurements. It is used to provide normalized water leaving radiance for SeaWiFS calibration and validation and the empirical development of radiative transfer algorithms for the exploration of ocean color satellite data.

The profiler was deployed twice per station to a depth of 200m. The reference was mounted on the compass deck and was never shadowed by any ship structures. The profiler fell at an average rate of 1ms^{-1} with tilts of less than 3 degrees.

These measurements provide data for the computation of key quantities required to characterize the underwater light field, such as profiles of reflectance, attenuation coefficients, photosynthetically available radiation (PAR), spectral water-leaving radiance, and remote sensing reflectance. These quantities are linked to the inherent optical properties of the ocean (IOP), and can be used to derive the concentration of sea-water constituents such as dissolved organic matter, suspended sediments, and the local chlorophyll concentration. The water-leaving radiance and remote sensing reflectance obtained from in-water profiles is the most accurate surface truth available for calibration/validation of ocean colour satellites.



Figure 1. Profiler configuration

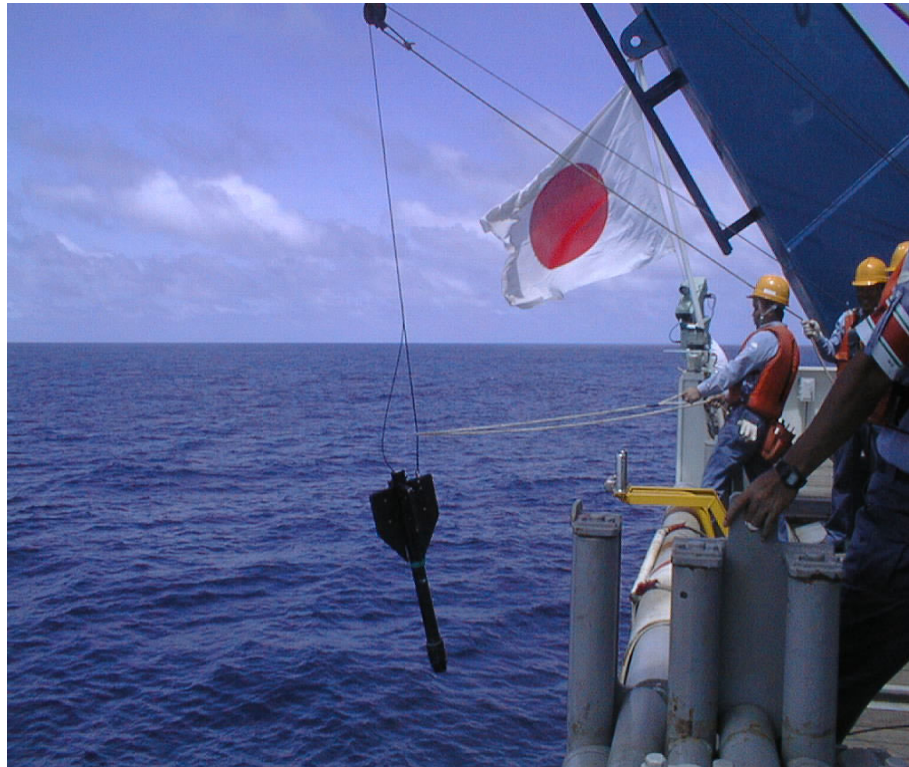


Figure 2. Profiler deployment

Table 5. Center wavelengths of the SPMR/SMSR

SMSR Es	379.5	399.6	412.2	442.8	456.1	490.9	519.0	554.3	564.5	619.5	665.6	683.0	705.9
SPMR Ed	380.0	399.7	412.4	442.9	455.2	489.4	519.8	554.9	565.1	619.3	665.5	682.8	705.2
SPMR Lu	380.3	399.8	412.4	442.8	455.8	489.6	519.3	554.5	564.6	619.2	665.6	682.6	704.5

Table 6. Specifications of the SPMR

Spatial Characteristics:		
Field of view	Irradiance	Cosine response
	Radiance	10° in water
Collector area	Irradiance	86.0mm ²
Entrance aperture	Radiance	9.5 mm diameter
Detector type	Irradiance	Custom 17mm ² and 33mm ² silicone photodiodes
	Radiance	Custom 13mm ² and 33mm ² silicone photodiodes
Spectral Characteristics:		
Number of channels	13	
Spectral bandwidth	10nm	
Bandwidth range	380-705nm	
Filter type	Custom low fluorescence interference	
Electrical specifications:		
Acquisition system	Two 14 channel 24bit DSP A/D system One 8 channel 16bit DSP A/D system	
System frame rate	10 Hz	
Data rate	57.6 kbps	
Data format	Binary	
Data interface	RS-422 / RS-232	
Power	56-80 VDC	
Telemetry	RS485 (RS485 to RS232 converter in deck unit)	
Physical specifications:		
Size	8.9 cm diameter x 122cm long	
Weight	15 kg	
Operating temp. range	-10°C to +60°C	
Depth rating	375m	

6.2 Hyperspectral Profiler

The second optical instrument package deployed was Satlantic's hyperspectral profiler, the HyperPro (NPR). The HyperPro data is accompanied by in-air surface irradiance (E_s) reference measurements obtained from an OCR3000 hyperspectral irradiance sensor. The HyperPro system has 138 surface irradiance channels, 138 downwelling irradiance channels and 138 upwelling radiance channels ranging from 350 to 800nm. The HyperPro also uses optical shutters for dark readings during deployment. Like the SPMR, the HyperPro free-falls through the water column, providing a profile of spectral upwelling radiance and downwelling irradiance.

These measurements provide data for the computation of key quantities needed to characterize the underwater light field, such as profiles of reflectance, attenuation coefficients, photosynthetically available radiation (PAR), spectral water-leaving radiance, and remote sensing reflectance. These quantities are linked to the inherent optical properties of the ocean (IOP), and can be used to derive the concentration of sea-water constituents such as dissolved organic matter, suspended sediments, and the local chlorophyll concentration. The water-leaving radiance and remote sensing reflectance obtained from in-water profiles is the most accurate surface truth available for calibration/validation of ocean colour satellites.



Figure 3. Satlantic's Hyperspectral Profiler



Figure 4. OCR3000 Hyperspectral surface reference



Figure 5. HyperPro deployment

Table 7. Specifications of the HyperPro

Optical Specifications:		
Spectral range	350-800nm	
Entrance slit	70 x 2500 μ m	
Detector type	256 channel Silicon photodiode array	
Pixel size	25 x 2500 μ m	
Spectral sampling	3.3nm/pixel	
Spectral resolution	10nm (3 pixel slit image)	
Spectral accuracy	0.3nm	
Stray light	$< 1 \times 10^{-3}$	
Field of view	Irradiance	Cosine corrected single collector
	Radiance	8.5° half angle baffled Gershun tube
Electrical specifications:		
Acquisition module	16 bit ADC	
Digital resolution	16 bits	
Frame rate	0.5 Hz	
Data rate	57.6 kbps	
Data format	Binary	
Data interface	RS-422 / RS-232	
Power	18-72 VDC at 3 Watts	
Telemetry options	Real time	
Physical specifications:		
Size	6 cm diameter x 32cm long (sensor length)	
Weight	1.07 kg	
Operating temp. range	-10°C to +50°C	
Absolute maximum spectrometer storage temperature range	-40°C to +60°C	

6.3 ISUS Nitrate Sensor

The third instrument deployed by Dalhousie/Satlantic was the In-Situ Ultra-violet Spectrometer (ISUS), or nitrate sensor. This instrument calculates nitrate and salinity concentrations in the water column by measuring absorption spectra in the 200 – 400nm wavelength range. The instrument calculates a nitrate concentration in μM and converts it to an analog signal to be logged by the CTD. The analog output provides a continuous, real-time profile of nitrate concentration in the water column (displayed in SeaSave in conjunction with the CTD data). The full measured spectra are also logged internally and can be downloaded and processed with more sophisticated post-processing software. This allows the user to manipulate the wavelength range and curve fitting function to improve accuracy and match the profile with the discrete data obtained with the TRACCS-800.

The main body of the ISUS is a PVC tube, 20 inches long and 5 inches in diameter. The bottom endcap contains power and telemetry ports, while the top endcap contains the measurement probe. For maximum flexibility, the ISUS can be used in a variety of user-selectable operating modes: CONTINUOUS, SCHEDULED, and TRIGGERED. For this cruise, the instrument was set-up in continuous mode or “profiling mode”. In this mode, the instrument began making measurements immediately after power-up, simultaneously saving the telemetry internally to a memory card and converting the nitrate and salinity values to an analog voltage to be read by JAMSTEC’s SeaBird 911Plus CTD.



Figure 6. ISUS mounted on rosette frame and connected SeaBird 911 CTD.

The telemetry format for the ISUS, as with all Satlantic instrumentation, follows the *Satlantic Data Format Standard*¹. This standard defines how Satlantic telemetry can be generated and interpreted. For every sample taken, the instrument will compose and transmit one frame of telemetry. The information contained in the frame will depend on the *telemetry mode* of the instrument. The instrument's *calibration file*² defines the specific format of the frame.

The format of an ISUS data frame when the instrument is in *FULL* Telemetry mode is given in the following table:

Table 8. ISUS data frame format.

Field Name	Size	Description
INSTRUMENT	6	An AS formatted field denoting the start of a frame of telemetry. The sequence normally starts with "SAT" for a Satlantic instrument.
SN	4	An AI formatted string denoting the serial number of the instrument. This field combined with the INSTRUMENT field uniquely identifies the instrument. This combination is known as the frame header or synchronization string.
DATE	7	An AI formatted field denoting the date at the time of the sample, using the year and Julian day. The format is YYYYDDD.
TIME	9	An AF formatted field denoting the GMT/UTC time of the sample in decimal hours, to 6 decimal places.
NTR CONC	7	An AF formatted field representing the Nitrate concentration ($\mu\text{Mol/L}$) to 2 decimal places, as calculated by ISUS.
SALINITY	7	An AF formatted field representing the Salinity (psu) to 2 decimal places, as calculated by ISUS.
RMS ERROR	10	An AF formatted field representing the Root Mean Square Error of the ISUS' concentration calculation, to 6 decimal places.
T_INT	7	An AF formatted field representing the temperature (to 2 decimal places) inside the ISUS housing, in degrees Celsius.
T_SPEC	7	An AF formatted field representing the case temperature (to 2 decimal places) of the spectrometer, in degrees Celsius.
T_LAMP	7	An AF formatted field representing the approximate temperature (to 2 decimal places) of the UV light source, in degrees Celsius.
REF AVG	7	An AF formatted field representing the average Reference Channel measurement (to 2 decimal places) taken during the sample time.
REF VAR	6	An AF formatted field representing the variance of the Reference Channel measurements (to 2 decimal places) taken during the sample time.

¹ For more information on this data format, refer to the *Instrument File Standard* document available from Satlantic

² For more information on calibration files, refer to the *Instrument File Standard* document available from Satlantic

SW DARK	8	An AF formatted field representing the Sea-Water Dark calculation (to 2 decimal places), in spectrometer counts.
SPEC AVG	8	An AF formatted field representing the average value of all spectrometer channels, to 2 decimal places.
S_CTD	7	RESERVED FOR FUTURE USE. An AF formatted field containing the Salinity measurement from an external CTD device.
T_CTD	7	RESERVED FOR FUTURE USE. An AF formatted field containing the Temperature measurement from an external CTD device, to 2 decimal places.
D_CTD	10	RESERVED FOR FUTURE USE. An AF formatted field containing the Depth measurement from an external CTD device.
RSRV1	10	RESERVED FOR FUTURE USE.
RSRV2	10	RESERVED FOR FUTURE USE.
RSRV3	10	RESERVED FOR FUTURE USE.
CHANNEL(λ_1)	5	An AI formatted field containing the A/D counts of the start channel of the spectrometer, at wavelength λ_1 .
CHANNEL(λ_2)	5	An AI formatted field containing the A/D counts of the spectrometer at wavelength λ_1 .
...
CHANNEL(λ_n)	5	An AI formatted field containing the A/D counts of the spectrometer at wavelength λ_n .
...
CHANNEL(λ_{256})	5	An AI formatted field containing the A/D counts of the end channel of the spectrometer, at wavelength λ_{256} .
TERMINATOR	2	This field indicates the end of the frame. The frame is terminated by a carriage return/line feed pair (0D _{hex} and 0A _{hex}).

The data in this frame is 1436 bytes in size, excluding delimiters. If the comma delimiters are included, the total maximum frame size is 1711 bytes.

The ISUS is capable of closing an on-board shutter over the UV light source before sampling. The instrument can be configured to do this periodically to help track measurement drift, and can be used to provide a dark correction during post processing. To distinguish between *Light* and *Dark* frames in the telemetry output, the instrument uses different frame headers. This allows any telemetry acquisition system to distinguish between sensor readings taken with the shutter opened and closed.

Full frames generated with the shutter open (*light* frames) normally output **SATNLF** in the INSTRUMENT field. SATNLF is an acronym for “SATlantic Nitrate Light Frame”. Full frames generated with the shutter closed (*dark* frames) normally output **SATNDF** in the INSTRUMENT field. SATNDF is an acronym for “SATlantic Nitrate Dark Frame”.

6.4 METSAS

The fourth instrument deployed was the METSAS meteorological station. This instrument package measures a wide range of physical and optical properties. In its present form, this instrument can measure physical properties such as GPS location, relative ship speed and direction, temperature and relative humidity, wind speed and wind direction and barometric pressure. It also measures solar radiation, sea surface skin temperature, downwelling irradiance (E_s) and upwelling above surface radiance (L_t). The last set of optical properties were measured with two 7 channel Satlantic MVD instruments. These two instruments running in unison are also known as the SAS (SeaWiFS aircraft Simulator).

The METSAS was set up and started collecting data immediately upon departure from Chuuk. This instrument package ran 24 hours a day and the data was collected using SatView 2.2a data logging software. These data files can become very large so it was decided to collect data files at two-hour intervals. This makes data processing much easier.



Figure 7. SAS radiance L_t sensor

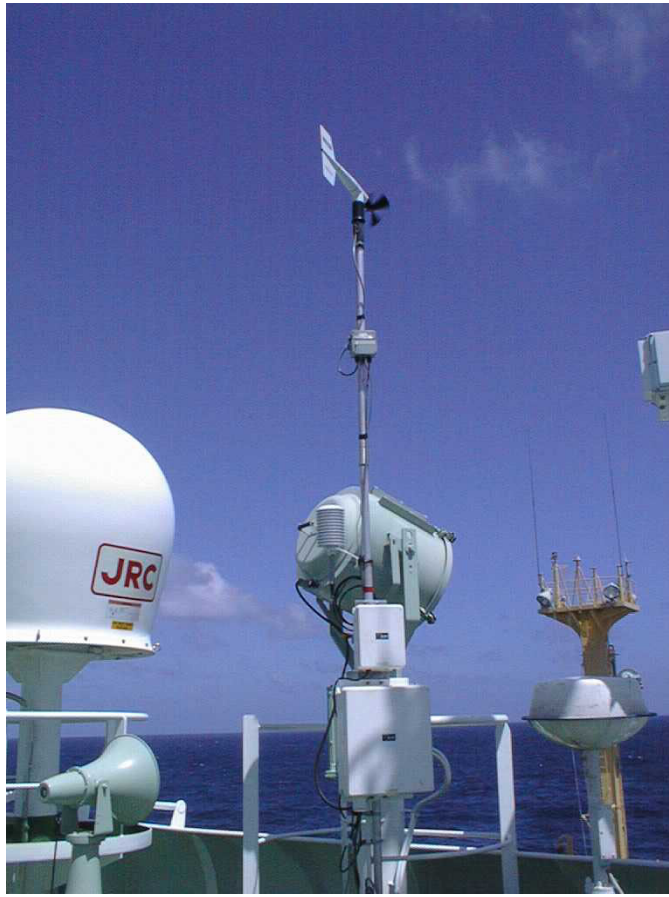


Figure 8. Weather station



Figure 9. Solar radiation sensor

6.5 MicroTops II Sunphotometer

The fifth instrument deployed on MR02-K06 was the MicroTops II Sunphotometer. This instrument has the capability of measuring the direct solar radiation at 440, 500, 675, 870, and 936nm. This data can then be used to determine optical thickness. A Garmin GPS was used in unison with the MicroTopsII and downloaded NMEA sentences to the sunphotometer in real time. The collected GPS position and time is then used to determine the solar zenith angle. It is very important only to collect sunphotometer data while the sun is in direct view, ie. clouds and high cirrus do not obstruct the solar disc. The sunphotometer files were collected during the SPMR deployment on days when the solar disc was unobstructed. The Microtops data can be found on the MR02K06 Cruise Data CD as text files using the naming protocol: MT[serial#][year][month][day].txt. For example, the filename MT377020020205.txt is a file from instrument #3770, captured on February 05, 2002.



Figure 10. Microtops II hand-held sunphotometer

6.6 Total and New Production

6.6.1 Methodology for measurements

A rosette system equipped with 30L General Oceanics Niskin bottles was used to collect seawater at seven optical depths for simulated *in-situ* at each station. A surface water sample was collected just prior to retrieval of the rosette system with a HDPE bucket. The optical depths were determined using Satlantic SPMR Profiler to correspond to seven light levels (100, 51, 22, 16, 13, 2 and 1 % of surface irradiance for new and primary production measures) available in the incubators aboard the R/V Mirai.

A summary of station locations, sample times and depths is shown in table 8. The incubators consisted of 0.6m long acrylic tubes covered with a neutral density screen. Measurement of light transparencies for the incubators is shown in Table 9. For estimation of ^{15}N and ^{13}C uptake rates, triplicate - 1L polycarbonate bottles were rinsed with sample water from each optical depth and filled to 1L using a silicon tube connected to the Niskin bottle to deliver the sample gently into the bottles, allowing a small air space at the top of the bottle. All sample bottles were then inoculated with $200\ \mu\text{M}$ ^{13}C -sodium bicarbonate and $0.5\ \mu\text{M}$ ^{15}N -potassium nitrate in the surface mixed layer above the chlorophyll-a maximum, and $1.0\ \mu\text{M}$ of ^{15}N -potassium nitrate at and below the chlorophyll maximum.

Immediately after inoculation with stable isotopes, sample bottles were placed into incubators corresponding to their nearest light level and then put into a large tank located on the deck with continuously flowing seawater pumped from 7 m below the surface to maintain stable temperatures in the sample bottles. All isotope additions were done in a dark room prior to placing sample bottles into incubators. All sample bottles were maintained just under the surface in the holding tanks during the 3-hour incubation under ambient irradiance and temperature conditions. At the end of the incubation, samples were filtered onto 21 mm pre-combusted ($475\ ^\circ\text{C}$ for 4 h) Whatman GF/F filters and placed into labelled Petri dishes and dried at $45\ ^\circ\text{C}$ for 20 h. Samples were then placed into plastic bags with dessicant and vacuum sealed. Sample filters will be maintained under vacuum and dessicant until analysis with an CN Analyzer coupled to a Europa Tracemass Spectrometer located at the Bedford Institute of Oceanography located in Dartmouth, Nova Scotia, Canada.

6.6.2 Sampling

Table 8. Summary of station locations, start times, and depths for simulated in-situ incubations.

station #	local date mm/dd/yy	local time hh:mm	Chl Max.	Mixed Layer	latitude	longitude	Sampling depths (m)
06	01/16/03	13:00	70	85	0 N	160 E	0,20,30,40,50,80,90
07	01/17/03	14:35	80	100	0 N	164 E	0,20,30,40,50,80,90
08	01/18/03	14:40	80	100	0 N	169 E	0,10,30,40,50,80,100
09	01/20/03	12:35	90	90	0 N	175 E	0,10,30,40,50,80,100
10	01/21/03	14:45	90	90	0 N	180 W	0,10,30,40,50,80,100
11	01/21b/03	14:30	75	90	0 N	175 W	0,10,30,40,50,80,100
12	01/23/03	12:55	60	120	0 N	170 W	0,10,30,40,50,80,100
13	01/25/03	14:30	60	130	0 N	166 W	0,10,20,30,40,70,90
14	01/27/03	13:10	60	120	0 N	160 W	0,10,20,30,40,70,90

Table 9. Summary of percent light transparencies for simulated *in-situ* (SIS) and uptake kinetics (UK) incubators measured under ambient photosynthetic active radiation (PAR 400-700 nm) with Li-Cor 1400 light meter.

Tube I.D.	Light transparency (% of ambient)
G	100
A	51
B	22
C	16
D	13
E	2
F	1

6.6.3 Data Processing

A total of 189 samples were collected for measurement of uptake rates of ^{15}N and ^{13}C for determination of new and total primary production. The uptake rate of nitrate into phytoplankton will be calculated using equation 1;

$$\rho_{\text{N}} = \frac{\Delta\text{APE PON } (^{14}\text{N} + ^{15}\text{N})}{100 \text{ } ^{15}\text{N} \Delta t} \quad \text{mg N m}^{-3} \text{ h}^{-1} \quad (1)$$

where ΔAPE = atom percent enrichment of ^{15}N in sample

PON = particulate organic nitrogen (mg N m^{-3})
 ^{15}N = μM concentration of labeled nitrate added to the sample bottle
 ^{14}N = μM concentration of ambient nitrate
 Δt = time of incubation in hours

The uptake rate of carbon into phytoplankton will be calculated using equation 2;

$$\rho_{\text{TC}} = \frac{\text{POC} (\text{AP}^{13}\text{C}_{\text{inc}} - \text{AP}^{13}\text{C}_{\text{n}})}{\Delta t (\text{AP}^{13}\text{C}_{\text{tic}} - \text{AP}^{13}\text{C}_{\text{n}}) f} \quad \text{mg C m}^{-3} \text{ h}^{-1} \quad (2)$$

where POC = particulate organic carbon (mg C m^{-3})
 $\text{AP}^{13}\text{C}_{\text{inc}}$ = atom percent enrichment of ^{13}C in sample
 $\text{AP}^{13}\text{C}_{\text{n}}$ = atom percent of ^{13}C in natural sample ($\text{AP}^{13}\text{C}_{\text{n}} = 1.1$)
 $\text{AP}^{13}\text{C}_{\text{tic}}$ = atom percent of total inorganic carbon
 Δt = incubation time in h
 f = discrimination factor of ^{13}C ($f = 1.025$)

6.7 Characterization

The instruments are characterized according to the detailed community consensus measurements embodied in SeaWiFS Technical Memorandum, Vol. 25 (RD 3), augmented with advances made by Satlantic in conjunction with NASA and NIST.

Spectral Range

The spectral range is determined by the nature of the spectrometer, the specifications of which are given by the manufacturer. The manufacturer's specifications are cross-checked by viewing a NIST standard source of spectral irradiance, and by viewing lamps with known spectral lines. The spectral range includes the wavebands from 350 to 800nm for the HyperPro and 400 to 800nm for the SPMR/SMSR.

Spectral Resolution

The spectral resolution is determined by the nature of the spectrometer, the specifications of which are given by the manufacturer. The spectral resolution is 10nm.

Spectral Accuracy

The spectral accuracy is determined to within +/- 0.3nm from the calibration sheet provided by the manufacturer.

Field of View

Field of view of the radiance sensor is determined by placing the instrument in a stepper motor controlled rotation table, and performing a rotation about the entrance optics center of rotation in

a collimated light beam. The accuracy and precision of the measurement is 0.1 degrees and 0.05 degrees respectively.

Linearity

The linearity of the instrument is determined by placing the instrument on an optical bench, viewing a collimated beam from a 1kW arc source. A series of calibrated neutral density screens are placed in the beam allowing the intensity to be varied by a factor of 1000. The system is linear to less than 1% over the measured range.

Cosine Response

The cosine response of the radiance sensor is determined by placing the instrument in a stepper motor controlled rotation table, and performing a rotation about the entrance optics center of rotation in a collimated light beam. The accuracy and precision of the measurement is 0.1 degrees and 0.05 degrees respectively. The acceptable range of response is within 3% from 0 to 60 degrees, and 10% from 60 to 85 degrees of the perfect cosine response to angle of incidence.

Thermal Response

The thermal response of the dark current is compensated for by using a shutter that measures the dark current every 6 frames. The thermal effects to responsivity are compensated by correction factors if the change in response is greater than 1% from the calibration values. This correction factor is measured by viewing a calibration source while the instrument is thermally stabilized at 5, 10, 15, 25, 30°C (calibrations are done in a thermally controlled room at 20°C±1°C).

Immersion Effects (Radiance)

Due to the difference in indices of refraction between air (where the instrument is characterized and calibrated) and water (where it is operated), a correction factor must be applied to obtain the effective in water radiances. This correction factor is referred to as the immersion factor. There are two effects contributing. First, the reduction in solid angle viewed by the sensors effectively reduces the amount of flux into the sensor. This correction is given by F1:

$$F1(\lambda) = (\eta_w(\lambda))^2$$

where η_w is the index of refraction of water.

To correct for the calibration values in air, the in-water values are multiplied by the effective loss of viewing area in water (F1).

The second effect is due to the change in index of refraction at the glass/air (glass/water) interface. This correction is given by F2:

$$F2(\lambda) = (\eta_w(\lambda) + \eta_g(\lambda))^2 / ((\eta_w(\lambda) \cdot (1 + \eta_g(\lambda))^2)$$

where η_g is the index of refraction of the window.

Since the indices of refraction of water and glass are better matched, there are less reflection losses at the window. The immersion factor thus increases the in-water values to correct for this effect.

The total immersion effect is then:

$$\text{Imm}(\lambda) = F1(\lambda) \cdot F2(\lambda)$$

Thus the correction for actual in-water radiance values is:

$$L_w(\lambda) = L(\lambda) \cdot \text{Imm}(\lambda)$$

6.8 Calibration

Each instrument is calibrated according to the detailed community consensus procedures embodied in SeaWiFS Technical Memorandum, Vol. 25 (RD 3), augmented with advances made by Satlantic in conjunction with NASA and NIST.

Absolute Radiometric Calibration, Radiance

Absolute radiometric radiance calibration is performed with a calibrated 1000W FEL lamp on a 5m optical bar using the 'plaque method'. The lamp is powered by an Optronics 83A current source. The flux from the lamp is normally incident on a 50cm diffuse reflectance target standard at a distance of D cm. The instrument views the target at an angle of 45.0° such that the field of view of all the sensors is completely covered by the target. The calibration radiances are determined using:

$$L(\lambda) = (E_{lamp}(\lambda, 50\text{cm}) / \pi) * (50.0 \text{ cm} / D \text{ cm})^2 * \rho(\lambda)$$

where:

$L(\lambda)$ is the calibration radiance

$E_{lamp}(\lambda, 50\text{cm})$ is the lamp standard spectral irradiance at 50cm

$(50.0 \text{ cm} / D \text{ cm})^2$ is the $1/r^2$ distance

$\rho(\lambda)$ is the target standard reflectance

Reflection Target: (Labsphere, calibration traceable to NIST)

Standard Lamp: (Optronics, calibration traceable to NIST)

The demonstrated uncertainty in this method is <3% absolute and <1% relative.

Absolute Radiometric Calibration, Irradiance

Absolute radiometric irradiance calibration is done using a calibrated 1000W FEL on a 5m optical bar using direct radiation from the lamp. The lamp is powered by an Optronics 83A current source. The flux from the lamp is normally incident on the irradiance sensor cosine collector at a distance of 50cm. The calibration irradiances are determined using equation 2:

$$E(\lambda) = E_{\text{lamp}}(\lambda, 50\text{cm}) \cdot (50.0 \text{ cm} / 50 \text{ cm})^2$$

where:

$E(\lambda)$ is the calibration irradiance

$E(\lambda, 50 \text{ cm})$ is the lamp calibration at 50 cm

$(50.0 \text{ cm} / 50 \text{ cm})^2$ is the lamp $1/R^2$ distance

Standard Lamp: Optronics, traceable to NIST standard

The demonstrated uncertainty in this method is <3% absolute and <1% relative.

6.9 Overview of Data Types

6.9.1 Reflectances and Profiles

The objective of this activity is the collection and collation of a library of reflectance signatures of the ocean, the “Ocean Background”.

- i. Above water reference downwelling irradiance ($E_s(\lambda)$)
- ii. Underwater profiler downwelling irradiance ($E_d(\lambda)$) of the water column
- iii. Underwater profiler upwelling radiance ($L_u(\lambda)$) of the water column

A data collection event includes ancillary data taken coincidentally with the radiance and irradiance measurement (“Instrument Measurement Data”). The following observations were recorded:

- i. Instrument Measurement Data
- ii. Time and location of acquisition

Instrument Measurement Data was acquired and processed as follows:

- i. Level 1 data (time series sample data, in digital instrument counts) was acquired from the sensors onboard the platform.
- ii. Level 2 data (calibrated physical units, i.e. $\mu\text{W cm}^{-2} \text{ nm}^{-1}$ for irradiance; $\mu\text{W cm}^{-2} \text{ nm}^{-1} \text{ sr}^{-1}$ for radiance) was generated using standard instrument software and calibration coefficients derived from a rigorous controlled laboratory absolute radiometric calibration.
- iii. Level 3 data (depth-binned) was generated using standard instrument software.
- iv. Level 4 data (computed reflectance spectrum and propagated surface properties) was generated using standard instrument software.

The ocean background reflectance (Level 4) is derived by analysis of the base measurement data. This analysis was performed using Satlantic software. The measurement of spectral upwelling radiance was propagated to, and through the sea-surface using radiative transfer calculations to provide the water-leaving radiances ($L_w(\lambda)$). These values were then normalized by the downwelling spectral irradiance to compute the remote sensing reflectance, $R_{rs} = L_w(\lambda) / E_s(\lambda)$.

6.9.2 Chlorophyll-a

At each cruise station, water samples were collected for the measurement of various properties, including chlorophyll-a. An estimate of chlorophyll-a distributions in the equatorial Pacific was made using fluorometric analysis and HPLC. Results for the HPLC measurements are not available at this time. The remainder of this section paraphrases the fluorometric chlorophyll-a measurement methods outlined in the JAMSTEC MIRAI Cruise Report (RD2).

Chlorophyll-a measurements were carried out using broadband and narrowband filter fluorometers. Broadband filter fluorometers are commonly used for measuring chlorophyll concentrations, but it is recognized that the acidification technique results in errors when chlorophyll-b is present. The new non-acidification method developed by Welschmeyer (1994) for narrowband filter fluorometers eliminates the effect of acidification error. Narrowband and broadband filter fluorometers are identical, with the exception of their excitation and emission filters and lamp. Though the Welschmeyer method alleviates the need to consider acidification error, an overestimation of chlorophyll-a concentration is still introduced, especially when chlorophyll-b is present.

During the cruise, seawater samples were collected at the twelve stations (see Table 2). Samples were collected at 14 depths from 0m to 200m using Niskin bottles, except for the surface water, which was taken by bucket. The samples (0.5L volume) were gently filtered by low vacuum pressure (<20 cmHg) through Nucleopore filters (pore size: 0.4µm; diameter: 47 mm) in the dark room. The sample filters were immediately extracted in the N,N-dimethylformamide (7 ml) and stored at -30 °C until the analysis, which was performed at room temperature.

Traditional acidification and Welschmeyer non-acidification methods were carried out using a Turner design model 10-AU-005 fluorometer. Analytical conditions of the two methods are indicated in Table .

Table 10. Characteristics of Turner fluorometer for chlorophyll-a measurements.

	Traditional method	Welschmeyer method
Excitation filter /nm	5-60 (340-500nm)	436nm
Emission filter /nm	2-64 (>665nm)	680nm
Optical kit	10-037R	10-040R
Lamp	Daylight White F4T5D	Blue F4T5, B2/BP (F4T4, 5B2 equiv.)
Acidification	Yes (1M HCl, 1min.)	No

6.10 Quality Assurance

Several layers of quality assurance were taken during the measurement program. The laboratory calibration provides a first order assurance in that the instrument response is referenced to an internationally traceable reference standard. This calibration took place immediately prior to the field program. Deviations greater than 3% in calibration coefficients are flagged for further investigation via controlled laboratory re-calibration checks. No deviations were noted.

During each field deployment, the operator views the spectrum of both upwelling radiance and downwelling irradiance. Visually identifiable departures from “normal” spectra are noted and are flagged for further investigation via controlled laboratory re-calibration checks.

7. Data Reduction/Analysis

The data collection is followed by a defined series of analysis steps, which reduce the collected data to geo-referenced, calibrated, and averaged data products for further statistical analysis. The steps include depth binning and derivation of products, and encompass transitions from Level 1 (raw data) to Level 4 (derived products). The analysis is carried out by the software package ProSoft (Ver. 6.3) developed by Satlantic (copies available on request).

Collected and processed data archiving and organization is based on the level of processing. Data processing was divided into four levels: Level 1, 2, 3 and 4.

- RAW – Level 1 binary data obtained as a result of data acquisition.
- REF – Level 2 ASCII data obtained as a result of SMSR and OCR3000 reference data calibration and some filtration.
- PRO – Level 2 ASCII data obtained as a result of SPMR and HyperPro profiler data calibration and some filtration.
- BIN – Level 3 ASCII data obtained by depth-binning the data.
- Level 4 files:
 - SPR – ASCII subsurface products for both SPMR/SMSR and HyperPro, containing all casts, one per line, obtained from BIN data propagation to subsurface level.
- PNG – Data plots for all casts. (PNG images within MR02K06-PLOTS.zip)

7.1 Level 1 to Level 2 Conversion

The first step in the analysis of the data is the conversion from Level 1 to Level 2 calibrated, dark corrected data. Calibration files are used, along with calibration darks for the SPMR/SMSR, and shutter darks for the HyperPro, to derive upwelling radiances ($L_u(\lambda)$), and downwelling irradiances ($E_s(\lambda)$), in calibrated physical units ($\mu\text{W cm}^{-2} \text{nm}^{-1} \text{sr}^{-1}$ and $\mu\text{W cm}^{-2} \text{nm}^{-1}$ respectively). The steps involved are:

1. Convert raw binary optical (light and dark) and ancillary data into an integer representation in counts.
2. Convert data counts into engineering units in accordance with the calibration equations (see *Satlantic Instrument File Standard V6.0*). The calibration equation for optical data is:

$$L_{DarkDat} = L_{CountsDarkDat} \cdot a \cdot ic \frac{it_1}{it_2}$$

$$L_{LightDat} = L_{CountsLightDat} \cdot a \cdot ic \frac{it_1}{it_2} \quad (1)$$

where a is a slope, ic is an immersion coefficient, it_1 is the first integration time and it_2 is the second integration time. a , ic and it_2 are taken from a calibration file, and it_1 is obtained from the same log file as optical data.

3. Check the sequence of frame numbers. Blank the frames that are out of sequence.
4. Deglitch dark data using a first difference filter (optional step for hyperspectral shutter darks only).
5. Smooth shutter darks using a running boxcar filter (hyperspectral instruments only).
6. Interpolate shutter darks as a function of measurement time to match the number of dark and light data measurements (hyperspectral instruments only).
7. Dark correct the light data:

$$L = L_{LightDat} - L_{DarkDat} \quad (2)$$

8. Correct light data using a derived temperature correction:

$$L = \frac{L}{0.01(c_1 \cdot w^3 + c_2 \cdot w^2 + c_3 \cdot w + c_4)(T - 20) + 1} \quad (3)$$

where c_1 , c_2 , c_3 and c_4 are constants, w is wavelength and T is temperature of the radiance or irradiance sensor (here $c_1 = 6.79131e-9$, $c_2 = -1.09902e-5$, $c_3 = 6.51646e-3$, $c_4 = -1.31056$).

7.2 Level 2 to Level 3 Conversion

The calibrated Level 2 data includes measured radiances, irradiances and ancillary data types. For the HyperPro, the nature of the spectrometer is such that the specific center wavelengths do not match precisely. In the Level 3 conversion, there are two options. The radiance and irradiance spectra can be interpolated using a linear interpolator, and the interpolated spectra subsampled at center wavelengths chosen by the operator. Alternatively, optical data can be used at the original wavelengths. For this dataset, the original wavelengths were retained for the

hyperspectral instruments. All profiler data is depth-binned at a 1 meter binning interval. The steps of the binning process are:

1. Interpolation of optical data into 1nm wavelength intervals (not performed for this dataset).
2. Natural logarithm transformation of the Level 2 optical data.
3. Data binning. The optical data is divided into equal depth layers. (Note that the number of data points within each layer can vary, since profiler's falling speed is not constant).
4. Data averaging.
5. Application of exponent to mean log transformed data.

7.3 Level 3 to Level 4 Conversion

The Level 3 data serve as the basis for the production of a number of derived information products: "Surface Products", "Remote Sensing Reflectance", and "Diffuse Attenuation Coefficient". These represent a series of mathematical manipulations of the data in the Level 3 files. The "Surface Products" represent the propagation of both radiance and irradiance to a common depth horizon, which is specified as just below the sea surface. For upwelling radiance taken at some depth below the sea-surface the radiance just below the surface is estimated by first computing the spectral attenuation coefficient for spectral radiance based on statistical computations using a ratio of blue to green wavebands as input. This attenuation coefficient governs the propagation of radiance to the surface based on an exponential model, and this model is used to determine the upwelling radiance just below the sea-surface. For irradiance, the above-water measurement is used and propagated through the sea-surface using an estimated albedo.

Subsurface values are derived from the near-surface data recorded at the start of a cast. Each set of these spectra is then combined to produce the Level 4 data.

Remote sensing reflectances are produced by propagating the radiance at a level just below the sea-surface through the surface by use of Fresnel reflectances, giving water-leaving radiances ($L_w(\lambda)$). These are then divided by the above-water irradiances on a band by band basis to produce remote sensing reflectances.

7.4 Processing Configurations

7.4.1 SPMR / SMSR

- Pressure Tare performed with Ed sensor just below surface
- Ed – Lu distance (1.14m)
- Es distance to surface (0m)
- Dark correction: calibration file used
- Number of bins regressed for computing K (NUM_K_BINS) = 9
- Binning interval: 1m

7.4.2 HyperPro

- Ed – Lu distance (0.35m)
- Es distance to surface (0m)
- Shutter darks used for dark correction
- Binning interval: 1m

8. Data SUBMISSION

This data submission includes the following:

Table 11. Data Submitted

Data type	Comments
SPMR/SMSR depth-binned data	Level 3 depth-binned data (BIN) files
HyperPro depth-binned data	Level 3 depth-binned data (BIN) files
SPMR/SMSR subsurface data	Level 4 subsurface spectra data (SPR) file
HyperPro subsurface data	Level 4 subsurface spectra data (SPR) file
Data plots (PNG image files)	Data plots for each station (MR02K06-PLOTS.ZIP)
Nitrate sensor raw data files	Full spectra internally logged data (Divexxx.raw files)
Nitrate sensor CTD output files	Nitrate conc's logged by CTD (CxxMxx.cnv files)
METSAS raw data	Raw files logged by METSAS (.RAW files)
METSAS processed data	.DAT ascii files and .AVE average files (50 frames ave)

9. Sample Plots

Sample plots from western (bluer water) and eastern station casts are included below. The complete set of plots for all casts is included with the submission in the file MR02K06-PLOTS.zip.

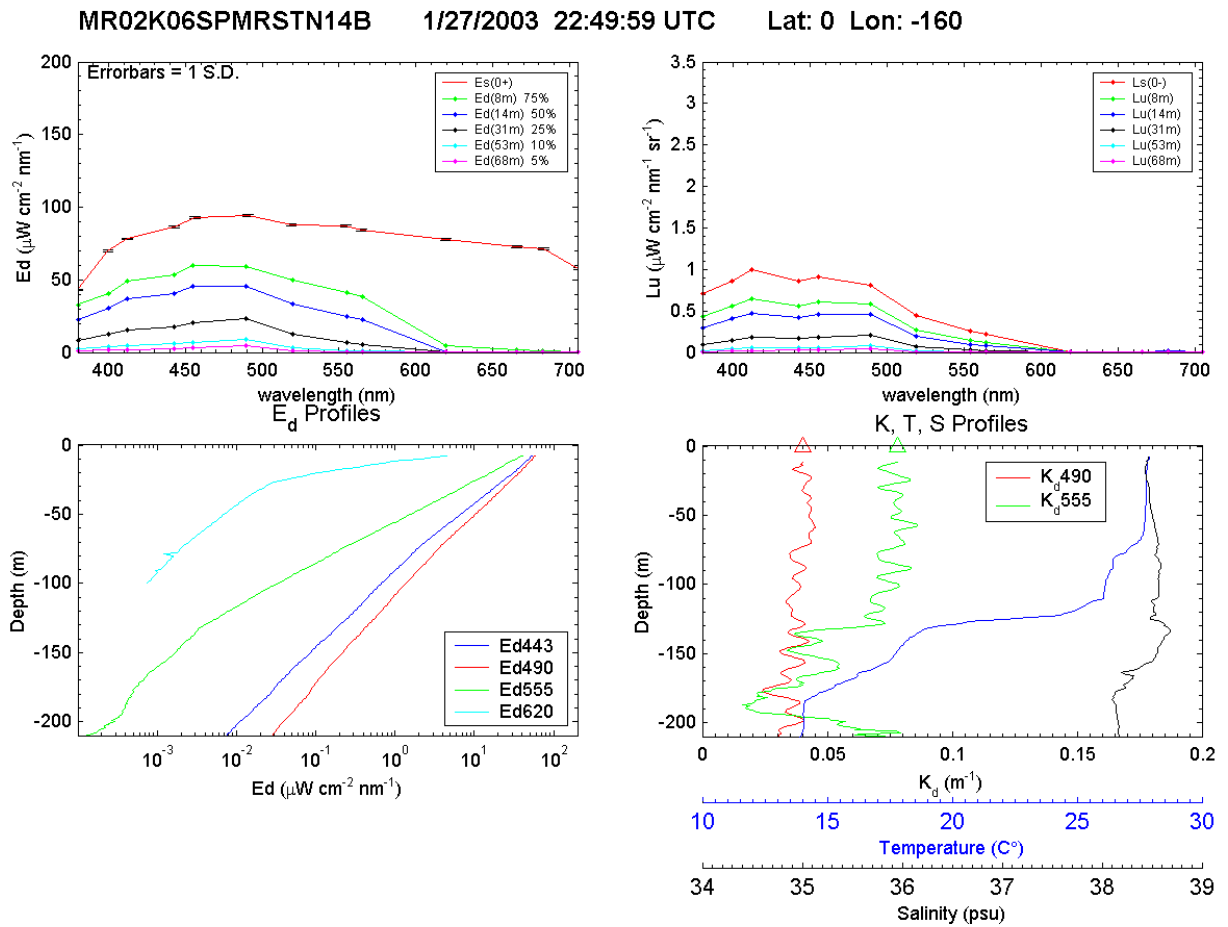


Figure 11. Sample plot 1 for Station MR02K06SPMRSTN14, Cast B.

MR02K06SPMRSTN14B 1/27/2003 22:49:59 UTC Lat: 0 Lon: -160

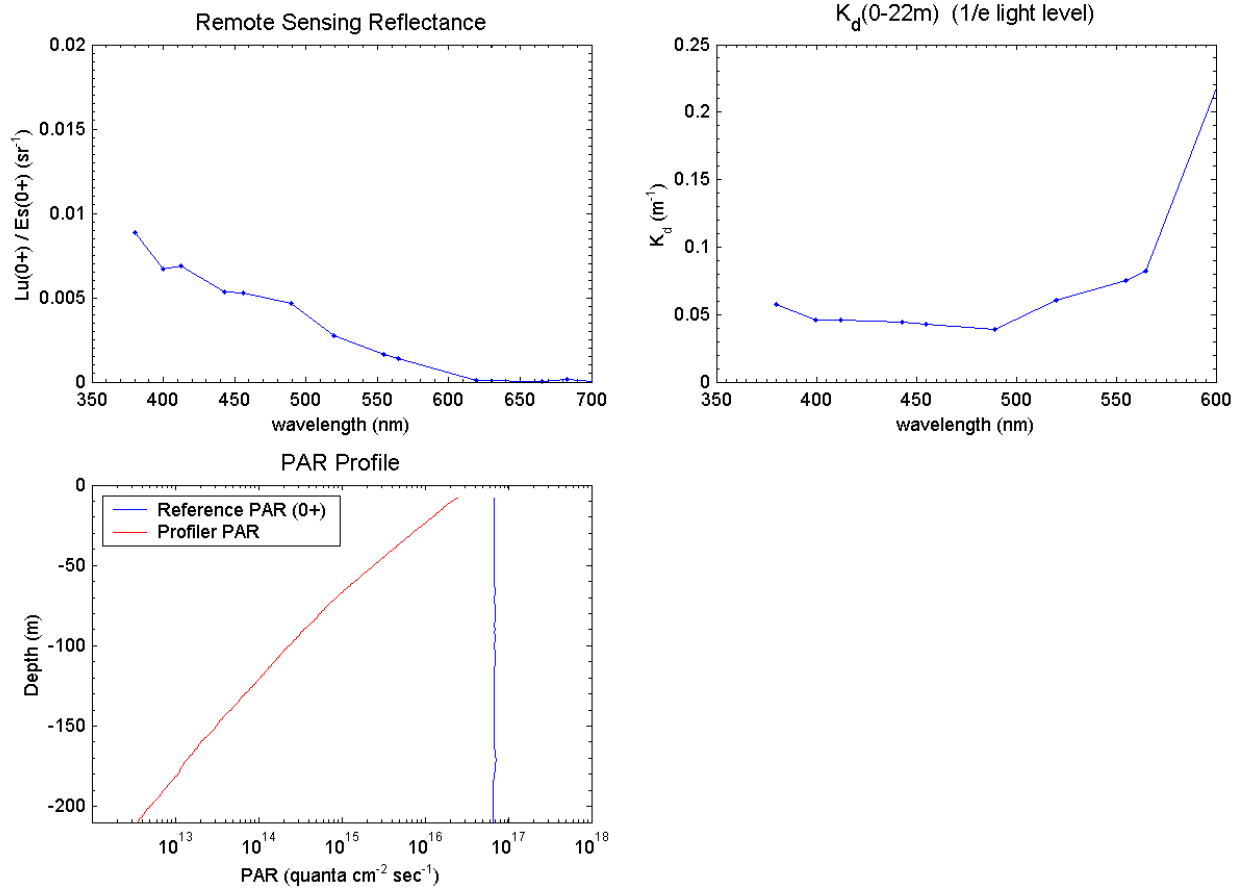


Figure 12. Sample plot 2 for Station MR02K06SPMRSTN14, Cast B.

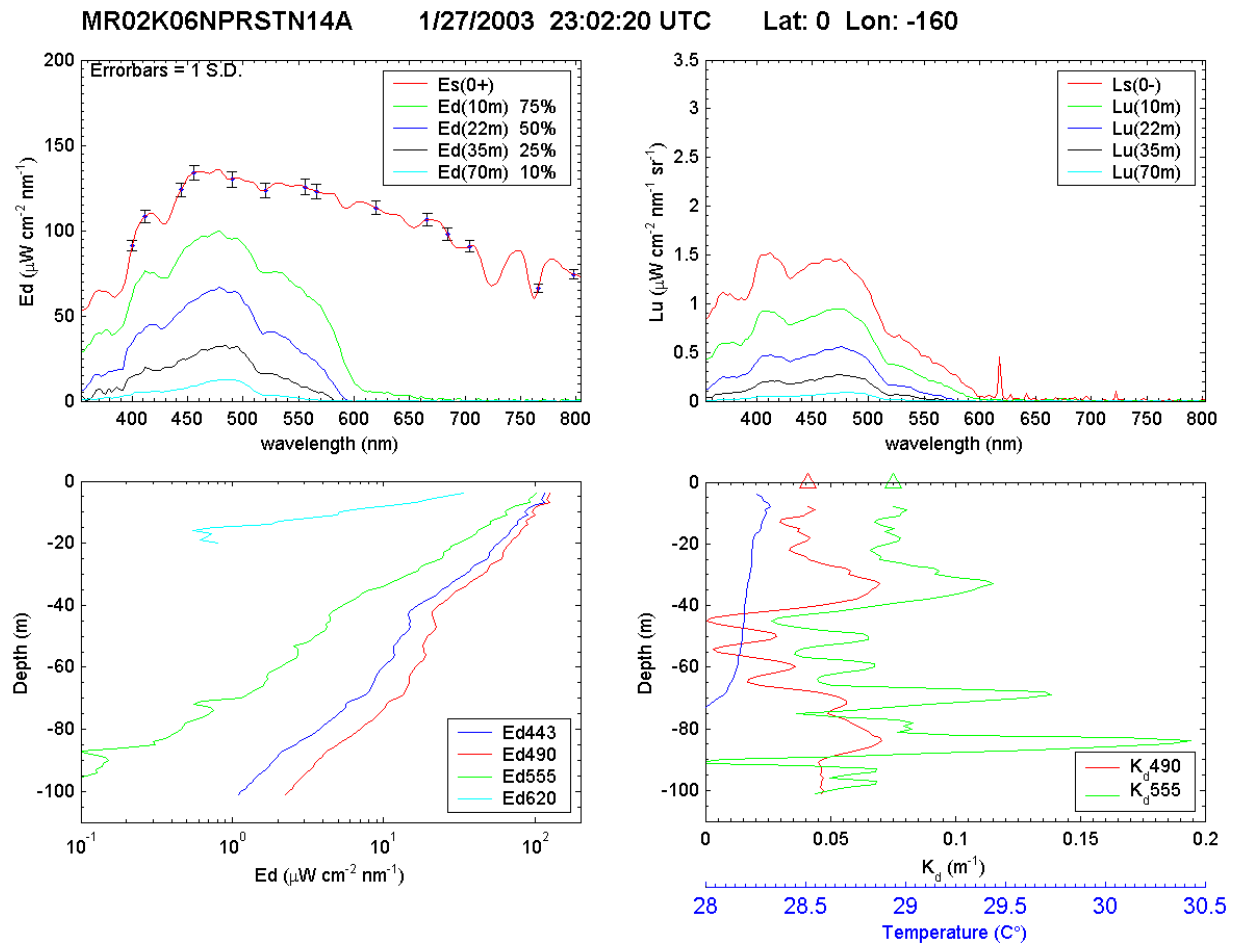


Figure 13. Sample plot 1 for Station MR02K06NPRSTN14, Cast A.

MR02K06NPRSTN14A 1/27/2003 23:02:20 UTC Lat: 0 Lon: -160

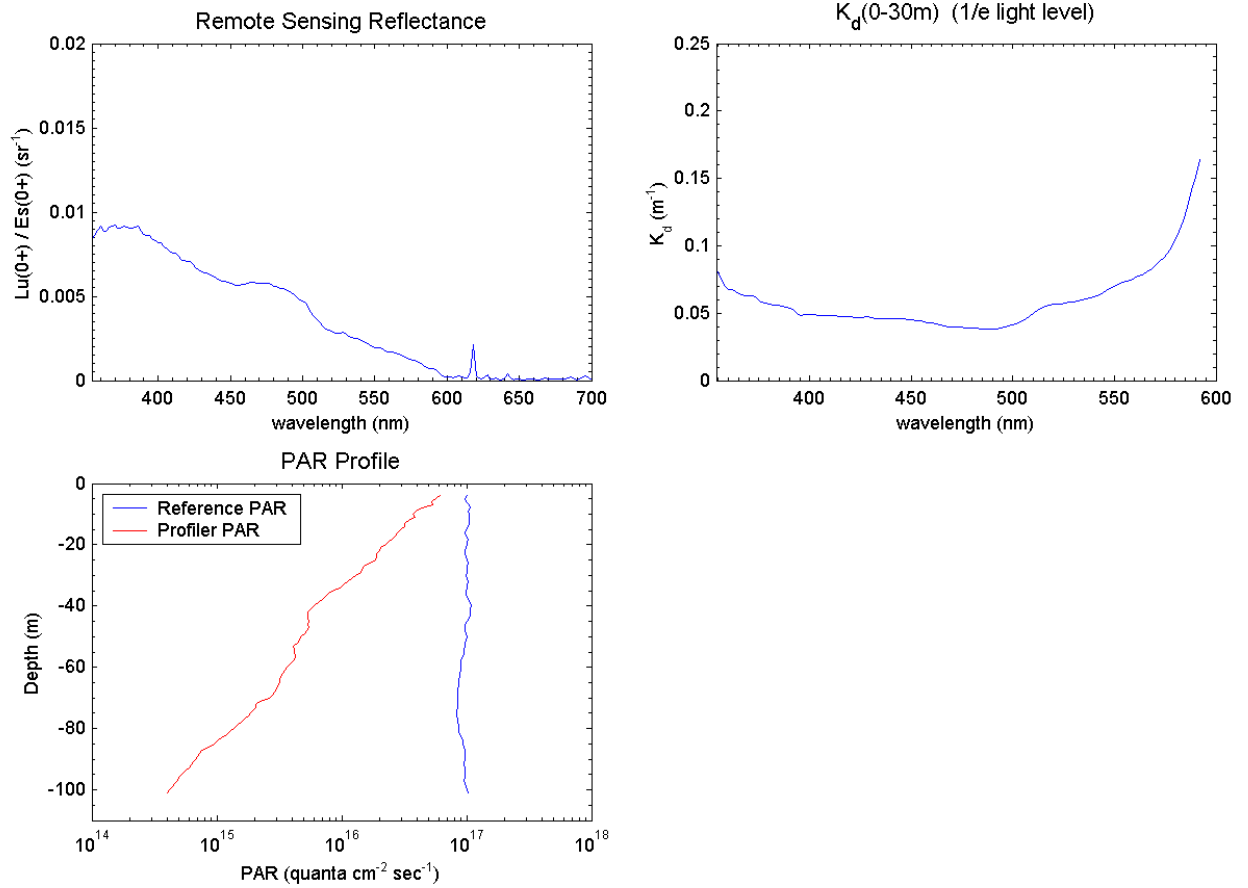


Figure 14. Sample plot 2 for Station MR02K06NPRSTN14, Cast A.

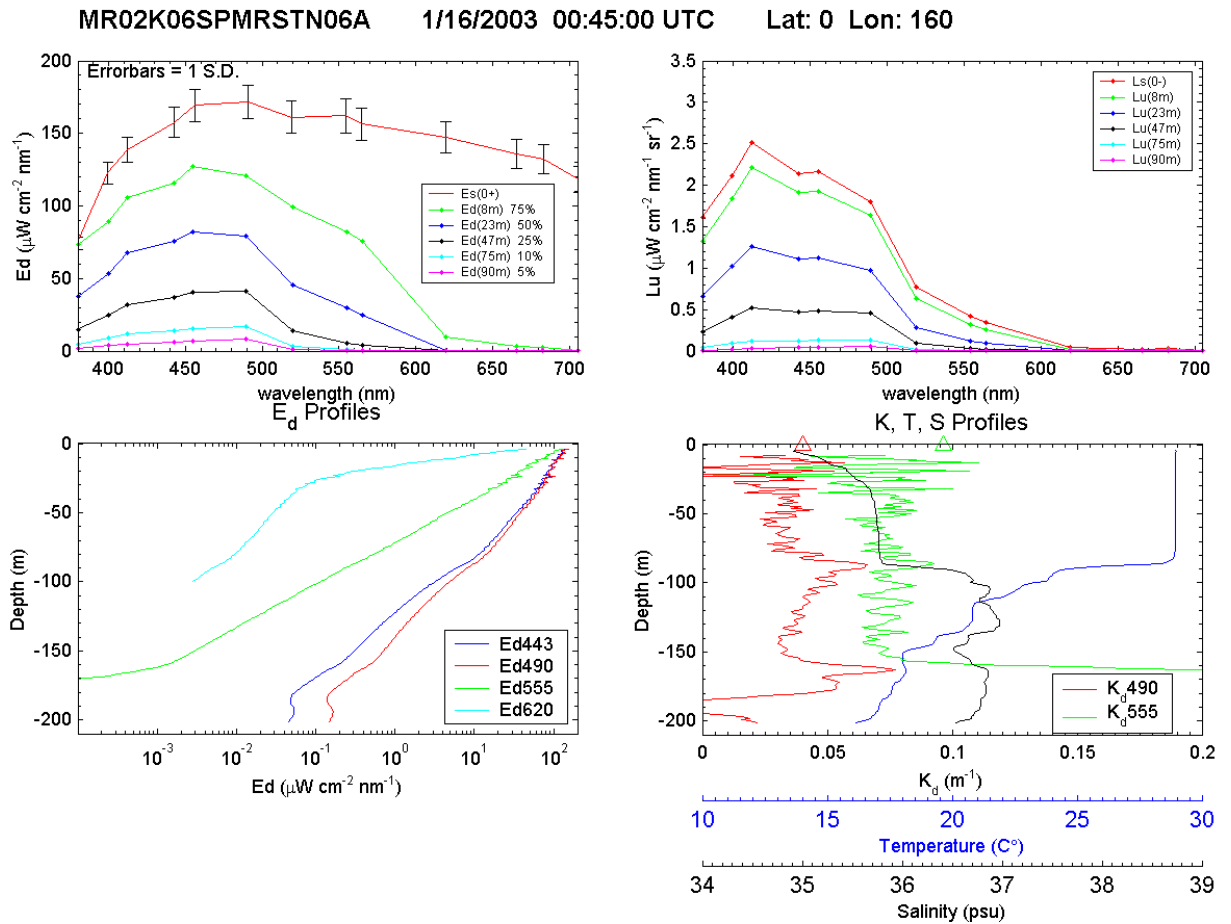


Figure 15. Sample plot 1 for Station MR02K06SPMRSTN06, Cast A.

MR02K06SPMRSTN06A 1/16/2003 00:45:00 UTC Lat: 0 Lon: 160

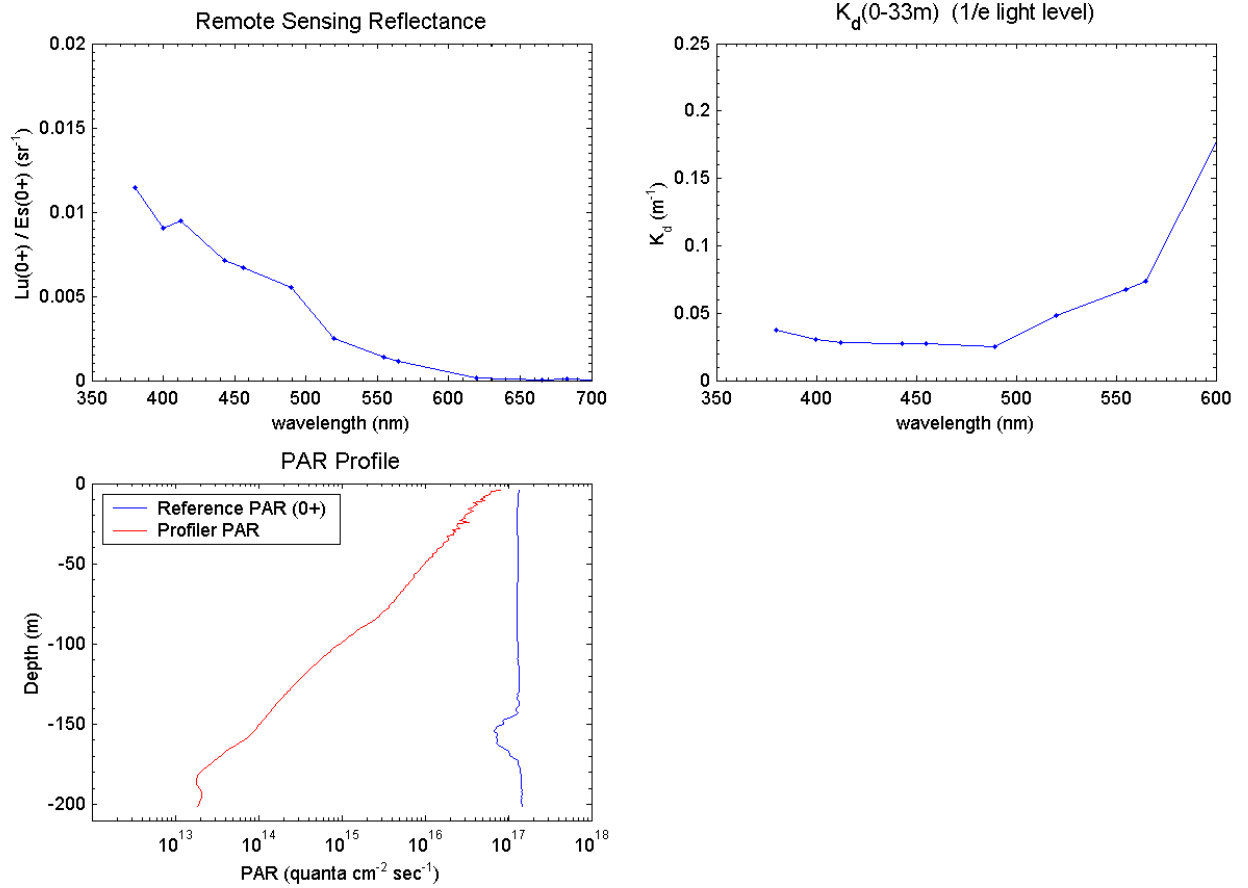


Figure 16. Sample plot 2 for Station MR02K06SPMRSTN06, Cast A.

MR02K06NPRSTN09B 1/20/2003 00:19:45 UTC Lat: 0 Lon: 175

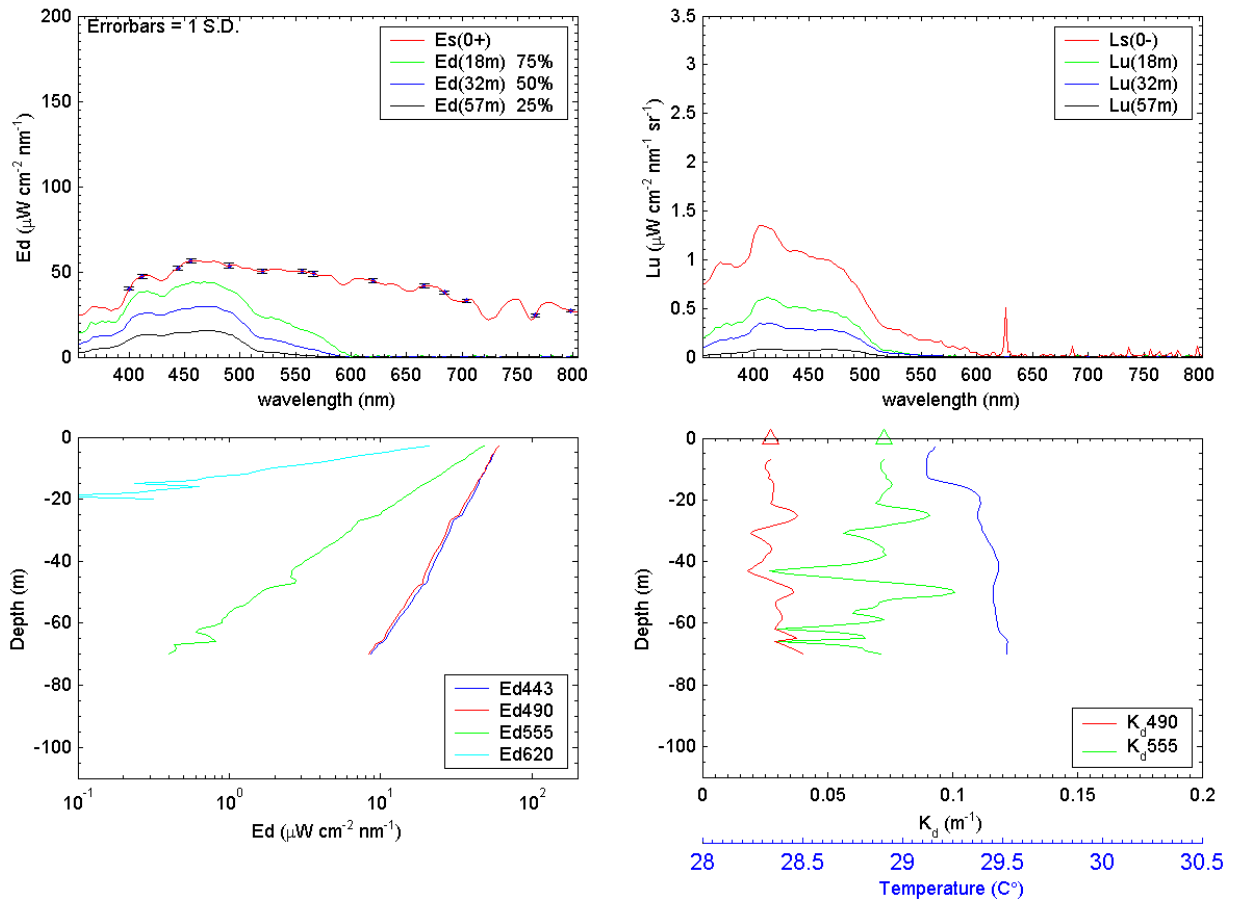


Figure 17. Sample plot 1 for Station MR02K06NPRSTN09, Cast B.

MR02K06NPRSTN09B 1/20/2003 00:19:45 UTC Lat: 0 Lon: 175

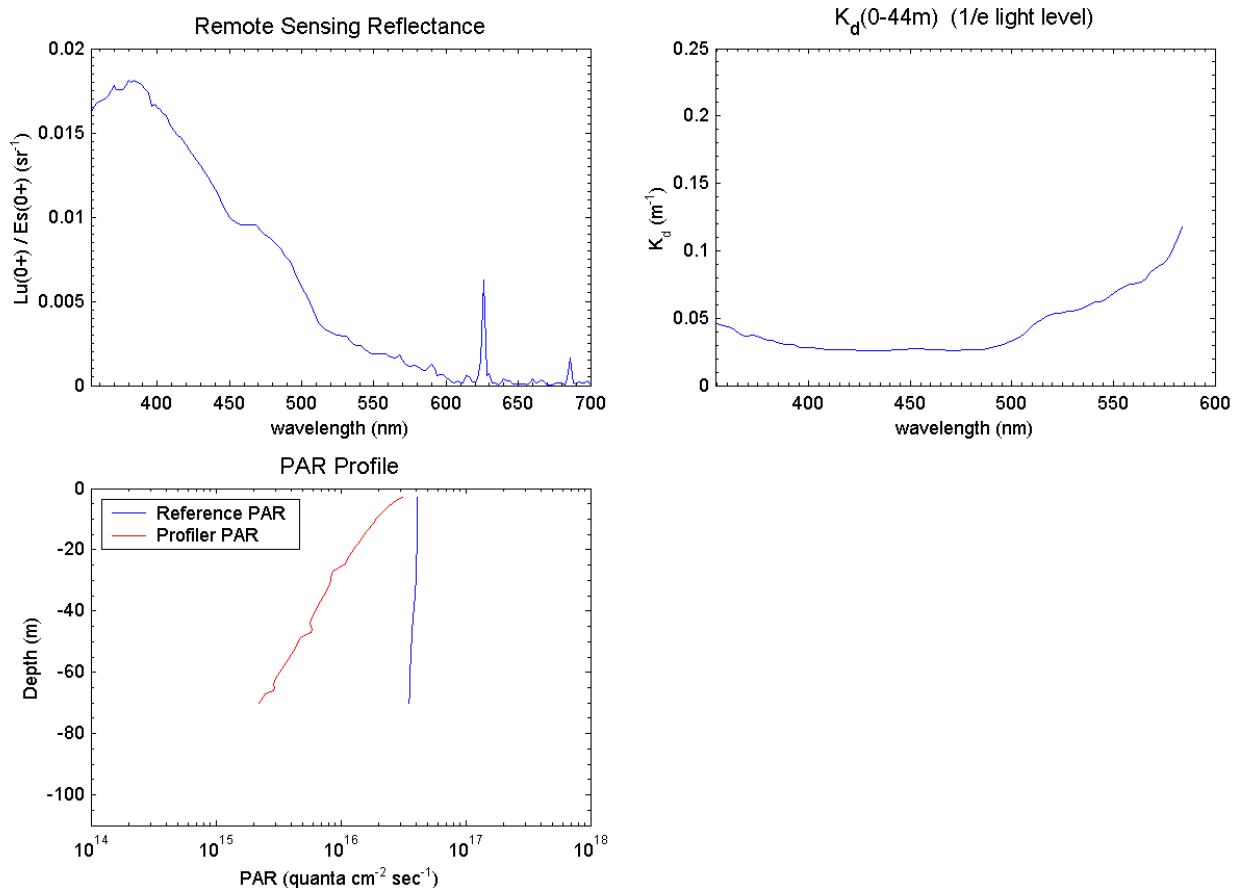


Figure 18. Sample plot 2 for Station MR02K06NPRSTN09, Cast B.

MR02K06 January 21b, 2003
Station 11: 0N 175W

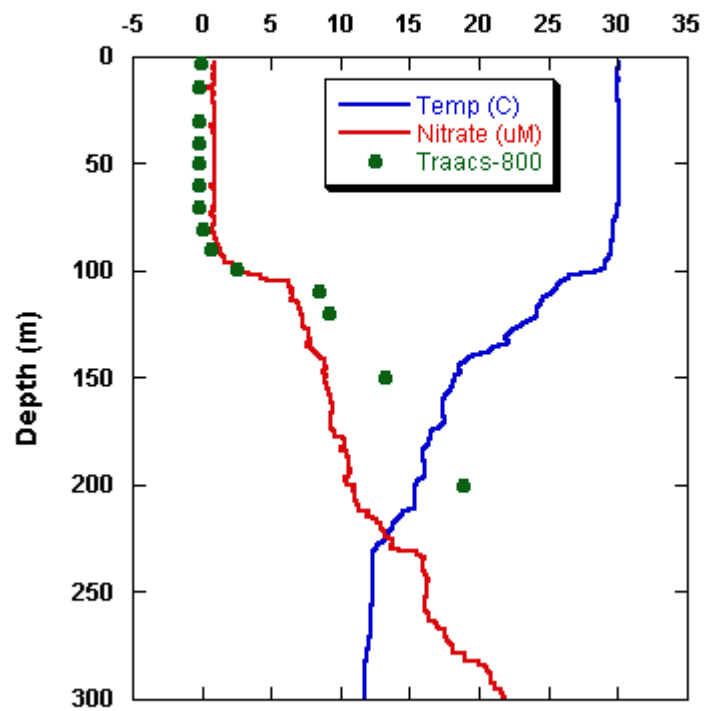


Figure 19. Sample ISUS nitrate plot for Station 11.

5.27. Argo float deployment

(1) Personnel

Kensuke Takeuchi	(FORSGC): Principal Investigator (not on board)
Nobie Shikama	(FORSGC) not on board
Eitarou Oka	(FORSGC)
Fujio Kobayashi	(MWJ)
Yasutaka Imai	(GODI)
Norio Nagahama	(GODI)

(2) Objectives

The objective of deployment is to clarify (1) variations of temperature and salinity in association with interannual variations such as ENSO events and intraseasonal variations and (2) subduction process in the mid-latitude, particularly the formation, circulation, and alteration of the Central Mode Water and the Subtropical Mode Water.

The profiling floats launched in this cruise measure vertical profiles of temperature and salinity automatically every ten days. The data from the floats will enable us to understand the variations mentioned above with time scales much smaller than those in the previous studies.

(3) Parameters

- water temperature, salinity, and pressure

(4) Methods

1) Profiling float deployment

We launched 26 APEX floats manufactured by Webb Research Ltd. Each float equips SBE41 CTD sensor manufactured by Sea-Bird Electronics Inc.

These floats usually drift at a predetermined depth, called the parking depth (1500 or 2000 decibar), and rise up to the sea surface every ten days by increasing their volume and changing the buoyancy. During the ascent, they measure temperature, salinity, and pressure. They stay at the sea surface for approximately nine hours, transmitting their positions and the CTD data to the land via the ARGOS system, and then return to the parking depth by decreasing volume. The status of floats and their launches are shown in Table 5.27-1.

2) XCTD observation

XCTD measurements to a depth of 1000 m were conducted between 165W and 152E on the cruise track from Honolulu to Hachinohe in Leg 4, in order to examine the sea condition around the float-deployment area (Sec. 4.2.2).

(6) Data archive

All data acquired through the ARGOS system is stored at FORSGC. The real-time data are provided to meteorological organizations via Global Telecommunication System (GTS) and utilized for analysis and forecasts of sea conditions.

Table 5.27-1 Status of floats and their launches

Float

Float Type	APEX floats manufactured by Webb Research Ltd.
CTD sensor	SBE41 manufactured by Sea-Bird Electronics Inc.
Cycle	10 days (approximately 9 hours at the sea surface)
ARGOS transmit interval	30 sec
Parking Depth	1500 decibar or 2000 decibar
Sampling layers	66 (1500, 1400, 1300, 1250, 1200, 1150, 1100, 1050, 1000, 975, 950, 925, 900, 875, 850, 825, 800, 780, 760, 740, 720, 700, 680, 660, 640, 620, 600, 580, 560, 540, 520, 500, 480, 460, 440, 420, 400, 380, 360, 340, 320, 300, 280, 260, 240, 220, 200, 190, 180, 170, 160, 150, 140, 130, 120, 110, 100, 90, 80, 70, 60, 50, 40, 30, 20, 10 decibar) for the floats with the parking depth of 2000 decibar and 71 (2000, 1900, 1800, 1700, 1600 decibar + 66 layers above) for the floats with the parking depth of 1500 decibar

Launches in Leg 3

Float S/N	ARGOS PTT ID	Date and time of Reset (UTC)	Date and Time of Launch (UTC)	Location of Launch	Parking Depth (decibar)
729	16359	00:37, Jan 18	02:45, Jan 18	0-00.22 S, 169-59.98 E	1500
731	16361	04:13, Jan 20	06:36, Jan 20	0-02.84 N, 175-06.11 E	1500
732	16362	23:34, Jan 20	01:52, Jan 21	0-00.97 S, 179-17.89 E	1500
733	16363	23:20, Jan 21	01:35, Jan 22	0-00.80 N, 175-37.82 W	1500
734	16364	21:44, Jan 24	23:28, Jan 24	0-00.08 S, 169-58.93 W	1500
735	16365	22:22, Jan 25	00:38, Jan 26	0-00.18 N, 164-48.32 W	1500
736	16366	03:41, Jan 28	05:01, Jan 28	0-04.23 N, 159-58.36 W	1500
737	16367	10:37, Jan 28	12:22, Jan 28	1-59.65 N, 159-48.52 W	1500
738	16476	05:48, Jan 29	07:30, Jan 29	6-59.37 N, 159-17.96 W	1500
692	13305	01:23, Jan 30	03:05, Jan 30	11-59.37 N, 158-46.81 W	2000
700	26558	18:09, Jan 30	19:24, Jan 30	15-59.64 N, 158-24.74 W	2000

Launches in Leg 4

Float S/N	ARGOS PTT ID	Date and time of Reset (UTC)	Date and Time of Launch (UTC)	Location of Launch	Parking Depth (decibar)
701	14061	18:23, Feb 03	20:03, Feb 03	25-28.38 N, 165-59.46 W	2000
702	14747	06:57, Feb 04	08:17, Feb 04	26-59.80 N, 168-59.18 W	2000
703	14748	18:51, Feb 04	20:51, Feb 04	28-21.73 N, 171-59.24 W	2000
706	15221	19:58, Feb 05	20:38, Feb 05	29-17.60 N, 175-59.14 W	2000
707	15467	06:08, Feb 06	07:50, Feb 06	30-17.89 N, 177-59.28 W	2000
708	16132	18:40, Feb 06	20:53, Feb 06	32-02.48 N, 179-00.84 E	2000
704	14800	06:03, Feb 07	07:43, Feb 07	32-58.79 N, 176-01.04 E	2000
705	15203	20:14, Feb 07	22:11, Feb 07	32-59.03 N, 173-01.18 E	2000
709	16206	11:02, Feb 08	13:11, Feb 08	32-58.78 N, 170-01.08 E	2000
710	16226	05:19, Feb 09	06:51, Feb 09	33-12.78 N, 167-01.21 E	2000
711	16324	14:29, Feb 09	16:58, Feb 09	33-54.35 N, 165-01.23 E	2000
712	16325	22:01, Feb 09	00:48, Feb 10	34-30.57 N, 163-00.59 E	2000
713	16326	06:31, Feb 10	08:19, Feb 10	35-05.74 N, 161-01.09 E	2000
714	16327	13:06, Feb 10	15:04, Feb 10	35-40.38 N, 159-00.52 E	2000
715	16328	07:59, Feb 11	10:27, Feb 11	37-24.45 N, 153-00.18 E	2000

5.28. TRITON Buoy recovery

(1) Personnel

Kazuhiko MATSUMOTO: Principal Investigator (JAMSTEC)

Akihiko MURATA : Scientist (JAMSTEC)

Masayuki FUJISAKI : Technical staff (MWJ)

Fujio KOBAYASHI : Technical staff (MWJ)

Ai YASUDA : Technical staff (MWJ)

Taeko OHAMA : Technical staff (MWJ)

Kentaro SHIRAISHI : Technical staff (MWJ)

Yuichi SONOYAMA : Technical staff (MWJ)

Masahiko NISHINO : Technical staff (MWJ)

Noriaki TERAMAE : Technical staff (MWJ)

Masato SUGIYAMA : Technical staff (MWJ)

(2) Objective

The large-scale air-sea interaction over the warmest sea surface temperature region in the tropical Pacific Ocean called warm pool affects the global atmosphere and causes El Nino phenomena. The formation mechanism of the warm pool and the air-sea interaction over the warm pool have not been well understood. Long term data sets of temperature, salinity, currents, so on have been required at fixed location. In particular, the ocean change due to the surface winds over the western tropical Pacific is important to study the relation with El Nino and rain fall over the ocean is also important parameter to study El Nino and Asia-Australian Monsoon. The TRITON program aims to obtain the basic data to improve the predictions of El Nino and variations Asia-Australian Monsoon system.

TRITON buoy array is integrated with the existing TAO (Tropical Atmosphere Ocean) array, which is presently operated by the Pacific Marine Environmental Laboratory / National Oceanic and Atmospheric Administration of the United States. TRITON is a component of international research program of CLIVAR (Climate Variability and Predictability), which is a major component of World Climate Research Program sponsored by the World Meteorological Organization, the International Council of Scientific Unions, and the Intergovernmental Oceanographic Commission of UNESCO. TRITON will also contribute to the development of GOOS (Global Ocean Observing system) and GCOS (Global Climate Observing system).

We could not recover TRITON buoy (Observation No.02005) during previous Leg(MR02-K06 Leg.2), so it was rough weather.

(3) Results

A TRITON buoy (Observation No.02005) had been successfully recovered during this Leg (MR02-K06 Leg.3).

The specifications of recovered TRITON buoy are as the following.

Nominal location	5N, 156E
ID number at JAMSTEC	02005
Number on surface float	T14
ARGOS PTT number	7962
ARGOS backup PTT number	07860
Deployed date	03 Mar. 2002
Recovered date	13 Jan. 2003
Exact location	04 - 58.47N, 156 - 02.23 E
Depth	3,602m

(4) Data archive

Hourly averaged data transmitted are through ARGOS satellite data transmission system in near real time. The real time data are provided to meteorological organizations via Global Telecommunication System and utilized for daily weather forecast. The data will be also distributed world wide through Internet from JAMSTEC and PMEL home pages. All data will be archived at JAMSTEC Mutsu Institute.

TRITON Homepage: <http://www.jamstec.go.jp/jamstec/triton>

5.29. Aerosol Measurement

(1) Personnel

On board scientists

Yuji Fujitani (Graduate school of Engineering, Hokkaido University) Graduate student

Co-workers not on board

Tatsuo Endoh (Institute of Low Temperature Science, Hokkaido University): Associate Professor

Sachio Ohta (Graduate school of Engineering, Hokkaido University): Professor

Tamio Takamura (Center for Environmental Remote Sensing, Chiba University): Professor

Teruyuki Nakajima (Center for Climate System Research, University of Tokyo): Professor

(2) Objectives

Anthropogenic aerosols affect on climate by perturbing radiation budget through scattering and absorbing solar radiation, which is called the direct effect of aerosol. At present, uncertainty of radiative forcing due to greenhouse gases is 15%, whereas it lies in a factor of 2 of the direct aerosol forcing. As in The Third Assessment Report of IPCC in 2001, a chapter was spared about aerosols effect on climate, this problem had been regarded as important. The larger uncertainty of aerosol forcing comes from little available information about aerosol distribution of optical properties. Aerosols have various sources and sinks, the lifetime is short as a week or 10 days. As a result, aerosols have various spatial and temporal distributions. Furthermore, aerosol optical properties are function of aerosol chemical species, aerosol size distribution, and mixed state (i.e. internal mixture or external mixture). To calculate radiative forcing, the various input parameters are needed, but there are still shortages of them. It is then necessary to conduct long term and large-scale observations to understand aerosol distribution of optical properties.

There are few measurements, in particular, of aerosol optical properties over the Pacific Ocean, whereas this region is very important. Anthropogenic materials are increasingly emitted from Asian countries, and more amounts of aerosols may be transported to the Pacific Ocean. Thus, it is important to monitor the atmospheric environment in the East Asia and western Pacific ocean. Satellite remote sensing is hoped for monitoring global aerosol distribution. For atmospheric correction of the remote sensing, surface measurements are indispensable to optical and chemical properties of atmospheric aerosols.

During this cruise, we measured spatial distribution of aerosol optical and chemical properties to estimate radiative forcing by aerosol accurately and to do ground truth for satellite remote sensing.

(3) Methods

Sky Radiometer (POM-01MK II ; PREDE), equipped on deck, measures direct and aureole sun light intensity every 5min. The sensor provides optical thickness, Åangstrom exponent and size distribution of atmospheric aerosols.

To confirm retrieved optical properties from skyradiometer data analysis, *in-situ* measurement is conducted during this cruise. Sample air is drawn through inlets 5m height on compass deck, to manifold in research room. Particle larger than $2 \mu\text{m}$ in diameter are removed by cyclone separators. From the manifold, the sample air is distributed to Particle Soot / Absorption Photometer (PSAP; Radiance Research), Integrating Nephelometer (IN; M903; Radiance Research)

and Optical Particle Counter (OPC; KC-01C; RION). PSAP measures volume absorption coefficient, IN measures volume scattering coefficient and OPC counts number concentration of aerosols larger than 0.3, 0.5, 1.0, 2.0 and 5.0 μm in diameter. All measurements are conducted every 1min. The aerosols are also collected on filter for chemical analysis by using another sampling system. The sampling system consists of three parts. One is Teflon filter sampling line (FP-500; 47mm ϕ ; SUMITOMO DENKOH), the second is quartz fiber filter sampling line (2500QAT-UP; 47mm ϕ ; Pallflex), and the third is teflon and quartz fiber filters in tandem use line. Aerosol sampling on Teflon filter are also conducted on the compass deck without cyclone separators. Aerosol sampling is performed with the special cautions not to be contaminated with chimney exhaust. The filters are stored in the refrigerator. From the aerosols collected on Teflon filters, amounts of inorganic and metal components are analysed by Ion chromatography and ICP-MS. From the sample on quartz fiber filters amounts of analyzed elemental and total carbons are determined by carbon analyzer.

(4) Results

Measurements were mainly conducted in fine day, the data are well acquired on Jan. 18, 22 to 27, 30 to Feb. 1, 3, 4, and 6 in 2003. In the analysis, we must exclude the effect of cloud. The volume scattering and absorption coefficients were $0.03 \sim 418 \times 10^{-7} \text{ m}^{-1}$ and $0.03 \sim 9.18 \times 10^{-7} \text{ m}^{-1}$, respectively. Figure 1 shows time series of particle concentration larger than 0.3 μm . The particle number was under 0.5 to 200 cm^{-3} . Tables 1 and 2 summarized the aerosol sampling results.

(5) Data archive

The data of skyradiometer, PSAP, IN, and OPC are numerically analyzed and filter samples are chemically analyzed. All data are archived at Hokkaido University (Endoh and Ohta), University of Tokyo (Nakajima) and Chiba University (Takamura), and submitted to JAMSTEC within 3-years.

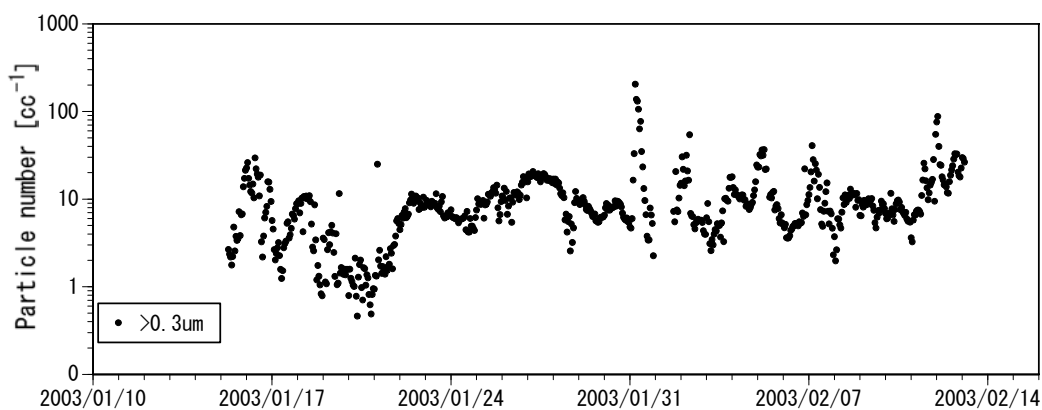


Figure 1. Time series of particle number concentration diameter larger than 0.3 μm

Table 1. Information of aerosol sampling on Teflon filter

No.	date and time (UTC)		total sampling period [min]	sampling volume [m ³]	start (deg)		end (deg)	
	start	end			Latitude	Longitude	Latitude	Longitude
1	13Jan. 0:51	14Jan. 21:03	2441	48.8	7.5	151.8	0.8	159.3
2	14Jan. 21:44	17Jan. 1:28	2162	43.2	0.7	159.4	0.0	164.5
3	17Jan. 2:12	18Jan. 22:28	2627	52.5	0.0	164.6	0.0	175.0
4	19Jan. 12:51	21Jan. 23:00	2897	57.9	0.0	175.0	0.0	-175.6
5	22Jan. 1:04	24Jan. 3:11	2427	48.5	0.0	-175.6	0.0	-170.0
6	24Jan. 3:29	26Jan. 2:45	2253	45.1	0.0	-170.0	0.0	-164.3
7	26Jan. 3:09	28Jan. 2:25	2288	45.8	0.0	-164.2	0.1	-160.0
8	28Jan. 2:43	29Jan. 17:53	2320	46.4	0.1	-160.0	9.6	-159.0
9	29Jan. 18:37	31Jan. 10:41	2356	47.1	9.8	-159.0	19.0	-158.1
10	31Jan. 10:47	31Jan. 21:45	655	13.1	19.1	-158.1	21.0	-157.9
11	2Feb. 10:30	4Feb. 4:33	2125	42.5	21.2	-158.4	26.5	-168.1
12	4Feb. 4:55	6Feb. 19:55	3503	70.1	26.6	-168.2	31.9	179.3
13	7Feb. 5:40	8Feb. 20:58	2326	46.5	32.8	176.5	34.2	164.0
14	8Feb. 21:14	10Feb. 2:28	1724	34.5	34.2	164.0	34.7	162.5
15	10Feb. 3:02	11Feb. 23:03	1151	23.0	34.7	162.4	38.5	149.2
16	11Feb. 23:42	12Feb. 21:02	1254	25.1	38.5	149.0	40.1	143.2

Table 2. Information of aerosol sampling on quartz fiber filter

No.	date and time (UTC)		total sampling period [min]	sampling volume [m ³]	start (deg)		end (deg)	
	start	end			Latitude	Longitude	Latitude	Longitude
1	13Jan. 0:51	17Jan. 1:28	4603	92.1	7.5	151.8	0.0	164.5
2	17Jan. 2:12	21Jan. 23:00	5523	110.5	0.0	164.6	0.0	-175.6
3	22Jan. 1:04	26Jan. 2:45	4681	93.6	0.0	-175.6	0.0	-164.3
4	26Jan. 3:09	29Jan. 17:53	4607	92.1	0.0	-164.2	9.6	-159.0
5	29Jan. 18:37	31Jan. 21:45	3011	60.2	9.8	-159.0	21.0	-157.9
6	2Feb. 10:30	6Feb. 19:55	5628	112.6	21.2	-158.4	31.9	179.3
7	7Feb. 5:40	10Feb. 2:28	4050	80.1	32.8	176.5	34.7	162.5
8	10Feb. 3:02	11Feb. 23:03	1151	23.0	34.7	162.4	38.5	149.2
9	11Feb. 23:42	12Feb. 21:02	1254	25.1	38.5	149.0	40.1	143.2

5.30. Lidar observations of clouds and aerosols

(1) Personnel

Nobuo Sugimoto, Ichiro Matsui, Atsushi Shimizu (National Institute for Environmental Studies), Yuji Fujitani (Hokkaido University, on board personnel)

(2) Objectives

Objectives of the observations and experiments in this cruise are to study distribution and optical characteristics of clouds and aerosols using a two-wavelength dual polarization lidar.

(3) Measured parameters

- Vertical profiles of backscattering coefficient at 532 nm and 1064 nm.
- Vertical profile of depolarization ratio at 532 nm.

(4) Method

Vertical profiles of aerosols and clouds were measured with a two-wavelength dual polarization lidar. The lidar employs a Nd:YAG laser as a light source which generates the fundamental output at 1064 nm and the second harmonic at 532 nm. Transmitted laser energy is typically 100 mJ per pulse at 1064 nm and 50 mJ per pulse at 532 nm. The pulse repetition rate is 10 Hz. The receiver telescope has a diameter of 25 cm. The receiver has three detection channels to receive the lidar signals at 1064 nm and the parallel and perpendicular polarization components at 532 nm. An analog-mode avalanche photo diode (APD) is used as a detector for 1064 nm, and photomultiplier tubes (PMTs) are used for 532 nm. The detected signals are recorded with a digital oscilloscope and stored on a hard disk with a computer. The lidar system was installed in a 20-ft container. The container has a glass window on the roof, and the lidar was operated continuously regardless of weather. Measurements were conducted during Jan. 13 - 31, Feb. 2- 13.

(5) Data archive

- raw data

- lidar signal at 532 nm (parallel polarization)
- lidar signal at 532 nm (perpendicular polarization)
- lidar signal at 1064 nm
- temporal resolution 10 sec/vertical resolution 6 m.

- processed data

- cloud base height, apparent cloud top height, cloud phase
- cloud fraction
- boundary layer height (aerosol layer upper boundary height)
- backscatter coefficient of aerosols
- depolarization ratio

5.31. Microwave radiometer and micro rain radar

(1) Personnel

Masayuki Sasaki (NASDA/EORC*): Principle Investigator (not on board)
Yozo Takayama (JMA/MRI**)

(2) Objectives

The satellite-borne microwave radiometers are the powerful device to obtain the spatial and temporal variation of the water vapor, cloud liquid water, etc, especially over the ocean where the ground-based observation is poor. To validate the products of AMSR (Advanced Microwave Radiometer) / ADEOS-II, brand-new satellite-borne microwave radiometer, the ground-based vertically-pointed rain radar is installed on the vessel and continuous observation is carried out.

(3) Methods

The micro rain radar MRR-2 (METEK GmbH) and the microwave radiometer WVR-1100 (Radiometrics Co.) are used for this observation.

The radar is a compact 24 GHz FM-CW-radar for the measurement of profiles of drip size distribution and rain rates, liquid water content and characteristic falling velocity of the raindrops. The transmitter power is 50 mW. In this observation, the data is obtained every 60 seconds, at every 200-m range gate to 6000-m height.

The radiometer obtained brightness temperature data for the two frequency, 23GHz and 31GHz. The brightness temperature data is converted to the vertically integrated water vapor amount and cloud liquid water amount.

The observation is performed continuously from 13 January to, 12 February 2003.

(4) Preliminary Results

The observed data will be checked and analyzed after the cruise.

(5) Data Archive

The original data will be archived at NASDA/EORC, and will be submitted to JAMSTEC.

*NASDA/EORC: National Space Development Agency of JAPAN / Earth Observation Research Center.

**JMA/MRI : Japan Meteorological Agency / Meteorological Research Institute

5.32. Surface Atmospheric Turbulent Flux

(1) Personnel

Norio Nagahama (GODI) : On-board collaborator

On-shore scientists:

Osamu Tsukamoto (Okayama University): Principal Investigator

Hiroshi Ishida (Maritime University of Kobe / Frontier Observational Research System for Global Change)

Kunio Yoneyama (JAMSTEC)

(2) Objective

For the understanding of air-sea interaction, accurate measurements of surface heat and fresh water budgets are necessary as well as momentum exchange through the sea surface. In addition, the evaluation of surface flux of carbon dioxide is also indispensable for the study of global warming. Sea surface turbulent fluxes of momentum, sensible heat, latent heat, and carbon dioxide were measured by using the eddy correlation method that is thought to be most accurate and free from assumptions. These surface heat flux data are combined with radiation fluxes and water temperature profiles to derive the surface energy budget.

(3) Methods

The surface turbulent flux measurement system consists of turbulence instruments (Kaijo Co., Ltd.) and ship motion sensors (Kanto Aircraft Instrument Co., Ltd.). The turbulence sensors include a three-dimensional sonic anemometer-thermometer (Kaijo, DA-600) and an infrared hygrometer (LICOR, LI-7500). The sonic anemometer measures three-dimensional wind components relative to the ship. The ship motion sensors include a two-axis inclinometer (Applied Geomechanics, MD-900-T), a three-axis accelerometer (Applied Signal Inc., QA-700-020), and a three-axis rate gyro (Systron Donner, QRS-0050-100). LI7500 is a CO₂/H₂O turbulence sensor that measures turbulent signals of carbon dioxide and water vapor simultaneously. Fig. 7.12-1 shows the installation of the instruments at the top of the foremast.

These signals are sampled at 10 Hz by a PC-based data logging system (Labview, National Instruments Co., Ltd.). By obtaining the ship speed and heading information through the Mirai network system it yields the absolute wind components relative to the ground. Combining wind data with the turbulence data, turbulent fluxes and statistics are calculated in a real-time basis.

(4) Results

Data will be processed after the cruise at Okayama University.

(5) Data Archive

All data are archived at Okayama University, and will be open to public after quality checks and corrections. Corrected data will be submitted to JAMSTEC Data Management Office.

Fig. 5.32-1 Turbulent flux measurement system on the top deck of foremast.

